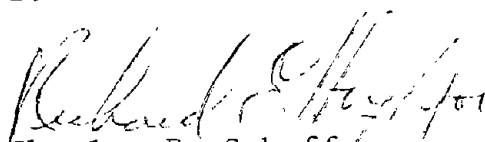




## FOREWORD

The use of high-strength bolts as connectors has produced bridge structural joints of superior quality and economy. However, the corrosion of untreated faying surfaces of friction-type bolted connections in steel bridges often results in joint separation and/or reduction of the coefficient of friction. Corrosion inhibiting coatings used on the faying surfaces or other forms of surface treatment such as blast-cleaning, can increase the slip resistance as well as reduce the scatter in the slip performance of a bolted joint.

Design recommendations and possible revisions in the AASHTO Bridge Specifications are presented. This is one of two final reports on the results of this research that are being distributed to the Washington and field offices of the Federal Highway Administration, State highway agencies and interested researchers. The other report is FHWA/RD-81/147, "Friction-type Bolted Connections with A588 Weathering Steel."



Charles F. Scheffey  
Director, Office of Research  
Federal Highway Administration

## NOTICE

The contents of this report reflect the views of the authors who are responsible for the facts and accuracy of the data presented herein. The contents do not necessarily reflect the views or policies of the Federal Highway Administration. This report does not constitute a standard, specification, or regulation.

There was no invention or discovery conceived or first actually reduced to practice in the course of or under this contract, including any art, method, process, machine, manufacture, design, or composition of matter, or any new and useful improvement thereof, or any variety of plant which is or may be patentable under the patent laws of the United States of America or any foreign country.

1. Report No. FHWA/RD-81/148		2. Government Accession No.		3. Recipient's Catalog No.	
4. Title and Subtitle AN EXPERIMENTAL STUDY OF BOLTED SHEAR CONNECTIONS				5. Report Date December 1981	
				6. Performing Organization Code	
7. Author(s) K. H. Frank, J. A. Yura				8. Performing Organization Report No.	
9. Performing Organization Name and Address Department of Civil Engineering University of Texas at Austin Austin, Texas 78712				10. Work Unit No. FCP 35L3-142	
				11. Contract or Grant No. DOT-FH-11-8900	
12. Sponsoring Agency Name and Address Offices of Research and Development Federal Highway Administration U.S. Department of Transportation Washington, D.C. 20590				13. Type of Report and Period Covered Final Report 2-5-76 - 6-1-81	
				14. Sponsoring Agency Code S 0 1 2 1 7	
15. Supplementary Notes FHWA Contract Manager: L. R. Cayes HRS-11					
16. Abstract <p>A large experimental program which involved approximately 700 tests was used to develop statistically reliable slip loads for bolted shear connections with coated contact surfaces. Four different painting systems were evaluated for use in friction-type connections. Variables included in the study were paint thickness, size of hole, type of steel, and magnitude of clamping force. An efficient and reliable slip test setup was developed to complete the research.</p> <p>Additional creep and fatigue tests on bolted butt splices were used to evaluate the suitability of the painting systems for bridges. Some large bolted connections were tested to evaluate the applicability of the single fastener slip test to multi-bolt connections. Ultimate load tests to determine the effect of undeveloped fillers on bolt shear strength and the interaction between bolt shearing stress and plate tensile stress are reported.</p> <p>The test program is used to develop design recommendations for friction connections for the AASHTO Bridge Specifications with coated faying surfaces. Vinyl paints were found unsatisfactory for the contact surfaces because of creep. Current provisions for undeveloped fillers are justified but current bearing stresses should be reduced when high tensile stresses are present.</p>					
17. Key Words Bolted connections, creep, fatigue, bearing, fillers, paints, slip resistance			18. Distribution Statement No restrictions. This document is available to the public through the National Technical Information Service, Springfield, Virginia 22161		
19. Security Classif. (of this report) Unclassified		20. Security Classif. (of this page) Unclassified		21. No. of Pages 246	22. Price

## TABLE OF CONTENTS

Part		Page
1	INTRODUCTION . . . . .	1
	Background . . . . .	1
	Objectives and Scope . . . . .	2
	Coating Systems . . . . .	3
	Preface . . . . .	6
2	EXPERIMENTAL METHODS . . . . .	7
	Slip Test Arrangement . . . . .	7
	Slip Specimens . . . . .	9
	Paint Thickness Measurement . . . . .	10
	Painting Procedure . . . . .	11
	Slip Test Procedure . . . . .	14
	Paint Curing Time . . . . .	15
	Bolt Tests . . . . .	20
	Surface Roughness Measurement . . . . .	23
3	SLIP TESTS . . . . .	26
	Factorial Slip Study . . . . .	26
	Discussion of Factorial Results . . . . .	48
	Other Coatings . . . . .	60
	Paint Curing Prior to Assembly . . . . .	63
	Tension Slip Tests . . . . .	65
	Full-Size Connections . . . . .	71
	Recommendations . . . . .	86
4	CREEP OF COATED SPECIMENS . . . . .	91
	Experiment Design . . . . .	91
	Experimental Procedures . . . . .	92
	Load Application and Specimen Deformation Measurement Procedures . . . . .	104
	Creep Test Results . . . . .	107
	Summary of Creep Test Results . . . . .	116
	Bolt Relaxation Results . . . . .	117
	Post Creep Slip Tests . . . . .	122
	Conclusions of Bolt Shortening and Post Creep Test Results . . . . .	126
5	FATIGUE STUDY OF COATED BOLTED JOINTS . . . . .	128
	Specimen Design and Testing Program . . . . .	128
	Test Equipment . . . . .	132
	Instrumentation . . . . .	133

Part	Page
Specimen Preparation . . . . .	133
Control Slip Tests . . . . .	137
Test Results . . . . .	138
Analysis of Results . . . . .	145
Summary and Conclusions of Fatigue Tests . . . . .	150
 6 SPLICE CONNECTIONS WITH UNDEVELOPED FILLERS . . . . .	 153
Introduction . . . . .	153
Splice Connection Tests . . . . .	155
Test Discussion . . . . .	163
Design Recommendations . . . . .	166
Summary . . . . .	167
 7 BEARING CRITICAL SPLICE CONNECTIONS . . . . .	 168
Introduction . . . . .	168
Test Program . . . . .	171
Test Results . . . . .	176
Analysis of Results . . . . .	190
Deflection Limits as a Failure Criterion in Bearing . . . . .	206
Conclusions and Recommendations . . . . .	208
 8 SUMMARY AND COMMENTS . . . . .	 211
 REFERENCES . . . . .	 215
 APPENDIX A - Draft Testing Specification to Determine the Design Slip Coefficient for Coatings Used in Bolted Joints . . . . .	   219
 APPENDIX B - Recommended Changes in the AASHTO Bridge Specifications . . . . .	  231

## List of Figures

<u>Figure</u>	<u>Title</u>	<u>Page</u>
1	Schematic of test specimens	8
2	Test setup schematic	8
3	Compression slip test setup	9
4	Slip test specimen	10
5	Paint film thickness gages	12
6	Painting racks	13
7	Definition of slip load	15
8	Comparison of slip coefficients	17
9	Comparison of slip coefficients	17
10	Comparison of slip coefficients	18
11	Comparison of slip coefficients	18
12	Comparison of slip coefficients	19
13	Skidmore-Wilhelm bolt calibrator	21
14	C-frame extensometer	21
15	Contact point fit with countersunk hole	22
16	Typical bolt calibration curves	22
17	Direct tension tests	24
18	The Keane-Tator surface profile comparator	24
19	Typical load-slip curve for sandblasted surfaces	29
20	Effect of steel type and clamping force	31
21	Histogram of slip coefficient for sandblasted surfaces	31
22	Effect of hole size and clamping force	32
23	Effect of clamping force	32
24	Effect of sandblasting on the average slip coefficient	34
25	Comparison of average slip coefficients for different surface roughness	34
26	Typical load-slip curve	36
27	Frequency distribution for organic zinc-rich coated A572 surfaces	36
28	Typical load-slip curve	43
29	Frequency distribution for organic zinc-rich with epoxy coated, A572 surfaces	43
30	Frequency distribution for inorganic zinc-rich with vinyl coated A572 surfaces	46
31	Typical load-slip curve	46
32	Typical load-slip curve	48
33	Comparison of average slip coefficient for different hole sizes	53
34	Comparison of average slip coefficient for different steel types	53
35	Comparison of average slip coefficient for different paint thickness	57
36	Comparison of average slip coefficient for different vinyl systems	57
37	Comparison of overall average slip coefficient for sandblasted and painted surfaces	58

List of Figures (cont.)

<u>Figure</u>	<u>Title</u>	<u>Page</u>
38	Typical load-slip curves	59
39	Typical load-slip curves	61
39a	Typical load-slip curves	61
40	Test sample assembled one hour after painting	65
41	Bolted tension slip specimen	66
42	Bolt calibration curves for tension specimens	66
43	Test setup for tension slip tests	68
44	Full size slip connection	72
45	Bolt force histograms and calibrations	74
46	Bolt force histograms, oversize holes	74
47	Bolt relaxation histograms, inorganic zinc, 15/16 holes	76
48	Bolt relaxation histograms, inorganic zinc, 1-1/16 holes	76
49	Bolt relaxation histograms, organic zinc, 15/16 holes	77
50	Bolt relaxation histograms, organic zinc, 1-1/16 holes	78
51	Bolt relaxation histograms, organic zinc and epoxy	79
52	Bolt tightening histograms, Fabricator A	81
53	Bolt tightening histograms, Fabricator B	81
54	Slip gages for truss connections	83
55	Contact area for full-size connections	83
56	A325 bolt calibrations	94
57	A490 bolt calibrations	94
58	A325 load-indicating washer calibrations	95
59	A490 load-indicating washer calibrations	95
60	Creep specimens in series	97
61	Slip gages	100
62	Specimen setup	102
63	Top support for specimen chain and load system	103
64	Precision micrometer measuring creep deformation	107
65	Inorganic zinc with vinyl topcoat (normal), chain #1	110
66	Inorganic zinc with vinyl topcoat (thick), chain #1	110
67	Inorganic zinc with vinyl topcoat (normal), chain #2	111
68	Inorganic zinc with vinyl topcoat (thick), chain #2	111
69	Vinyl primer (normal), chain #3	112
70	Vinyl primer (thick), chain #3	112
71	Vinyl primer (normal), chain #4	113
72	Vinyl primer (thick), chain #4	113
73	Creep of thick organic zinc, chain #2	115
74	Creep-time response, organic zinc specimen, outdoor test	115
75	Average bolt shortening--inorganic zinc with vinyl and organic zinc	118
76	Average bolt shortening--vinyl primer and organix zinc with epoxy topcoat	119
77	Bolt force reduction specimen	121
78	Specimen 2-1 bolt relaxation	122
79	Unloading test of bolts	123
80	Specimen and plate dimensions	130
81	Shear force diagram	131

## List of Figures (cont.)

<u>Figure</u>	<u>Title</u>	<u>Page</u>
82	Fatigue testing setup	132
83	LVDT mount	134
84	LVDT and strain gage mount	135
85	Bolt tension histogram of fatigue specimens	138
86	Organic zinc specimen	139
87	Organic zinc/epoxy specimen	139
88	Inorganic zinc specimen	140
89	Fatigue test results	147
90	Previous fatigue test results	147
91	Filler plates	154
92	Idealized loads on bolts	154
93	Test specimen and instrumentation	156
94	Torqued tension tests	158
95	Single shear test	159
96	Load-deformation for 3 X 0.25 in. fillers	159
97	3 X 0.25 in. fillers--intermediate load	160
98	0.75 in. fillers--intermediate load	160
99	Summary of filler tests	162
100	Bolts after test failure	162
101	Effect of filler thickness on shear capacity	166
102	Plate failure modes in bolted lap splices	169
103	Connection types for bearing tests	169
104	Bearing critical test specimens	173
105	Test setup	173
106	Steel stress-strain	175
107	Failure modes	177
108	Stress-displacement curves, Test 8-H3-1	178
109	Stress-displacement curves, Test 6-H3-1	181
110	Stress-displacement curves, Test 8S-H3-1	182
111	Bearing deformation at slotted holes, Test 8S-H3-1	183
112	Stress-displacement curves, Test 6S-H3-2	185
113	Net section failure, slotted holes, Test 6S-H3-2	186
114	Stress-displacement curves, Test 8-H3-2	187
115	Effect of short edge distance, Load Stage 2	188
116	Stress-displacement curves, Test 6-H3-2	189
117	End tearout model	191
118	Effect of end distance, 8 in. wide plates	192
119	Effect of end distance, 6 in. wide plates	193
120	Effect of clamping force, 2 in. plates	195
121	Effect of clamping force, 8 in. plates	196
122	Effect of clamping force, 6 in. plates	197
123	Effect of slotted holes, 8 in. wide plates	199
124	Test data at ultimate load	201
125	Test data at 0.25 in. total deflection	202
126	Comparison: Ultimate load vs. 0.25 in. deflection	203
127	Typical load-deflection behavior	208
128	Compression test specimen	221
129	Creep test specimens	222
130	Test setup	223
131	Definition of slip load	226



## List of Tables

<u>Table</u>	<u>Title</u>	<u>Page</u>
1	Steel type factorial experiment	27
2	Paint thickness factorial experiment	27
3	Hole size factorial experiment	27
4	Steel type effect--blasted surfaces, 15/16 holes	30
5	Hole size effect --blasted surfaces, A572	30
6	Steel type effect--organic zinc, 15/16 holes, normal paint	37
7	Paint thickness effect--organic zinc, A572, 15/16 holes	37
8	Paint thickness effect--organic zinc, A514, 15/16 holes	38
9	Hole size effect--organic zinc, A572, normal paint	38
10	Hole size effect--organic zinc, A572, normal paint	39
11	Steel type effect--organic zinc with epoxy, 15/16 holes, normal paint	41
12	Paint thickness effect--organic zinc with epoxy, A572 15/16 holes	41
13	Paint thickness effect--organic zinc with epoxy, A514 15/16 holes	42
14	Hole size effect--organic zinc with epoxy, A572, normal paint	42
15	Steel type effect--inorganic zinc with vinyl, 15/16 holes, normal paint	44
16	Paint thickness effect--inorganic zinc with vinyl, A572, 15/16 holes	44
17	Paint thickness effect--inorganic zinc with vinyl, A514, 15/16 holes	45
18	Hole size effect--inorganic zinc with vinyl, A572, normal paint	45
19	Steel type effect--vinyl primer, 15/16 holes, 2.5 mil paint	47
20	Comparison of systems with vinyl top coat, A514, 15/16 holes	47
21	Summary -- all test results	49
22	Overall average slip coefficients	56
23	Average slip coefficients for inorganic zinc primer	60
24	Average slip coefficients for additional organic zinc primer	63
25	Effect of curing time on the slip coefficient, phenoxy zinc primer	64
26	Slip coefficients from tension test	69
27	Measured clamping force for 1/3 turns	73
28	Paint thickness and bolt shortening data	80
29	Test results, full-size specimens	84
30	Safety factor for different surface treatments	86
31	Allowable working stress, ksi, based upon surface condition of bolted parts, for friction-type shear connections	87
32	Allowable slip coefficients	89
33	Design recommendations for slip-critical shear connections	89

List of Tables (cont.)

<u>Table</u>	<u>Title</u>	<u>Page</u>
34	Average faying surface coating thickness for creep specimens	98
35	Slip coefficients for short-term loading	105
36	Creep specimen test arrangement	106
37	Slip, service, and allowable loads	106
38	Summary of average total creep deformations	108
39	Average bolt shortening of creep specimens	120
40	Compression creep tests	121
41	Post creep slip test results	124
42	Analysis of chain #1 organic zinc post creep slip tests	126
43	Testing program	128
44	Average paint thickness	136
45	Slip coefficients from control specimens	137
46	Test results--organic zinc specimens	141
47	Test results--organic zinc/epoxy top coat specimens	144
48	Test results--inorganic zinc specimens	146
49	Test results--blasted specimens	148
50	Mean ultimate bolt capacity in kips	157
51	Slip loads	163
52	Splice test summary	164
53	Factors of safety for deformation-limited loads	165
54	Material properties	174
55	Summary of bearing tests	200

## 1. INTRODUCTION

### Background

During the past twenty years a significant amount of research has been reported on high-strength bolted connections. In 1974, Fisher and Struik [15] coordinated and summarized the research available at that time into a guide to aid the development of reliable design procedures for bolted connections. Prior to this publication, the design methods and allowable bolt stresses had basically followed past recommendations for riveted construction with one principal exception. In high-strength bolted shear connections the load transfer between plate components is initially provided by the frictional forces developed by the high bolt clamping forces and the friction characteristics of the contact surfaces. A connection which relies on this slip resistance to transfer load is called a friction connection. When the slip resistance is exceeded, the connection slips into bearing to develop the bearing strength (bearing connection). Paints on the contact surfaces were prohibited in friction connections because some early tests showed they adversely affected the slip load.

The American Association of State Highway and Transportation Officials - Bridge Specification [2], hereinafter called AASHTO, requires all shear connections to be the friction-type except for compression members and secondary members. Since coatings were prohibited on the contact surfaces, the fabricator had to mask off the connection area, thus increasing the cost. In exposed environments, the unpainted contact surfaces resulted in crevice corrosion and a subsequent deterioration of the structural painting system. In some instances this corrosion caused separation of the plates and elongation of the fasteners. In 1975, a revision to AASHTO permitted hot-dip galvanizing, inorganic zinc-rich paints and metallized zinc or aluminum on the surfaces, following the recommendations of the Research Council on Structural Connections, RCSC [30]. This change was based on research which showed that these surface coatings provided slip resistance at least equivalent to a mill scale surface for which the allowable friction capacity was developed.

In 1976, the RCSC, based on the criteria developed by Fisher and Struik [15], adopted three major changes to its high-strength bolt specification, hereinafter called Bolt Spec, as follows:

1. The allowable friction strength was developed for nine different surface conditions, including organic zinc and vinyl wash paints based on a probability of slip concept.
2. The allowable shear capacity of a bearing connection was increased 36 percent to reflect the high strength of the connector.
3. The allowable bearing stress on plate material adjacent to the bolt was increased from  $1.35F_y$  to  $1.5F_u$ , where  $F_y$  is the yield strength

of the connected member and  $F_u$  is the ultimate strength.

These changes had considerable impact on bolted construction. Generally, fewer bolts would be required to transfer the required forces, and perhaps more importantly, the costly practice of masking connection surfaces could be eliminated. Also, the differences in slip resistance among various types of surfaces were recognized.

Many coatings and painting systems have been developed in the past twenty years which show significant improvement in corrosion protection. For example, vinyl is a high performance coating for use in corrosive environments and its life expectancy is fifteen years or more. Excellent epoxy coatings have also been developed. They are highly abrasion resistant and have excellent corrosion protective qualities. Their outdoor life is from fifteen to twenty years. A National Bureau of Standards (NBS) study of various systems to protect steel reinforcing bars found that powdered epoxy coating provided outstanding corrosion protection and satisfactory structural performance in reinforced concrete members [40].

The systems described above are not reflected in the RCSC recommendations, so their status for use on friction surfaces is unknown. Therefore, a research program was initiated to choose four superior coating systems and determine their suitability for the contact surfaces of friction joints. After the research was started, the program was broadened to include an evaluation of the 1976 Bolt Spec for use by AASHTO.

### Objectives and Scope

A statistically reliable (factorial) experimental program was developed to study the slip characteristics of four primary surface coatings. The effects of paint curing time, clamping force, steel strength, hole size, and paint thickness were considered. Since the program involved hundreds of slip experiments, a reliable slip test had to be developed. Creep and fatigue tests were also used to assess the suitability of the coatings for structural use. Some large multi-bolt connections were tested to evaluate the extrapolation of design recommendations based on small slip tests to more realistic applications. Consideration was also given to the possible difference between carefully controlled laboratory tests and joints constructed under typical field conditions. Based on the tests contained herein and those reported by others, design recommendations for friction joints are presented.

An evaluation of the provisions in the Bolt Spec for bearing connections indicated two areas where additional research was needed. First, some experimental evidence was needed on the effect of thickness of filler plates on the shear strength of high strength bolts. Second, data used to justify an increase in bearing stress from  $1.35F_y$  to  $1.5F_u$

did not consider the problem of high tension and high local bearing stress acting simultaneously. In addition, there are little data on the bearing strength of slotted holes. These problems were addressed by conducting tests on butt splices.

### Coating Systems

A survey was conducted to determine the coating systems to be used in the slip resistance studies. Literature was examined, paint experts and bridge maintenance engineers contacted, and recommendations established for protection of offshore structures were studied. The Structural Steel Painting Council (SSPC) was an excellent source for recommendations for particular corrosive environments.

The survey, which is discussed in detail elsewhere [16], developed four systems for the factorial experiment:

- (1) organic zinc-rich primer
- (2) organic zinc-rich primer with an epoxy topcoat
- (3) inorganic zinc-rich primer with a vinyl topcoat
- (4) vinyl primer with and without vinyl topcoat

According to present painting practice, topcoats are usually applied after erection. However, as painting technology advances, there will be a trend to shop-applied primer and single topcoat and one field coat or field-applied topcoat before erection. This was the main reason for selecting systems with topcoats in this study, since the present practice of masking-off the contact surfaces of the bolted friction joints when applying topcoats is costly. Also, previous research work on coated friction joints did not consider paint systems with topcoats on the contact surfaces. These selected systems have superior corrosion protection properties and are usually recommended for highway bridges and important steel structures.

It should be noted at this early stage of the report that current trends for protecting steel against corrosion involve paint systems at least 4 mils thick. The paint thickness on the faying surfaces of friction-type structural joints tested to date has been usually less than 1.5 mils, conforming to past painting practices. Therefore, for all the coating systems, a paint thickness of at least 3 mils is used on each plate in contact.

Discussions were held with paint manufacturers, highway department experts, and steel fabricators to obtain opinions on specific paint products, application of paints, surface preparation, field experience, paint film thickness measurement, and cost. Based on these discussions and the limited number of systems to be studied, it was decided to use paint products from a single manufacturer in the factorial experiment. This permitted the study of compatible primers and top coats. A

detailed discussion of the coatings used in the factorial experiment and some other coatings used in peripheral studies follows.

Organic Zinc-Rich Primer. Organic zinc-rich paints have a minimum zinc content of 80 percent by weight of the nonvolatile portion according to SSPC Specification (SSPC-PS 12.00-68T) [32]. Simply, they are an organic primer with large quantities of zinc dust. They require a near-white metal blast-cleaned surface for best results, and are usually applied in one coat with a minimum average dry film thickness of about 2-4 mils\* over the cleaned steel, according to the SSPC Specification. Compared with the inorganics, the organic coatings are generally more tolerant of variation in surface preparation quality. They tend to have better compatibility with topcoats and to be more flexible. The organic zinc paint was a modified phenoxy.

Organic zinc-rich paints are mainly intended for use under conditions of high humidity or marine atmospheric exposures and for fresh water immersion. They are commonly used on bridges in severe environments.

Current specifications and practice require at least a 3 mil thickness (Texas State Department of Highways and Public Transportation requirements are 3.5 mils minimum to 10 mils maximum). However, most of the friction-type joint tests which have been conducted up to the present time by other researchers used thicknesses which were less than 1.5 mils [15]. Thus, the effect of increased thickness on the friction characteristics is not known.

Organic Zinc-Rich Primer Plus Epoxy Topcoat. The epoxy polyamide widely used as a topcoat is a two-component system and is usually applied in one coat at a thickness of 3 to 6 mils. This coating is capable of providing long-term protection to steel surfaces in environments involving fresh or seawater immersion, tidal and splash zone exposure, condensation, burial in soil, and exposure to brine, crude oil, alkalis, chemical fumes, and chemical splashings.

The organic zinc-rich primer with an epoxy topcoat system has been used successfully for protecting offshore oil drilling platforms and is recommended by the American Petroleum Institute (API) for use on offshore structures. No friction-type joint tests have been conducted with this system on the faying surfaces of the joints.

Inorganic Zinc-Rich Primer plus Vinyl Topcoat. The inorganic zinc-rich primer must have a minimum zinc content of 75 percent by weight of the nonvolatile portion (SSPC-PS 12.00 6BT). Usually the coating is supplied with the zinc dust packaged separately to be mixed at the time of application with the inorganic vehicle, i.e., silicates,

---

\*Mil is a common term in the painting industry and will be used throughout this report (1 mil = 0.001 in. = 0.025 mm).

silicate esters, or phosphates. The primer used had a silicate vehicle. As in the case of organic zinc-rich primers, inorganic coatings have outstanding ability to withstand exposure to solvents, oils, and most petroleum products, and are very resistant to high humidity, splash, and spray. However, they are unsuitable for acidic or alkaline service without overcoating, and should be topcoated for prolonged continuous salt water exposure.

A high-build vinyl topcoat is suitable for fresh water immersion, industrial, rural, and marine atmospheres, and chemical exposures. It is applied at thicknesses of 3 to 5 mils in one coat. Generically, the topcoat used was a vinyl, copolymer.

The inorganic zinc-rich primer with a vinyl topcoat system is also recommended by the American Petroleum Institute in its corrosion specification.

The reason for selecting this system is to study the effect of the topcoat and its friction characteristics, since most of the previous research considered only the inorganic zinc-rich primer without a topcoat.

Vinyl System. The Steel Structures Painting Council recommends this system for highway bridges exposed mainly to fresh water. Vinyl paint systems are excellent for very severe exposures, including most chemical atmospheres, and are highly recommended for complete or alternate immersion in fresh or salt water, high humidity, and condensation, and exposure to the weather. Usually the vinyl system is required in three or four coats as a minimum, according to the severity of the exposure, and is applied with a dry film thickness of about 1.5 mils per coat. This system does not require as careful a surface preparation as systems described previously.

Joint tests have been conducted with faying surfaces treated with a vinyl wash (less than 1 mil thick). No tests have been conducted for thickness approaching the recommended values. In this research, both a vinyl primer (a modified vinyl-alkyd) applied in two coats and a vinyl primer applied in two coats with a vinyl topcoat were studied. Thickness ranges from 3 mils for the former system to 6 mils for the latter system (all vinyl system).

Other Coatings. (1) Powder Epoxy System. Initially, a powder epoxy was selected as one of the main systems in this study, since epoxies proved to be the best performers in the rebar study conducted by NBS [40]. Preliminary tests on specimens coated with a powder epoxy product that was an approved AASHTO coating for steel reinforcing bars gave slip coefficients which were too small to provide a reasonable shear strength in a friction-type bolted joint. Thus, powdered epoxy was eliminated from being one of the main coating systems extensively tested in this research work and only a few tests were conducted.

(2) Inorganic Zinc Primers. Previous research has established that inorganic zinc-rich primers sprayed on a blasted surface give a slip resistance slightly superior to a blasted surface [15]. Some tests were conducted with inorganic zinc used in the factorial experiment described previously for determining the curing time. A different primer from the same manufacturer but with reduced zinc content (75 percent rather than 80 percent) was used in a study to determine the effect of zinc content on slip resistance.

(3) Organic Zinc Primers. The Bolt Spec categorized coatings into broad classes only by paint type, e.g., organic zinc. In order to check the scatter within a category, two other organic zinc primers were tested. Both primers were manufactured by the same company but they had different vehicles, an epoxy resin and a phenoxy. The epoxy zinc-rich was a three-component paint and the phenoxy zinc-rich had a single component. Both primers satisfied the SSPC Specification for organic zinc-rich paints.

### Preface

In the following chapters the results of the research are presented. Because of the wide variation in subject matter, there is generally a summary at the end of each chapter. In Chapter 2, experimental methods throughout the study are documented. In Chapter 3, all the tests related to the slip resistance of joints, including the factorial experiment, tension slip tests, and full size truss joints, are presented. The shear creep studies up to one year duration are reported in Chapter 4, and the fatigue tests in Chapter 5. Chapters 6 and 7 document the ultimate strength tests on bolts in butt splices with undeveloped fillers and the strength of bearing critical connections. An overview of the entire project is given in the last chapter.



## 2. EXPERIMENTAL METHODS

### Slip Test Arrangement

Because of the large number of slip tests required, the test setup was designed to keep testing time and specimen fabrication to a minimum. The compression-type slip setup shown in Figure 1a accomplished these goals. This setup requires three plates with the same hole pattern. The shearing load is applied directly to the specimen without the use of the additional end fixtures usually required for the tension arrangement shown in Figure 1b. Hechtman [20] reported slip tests using both the tension and compression arrangements which showed that the compression setup produced slightly higher mean slip resistance compared to the tension setup (12 percent for millscale surfaces). However, Hechtman attributed this difference to normal scatter in the test results, which are approximately 10 percent of the mean.

It has been reasoned that in a compression-type slip test the Poisson's ratio effect may lead to an increase in the bolt force and consequently an increase in the slip load [15]. This objection was eliminated in the test setup shown in Figure 2, where the clamping force is applied by means of a high-strength steel rod acting with a center-hole hydraulic jack. A threaded rod passes through a centerhole ram and is locked in position by nuts at both ends. Oil pressure is applied to the ram, which forces the drilled nut (a 7/8 (22mm) 2H nut with the threads drilled out so it can slip along the threaded rod) against the connection plate. The drilled nut provides the same plate contact area as a bolt. Oil pressure is increased until the desired clamping force is reached. The clamping force was measured by the 50 kip (222 kN) load cell. The arrangement maintained the clamping force, thus eliminating the problem of bolt variations and calibrations. Two different clamping forces were applied in the study: 39 kips (173 kN) and 49 kips (218 kN). They represented the minimum tension required from a 7/8 in. (22mm) ASTM A325 and A490 high-strength bolts, respectively. A somewhat similar "hydraulic bolt" setup was used in a bolt test in Japan [27].

The whole arrangement was placed on the load table of a hydraulic testing machine. The two outer specimen plates rested on a specially machined and hardened circular steel base plate, as shown in Figure 3. The base plate transmitted the applied load from the specimen to a 100-kip (445 kN) centerhole load cell, resting directly on the load table of the testing machine. A wooden frame supported the hydraulic jack and was placed on the load table of the testing machine. The frame had four screws for horizontal adjustment of the setup and to provide ease in aligning the specimen.

Two electrical deflection gages (DCDT) were used to measure the slip. The gages were supported by aluminum holders attached by epoxy to the base plate on which the two lap plates of the specimen rested. The two plungers of the deflection gages bore against the head of brass

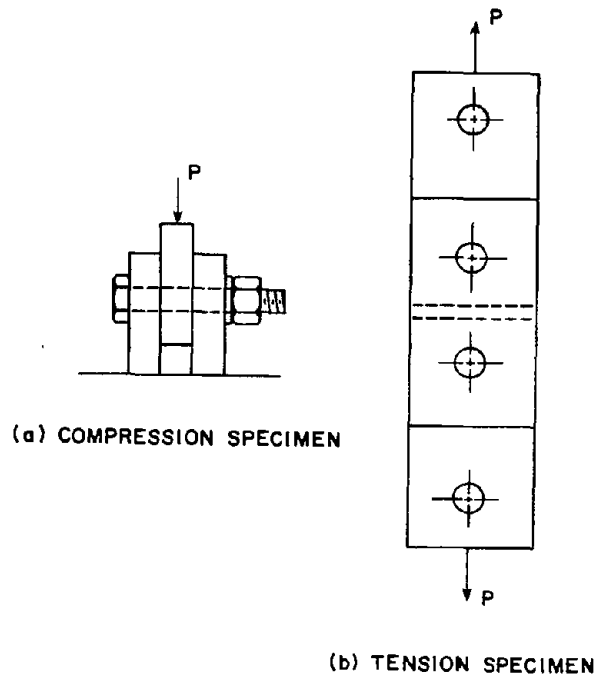


Figure 1. Schematic of test specimens

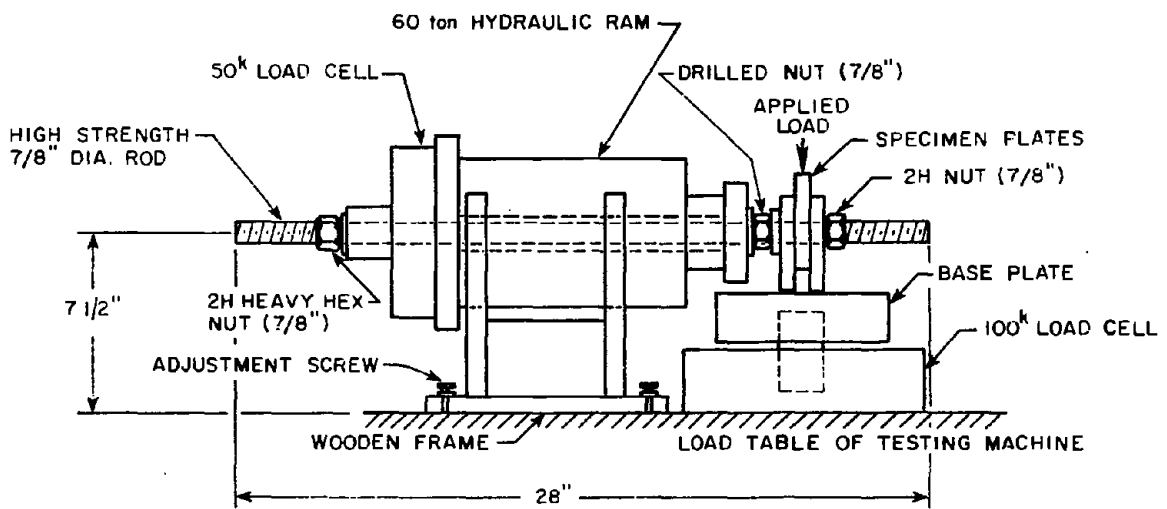


Figure 2. Test setup schematic

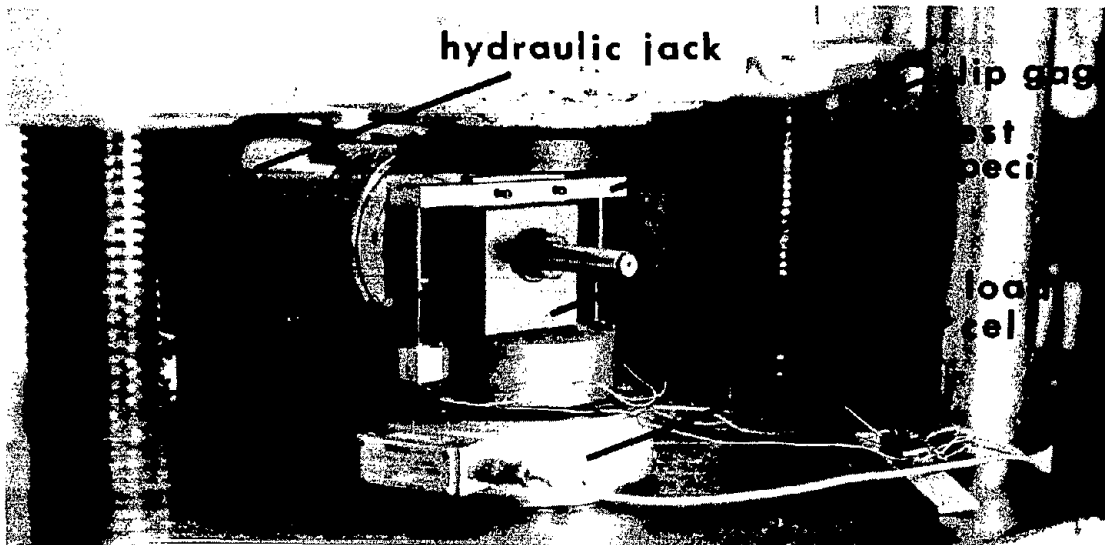


Figure 3. Compression slip test setup

thumb screws connected to an aluminum fixture that could be mounted and dismantled easily on the middle plate of the specimen by means of screws. The DCDT measured the relative movement between the middle specimen plate and the base plate. The outputs from the 100 kip (445 kN) load cell and the DCDT's were attached to an X-Y plotter. A voltmeter attached to the DCDT output was used to monitor the rate of slip, since a reasonably constant rate was desired.

#### Slip Specimens

Pilot tests were conducted to establish the influence of specimen plate size on the slip load. Tests were performed on clean millscale specimens and on blast-cleaned specimens. Two specimen sizes were considered: a 4 × 4 in. (102mm × 102mm) and a 5 × 6 in. (127 × 152 mm) specimen size.

The test setup performed very well and the results of the slip tests were evaluated and found to give values which were consistent with the work of other researchers. Results of the 4 in. (102mm) and 5 in. (127mm) specimens were compared and were found to be almost identical (mean slip load of 47.4 kips (211 kN) vs. 50.1 kips (223 kN), respectively, for sandblasted clean surfaces). The contact areas for both specimen sizes were measured after testing and they were about the same. The 4 in. (102mm) specimen, as shown in Figure 4, was chosen, since the contact was generally within 1 in. (25mm) from the edge of the hole and not close to the end of the plate.

A specimen consisted of three identical plates which were bolted up by a steel rod 7/8 in. (22 mm) in diameter using the test setup.

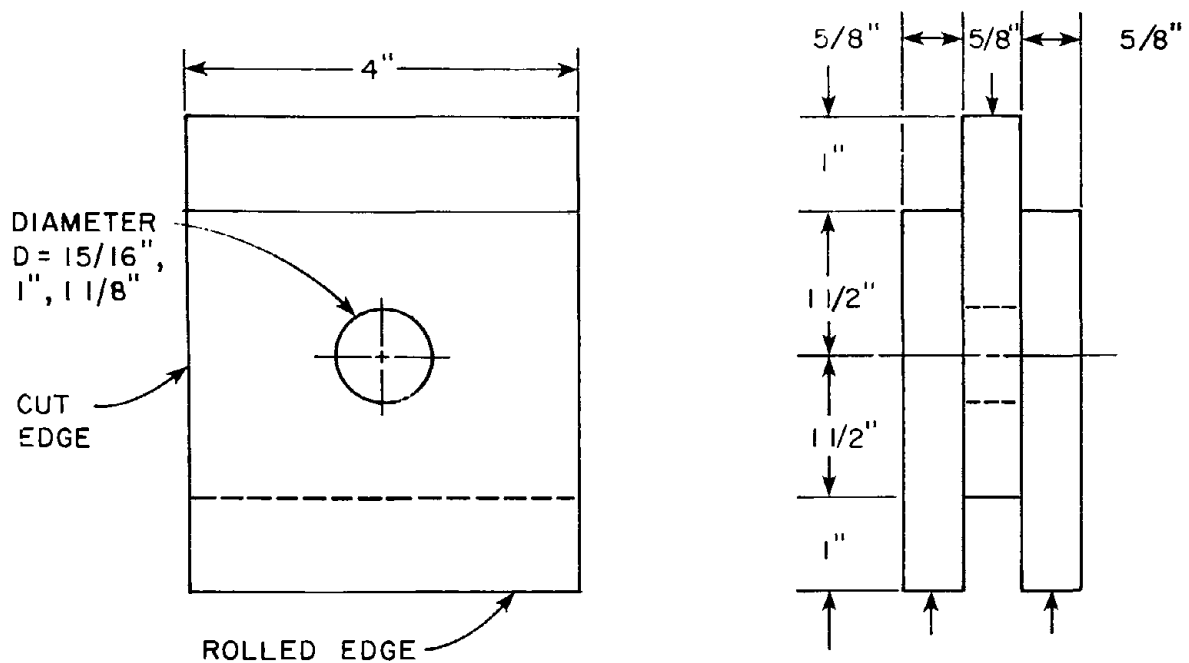


Figure 4. Slip test specimen (1 in. = 25.4 mm)

The clearance in the holes was either 1/16 in. (1.6mm) standard, 1/8 in. (3.2mm), or 1/4 in. (6.4mm) oversize holes. The joints were fabricated from three types of steel: A36, A572, and A514. The three steel types were cut from plates 5/8 in. (15.9mm) thick, 4 in. (102mm) wide, and 20 ft (6.1m) long. Each plate length was cut into square plates 4 in.  $\times$  4 in. (102  $\times$  102 mm) using a power hacksaw, and the sharp cut edges were filed. Three square plates which formed a specimen were chosen from the same plate length, and an identifying number was punched on the edge of the plates. Each group of three plates forming a specimen was aligned and clamped together in a vice prior to drilling. Then, a pilot hole 3/8 in. (10mm) in diameter was drilled through them in one operation. The required holes were then drilled through each plate separately. This operation was repeated for every specimen and assured proper alignment of holes. The edges of the drilled holes were slightly countersunk to remove burrs. During all the phases of fabrication, the steel was in the as-received millscale surface condition.

#### Paint Thickness Measurement

The paint film thickness was one of the important variables considered in this research study. Three instruments were used for measuring the film thickness in this research study. A brief description of the three film thickness gages is given below. The principle of their operation is given elsewhere [32].

(1) Tooke Gage. This is a scratch-type gage which is slightly destructive. It operates on the principle of cutting the coating film

at a predetermined angle, normally 45°, magnifying the view of the cut, and comparing the cut edge of film to a calibrated scale viewed in the eyepiece (see Figure 5).

(2) Mikrotest Gage. It is a nondestructive magnetic gage used only to measure nonmagnetic coatings on ferrous material. The Mikrotest utilizes one contact probe and measures the magnetic force between this probe and a ferrous surface by means of a calibrated spring.

(3) Prong Gage (wet thickness). As shown in Figure 5, the two outside prongs of the gage form a reference plane. The inner prongs are machined to various distance variations from this reference plane. The distance or gap between the prongs and reference plane is marked on the prongs in mils. To determine wet film thickness with the prong-type gage, both side prongs are pressed firmly against the plate surface while maintaining the gage perpendicular to the surface. The last tip of the measuring prongs that is coated with paint indicates the wet thickness.

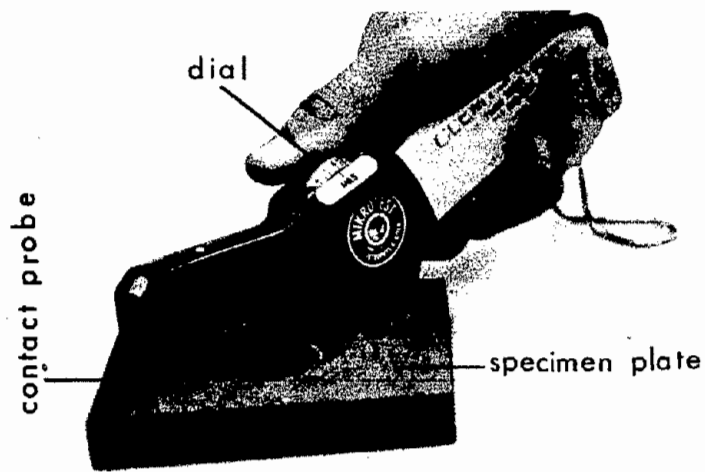
The three paint film-thickness gages were used extensively throughout this research study. The wet film-thickness gage (prong gage) was used during the painting process to determine the spraying speed that provided the desired wet film thickness. It was not used on the specimen plates but on control panels mentioned in the next section.

The Mikrotest gage was used to measure the paint thickness of the cured specimens. Usually eight readings were taken for each plate (four on each side) or twenty-four readings per specimen. These readings were recorded for every specimen, and were the basis for selecting the plate sides which were to be in contact. Sides which showed less variations in the Mikrotest gage readings and at the same time had an average thickness closer to the desired dry film thickness were chosen to be in contact.

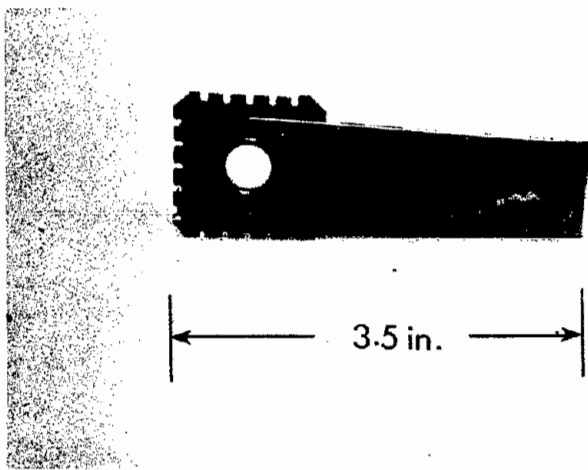
The Tooke gage was used primarily to check the Mikrotest readings. Specimens were randomly chosen for the check. The scratch was made near the edges of the specimen plates in order not to disturb the actual contact surfaces. The Tooke gage was also used to measure the thickness at particular points marked on the painted control panels, which were already measured by the Mikrotest gage, in order to check the calibration of the Mikrotest gage. The results of both gages were always consistent, so only results of the Mikrotest gage are reported herein.

### Painting Procedure

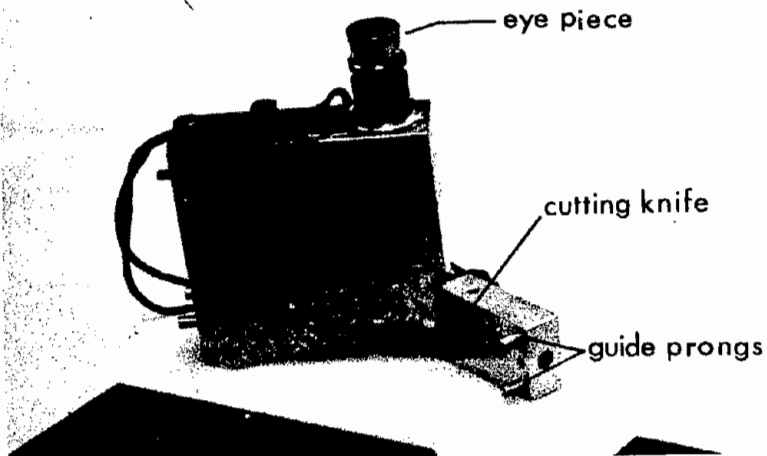
Specimens were sandblasted at a local sandblasting shop. The steel surfaces were specified to be blast-cleaned to a white metal finish by dry sandblasting and meeting the requirements of the SSPC-SP5-63 [32]. Each group consisted of twenty to thirty specimens; some were to be painted by one of the selected coating systems, and the



Mikrotest gage



Prong gage



Tooke gage

rest were used as control test specimens with blast-cleaned surfaces. Usually, for every ten specimens there were four control specimens.

After the specimens were brought back from the sandblasting shop, all surfaces were cleaned with acetone to remove any sand particles or dust, and were then ready for painting. The surface roughness of the control specimens was studied using the Keane-Tator surface comparator. Usually the sandblasted control specimens were tested within a week from sandblasting.

All painting was done in the laboratory according to the paint manufacturer's as well as painting experts' recommendations. A spray gun and a pressure cup were used for all the painting. Figure 6 shows the racks which were built to control overspraying of the specimens and to minimize surface disturbance of the painted surfaces. Directly before every painting of a group of specimens, several cold formed steel panels with smooth surfaces were used for practice spraying in order to achieve a good spraying pattern, and to develop a spraying tempo which would give the required wet film thickness determined by the prong gage. Under these laboratory conditions, a coat could be applied to a dry film tolerance of  $\pm 1$  mil. Some of the steel panels were also placed on the racks with the specimens so that the dry film thickness could be measured using a destructive paint-measuring device (Tooke gage) for comparison with the magnetic gage. Utilizing the percent solids of each paint, the necessary wet film thickness could be judged to provide the desired film thickness. A dry film thickness of 3 mils per coat at most was used, based upon recommendations from paint experts.

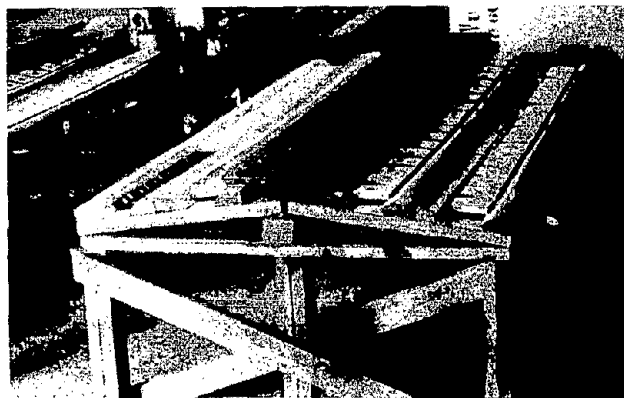


Figure 6. Painting racks

The curing time between the application of one coat and another was usually 24 hours (minimum time specified by paint manufacturers was usually less than that). However, if the specimens were to be topcoated, the primer was left to cure for a particular number of days, based on the curing tests discussed in this chapter. After all the coats were

applied, the specimens were placed in an air conditioned room (at room temperature) to cure before testing. The inorganic zinc-rich paint required a humid atmosphere to cure well. Thus, the painted specimens were covered by wet burlap (at least one hour after painting) to provide the recommended atmosphere.

#### Slip Test Procedure

Individual specimen plates were assembled so that the coated surfaces which showed the smallest variation in thickness and were close to the desired thickness would be placed in contact. The specimen was inserted into the hydraulic bolt setup shown in Figure 3 and aligned in the test machine to minimize eccentricities. A spherical head on the test machine ensured uniform compression along the edge of the plate. The slip gage shown in Figure 3 was attached and the DCDT's located on each side of the specimen were connected to give the average of two readings. The gages measured the relative displacement (slip) between the interior connection plate and the two side plates. The arrangement shown includes the axial deformation of plates in the slip measurement, but it is very small compared to the slip. The specimen was checked to make sure the plates were not bearing on the hydraulic bolt prior to the application of the clamping force. The clamping force was measured by a load cell and checked by pressure gages on the hydraulic pump.

The slip and the load applied to the specimen were plotted automatically using an X-Y recorder. The applied loading rate was approximately 25 kips (111 kN) per minute or 0.003 in. (0.076 mm) of slip per minute. The test was terminated when a total slip reached approximately 1/16 in. (1.6 mm), the nominal hole clearance.

Pilot tests indicated that the rate of slip (or deformation) has an effect on the slip coefficient for some paints. Thus, it was decided to conduct all the slip tests at the rate of 3 mils per minute to achieve fair comparisons of slip coefficient and to minimize the influence of the operator on the shape of the load-slip curves. The rate of 3 mils/min was chosen because of its practicality, since a test could be conducted within a reasonable amount of time (less than 20 minutes). In recent research conducted in Australia (1977) [33], slip tests were performed using displacement as a control parameter. The loading rate (slip rate) was 10 mils/min, which is about three times faster than the rate used in the research described herein.

The slip load was determined from the connection load-deflection plot, some typical types of which are shown in Figure 7. The slip load was recorded as one of the following:

- (a) The maximum load provided this maximum occurred before a total slip of 0.020 in. (0.51mm) occurred.



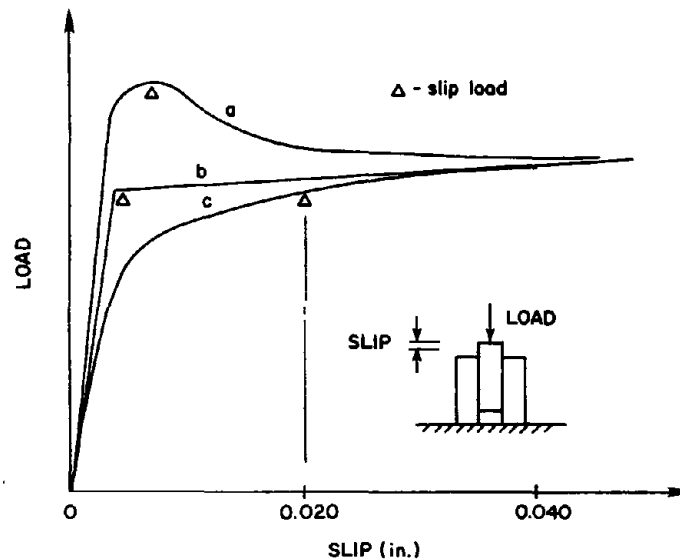


Figure 7. Definition of slip load

- (b) The load at which the deflection rate suddenly increases, typically as shown in curve b.
- (c) The load measured when the slip is 0.020 in. (0.51mm). This definition controls when the load-deflection curves show a gradual change in response, as shown by curve c.

The experimental slip coefficient  $k_s$  is calculated as

$$k_s = \frac{\text{slip load}}{\text{clamping force} \times \text{number of slip planes}} \quad (1)$$

#### Paint Curing Time

Preliminary slip tests at an early stage in the research indicated that time lapse between painting and testing was a significant parameter. Since this was not considered in the basic factorial experiment, a series of slip tests was conducted to determine the time required for the paint to cure. The drying time for a coating system, as specified by paint manufacturers, is intended only for handling and recoating purposes and does not imply curing of the paint.

For each paint system in the factorial experiment, from six to ten specimens were painted at the same time. One or two slip tests were conducted at different intervals, so that the relationship between  $k_s$  and curing time could be determined. In each case the individual plates cured in the unassembled state until testing.

Organic Zinc-Rich Primer. Eight slip specimens of A36 steel with 15/16 in. (24mm) diameter holes were painted with two coats of organic zinc-rich paint with an average dry film thickness of 5 mils. A one day interval was used between coats. The individual plates were cured at room temperature before they were clamped together for testing. Specimens were then tested, two at a time, after 3, 5, 7, and 9 days curing, respectively.

A summary of the observed slip coefficients as a function of the curing time is shown in Figure 8. In the figure, slip coefficients after 36 days were obtained from another set of specimens, A36 steel and 15/16 in. (24mm) diameter holes, which were coated at a different time. The dashed line is drawn through the average  $k$  at 36 days. These two slip coefficients were used in determining the  $s$  required curing period, since it was felt that the data available up to 9 days curing alone was not sufficient to establish a reliable curing period. The general trend of Figure 8 indicates that a 9-day period will be sufficient for the organic zinc-rich primer to cure.

Organic Zinc-Rich Primer with an Epoxy Topcoat. Fourteen slip specimens of A36 steel with 15/16 in. (24mm) diameter holes were painted with two coats of organic zinc-rich primer with an average total dry film thickness of 6.5 mils. The specimens were left to cure at room temperature for 9 days, as indicated in the previous section, and then were topcoated by an epoxy polyamide paint with an average dry film thickness of 2.5 mils. The specimens were tested two at a time after 5, 9, 12, and 18 days curing, respectively, and the results are shown in Figure 9. The remaining six specimens were tested after 44 days, and yielded an average slip coefficient which was the same as that for 18 days, so that data are not shown. It was concluded that a 9-day primer cure followed by a 7-day curing period for the topcoat would be sufficient to cure the specimens prior to testing.

Inorganic Zinc-Rich Primer. Ten specimens of A572 steel with 1 in. (25mm) diameter holes were coated with two coats of inorganic zinc-rich paint, with a total average dry film thickness of 6 mils. The specimens were tested two at a time, after 3, 5, 7, 9, and 11 days curing, respectively. Comparing the average slip coefficients in Figure 10, obtained at different testing days, it was found that the average slip coefficient at 3 days is approximately equal to that at 11 days. A 3-day curing period was chosen before applying a topcoat.

Inorganic Zinc-Rich Primer with a Vinyl Topcoat. Ten slip specimens of A36 steel with 15/16 in. (24mm) diameter holes were painted with two coats of inorganic zinc-rich paint with a dry film thickness of 7 mils. The specimens were left to cure at room temperature for 3 days (as indicated in the previous section) and then were topcoated by a vinyl paint with an average dry film thickness of 2 mils. The specimens were tested after 9, 11, 14, 16, 20, and 26 days curing, respectively.

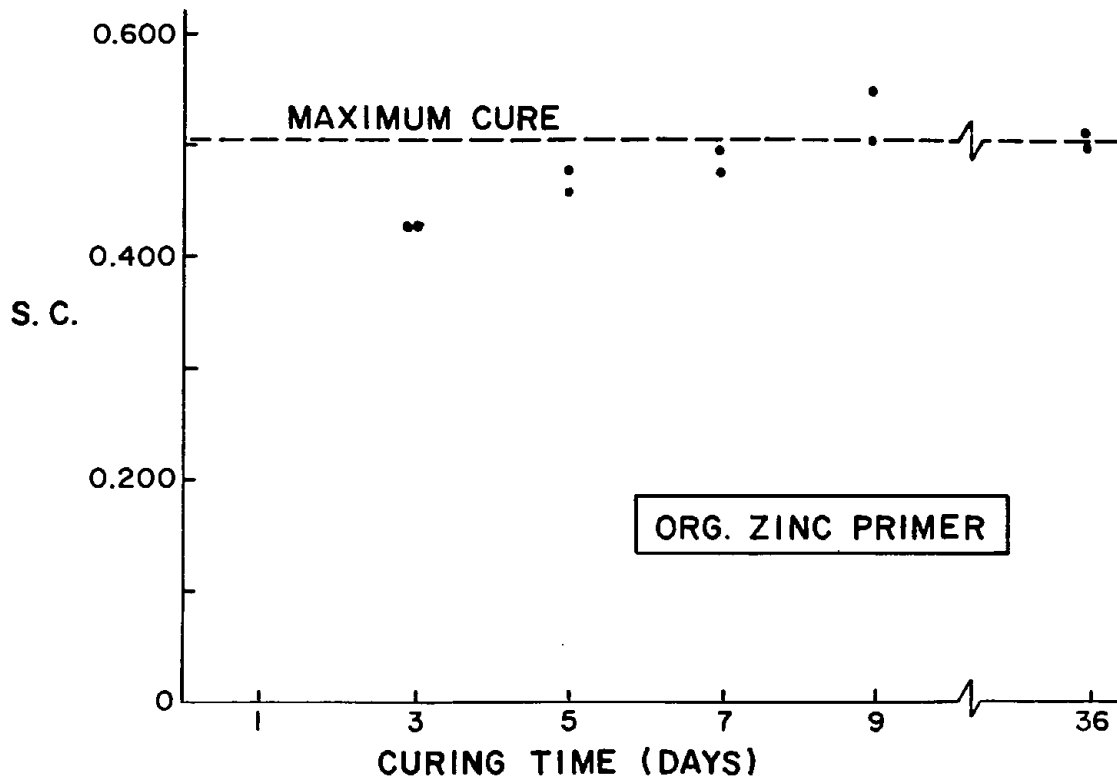


Figure 8. Comparison of slip coefficients

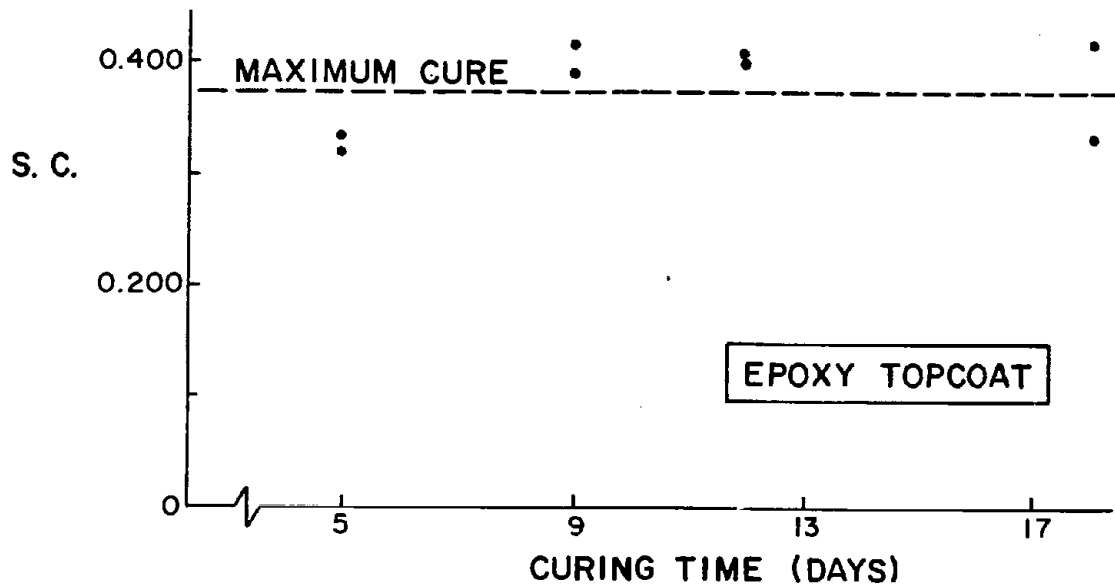


Figure 9. Comparison of slip coefficients

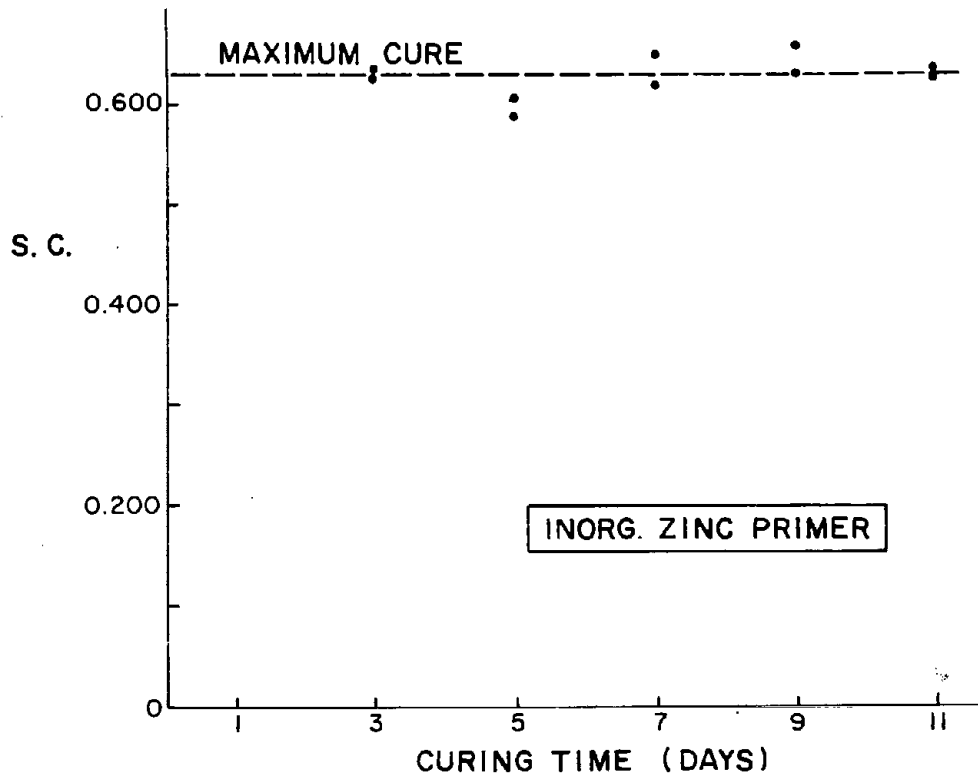


Figure 10. Comparison of slip coefficients

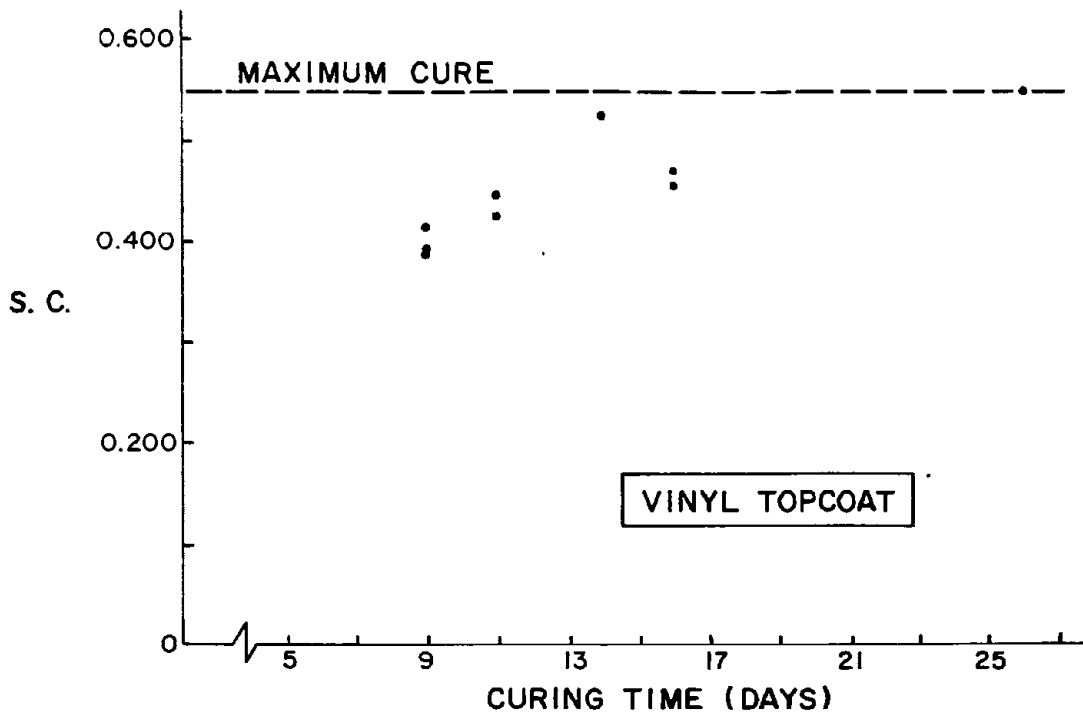


Figure 11. Comparison of slip coefficients

Figure 11 summarizes the results of the tests. The slip coefficients show significant scatter with time. Slip coefficients obtained at 16 days are low for some reason. Slip coefficients at 14 and 20 days are higher than those at 16 days. It was concluded that a 3-day primer cure followed by an 18-day curing period for the vinyl coat was sufficient to cure the specimens before testing.

Vinyl Primer. Six slip specimens of A572 steel with 15/16 in. (24mm) diameter holes painted with four coats of the vinyl primer with a final average dry film thickness of 4 mils were tested after 17, 19, and 21 days curing, because of the long curing time required for the vinyl topcoat in the previous section.

Figure 12, which summarizes the observed slip coefficients as a function of the curing time, indicates that curing time did not affect the slip coefficient for the time interval chosen. However, no tests were conducted on specimens with less than 17 days curing, so the minimum curing time could not be established. Because of time constraints, the experiment could not be repeated so a 17-day time interval was chosen for the curing period.

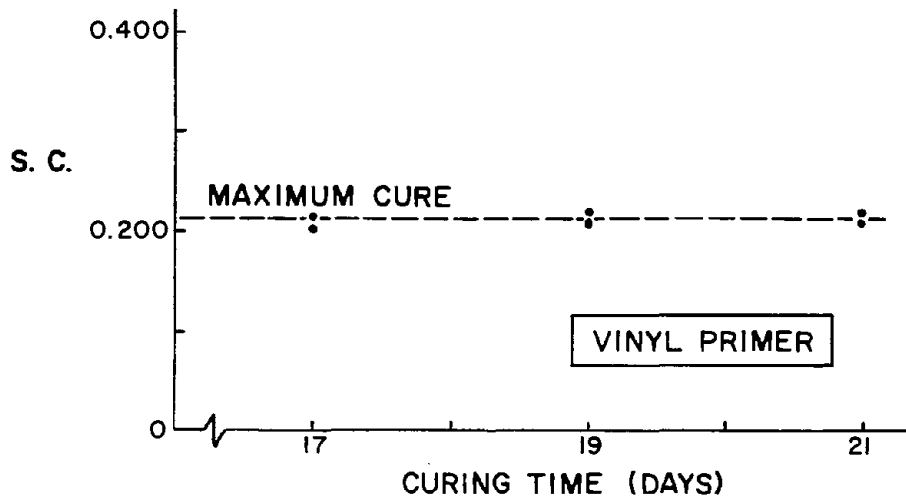


Figure 12. Comparison of slip coefficients

Summary. Slip tests were conducted to determine the reasonable time limit during which the painted faying surfaces should be left unclamped in order to allow for paint curing. The curing period would ensure that the effect of incomplete paint curing on the test results is reduced to a practical minimum.

The following listing gives the minimum curing time used for each coating system:

<u>Coating System</u>	<u>Minimum Curing Time (days)</u>
1. Organic zinc-rich primer	9
2. Organic zinc-rich primer + epoxy topcoat	9 + 7
3. Inorganic zinc-rich primer	3
4. Inorganic zinc-rich primer + vinyl topcoat	3 + 18
5. Vinyl primer	17

### Bolt Tests

High-strength bolts were used in many aspects of this research. Some slip tests were performed with real bolts, and the creep, fatigue, filler and bearing portions all used high-strength bolts. In general, the bolt and nut threads were measured to establish their compliance with the American National Standards Institute (ANSI) specification [4]. The tensile strength of each bolt lot was determined by testing three bolts in torqued tension (usually called bolt calibration). In some instances, direct tension tests of the bolts were also conducted.

Bolt Calibration (Torqued-Tension Test). The purpose of a bolt calibration is to develop a relationship between the tension developed in a bolt as it is tightened in a normal fashion by turning the nut and the elongation of the bolt. This relationship can then be used to determine the actual tension (clamping force) in an installed bolt from the same lot if the elongation is known.

The calibrations were achieved by utilizing a Skidmore Wilhelm load indicating device, as shown in Figure 13. Actual specimen conditions were duplicated by fabricating a small insert into the back side of the Skidmore Wilhelm, causing the bolts being calibrated to experience identical grip lengths. Prior to any bolt calibrations, the Skidmore Wilhelm (SW) was checked for accuracy against a 120-kip (534 kN) testing machine. Usually, the SW readings were 1 kip (4.45 kN) low, so adjustments were made to the data. All bolts were machined flat on each end and were center-drilled with a 1/8 in. (3.2mm) 60° countersink drill. Bolt elongations were measured utilizing a specially designed C-frame mounted with a dial gage capable of measuring to 0.0001 in. (0.0025 mm) (see Figure 14). A diagram of the contact points with the countersunk hole in the bolt is provided in Figure 15. The bolt elongation measurements were found to be repeatable to within  $\pm 0.0001$  in. (0.0025 mm).

The calibration procedure was as follows. The bolt was placed in the Skidmore Wilhelm calibrator, with the nut tightened to a finger-tight position on the front side. An initial reading was taken of the

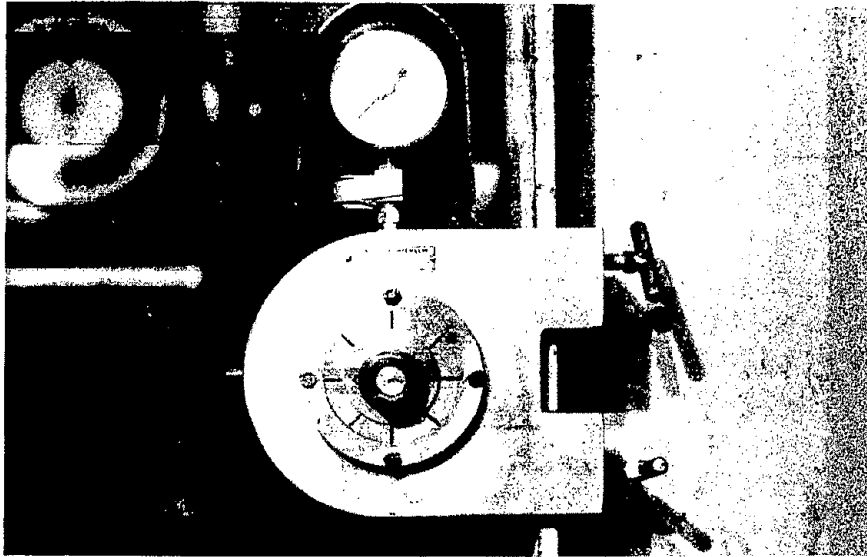


Figure 13. Skidmore-Wilhelm bolt calibrator

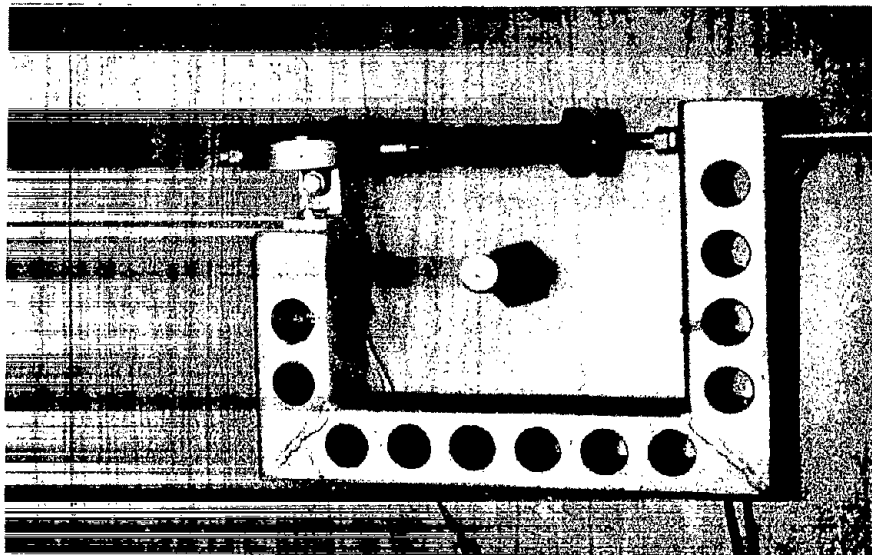


Figure 14. C-frame extensometer

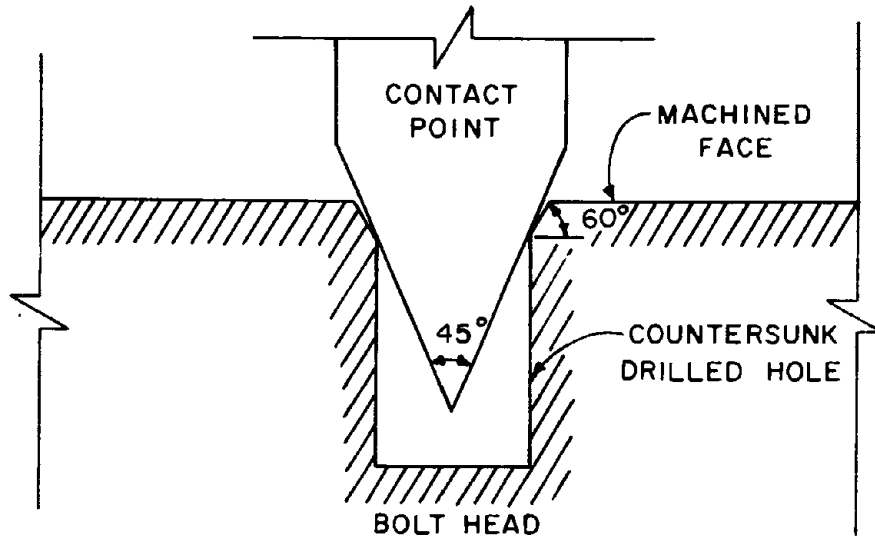


Figure 15. Contact point fit with countersunk hole

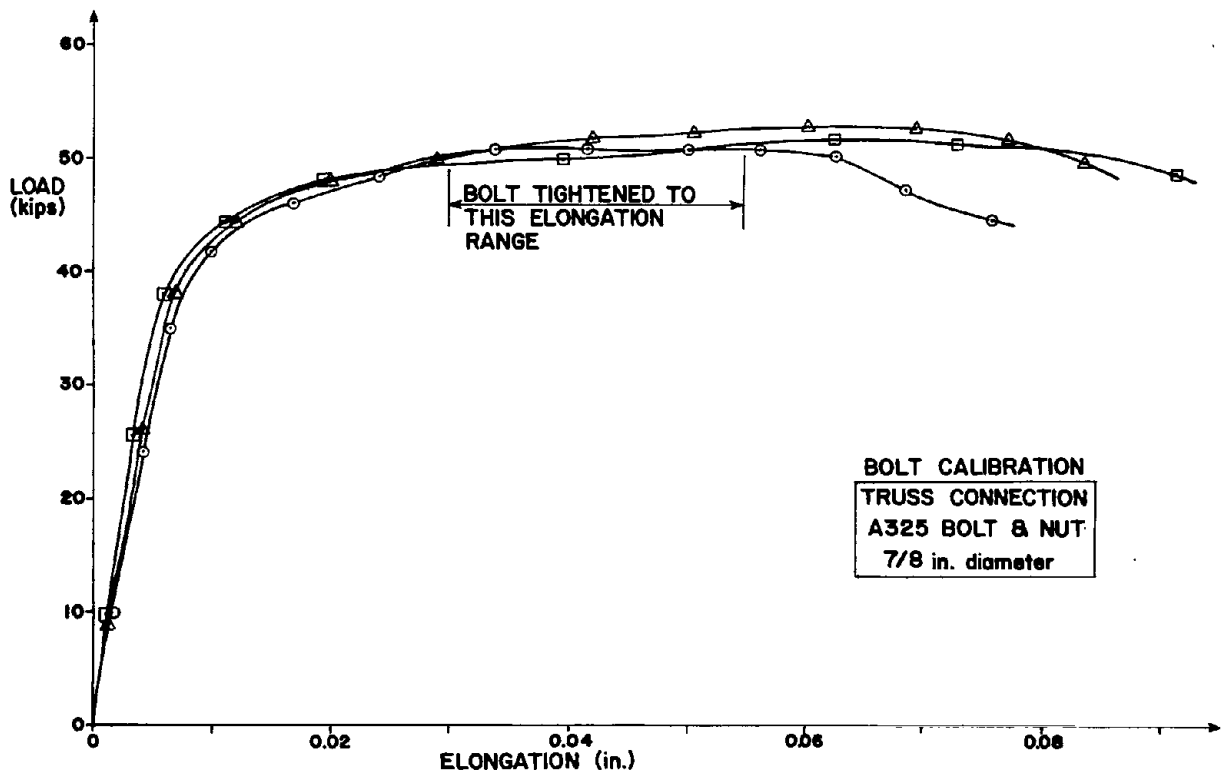


Figure 16. Typical bolt calibration curves  
(1 in. = 25.4 mm, 1 kip = 4.45 kN)



length of the bolt. The bolt was tightened to a snug position that corresponded to a load of 8 kips (36 kN) while holding the bolt head. This load was reached by using a hand wrench and reading directly from the calibrator. Three elongation measurements using the C-frame were taken immediately after reaching this load, and the average was used to compute the elongation experienced by the bolt. A pneumatic impact wrench was utilized to turn the bolt after the snugging, using a hand-held wrench to hold the opposite end. The nut was turned in stages of 1/8 of a turn to failure, reading the load corresponding to each stage from the calibrator. Measurements of elongation were taken at each stage similar to the snug tight position described above. Results of each calibration were plotted on a load versus elongation curve.

Three bolt calibrations from the bolt lot used for the truss-type connections discussed in Chapter 3 are given in Figure 16. Initially, the bolts follow an elastic response and then the load is almost constant over a wide range of deformation. This factor was utilized in developing bolt installation procedures for the test specimens. It was desirable to keep the scatter in bolt tension to a minimum so consistent clamping force could be developed among various specimens. The bolt calibration curves were used to define a range of bolt elongations over which the bolt tension could be considered constant. It is assumed that the average of three bolts represented the entire lot. This simplified the installation of the bolts. For the curves shown in Figure 15, a nut turned 3/4 turns from snug would give bolt elongations near the midpoint of the flat range. Once the bolt was installed, the actual bolt tension reported herein is always based on the actual elongations measured and the average of the three calibrations at that elongation. In instances where bolt relaxation was monitored (bolt unloading due to factors such as creep), it was assumed that the bolt unloaded elastically following the slope of the initial portion of the load-elongation curves.

Direct Tension Test. The bolt to be tested was placed in the direct tension rig shown in Figure 17 to produce the desired grip. After the desired grip was established a washer was placed under the nut and the nut was hand tightened onto the bolt. The bolt was then loaded slowly and continuously until the ultimate load was reached.

#### Surface Roughness Measurement

The surface roughness or, in other words, the anchor pattern profile depth of the sandblasted surfaces was determined using the Keane-Tator Surface Profile Comparator shown in Figure 18. It consists of a reference disc and a magnifier with a magnetic disc holder. The reference disc is composed of five sections, each with a different anchor pattern depth which is marked in mils (0.001 in. = 0.0254 mm). The comparator disc was used as a visual as well as a tactile reference. As a visual reference, the disc was centered on the bottom of the magnifier and then the magnifier placed on the sandblasted surface. The reference

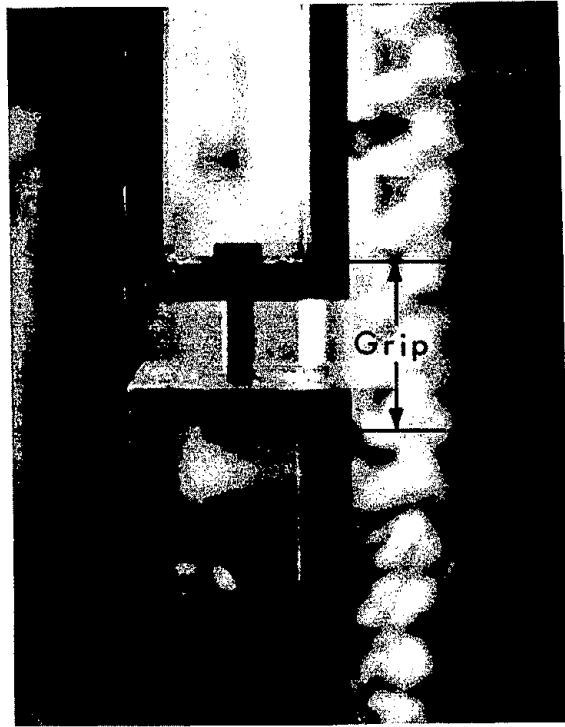


Figure 17. Direct tension tests

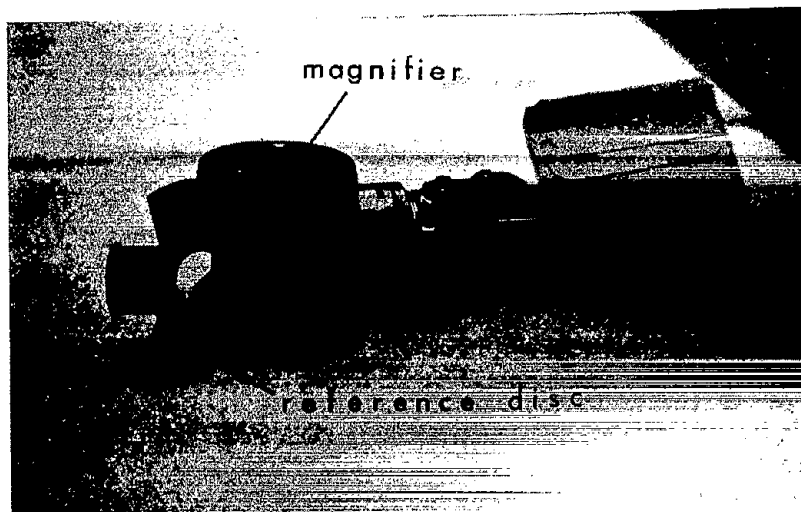


Figure 18. The Keane-Tator surface profile comparator

section most closely approaching the roughness of the sandblast was selected. Comparing the sandblasted surface in the "v" notch separating two reference segments usually provided a greater accuracy. As a tactile reference, the roughness of the sandblasted surface as felt by one's fingertip, or a plastic card, was compared with the roughness of a segment on the comparator disc. The surface roughness was measured for the three plates of a specimen. Two readings for each plate were recorded, each representing the roughness of one of the plate's sides. Based on these readings, the specimen's plates were so arranged that the average roughness for the contact surfaces was about the same. The average surface roughness of a specimen as reported was calculated by averaging the roughness of the four surfaces in contact.

### 3. SLIP TESTS

The results of the various slip tests are presented in this chapter. The principal data are from the large factorial experiment using the hydraulic bolt test setup. More than 400 slip tests on connections with painted contact surfaces and another 77 on blasted surfaces are summarized. Additional studies are reported on the effect of zinc content of paint and variations among organic zinc-rich paints on the market. Some tension-type slip tests as shown in Figure 1 were conducted to compare with the hydraulic bolt data. A number of large truss type shear joints were tested to assess the reliability of using small joint slip coefficients in determining the slip load of large bolted joints. Design recommendations for friction-type bolted connections are given at the end of the chapter.

#### Factorial Slip Study

The experiment design was a factorial design. This will allow a statistical analysis of the results and provide a firm basis for the design specification recommendations. In its simplest form, a factorial experiment is one in which all levels of a given factor (variable) are combined with all the levels of every other factor in the experiment. It should be pointed out that a factorial experiment design is more efficient than a one-factor-at-a-time experiment, since it requires a smaller number of tests to be performed. Also, in a factorial experiment design, some information is gleaned on possible interaction between the variables considered in the experiment.

The effect of the following variables on the slip behavior of friction-type bolted joints with coated contact surfaces was the main concern of this research.

- (1) Three types of steel: A36,  $F_y = 36$  ksi (248 MPa); A572,  $F_y = 50$  ksi (345 MPa); A514,  $F_y = 100$  ksi (690 MPa)
- (2) Three hole sizes for a 7/8-in. (22mm) fastener: Standard diameter = 15/16 in. (24mm), oversize diameter = 1 in. (25mm), oversize diameter = 1-1/8 in. (29mm)
- (3) Two magnitudes of clamping force: 39 kips (174 kN) and 49 kips (218 kN), corresponding to the minimum specified clamping forces for 7/8 in. (22mm) and A325 and A490 bolts, respectively
- (4) Four paint systems as described in Chapter 1
- (5) Three paint thicknesses on each plate in contact: thin (~ 3 mils), normal (~ 6 mils), and thick (~ 9 mils)

Only one fastener size, 7/8 in. (22mm) diameter, was used throughout the research program. These variables were studied statistically, using a factorial experiment design.

The typical factorial experiment designs are shown in Tables 1, 2, and 3, which were used for each of the paint systems.

Table 1. Steel type factorial experiment  
(1 kip = 4.45 kN)

Clamping Force	Steel Type		
	A36	A572	A514
39k	5	5	5
49k	5	5	5

Table 2. Paint thickness factorial experiment  
(1 kip = 4.45 kN)

Clamping Force	Steel Type					
	A572			A514		
	Thickness Type			Thickness Type		
	Thin	Normal	Thick	Thin	Normal	Thick
39k	5	5	5	5	5	5
49k	5	5	5	5	5	5

Table 3. Hole size factorial experiment  
(1 kip = 4.45 kN, 1 in. = 25.4 mm)

Clamping Force	Hole Size (in.)		
	15/16	1	1-1/8
39k	5	5	5
49k	5	5	5

Table 1 shows a data layout for the "steel type" experiment. The number 5 in each box represents the number of replications per cell. The experiment is a 3 × 2 factorial experiment. In this experiment the paint thickness and hole size were not variables; that is to say, all specimens for a paint system had the same hole size, 15/16 in. (24mm), and about the same paint thickness, normal ~ 6 mils. Table 2 shows a data layout for the "paint thickness" experiment. This experiment is a 2 × 3 × 2 factorial experiment. (The vinyl system was not included in

this thickness experiment.) It should be pointed out that Columns 2 and 5 concern tests which were already considered in Columns 2 and 3 in the "steel type" experiment. Thus, no additional testing was done in this case; that is, Columns 2 and 5 in Table 2 shared the same test data with Columns 2 and 3 in Table 1 for each paint system. Table 3 shows a data layout for the "hole size" experiment. This experiment is a  $3 \times 2$  factorial experiment and was repeated for each of the selected paint systems (excluding the vinyl system). Again, Column 1 in this experiment shared test data with Column 2 in Table 1. The order in which individual tests were completed was randomized within practical limits.

As part of the study, a large number of blasted specimens without coated faying surfaces were tested. These tests were considered "control tests" and were taken from each group of specimens sent for sandblasting.

Blasted Surfaces. Slip behavior of blast-cleaned uncoated surfaces have been studied by other researchers. Extensive test data were reported by both Fisher (1975) [15] and the Office of Research and Experiments of the International Union of Railways (ORE) (1974) [28]. With the wealth of data already available, this research project was directed toward a study of slip behavior of coated surfaces. Nevertheless, a large number of blast-cleaned uncoated surfaces were tested that will be referred to as "control specimens" throughout this study. The purpose of these control specimens was to provide a base condition for determining the influence of the coating on the slip behavior and provide additional needed data on A514 steel.

(1) Test Methods. Specimens were sent in groups to a local sandblasting shop to be sandblasted. Usually, each group of 14 specimens contained 4 control specimens. Blast-cleaned control specimens were usually tested within a week after sandblasting. All specimens were sandblasted to a white surface finish according to SSPC-SP5-63. This surface preparation is highly recommended by the SSPC and paint manufacturers for coated steel exposed to severe environments. The surface roughness of the control specimens was measured before testing, since it was felt that it might be directly related to the slip coefficient. The surface roughness of the control specimens served as an indicator of the base metal roughness of the coated specimens of the same group. The procedure for measuring the surface roughness is explained briefly in Chapter 2.

Pilot tests indicated that the speed of testing has no effect on the slip coefficient for sandblasted surfaces as compared to some coated surfaces. Nevertheless, all control specimens were loaded at a slip rate of 3 mils per minute (same as for coated surfaces) up to the slip load. When the slip load was reached, the specimen slipped suddenly and it was difficult to control the rate of slip. Figure 19 shows a typical load-slip relationship for a blast-cleaned steel surface. The shape of the response curves was not affected by steel type or size of hole. The load-slip response is almost linear until the load approaches the slip

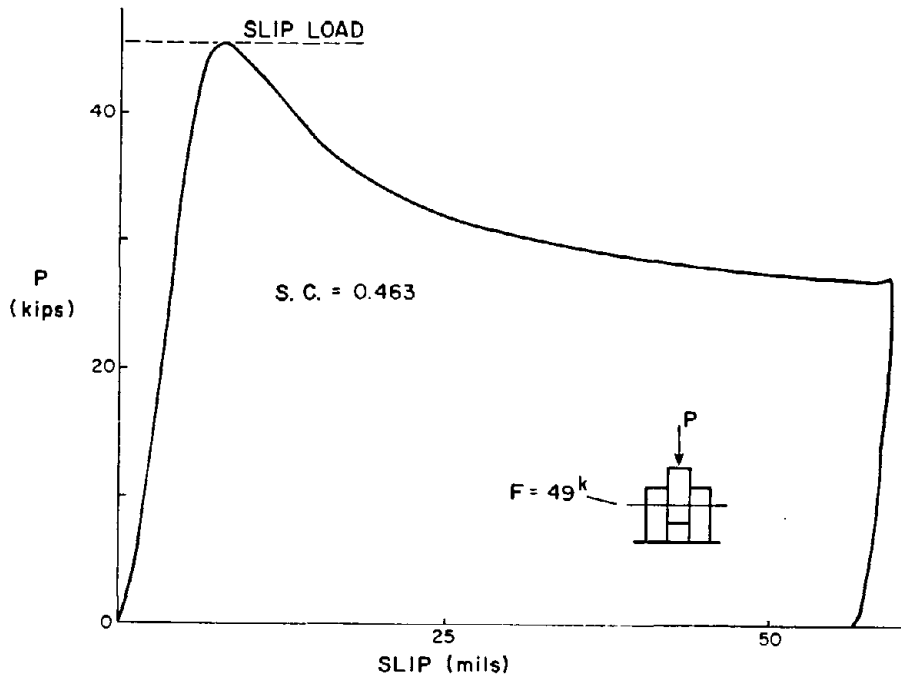


Figure 19. Typical load-slip curve for sandblasted surfaces  
(1 kip = 4.45 kN)

load. After the maximum load is reached the load drops suddenly and the plates slip with extreme rapidity. The data for each test including surface roughness are given in Ref. 16.

(2) Summary of Results. Table 4 and Figure 20 provide a comparison of the average slip coefficients (ASC) for the three steel types where  $n$  is the number of tests in the sample. They also compare the average slip coefficients (ASCs) for 39 kip (174 kN) and 49 kip (218 kN) clamping forces. It is evident that the ASCs for A36 and A514 are comparable (difference less than 4 percent). On the other hand, A572 steel has a slightly higher ASC (maximum difference about 15 percent). It seems that the effect of clamping force on the slip coefficient is almost negligible. Figure 22 shows the frequency distribution of the test results from the 77 tests in Figure 20. The results are approximately normally distributed with mean of 0.509 and standard deviation of 0.077. The ASC reported by Fisher [15] was 0.493 for 168 tests and the standard deviation was 0.074. These figures are in close agreement with the results of this research.

The test results for all the steels are grouped together in Figure 23, which shows that the clamping force had no significant effect on the slip coefficient (difference less than 2 percent).

Table 4. Steel type effect--blasted surfaces, 15/16 holes  
(1 kip = 4.45 kN, 1 in. = 25.4 mm)

Steel Type Clamping Force	A36			A572			A514		
	No. of Tests	Avg. SC	Std. Dev.	No. of Tests	Avg. SC	Std. Dev.	No. of Tests	Avg. SC	Std. Dev.
Low Clamping F = 39.0 <sup>k</sup>	11	0.461	0.059	16	0.540	0.087	8	0.494	0.085
High Clamping F = 49.0 <sup>k</sup>	8	0.484	0.069	20	0.542	0.067	14	0.488	0.067
TOTAL	19	0.471	0.063	36	0.541	0.075	22	0.490	0.072

Table 5. Hole size effect--blasted surfaces, A572  
(1 kip = 4.45 kN, 1 in. = 25.4 mm)

Hole Diameter Clamping Force	1 in.			1-1/8 in.			15/16 in.		
	No. of Tests	Avg. SC	Std. Dev.	No. of Tests	Avg. SC	Std. Dev.	No. of Tests	Avg. SC	Std. Dev.
Low Clamping F = 39.0 <sup>k</sup>	8	0.536	0.107	6	0.638	0.036	16	0.540	0.087
High Clamping F = 49.0 <sup>k</sup>	6	0.437	0.038	6	0.622	0.073	20	0.542	0.067
TOTAL	14	0.494	0.097	12	0.630	0.055	36	0.541	0.075



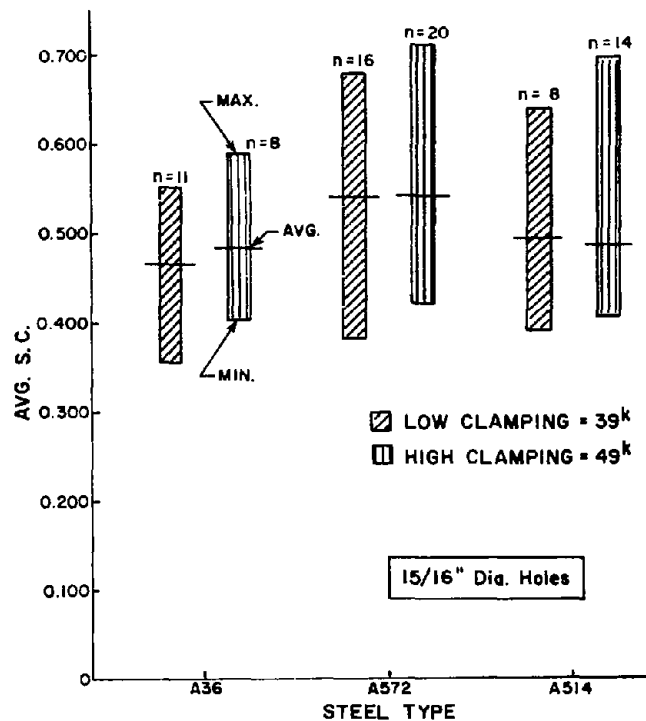


Figure 20. Effect of steel type and clamping force (1 kip = 4.45 kN, 1 in. = 25.4 mm)

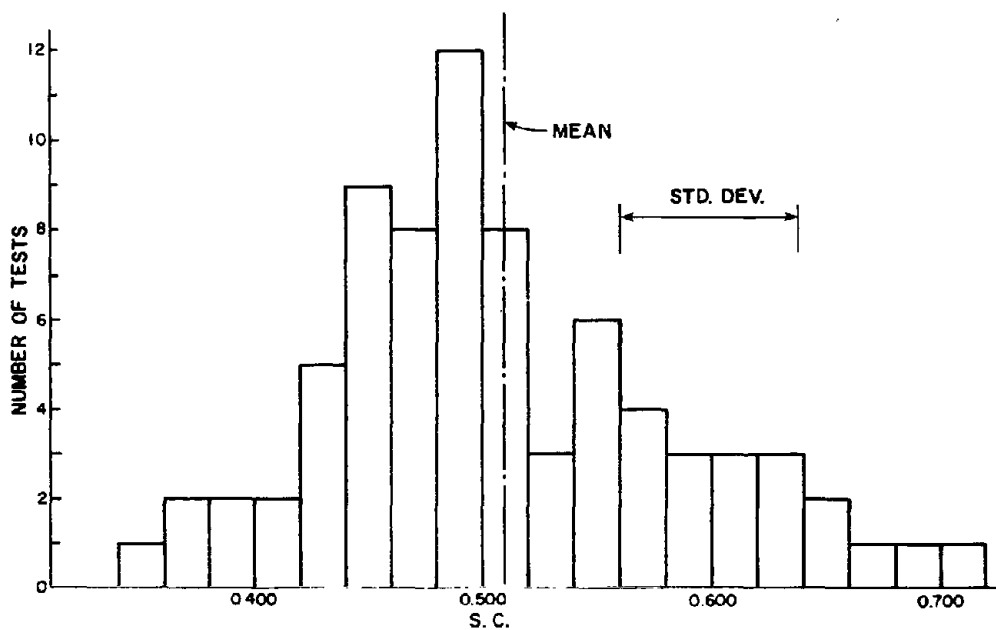


Figure 21. Histogram of slip coefficient for sandblasted surfaces, Table 4

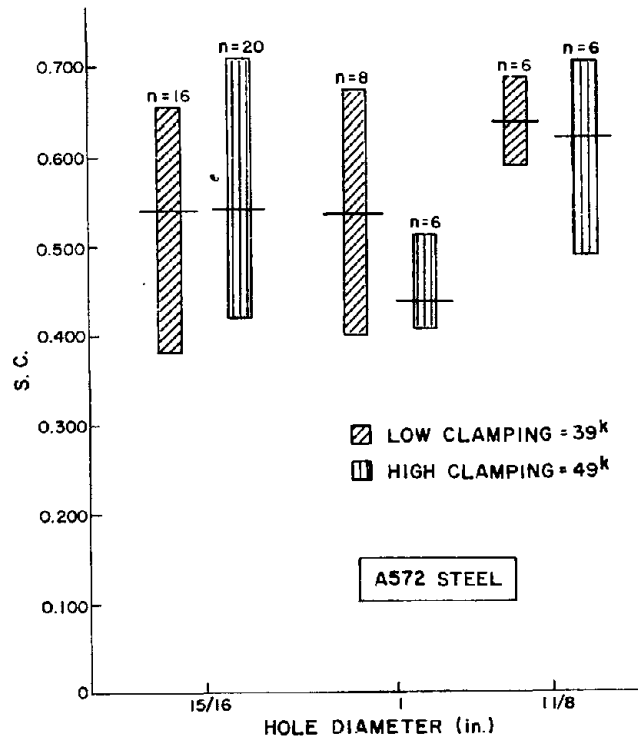


Figure 22. Effect of hole size and clamping force (1 kip = 4.45 kN, 1 in. = 25.4 mm)

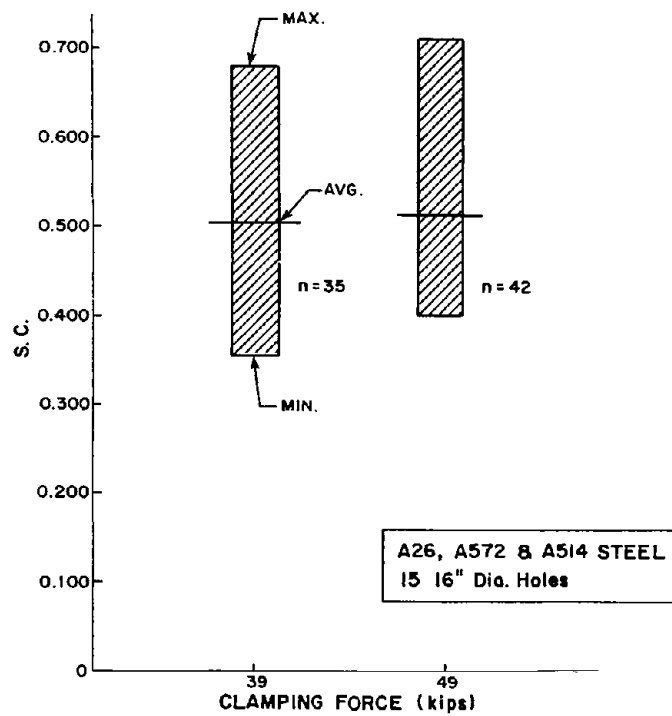


Figure 23. Effect of clamping force (1 kip = 4.45 kN, 1 in. = 25.4 mm)

Table 5 and Figure 22 compare the ASC for specimens with different hole diameters. The ASC for 15/16 in. (24mm) diameter holes is higher than that for 1 in. (25mm) diameter holes and lower than that for 1-1/8 in. (29mm) hole specimens. There is not any clear explanation for these differences, especially since the load-slip response for the three hole sizes was identical and the contact areas observed after testing were about the same. Although the number of tests for specimens with oversize holes is too few to be conclusive, no relationship between the slip coefficient and the hole diameter seems to exist. The differences observed may be attributed to scatter in the test results, as well as due to the fact that the results of 1-1/8 in. (29mm) diameter holes were obtained from two sandblastings only.

Figure 24 shows a comparison of the ASCs as obtained from the individual slip tests for fifteen different sandblasting groups. The standard deviation for each sandblasting sample is also shown with the number of samples shown in parentheses. The average of these ASCs is 0.504, with a standard deviation of 0.045. Comparing the standard deviations, it is apparent that the scatter in the mean values at different sandblasting is in most cases less than the variations within a sample of specimens sandblasted at one time.

A summary of the observed slip coefficients as a function of the surface roughness is shown in Figure 25. The general trend indicates that there is a slight increase in slip coefficient with deeper anchor pattern. However, a definite relationship cannot be established, since it is felt that the roughness as measured by the Keane-Tator surface comparator is very sensitive to the influence of the person taking readings.

The statistical analysis of the results of sandblasted surfaces is discussed later.

(3) Other Observations. The A514 steel plates were supplied with ridges at the rolled edges. The plates were reasonably flat through most of their width, but near both rolled edges the thickness increased gradually 1/32 in. (0.8mm). Nevertheless, the plates satisfied all specifications.

Some pilot tests were conducted on coated as well as uncoated sandblasted surfaces to observe the effect of out-of-flatness on the slip coefficient. The out-of-flatness was large enough so that approximately 80 percent of the surface area was not in contact after clamping the specimen. Most contact was at the ridges at the edges. This did not affect the slip coefficient of the sandblasted surfaces. The tests yielded results comparable to previous work. However, test results proved unsatisfactory for coated surfaces. The slip coefficient was significantly reduced. The specimens with the most contact area had the highest slip coefficient. Thus, it was concluded that it was necessary

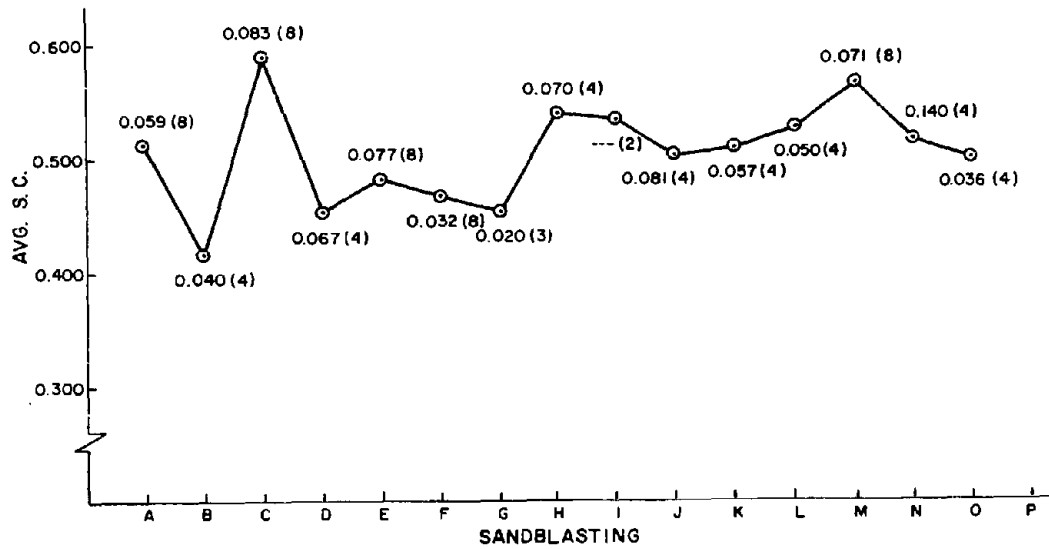


Figure 24. Effect of sandblasting on the average slip coefficient

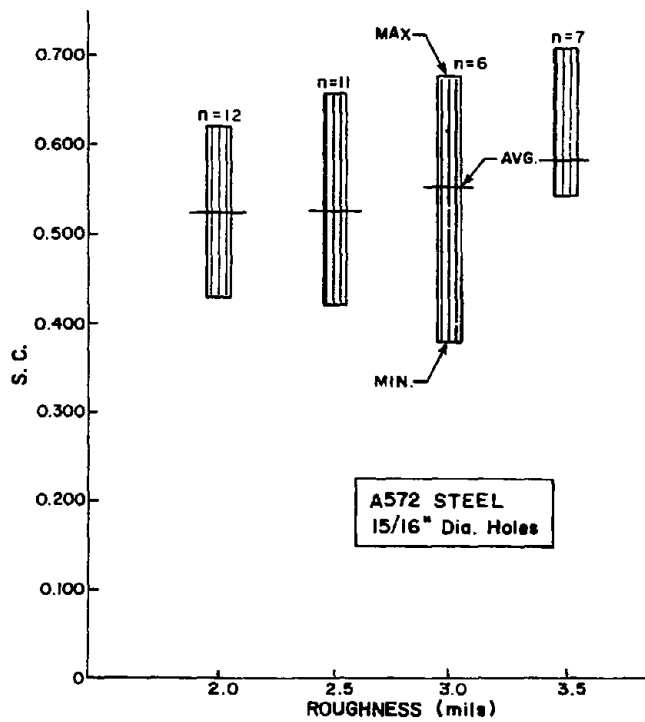


Figure 25. Comparison of average slip coefficients for different surface roughness (1 in. = 25.4 mm)

to mill or grind off the high edges on the plates in order to obtain valid test data on the different coatings considered. The edges were ground using a grinding wheel, which left the surface undisturbed in the vicinity of the hole.

Six tests were conducted on sandblasted surfaces which had the edges ground off after sandblasting. The tests yielded an average slip coefficient of 0.356, with a standard deviation of 0.050. The specimens did not slip rapidly as most sandblasted surfaces did; rather, the slip was steady. This was due to the smooth edge surfaces resulting from grinding. The value of 0.356 is rather low when compared to the average slip coefficient for specimens tested with the out-of-flatness not corrected, which was 0.472 with a standard deviation of 0.046. Therefore, it was decided to grind off the edges first and then sandblast the plates. The results of the tests which had edges ground off after sandblasting are not included in any of the previous results.

Painted Surfaces. In this section the test results of all the coated surfaces are presented and summarized. Each of the following sections considers one coating system. All tests were performed at a rate of 3 mils of slip per minute, which is approximately 25 kips (111 kN) per minute.

(1) Organic Zinc-Rich Primer. A typical load-slip relationship is shown in Figure 26. In general, the relationship was linear up to about 80 percent of the slip load. Then, the load-slip relationship became nonlinear and eventually a flat plateau was formed which was used to define the slip load. In some of the tests, the loading rate was increased after a total slip of about 30 to 40 mils to determine the effect of higher loading rate on the slip coefficient. Usually, by increasing the loading rate, a hump was formed, indicating an increase in the slip resistance of the specimen, as shown in Figure 26. This increase in slip resistance was dependent on several factors, such as the loading rate, curing time, and the paint film roughness. The slip coefficients reported herein were always based on the first slip load and before increasing the loading rate. The slip coefficients obtained are conservative, since most researchers conducted their tests at higher loading rates. In recent research conducted in Australia, Vitelleschi and Schmidt [33] performed their slip tests at a rate of 10 mils per min, which is about three times the rate used in this research.

Investigation of the contact surfaces of the specimens indicated that damage to the organic zinc painted surfaces was fairly uniform all over the contact areas. However, in some cases the severe damage was confined mostly to the areas adjacent to the holes.

Tables 6 through 9 summarize the test results in a factorial form. The standard deviation was generally less than 10 percent of the mean within each sample of five specimens. Table 10 is a summary of an additional experiment which was conducted to study more carefully the effect

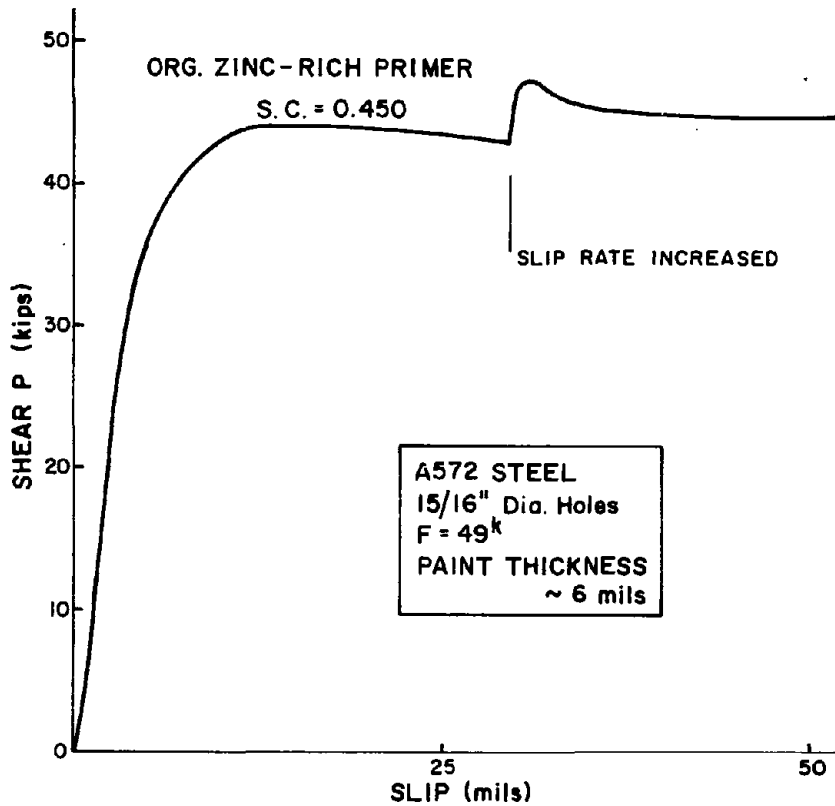


Figure 26. Typical load-slip curve  
 (1 kip = 4.45 kN, 1 in. = 25.4 mm)

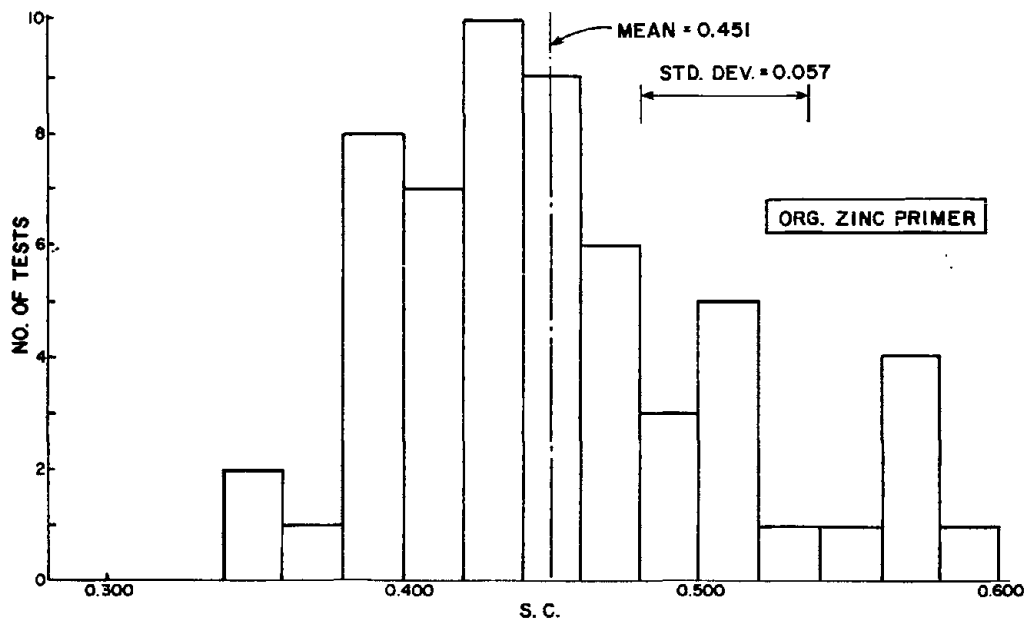


Figure 27. Frequency distribution for organic zinc-rich coated A572 surfaces (58 tests)

Table 6. Steel type effect--organic zinc, 15/16 holes, normal paint  
(1 kip = 4.45 kN, 1 in. = 25.4 mm)

Clamping Force \ Steel Type	A36			A572			A514		
	No. of Tests	Avg. SC	Std. Dev.	No. of Tests	Avg. SC	Std. Dev.	No. of Tests	Avg. SC	Std. Dev.
Low Clamping F = 39.0 <sup>k</sup>	7	0.558	0.024	7	0.493	0.058	5	0.476	0.060
High Clamping F = 49.0 <sup>k</sup>	7	0.553	0.026	7	0.474	0.055	5	0.483	0.075
TOTAL	14	0.555	0.025	14	0.484	0.055	10	0.479	0.066

Table 7. Paint thickness effect--organic zinc, A572, 15/16 holes  
(1 kip = 4.45 kN, 1 in. = 25.4 mm)

Clamping Force \ Paint Thickness	Thin ~ 3 mils			Normal ~ 6 mils			Thick ~ 9 mils		
	No. of Tests	Avg. SC	Std. Dev.	No. of Tests	Avg. SC	Std. Dev.	No. of Tests	Avg. SC	Std. Dev.
Low Clamping F = 39 <sup>k</sup>	5	0.441	0.023	5	0.463	0.030	5	0.520	0.053
High Clamping F = 49 <sup>k</sup>	5	0.405	0.016	5	0.444	0.020	5	0.467	0.039
TOTAL	10	0.423	0.027	10	0.453	0.030	10	0.494	0.039

Table 8. Paint thickness effect--organic zinc, A514, 15/16 holes  
(1 kip = 4.45 kN, 1 in. = 25.4 mm)

Paint Thickness Clamping Force	Thin ~ 3 mils			Normal ~ 6 mils			Thick ~ 9 mils		
	No. of Tests	Avg. SC	Std. Dev.	No. of Tests	Avg. SC	Std. Dev.	No. of Tests	Avg. SC	Std. Dev.
Low Clamping F = 39 <sup>k</sup>	5	0.351	0.043	5	0.476	0.060	5	0.484	0.071
High Clamping F = 49 <sup>k</sup>	3	0.362	0.004	5	0.483	0.075	5	0.455	0.079
TOTAL	8	0.355	0.032	10	0.479	0.066	10	0.470	0.072

Table 9. Hole size effect--organic zinc, A572, normal paint  
(1 kip = 4.45 kN, 1 in. = 25.4 mm)

Hole Diameter Clamping Force	15/16 in.			1 in.			1-1/8 in.		
	No. of Tests	Avg. SC	Std. Dev.	No. of Tests	Avg. SC	Std. Dev.	No. of Tests	Avg. SC	Std. Dev.
Low Clamping F = 39.0 <sup>k</sup>	5	0.463	0.030	5	0.456	0.020	5	0.396	0.016
High Clamping F = 49.0 <sup>k</sup>	5	0.444	0.020	5	0.422	0.015	5	0.369	0.027
TOTAL	10	0.453	0.030	10	0.439	0.020	10	0.382	0.025



Table 10. Hole size effect--organic zinc, A572, normal paint  
 (1 kip = 4.45 kN, 1 in. = 25.4 mm)

Hole Diameter Clamping Force	15/16 in.			1 in.			1-1/8 in.		
	No. of Tests	Avg. SC	Std. Dev.	No. of Tests	Avg. SC	Std. Dev.	No. of Tests	Avg. SC	Std. Dev.
High Clamping F = 49.0 <sup>k</sup>	5	0.368	0.026	5	0.379	0.021	5	0.371	0.025

of hole size on the slip coefficient. In this experiment all specimens were coated at the same time. This provided a fair comparison, since it was observed that the slip coefficient is affected by the painting process in the case of organic zinc-rich primer. Figure 27 is a histogram for all A572 Grade 50 steel data considering variations in paint thickness and hole diameters.

(2) Organic Zinc with Epoxy Topcoat. Tables 11 through 14 provide summaries for the test results in factorial form. Figure 29 is a histogram for all Grade 50 steel data. A typical load-slip relationship is shown in Figure 28.

The load-slip response was linear up to about 95 percent of the slip load. Unlike organic zinc-rich primer, when the slip load was reached a sudden drop in load accompanied by major slip occurred. In most cases the drop in load amounted to about 50 percent of the slip load. This indicated that the dynamic friction was much lower than the static friction. The loading rate did not seem to have any effect on the shape of the load-slip curve, as compared to the case of specimens coated with the primer only.

Investigation of the faying surfaces of the specimens after testing indicated that there was no damage to the epoxy topcoat surface. The epoxy topcoat was so hard that it was barely injured by slip.

(3) Inorganic Zinc-Rich Primer with Vinyl Topcoat. Tables 15 through 18 provide summaries for the test results in factorial form. Figure 30 is a histogram of all Grade 50 steel data. Figure 31 shows a typical load-slip relationship.

The load-slip response was linear up to about 80 percent of the slip load. Then, the relationship became nonlinear and eventually a flat plateau was formed. There was no drop in the slip load and its value was almost constant during slip. The loading rate had an effect on the shape of the load-slip curve. An appreciable increase in slip resistance occurred when the loading rate was increased. The behavior of this coating system is very similar to that of organic zinc-rich primer.

Investigation of the faying surfaces of the specimens after testing indicated that in most cases the damage to the vinyl topcoat was fairly uniform. The white vinyl topcoat peeled off, exposing the yellow inorganic zinc-rich primer.

(4) Vinyl Primer and All-Vinyl System. Tables 19 and 20 provide summaries of test results in factorial form. Figure 32 shows typical load-slip relationships.

For vinyl primer, the load-slip response was linear up to about 85 percent of the slip load. When the slip load was reached, a drop in load occurred accompanied by major slip (rapid slip of specimen). The

Table 11. Steel type effect--organic zinc with epoxy, 15/16 holes, normal paint  
(1 kip = 4.45 kN, 1 in. = 25.4 mm)

Steel Type Clamping Force	A36			A572			A514		
	No. of Tests	Avg. SC	Std. Dev.	No. of Tests	Avg. SC	Std. Dev.	No. of Tests	Avg. SC	Std. Dev.
Low Clamping F = 39.0 <sup>k</sup>	5	0.317	0.038	5	0.285	0.013	5	0.276	0.020
High Clamping F = 49.0 <sup>k</sup>	5	0.293	0.026	5	0.257	0.024	5	0.274	0.040
TOTAL	10	0.305	0.033	10	0.271	0.023	10	0.275	0.030

Table 12. Paint thickness effect--organic zinc with epoxy, A572, 15/16 holes  
(1 kip = 4.45 kN, 1 in. = 25.4 mm)

Paint Thickness Clamping Force	Thin ~ 6 mils			Normal ~ 9 mils			Thick ~ 12 mils		
	No. of Tests	Avg. SC	Std. Dev.	No. of Tests	Avg. SC	Std. Dev.	No. of Tests	Avg. SC	Std. Dev.
Low Clamping F = 39.0 <sup>k</sup>	5	0.291	0.020	5	0.285	0.013	5	0.281	0.039
High Clamping F = 49.0 <sup>k</sup>	5	0.275	0.024	5	0.257	0.024	5	0.268	0.022
TOTAL	10	0.283	0.023	10	0.271	0.023	10	0.274	0.030

Table 13. Paint thickness effect--organic zinc with epoxy, A514, 15/16 holes  
(1 kip = 4.45 kN, 1 in. = 25.4 mm)

Paint Thickness Clamping Force	Thin ~ 6 mils			Normal ~ 9 mils			Thick ~ 12 mils		
	No. of Tests	Avg. SC	Std. Dev.	No. of Tests	Avg. SC	Std. Dev.	No. of Tests	Avg. SC	Std. Dev.
Low Clamping F = 39.0 <sup>k</sup>	5	0.288	0.028	5	0.276	0.020	5	0.283	0.026
High Clamping F = 49.0 <sup>k</sup>	4	0.288	0.024	5	0.274	0.040	5	0.271	0.034
TOTAL	9	0.288	0.024	10	0.275	0.030	10	0.277	0.029

Table 14. Hole size effect--organic zinc with epoxy, A572, normal paint  
(1 kip = 4.45 kN, 1 in. = 25.4 mm)

Hole Diameter Clamping Force	15/16 in.			1 in.			1-1/8 in.		
	No. of Tests	Avg. SC	Std. Dev.	No. of Tests	Avg. SC	Std. Dev.	No. of Tests	Avg. SC	Std. Dev.
Low Clamping F = 39.0 <sup>k</sup>	5	0.285	0.013	5	0.251	0.009	5	0.261	0.028
High Clamping F = 49.0 <sup>k</sup>	5	0.257	0.024	4	0.256	0.014	5	0.255	0.023
TOTAL	10	0.271	0.023	9	0.253	0.011	10	0.258	0.024

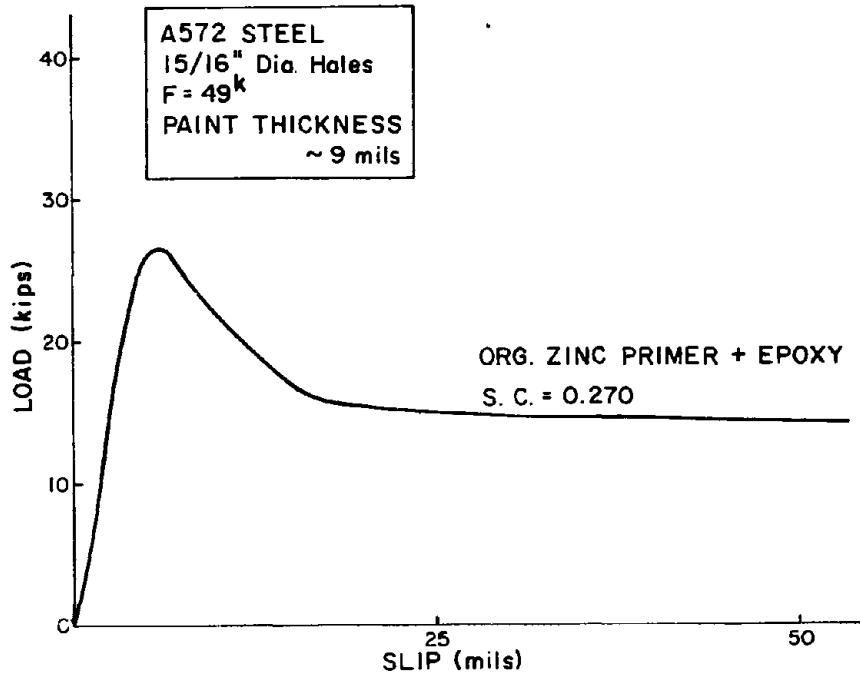


Figure 28. Typical load-slip curve (1 kip = 4.45 kN, 1 in. = 25.4 mm)

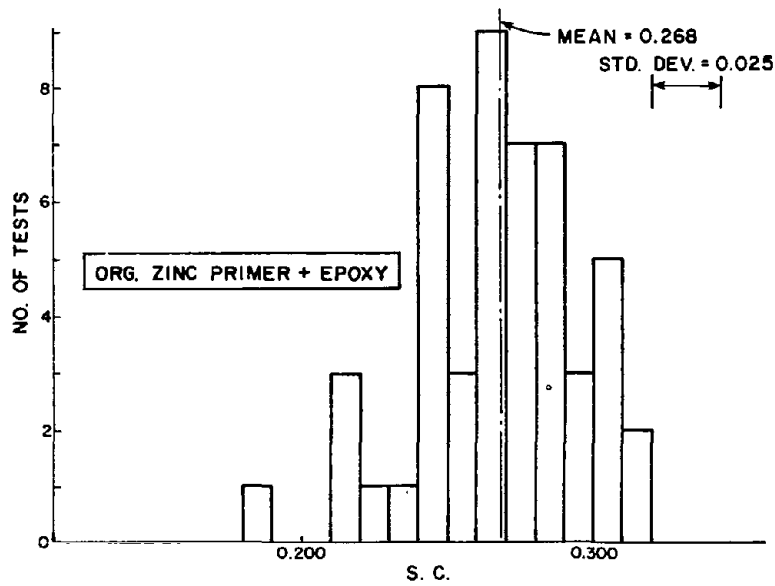


Figure 29. Frequency distribution for organic zinc-rich with epoxy coated, A572 surfaces (49 tests)

Table 15. Steel type effect--inorganic zinc with vinyl, 15/16 holes, normal paint  
(1 kip = 4.45 kN, 1 in. = 25.4 mm)

Steel Type Clamping Force	A36			A572			A514		
	No. of Tests	Avg. SC	Std. Dev.	No. of Tests	Avg. SC	Std. Dev.	No. of Tests	Avg. SC	Std. Dev.
Low Clamping F = 39.0 <sup>k</sup>	9	0.501	0.085	5	0.498	0.030	5	0.510	0.065
High Clamping F = 49.0 <sup>k</sup>	3	0.543	0.005	5	0.487	0.030	4	0.504	0.023
TOTAL	12	0.512	0.075	10	0.493	0.020	9	0.507	0.048

Table 16. Paint thickness effect--inorganic zinc with vinyl, A572, 15/16 holes  
(1 kip = 4.45 kN, 1 in. = 25.4 mm)

Paint Thickness Clamping Force	Thin ~ 6 mils			Normal ~ 10 mils			Thick ~ 14 mils		
	No. of Tests	Avg. SC	Std. Dev.	No. of Tests	Avg. SC	Std. Dev.	No. of Tests	Avg. SC	Std. Dev.
Low Clamping F = 39.0 <sup>k</sup>	5	0.489	0.038	5	0.498	0.030	5	0.555	0.008
High Clamping F = 49.0 <sup>k</sup>	5	0.446	0.057	5	0.487	0.030	5	0.544	0.026
TOTAL	10	0.468	0.051	10	0.493	0.020	10	0.550	0.019

Table 17. Paint thickness effect--inorganic zinc with vinyl, A514, 15/16 holes  
(1 kip = 4.45 kN, 1 in. = 25.4 mm)

Paint Thickness Clamping Force	Thin ~ 6 mils			Normal ~ 10 mils			Thick ~ 14 mils		
	No. of Tests	Avg. SC	Std. Dev.	No. of Tests	Avg. SC	Std. Dev.	No. of Tests	Avg. SC	Std. Dev.
Low Clamping F = 39.0 <sup>k</sup>	5	0.466	0.053	5	0.510	0.065	5	0.520	0.088
High Clamping F = 49.0 <sup>k</sup>	5	0.424	0.054	4	0.504	0.023	5	0.511	0.059
TOTAL	10	0.445	0.055	9	0.507	0.048	10	0.515	0.071

Table 18. Hole size effect-inorganic zinc with vinyl, A572, normal paint  
(1 kip = 4.45 kN, 1 in. = 25.4 mm)

Hole Diameter Clamping Force	15/16 in.			1 in.			1-1/8 in.		
	No. of Tests	Avg. SC	Std. Dev.	No. of Tests	Avg. SC	Std. Dev.	No. of Tests	Avg. SC	Std. Dev.
Low Clamping F = 39.0 <sup>k</sup>	5	0.498	0.030	5	0.563	0.005	5	0.565	0.030
High Clamping F = 49.0 <sup>k</sup>	5	0.487	0.030	5	0.546	0.018	5	0.530	0.023
TOTAL	10	0.493	0.020	10	0.555	0.018	10	0.548	0.031

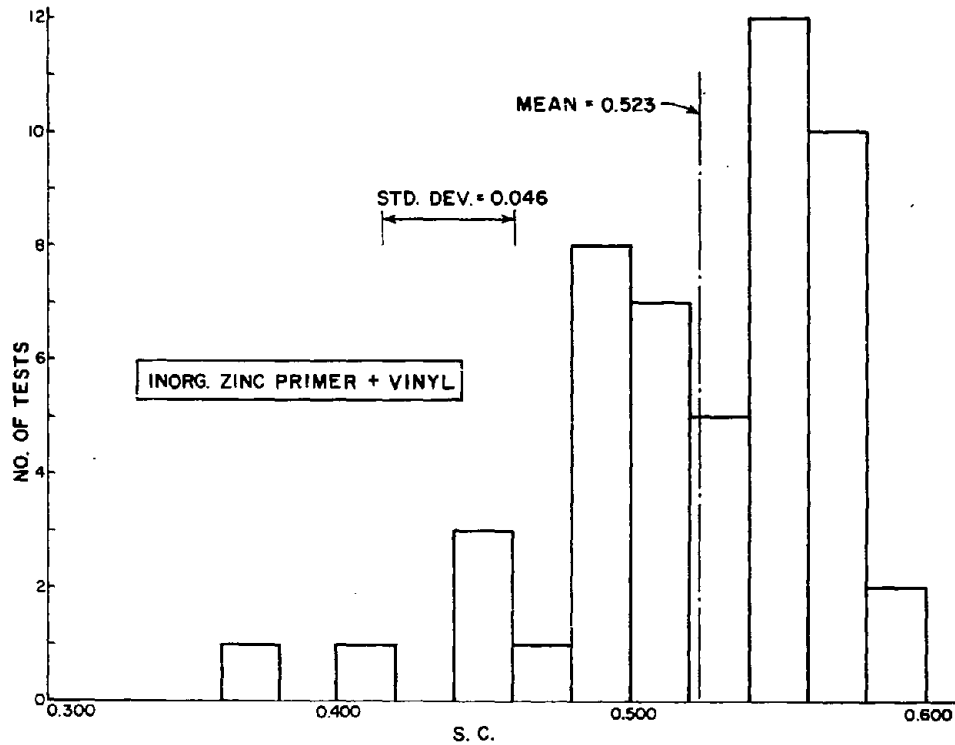


Figure 30. Frequency distribution for inorganic zinc-rich with vinyl coated A572 surfaces (50 tests)

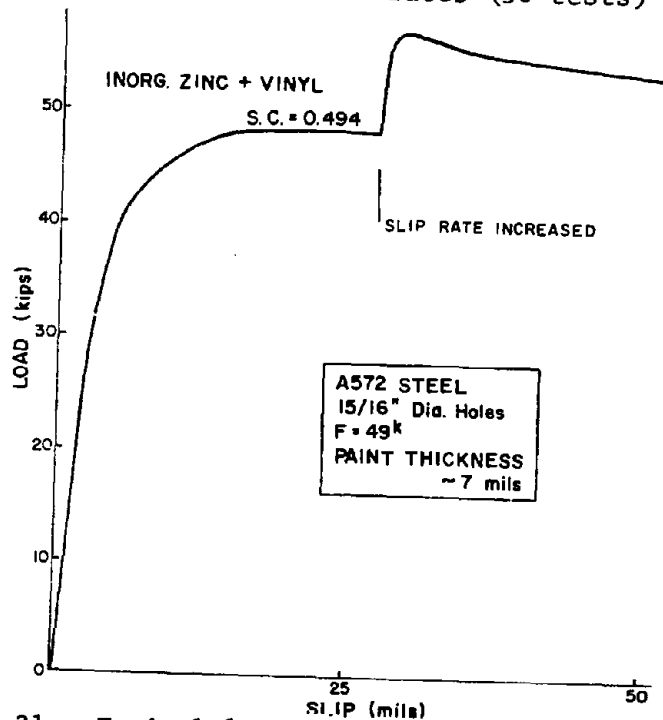


Figure 31. Typical load-slip curve (1 kip = 4.45 kN, 1 in. = 25.4 mm)



Table 19. Steel type effect--vinyl primer, 15/16 holes, 2.5 mil paint  
(1 kip = 4.45 kN, 1 in. = 25.4 mm)

Steel Type Clamping Force	A36			A572			A514		
	No. of Tests	Avg. SC	Std. Dev.	No. of Tests	Avg. SC	Std. Dev.	No. of Tests	Avg. SC	Std. Dev.
High Clamping F = 49.0 <sup>k</sup>	5	0.206	0.015	5	0.186	0.012	5	0.187	0.014

47

Table 20. Comparison of systems with vinyl topcoat, A514, 15/16 holes  
(1 kip = 4.45 kN, 1 in. = 25.4 mm)

Paint Clamping Force	Vinyl Primer			Vinyl Primer with Vinyl Top			Inorganic Zinc Primer with Vinyl Top		
	No. of Tests	Avg. SC	Std. Dev.	No. of Tests	Avg. SC	Std. Dev.	No. of Tests	Avg. SC	Std. Dev.
High Clamping F = 49.0 <sup>k</sup>	5	0.187	0.014	6	0.195	0.014	29	0.489	0.066

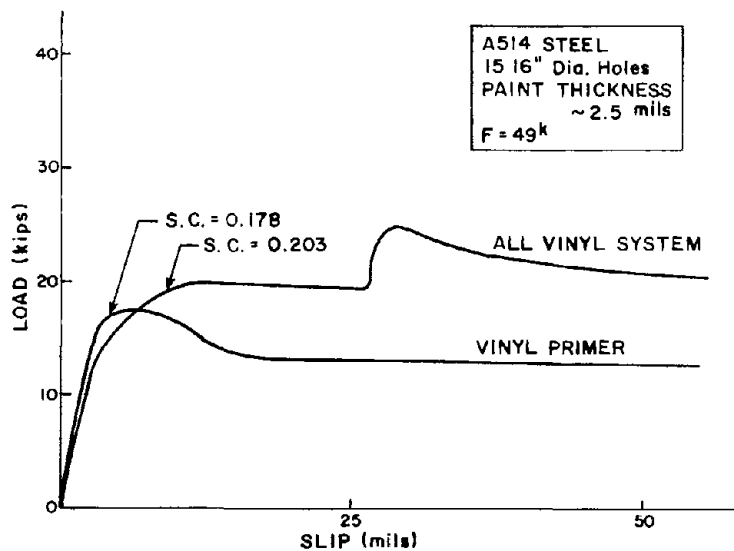


Figure 32. Typical load-slip curve  
 (1 kip = 4.45 kN, 1 in. = 25.4 mm)

specimens did not exhibit any loading rate effects, that is, when the loading rate was increased, there was no change in the load-slip response. Surface inspection after testing indicated that most contact was confined around the holes. Damage of the paint was negligible.

For the all-vinyl system (vinyl primer with vinyl topcoat), the load-slip response was linear up to about 70 percent of the slip load. Then, the load-slip relationship became nonlinear and eventually a flat plateau was formed without any drop in load. Increasing the loading rate increased the slip resistance. Surface inspection after testing indicated that in most cases the white vinyl topcoat was damaged (peeled off) exposing the dark red vinyl primer.

(5) Summary. Table 21 is a summary of all the results on the coated surfaces. Two systems shown, inorganic zinc (A572) and powder epoxy, are presented in a later section. The statistical analysis and discussion of the test results are given in the next sections. A full factorial experiment on the vinyl system was not completed because it became evident from the creep experiment discussed in the next chapter that the vinyl system with thicknesses greater than 2 mils were not satisfactory.

#### Discussion of Factorial Results

Method of Analysis. A statistical analysis was made of the test results given in the two previous sections to investigate the effects of the different variables considered in this study. A computer program (AOVRNC) available at The University of Texas at Austin computer library was used. AOVRNC is a self-contained routine for performing fixed

Table 21. Summary--all test results  
(1 in. = 25.4 mm)

		Thickness			Oversize Holes	
		Thin	Normal	Thick	D = 1"	D = 1-1/8"
Organic Zinc	A36		0.555* (0.025)**			
	A572	0.446 (0.046)	0.484 (0.055)	0.494 (0.039)	0.439 (0.020)	0.380 (0.025)
	A514	0.355 (0.032)	0.479 (0.066)	0.470 (0.072)		
Organic Zinc with Epoxy Topcoat	A36		0.305 (0.033)			
	A572	0.283 (0.023)	0.271 (0.023)	0.274 (0.030)	0.253 (0.011)	0.258 (0.024)
	A514	0.288 (0.024)	0.275 (0.030)	0.277 (0.029)		
Inorganic Zinc with Vinyl Topcoat	A36		0.512 (0.075)			
	A572	0.468 (0.051)	0.493 (0.020)	0.550 (0.019)	0.555 (0.018)	0.548 (0.031)
	A514	0.445 (0.055)	0.507 (0.048)	0.515 (0.071)		
Vinyl Primer	A36		0.206 (0.015)			
	A572		0.186 (0.012)			
	A514		0.187 (0.014)			
All Vinyl System	A514		0.195 (0.014)			
Inorganic Zinc (A572)	80% Zinc		0.607 (0.030)		0.628 (0.020)	
	75% Zinc		0.507 (0.010)			
	0% Zinc (ethyl silicate base)		0.276 (0.003)			
Powder Epoxy			0.079 (0.010)			

\*Average slip coefficient  
\*\*Standard deviation

effects analysis of variance requiring user-specified hypotheses. The routine could be used for analyzing factorial experiments with any number of levels. It can also handle situations where the number of replications in each cell is not equal. For statistical testing, a 5 percent level of significance was usually used. In comparing means, this indicates a 5 percent chance of falsely assuming a mean to be significantly different from the population studied. The Scheffé test on means, which is a conservative test for protection against the probability of making a Type I error, was also performed at the 5 percent level. Type I error is the rejection of the hypothesis which states that all the means are equal when the hypothesis is actually correct.

Blasted Surfaces. A 3 × 2 factorial experiment was analyzed statistically to determine the effect of oversize holes and clamping force level

on the slip resistance of A572 steel. There were three different hole sizes and two different clamping forces. Results of the analysis indicated that at a 5 percent level of significance the hole size exhibited significant contrasts, whereas the clamping forces' contrast was insignificant. The average slip coefficient (ASC) for 15/16 (24mm) and 1 in. (25mm) diameter holes was comparable, but was noticeably lower than the ASC for 1-1/8 in. (29mm) diameter hole which was about 20 percent higher than the ASC for both 15/16 (24mm) and 1 in. (25mm) diameter holes. This increase in slip resistance provided by the 1-1/8 in. (29mm) diameter hole specimens could not be explained, especially since the load-slip response for the three hole sizes was identical and the contact areas observed after testing were about the same. However, test results on the 1-1/8 in. (29mm) diameter hole specimens were obtained from two sandblastings only, as compared to the test results on 15/16 in. (24mm) diameter hole specimens which were obtained from a total of twelve sandblastings. Because of the considerable scatter in the test results, due to different sandblastings (see Figure 24), it is a reasonable possibility that the limited data on the 1-1/8 in. (29mm) diameter hole joints (two sandblastings only) may be responsible for the apparent higher slip resistance. However, it may be confidently concluded that for 7/8 in. (22mm) diameter bolts, there is no decrease in the slip coefficient for oversize holes with up to 1/4 in. (6mm) clearance. This conclusion is in agreement with the work done by Allan and Fisher on millscale joints with oversize holes [1].

Similar statistical analysis of the  $3 \times 2$  factorial experiment was performed to evaluate the effect of steel type on the slip resistance. Only joints with 15/16 in. (24mm) diameter holes were used. Steel types were A36, A572 Grade 50, and A514. Clamping force was at the two levels, 39 kips (174kN) and 49 kips (218 kN). This analysis merely confirmed that clamping force was an insignificant variable, because it was apparent from Figures 20 and 23 that the ASC was almost unaffected by the level of clamping force. Obviously, the clamping force directly affects slip load but not the slip coefficient. On the other hand, the analysis indicated that steel type was a significant variable. The ASC for A36 and A514 steel was about equal (0.471 and 0.490, respectively), but was noticeably lower than the ASC for A572 steel (0.541), as shown in Figure 20. The slip resistance offered by A572 steel was only 12.5 percent higher than that of A36 and A514 steel. It is debatable if this modest increase in slip resistance should be taken into consideration in the design, since each steel type tested came from a single heat.

It might also be mentioned that tests reported by Fisher and Struik [15] indicated that A514 heat-treated steel provided lower resistance to slip as compared to A36 steel. This was attributed to the harder surface of A514 steel that influences the roughness achieved by blast cleaning. They reported a reduction in the slip resistance of about 33 percent for blast-cleaned A514 surfaces. However, the ASCs for A36 and A514 steel specimens studied herein were about the same, a difference of about 3.5 percent. This result seems to be reasonable, since blasted surfaces of

A36 and A514 steel inspected under a powerful microscope did not exhibit any drastic differences in texture. The measured surface roughness also, when compared for A36 and A514 steel plates which were blasted together, did not indicate any significant differences.

A simple one-variable analysis of variance was performed to study the effect of surface roughness on the slip coefficient. A572 steel joints with 15/16 in. (24mm) holes were arranged into four groups according to roughness (2, 2.5, 3, and 3.5 mils). Each group represented an average anchor pattern profile depth as measured by the Keane-Tator surface comparator. As can be seen in Figure 25, the ASC tends to increase slightly as the surface gets rougher. However, the statistical test at 5 percent significance level indicated that roughness was insignificant.

Another similar simple analysis was done to find out if different sandblastings significantly affected the ASC. For each steel type, a separate analysis compared the ASCs as obtained from each sandblasting group. It was found that for any of the three steel types considered, the ASC is not significantly affected by different sandblasting. The ASC, as a function of sandblasting time, is given in Figure 21. This conclusion is helpful in design, since sandblasting is eliminated as a variable. This means that in spite of the fact that the joints in a structure might be blasted at different times, still the ASCs for all joints will be about the same within a 95 percent confidence level.

Painted Surfaces. (1) Oversize Holes and Clamping Force. A  $3 \times 2$  factorial experiment for each coating system was analyzed statistically to determine the effects of oversize holes and clamping force level on the slip coefficient. The hole sizes were 15/16, 1, and 1-1/8 in. (24, 25, and 29 mm) in diameter; the clamping force was at the two levels, 39 and 49 kips (174 and 218 kN). The coating systems used were organic zinc primer, organic zinc primer with an epoxy topcoat, and inorganic zinc primer with vinyl topcoat. All joints were of A572 steel and had normal paint thickness (~6 mils for primer and ~3 mils for topcoat). For the surfaces coated with organic zinc primer, the analysis indicated that hole size was a significant variable, whereas the clamping force was not. The 15/16 and 1 in. (24 and 25mm) diameter hole joints had comparable ASCs (difference of about 3 percent), which were higher than the ASC for 1-1/8 in. (29mm) diameter hole joints by about 14 percent. However, the friction characteristics of organic zinc primer coated surfaces showed sensitivity to painting in a group. For each group of joints (specimens) painted at a single time, the standard deviation was very low (~0.020) and was about equal for all the groups. But the average slip coefficient exhibited large differences from one painting job to another, amounting to about 15 percent. This is believed to be due to the slight variations in paint surface roughness resulting from different painting conditions (humidity, temperature, spray gun setting, etc.). The results of the joints with different hole sizes were not all obtained from one painting job. The 15/16 and 1 in. (24 and 25mm) diameter hole joints were painted

at the same time, whereas the 1-1/8 in. (29mm) diameter hole joints were painted separately.

Thus, it was felt that the low ASC exhibited by the 1-1/8 in. (29mm) diameter hole joints might have resulted from different painting jobs. Therefore, an additional experiment was conducted with the hole size as the only variable and all the joints were painted at the same time. The results summarized in Table 10 show that the effect of hole size on the ASC was insignificant (0.368 and 0.371 for 15/16 and 1-1/8 in. (24 and 29 mm) diameter holes, respectively), and the effect of different paintings was verified.

As for the organic zinc primer topcoated with epoxy, the analysis of the  $3 \times 2$  factorial experiment indicated that neither hole size nor clamping force was significant as a variable. The effect of different paintings on the ASC was very slight as compared to the case of the primer without topcoat. It is believed that the hard epoxy topcoat provided surfaces which possess more uniform friction characteristics.

For the inorganic zinc primer with a vinyl topcoat, the analysis indicated that hole size as well as clamping force was significant at the 5 percent level. The clamping force exhibited insignificant contrasts at the 1 percent level. This indicated that the clamping force effect was very small. The maximum difference in the ASC due to clamping force level was about 6 percent for the 1-1/8 in. (29mm) diameter hole joints. The 39 kip (174 kN) clamping force always offered the higher slip resistance. The ASCs for 1 and 1-1/8 in. (25 and 29mm) diameter hole joints were about equal (1 percent difference), but were noticeably higher than the ASC for the 15/16 in. (24mm) diameter hole joints (12 percent difference). The relatively high value of the ASC for the joints with oversize holes cannot be fully explained. However, it is very possible that the observed differences were due to different paintings. The joints with 1 and 1-1/8 in. (25 and 29 mm) diameter holes were painted at the same time and provided comparable ASCs. Joints with 15/16 in. (24mm) diameter holes were painted separately and provided a lower ASC. However, an additional experiment, as in the case of the organic zinc primer, was not designed since the oversize holes, contrary to the previous case, offered a higher slip resistance. Some additional tests were conducted on inorganic zinc (no topcoat) coated surfaces with 15/16 and 1 in. (24 and 25 mm) diameter holes, A572 steel, and a clamping force of 39 kips (174 kN), which yielded ASCs of 0.620 (five tests) and 0.628 (ten tests), respectively. The values are about equal and indicate very clearly the insignificance of hole size as a variable. Figure 33 shows the effect of oversize holes for the different coating systems. The narrow black boxes shown in the figure for organic zinc primer represent the additional experiment done for this paint. From the above discussion, it may be concluded that for joints coated with any of the above-mentioned paint systems, there will be no decrease in the slip coefficient for oversize holes with up to 1/4 in. (6mm) clearance for 7/8 in. (22mm) diameter bolts.

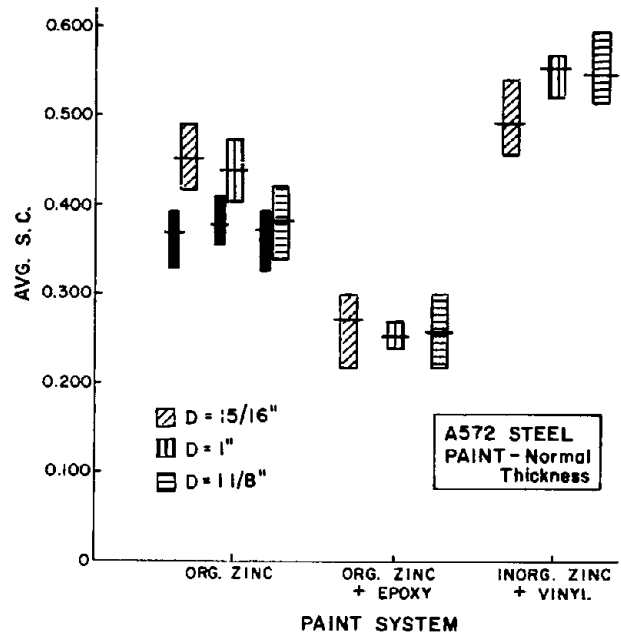


Figure 33. Comparison of average slip coefficient for different hole sizes (1 in. = 25.4 mm)

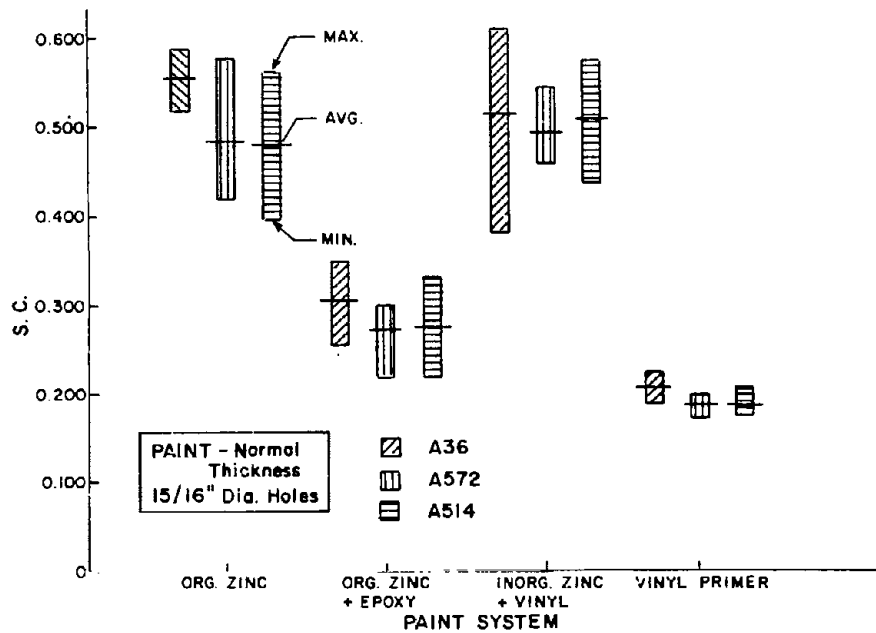


Figure 34. Comparison of average slip coefficient for different steel types (1 in. = 25.4 mm)

In Table 2a of the 1978 Bolt Specification [30], a reduction of about 15 percent is specified for joints with oversize holes. This was based on data which showed that the clamping force is expected to be reduced by about 15 percent for oversize holes [15]. This reduction was attributed to plate depressions occurring under the bolt heads during tightening by the turn of the nut method. Thus, rotation of the nut does not result in the degree of bolt elongation desired. However, if torque-controlled bolts or the load-indicating washer method is used in tightening the bolts, perhaps this reduction may not exist. Further research is needed to determine if oversize holes cause reduction in the clamping force for these tightening methods. Also, it should be pointed out that the reduction in clamping force (when using turn-of-the-nut method) was 15 percent lower than the average tension that resulted in joints with a 1/16 in. (2mm) hole clearance. But, bolt tension was still above the minimum required tension by about 18 percent. Thus, if a specification is based on the minimum clamping force, no reduction should be considered, even when turn of the nut method is used.

(2) Type of Steel. A similar experiment to that of the oversize holes was analyzed to determine the effects of steel type and clamping force on the slip coefficient of the joints. The steel types were A36, A572, and A514, and the clamping forces were 39 and 49 kips (174 and 218 kN). The coating systems used were organic zinc primer, organic zinc primer with an epoxy topcoat, inorganic zinc primer with a vinyl topcoat, and a vinyl primer. All joints had 15/16 in. (24mm) diameter holes and normal paint thickness. Results of the analyses for the different paint systems indicated that the effect of the clamping force was insignificant. Usually, the low clamping force 39 kips (174 kN) offered a slightly higher slip coefficient than the high clamping force 49 kips (218 kN). The maximum difference amounted to about 6 percent in the case of the organic zinc primer with epoxy topcoat. However, the statistical analyses suggested that the differences are too small and are mainly due to the estimate of the variance and scatter in the test results. No real differences exist between the 39 kip (174 kN) and 49 kip (218 kN) ASCs.

On the other hand, the analyses indicated that the steel type was a significant variable for most of the coated surfaces. For the organic zinc primer, organic zinc primer with epoxy topcoat, and vinyl primer coated surfaces, the ASCs for A572 and A514 steel were about the same (differences less than 1.5 percent for any of the three paint systems), but were noticeably lower than the ASC for A36 steel of the same paint system. The percentage increase in slip resistance provided by the A36 steel was 15 percent, 12 percent, and 11 percent for the three paint systems, respectively. As for the surfaces coated with inorganic zinc primer with a vinyl topcoat, the analyses indicated that steel type was an insignificant variable. Figure 34 shows a comparison of the ASCs for the different steel types and paint systems. In the figure, it can be seen that the ASC of A36 steel always plots slightly higher than the ASCs of A572 and A514 steel.



The increase in slip resistance provided by A36 steel for some coatings cannot be explained, since the blasted specimens did not show a similar increase. Also, the inorganic zinc primer with vinyl topcoat did not show an increase in the slip resistance. Since the maximum observed increase was only 15 percent, it is recommended that the steel type effect not be considered in a design specification. The small potential benefit for some coatings does not justify the complications resulting from the inclusion of steel as a factor in design specifications.

(3) Paint Thickness. A  $2 \times 3 \times 2$  factorial experiment was analyzed to determine the effect of paint film thickness on the slip coefficient of the joints. The factorial experiment was also used to check the possibility of interaction between steel type at two levels--A572 and A514 steel, paint thickness at three levels--thin, normal, and thick, clamping force at two levels--39 and 49 kips (174 and 218 kN). The same three paint systems were considered; namely, organic zinc primer with and without an epoxy topcoat, and the inorganic zinc primer with vinyl topcoat system. Topcoats (epoxy or vinyl) had constant thickness of about 3 mils. Thickness of the primer was the variable. The three levels of thickness were 3, 6, and 9 mils for organic zinc primer; and 3, 7, and 11 mils for the inorganic zinc primer. All joints had 15/16 in. (24mm) diameter holes.

The results of the analyses confirmed that steel type (A572 and A514 only) and clamping force were insignificant variables for all of the three paint systems. Also, the analyses indicated that all interaction effects between the three variables (steel, clamping force, and paint thickness) were insignificant. These results were expected since (1) the steel type experiment discussed above concluded that the ASCs for A572 and A514 steel were practically equal for any of the paint systems and the clamping force was insignificant, and (2) it was felt that the paint thickness as a variable will not affect the steel type or the clamping force level effects. As to the paint thickness, the analyses indicated that thickness was insignificant in the case of organic zinc primer with and without epoxy topcoat paint systems. Table 8 shows an apparent decrease in the ASC for thin thickness of organic zinc primer on A514 steel joints (about 25 percent). However, this was mainly due to edge effects present in this set of eight specimens. A verification for this reasoning is provided by the A572 steel joints that have no edge effects and did not exhibit this reduction in ASC due to thin thickness. For inorganic zinc primer with vinyl topcoat, statistical analysis indicated that the ASCs for thin and normal thickness were comparable. Also, the ASCs for thick and normal thickness were comparable. But the ASCs for thick and thin thicknesses showed some differences. The ASC for thin thickness was lower than that for thick thickness by about 15 percent. Since the ASC for normal thickness was comparable with the ASCs for both thin and thick thicknesses, this would suggest using the ASC based on normal thickness and eliminate the effect of thickness. Thus, based on the above discussion concerning thickness of paint, it may be concluded that thickness is not an important variable and its effect on the slip resistance of the joint for all practical

reasons is negligible. Figure 35 shows the effect of paint thickness on the ASC for A572 and A514 steel joints.

(4) Primer. A simple one variable analysis was performed to compare between the following paint systems: vinyl primer (~ 2.5 mils), vinyl primer with a vinyl topcoat (all vinyl system) (~ 2.5 + 2.5 mils), and inorganic zinc primer with vinyl topcoat (~ 7 + 2.5 mils). All joints were of A514 steel and had 15/16 in. (24mm) diameter holes. The results indicated that the vinyl primer and all vinyl system had comparable ASCs, which were significantly lower than the ASC of the inorganic zinc primer with vinyl topcoat. The all vinyl system and the inorganic zinc primer with vinyl topcoat had the same topcoat. However, the slip resistance of the all vinyl system was 60 percent lower. It is quite apparent that the vinyl primer, which has a low ASC (0.187), when topcoated with vinyl still exhibited a low ASC (0.195), whereas the inorganic zinc which has a high ASC (0.607), when topcoated (with the same vinyl topcoat) exhibited a relatively high ASC (0.489). This behavior indicates that the kind of primer considerably affects the slip resistance even when it is topcoated. Figure 36 clearly shows this phenomenon.

(5) Summary. In summary, Table 22 lists the overall average slip coefficient (ASC), standard deviation and number of tests for each of the coating systems. Figure 37 shows the ASC and the range of slip coefficient and Figure 38 shows typical load-slip curves for the coatings considered in the factorial experiment as well as some other coatings discussed in the next section. From the summaries, it is evident that the coated surfaces have lower standard deviations than blast-cleaned uncoated surfaces. Based on this statistically designed experiment, the effect of the following variables may be considered insignificant with respect to the the static slip behavior of friction-type joints with coated and uncoated contact surfaces:

Table 22. Overall average slip coefficients

Surface Treatment	Average Slip Coeff.	Standard Deviation	Total No. of Tests
Sandblasted	0.521	0.077	103
Organic zinc primer	0.464	0.061	106
Organic zinc primer with epoxy topcoat	0.276	0.031	88
Inorganic zinc primer with vinyl topcoat	0.510	0.057	94
Vinyl primer	0.193	0.016	15
All vinyl system	0.195	0.014	5

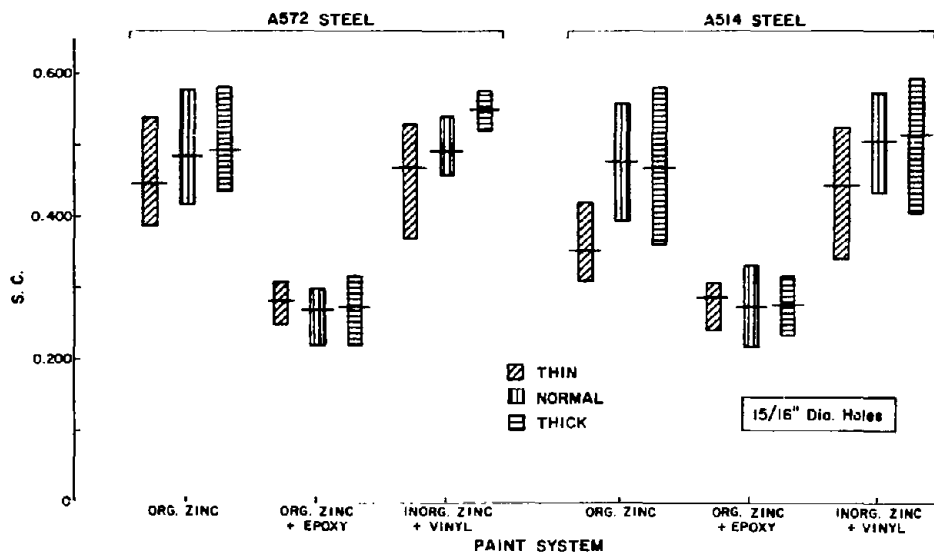


Figure 35. Comparison of average slip coefficient for different paint thickness (1 in. = 25.4 mm)

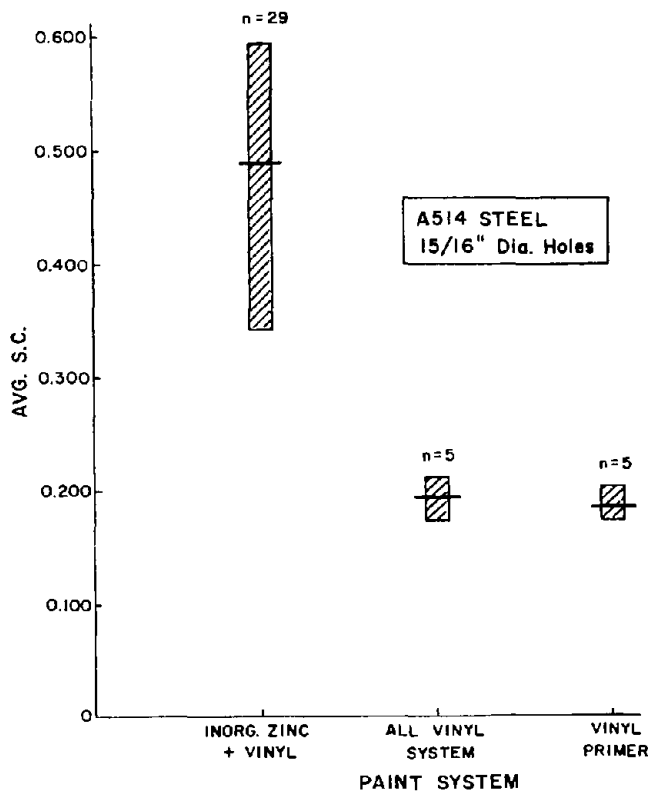


Figure 36. Comparison of average slip coefficient for different vinyl systems (1 in. = 25.4 mm)

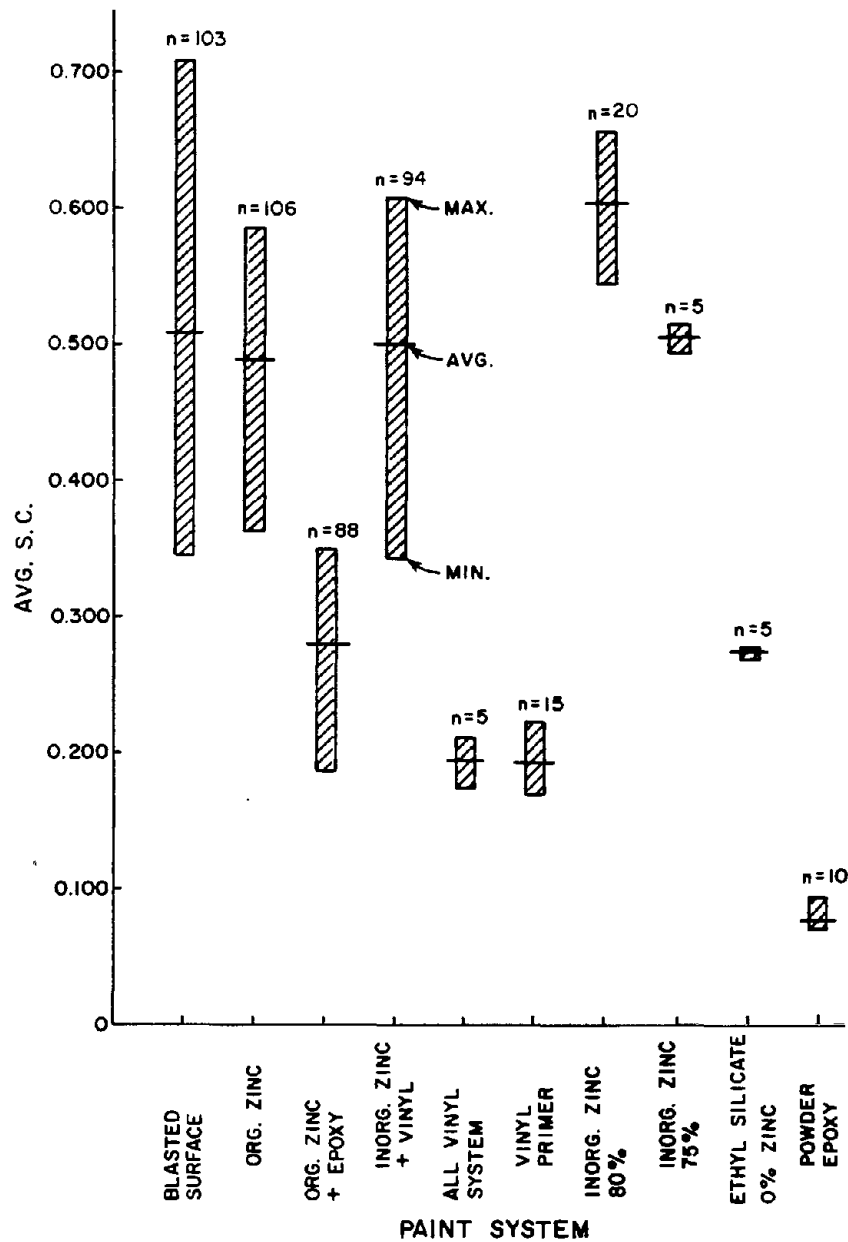


Figure 37. Comparison of overall average slip coefficient for sandblasted and painted surfaces (blasted and painted surfaces: A36, A572, and A514 steel; hole sizes: 15/16, 1, and 1-1/8 in. diameter; clamping force: 39 and 49 kips; paint thickness: 3 to 15 mils) [1 kip = 4.45 kN, 1 in. = 25.4 mm]

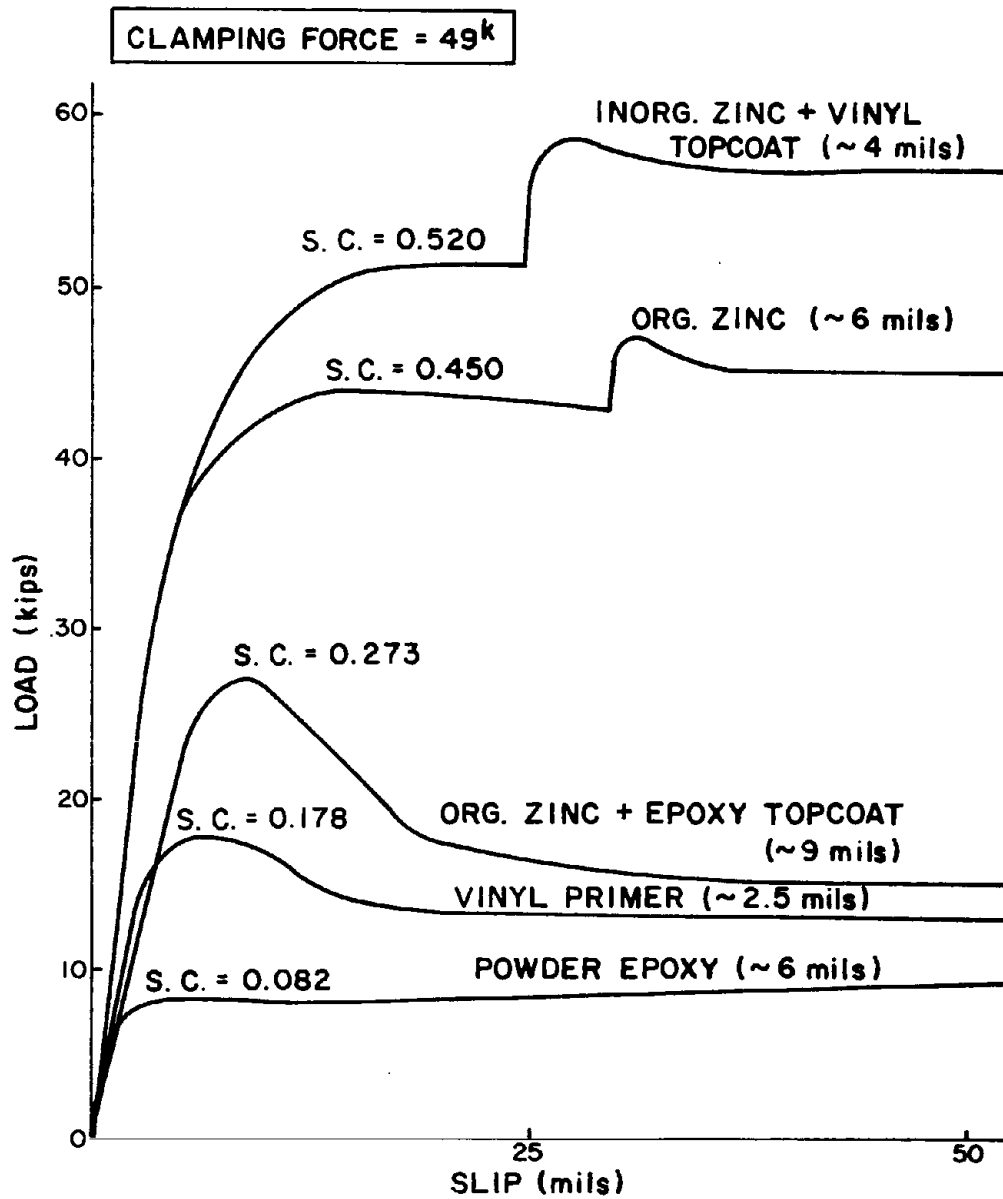


Figure 38. Typical load-slip curves (1 kip = 4.45 kN)

- (i) Hole size up to 1/4 in. (6mm) clearance for 7/8 in. (22mm) diameter bolts
- (ii) Type of steel (A36, A572, and A514)
- (iii) Paint thickness on each plate in contact (3 mils to 14 mils)

It was also established that clamping force did not significantly affect the slip coefficient, so the slip load of a high-strength bolted connection is directly related to the clamping force provided.

### Other Coatings

Powder Epoxy. As indicated in Chapter 1, a powder epoxy system was initially suggested for the main factorial experiment but the low slip coefficient developed limited the use of such a coating. A typical load-slip curve is given in Figure 39a. The average slip coefficient from ten tests was 0.079 with a standard deviation of 0.01. This slip coefficient is about one-fourth of the value for a standard millscale surface. The low coefficient may be attributed to the very hard and smooth powder epoxy surface. After disassembling the specimens, an examination of the surface showed no evidence of damage.

Inorganic Zinc Primer. The Steel Structures Painting Council Specification SSPC-PS-12.00 C8T requires at least 75 percent zinc by weight for the paint to be acceptable on exposed structural steel [32]. The zinc content of the inorganic zinc primer used in the factorial experiment contained 80 percent zinc. Because this percentage was greater than required, another inorganic zinc paint from the same manufacturer with the same vehicle and 75 percent zinc was tested. Both zinc-rich paints were two component products, vehicle and zinc dust. Slip tests were also conducted on plates sprayed with the vehicle alone, so the contribution of the zinc dust to the slip resistance could be clearly established. Thirty tests were performed and the individual data are presented in Ref. 16. A summary is given in Table 23.

Table 23. Average slip coefficients for inorganic zinc primer

Percent Zinc	No. of Tests	Average Slip Coefficient	Standard Deviation	Range
80	20	0.618	0.030	0.66-0.55
75	5	0.507	0.010	0.52-0.49
0 (base)	5	0.276	0.003	0.27-0.28

Figure 40 shows the typical load-slip response for the three levels of zinc content. The response was linear up to about 85 percent of the

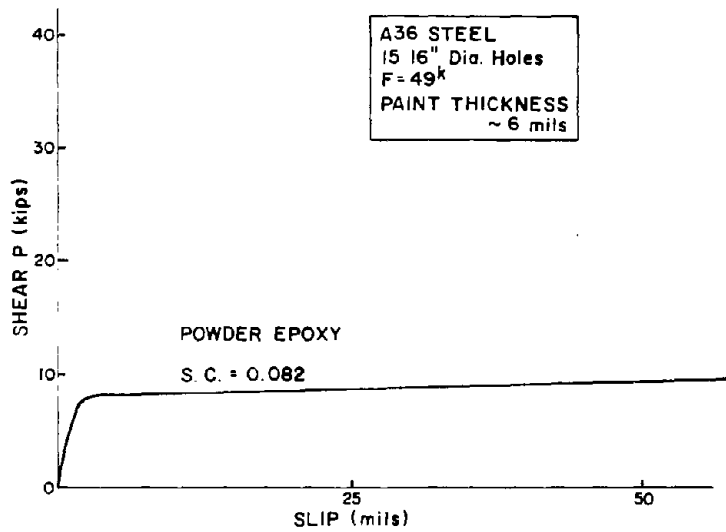


Figure 39. Typical load-slip curve (1 kip = 4.45 kN, 1 in. = 25.4 mm)

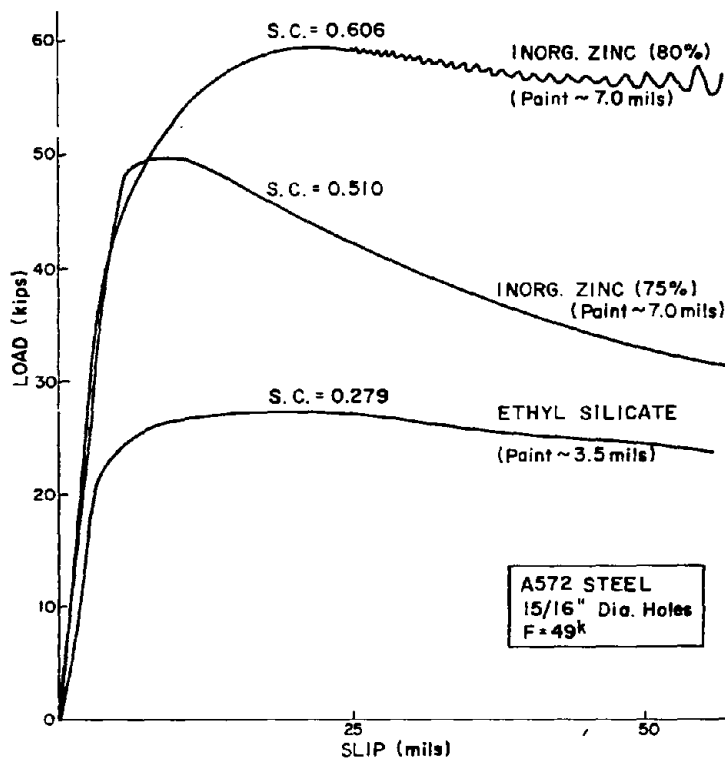


Figure 39a. Typical load-slip curves (1 kip = 4.45 kN, 1 in. = 25.4 mm)

slip load. When the slip load was reached, the specimen slipped slowly with a gradual drop in load. A larger reduction in load occurred in the case of the 75 percent zinc primer as compared to the 80 percent zinc primer. For the ethyl silicate base (0 percent zinc), there was no drop (reduction) in the slip load, while the flat plateau was formed. The 80 percent zinc primer showed a different behavior. After a total slip of about 30 mils to 40 mils, a banging noise was heard. The sound was low at first, and then became louder as slip progressed. This led to the cyclic pattern on the load-slip curve shown in Figure 40.

Investigation of the faying surfaces after testing indicated that damage to the inorganic zinc-rich primer was fairly uniform. Sometimes the damage was mostly around the holes. In case of the zincless paint (ethyl silicate base), slip caused the faying surfaces to become shiny and smooth. However, no damage occurred to the surface.

It is clear that the percentage of zinc considerably affects the slip resistance. The ethyl silicate base (0 percent zinc) provided the least ASC with a reduction in ASC of 55 percent compared to the best zinc primer. The reduction in zinc from 80 to 75 percent reduced the ASC by 18 percent. No tests were done to investigate the effect of the percentage of zinc between 0 and 75 percent. Therefore, it is felt that further study is needed in order to establish a direct mathematical relationship between the percentage of zinc and the ASC. These results also indicate that the paint should be agitated continuously, so that a reliable slip load can be obtained.

Additional Organic Zinc Primers. The factorial experiment discussed earlier established an average slip coefficient of 0.46 for one particular brand of organic zinc-rich primer. In order to get an indication of the scatter to be expected within one of the current surface classifications in the Bolt Specification, two additional organic zinc primers were tested. Both came from the same manufacturer; one paint had a phenoxy base and the other an epoxy base. The phenoxy base satisfied the more stringent California Specification of 90 percent zinc [41]. The supplier was different from the one used in the factorial experiment. Two painting groups separated by two weeks were established for each primer because the factorial experiment indicated that the slip coefficient was affected by the painting schedule. An equal number of slip specimens were prepared using 7/8 in. (22mm) A325 bolts and using the hydraulic bolt arrangement. The two types of tests were planned to provide a direct indication of bolt relaxation due to creep. The thickness of the paint which was applied in two coats was between 4 and 6 mils.

Originally 40 tests were planned, 2 paints  $\times$  2 types of tests  $\times$  2 paintings  $\times$  5 replicates. However, as will be discussed shortly, one of the painting groups showed an unusually low slip coefficient, so an additional ten specimens were tested. The average of five replicates and the standard deviations are summarized in Table 24.



Table 24. Average slip coefficients for additional organic zinc primer

Type of Test	Epoxy base			Phenoxy base			
	Group 1	Group 2	Total	Group 1	Group 2	Group 3	Total*
Real bolts	0.45 (0.032)**	0.38 (0.010)	0.41 (0.040)	0.14 (0.015)	0.30 (0.024)	0.26 (0.021)	0.28 (0.031)
Hydraulic bolts	0.44 (0.012)	0.42 (0.016)	0.43 (0.017)	0.12 (0.019)	0.30 (0.021)	0.32 (0.040)	0.31 (0.032)

\*Only Groups 2 and 3

\*\*Standard deviation

The scatter within each group is quite small; the coefficient of variation is usually less than 10 percent. Two groups show greater slip coefficients for the A325 bolted connections, and two groups show a reduced value. For each type of paint, one painting group showed an increase in slip coefficient while another group showed just the opposite. It is apparent that the bolted specimens give about the same result as the hydraulically bolted specimens. It can be concluded that creep in the organic zinc primer will not significantly affect the clamping force in an A325 bolt for paint thickness less than 6 mils. A similar observation is made in the next chapter related to creep studies.

Group 1 of the phenoxy base data is significantly lower than the other two samples. Apparently this was due to improper mixing and agitation of the primer during paint spraying. This incident points out one of the variables that can have a significant effect on the slip resistance which is beyond the control of the design engineer. The average of Groups 2 and 3 gave an ASC = 0.31, which is close to the ASC = 0.33 reported by others for this same paint (3 to 6 mils thick) and using a multi-bolt tensioning setup [42]

Both the hydraulic bolt and real bolt data indicate a significant difference between the ASC of the two primers. The phenoxy base which had a zinc content of 90 percent gave an average slip coefficient of 0.31 compared to 0.46 for the phenoxy (organic) zinc supplied by another manufacturer for the factorial experiment. The average of the epoxy zinc-rich paint is 0.43.

This study shows that paints within a particular category can show a wide variation in average slip coefficient. Further discussion of this matter is given at the end of this chapter.

#### Paint Curing Prior to Assembly

The current Bolt Specification does not have any guidelines related to the amount of curing required before contact surfaces are bolted. The

curing time experiments described in Chapter 2 show that paints vary in their curing requirements and in the factorial experiment periods from 3 days to 21 days were used before joints were assembled. Examination of the research on coated faying surfaces reported in Ref. 15 has shown that usually a significant period of time elapsed between painting and assembling. In most instances, at least a two-week period was used.

From a fabricator's viewpoint, it is best to assemble the connection as soon as practical to avoid the cost of storage of clip angles, bolts, etc., or the more costly field erection of such items. But, if the connection is assembled without the paint properly cured, the slip coefficient upon which the allowable bolt stress is based may not be achieved. It could be argued, however, that the paint can cure in place. To get some perspective on the problem a pilot study was undertaken on one organic zinc primer.

Twenty small single bolt compression slip specimens were blasted and painted with the phenoxy zinc-rich paint used in the previous section with a slip coefficient = 0.31. One coat, 2 mils dry, was applied first and one day later the final coat was applied to produce the same dry thickness. After applying the second coat, plates were bolted together one hour, five hours, one day, and two weeks after painting. The final dry paint thickness varied between 3 and 4 mils. Five specimens were prepared within each group. Previous slip data were developed using specimens which cured for a full two weeks prior to assembly. Two weeks after painting, three specimens from each group were tested. One month after painting, the remaining specimens were tested. Table 25 gives the average slip coefficients. A photo of one of the specimens bolted after 1 hr is shown in Figure 40. Note that some paint has been squeezed out at the top edge.

Table 25. Effect of curing time on the slip coefficient, phenoxy zinc primer

Time before assembly	1 hr	5 hrs	1 day	2 weeks
Tested after two weeks*	0.077	0.145	0.337	0.391
Tested after one month**	--	0.240	0.358	0.394

\*Average of three specimens

\*\*Average of two specimens

The two-week specimens gave greater slip coefficients than similar specimens in the previous section on the same paint (0.31 vs. 0.39). The data indicate that curing time prior to assembly has a significant effect on slip resistance. Five hours of curing produced only 57 percent of the slip resistance recorded for the two-week cured control specimens. Waiting an additional two weeks before testing gave an improved slip

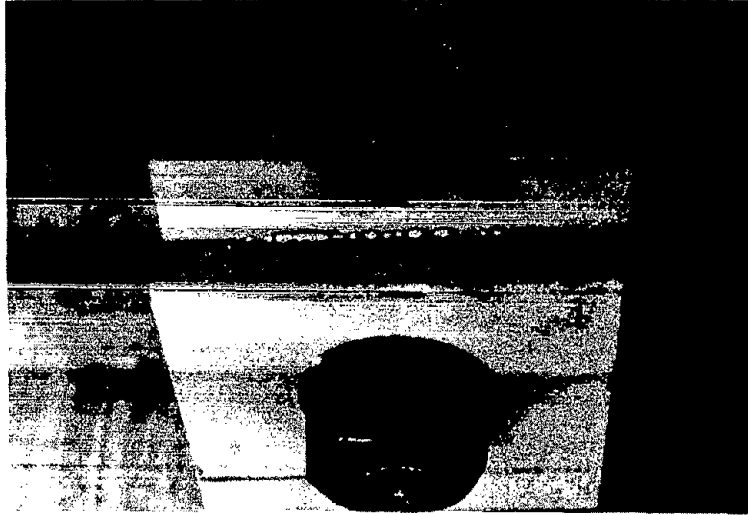


Figure 40. Test sample assembled one hour after painting

coefficient (0.240 vs. 0.145), but it is still less than the coefficient from the two-week control group (0.39).

The purpose of these tests was to establish if the curing time prior to assembly has a significant effect on slip resistance. For the particular paint product tested, the data indicate that the curing time is a significant variable which should be considered in developing design and fabrication procedures.

#### Tension Slip Tests

The slip data presented so far were derived mainly from the simple hydraulic compression slip test. In the previous section, a few single bolted connections were presented to obtain a measure of losses to be expected due to bolt relaxation. In this section, tests on tension-type connections of the type shown in Figure 41 are reported which had the following purposes:

- (1) Determine if the hydraulic bolt compression test setup gives the same results as a bolted tension arrangement.
- (2) Evaluate the bolt relaxation due to paint creep.
- (3) Develop some additional data on uncoated steel surfaces, both millscale and blasted.

Item 1 was considered by testing some A588 (weathering steel) millscale surfaces using tension specimens and hydraulic bolt specimens. These

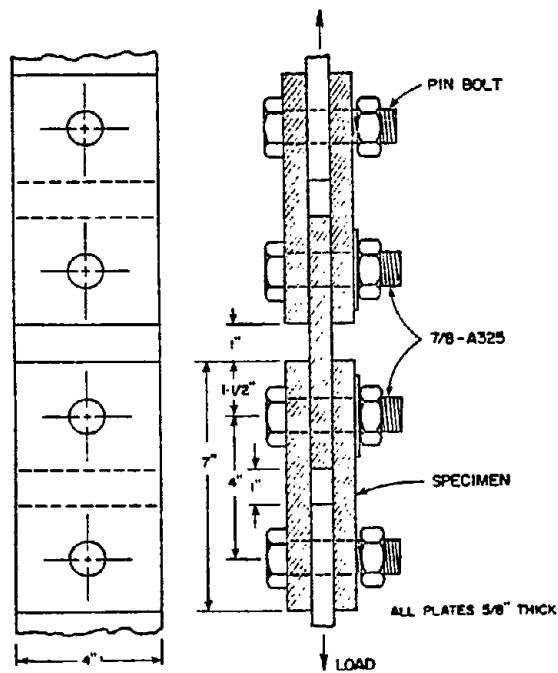


Figure 41. Bolted tension slip specimen (1 in. = 25.4 mm)

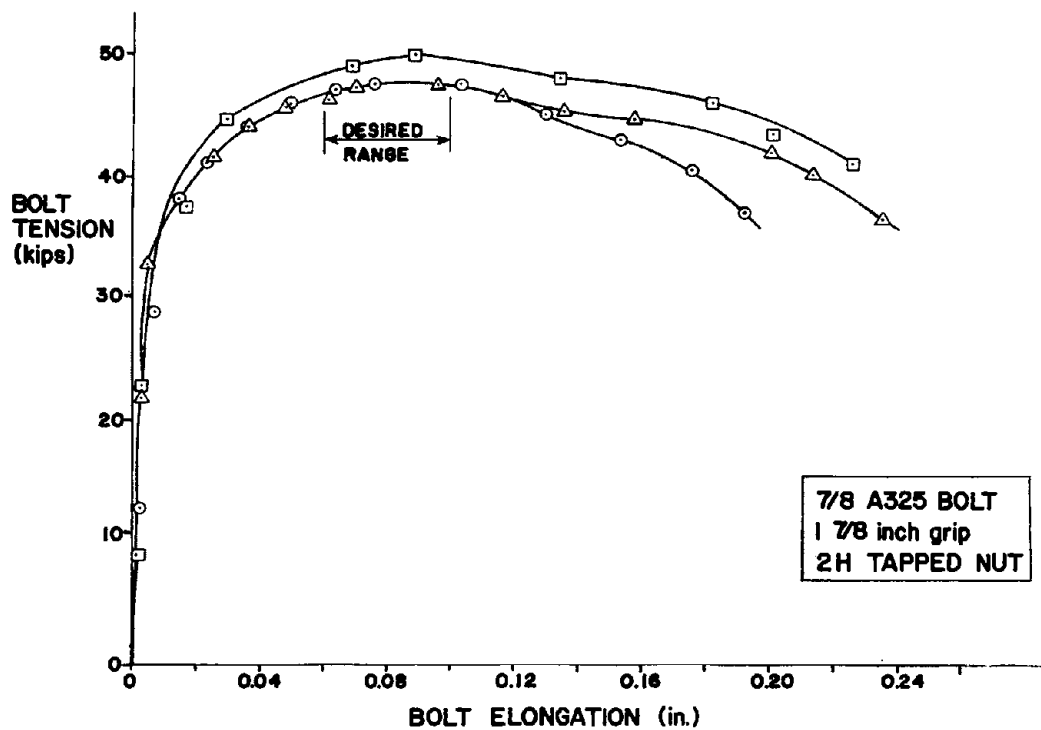


Figure 42. Bolt calibration curves for tension specimens (1 kip = 4.45 kN, 1 in. = 25.4 mm)

results, which are reported elsewhere [36], showed that the two methods give the same slip coefficients. This is reasonable, since there is very little bolt relaxation in a connection with uncoated steel contact surfaces. The tests presented herein will be concerned principally with Items 2 and 3.

Forty-two tension slip tests are reported, 22 on connections with painted faces and the remaining with millscale and blasted surfaces. In all the painted specimens, A572 steel was used but the hole size varied between 15/16 and 1-1/8 in. (24 and 29 mm). Since bolt relaxation was a principal variable, the paint thickness was high, and it was kept constant within the paint group:

- (1) organic zinc primer, 6 mils thick
- (2) organic zinc primer, 8 mils, with a 3 mil epoxy topcoat applied in two thin coats
- (3) inorganic zinc, 3 mils thick

The millscale and sand-blasted specimens were constructed from A36, A572, and A514 steel. All steel and paint are the same as those used in the factorial experiment presented earlier.

Test Setup and Procedure. The symmetrical design of the test specimen, shown cross-hatched in Figure 41, permits two independent slip load tests. The end fixture plate shown solid fits between the plates of the test specimen and is gripped by the tension test machine. The pin bolts are left loose for alignment.

The test specimens were assembled in an alignment jig using 7/8 A325 bolts (22mm) with 2H nuts. The 2H nuts were tapped in the laboratory because initial bolt calibration on the material supplied showed stripping-type failures and limited bolt ductility. This performance was due principally to very rough surfaces in the threads of the nut, which caused considerable friction in the threaded area. After the nuts were tapped, the performance improved considerably, although there was still some scatter in the bolt calibration curves, as shown in Figure 42. A hardened washer was used under the nut; in addition, an oversize washer was used on all specimens with 1-1/8 in. (29mm) holes.

For the purposes of the test program it was desirable to minimize scatter in the clamping force level. This was accomplished by installing the bolt so that the bolt elongation was in the range of 0.06 to 0.09 in. (1.5 to 2.3 mm). In general, from 5/8 to 7/8 turns were required from the snug position to get within the range. Bolt elongations were monitored as described in Chapter 2.

Slip gages were attached to the specimen with set screws, as shown in Figure 43. Linear potentiometers were located on each side of the specimen and connected in a manner to give the average of two readings. The gages measured the relative displacement (slip) between the interior plate and the two side plates. Both sides of the specimen were monitored

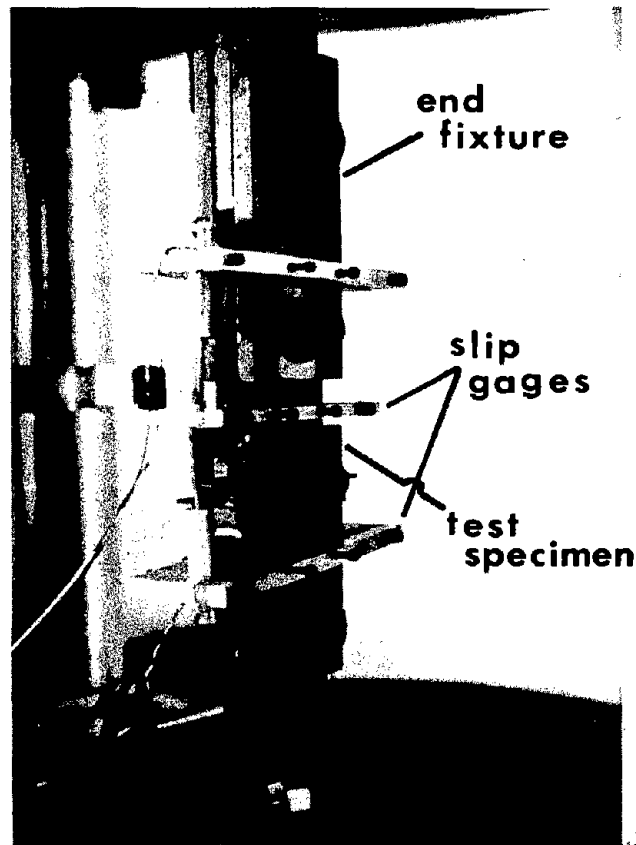


Figure 43. Test setup for tension slip tests

on two X-Y recorders and the load was applied until both sets of side plates slipped. Load rates and determination of slip load are the same as those used in previous sections.

Test Results. The slip coefficients for the 42 tests are given in Table 26. The initial clamping force in each specimen varied within the narrow range of 47.5 to 48.5 kips (211 to 216 kN), based on the measured installation elongations and the average of the three bolt calibrations given in Figure 41. The slip coefficient in Table 26 under the heading Slip Coefficient (no loss) is based on the initial clamping force. Changes in bolt elongations were recorded for the approximate two week period between the bolting of the specimen and the slip test. Specimens were painted approximately three months before testing.

The elongations showed considerable scatter, much of it due to experimental methods. In some instances the elongations at bolt installation were not measured carefully. A change in elongation of 0.001 in. (0.025mm) corresponds to a load of 5 kips (22 kN), and while the C frame

Table 26. Slip coefficients from tension test  
(1 in. = 25.4 mm)

Coating	Painted			Uncoated			
	Hole Size (in.)	Slip Coef. (No loss)	Slip Coef. (Average Loss)	Steel	Surface	Hole Size (in.)	Slip Coef. (No loss)
Organic Zinc 6 mils thick	15/16	0.48	0.56	A36	Millscale ↑ ↓ A572	1	0.29
	15/16	0.52	0.61	A36		1	0.41
	1	0.40	0.46	A572		15/16	0.20
	1	0.48	0.56			15/16	0.21
	1	0.43	0.50			1	0.23
	1	0.47	0.55			1	0.21
	1-1/8	0.48	0.56			1-1/8	0.24
	1-1/8	0.41	0.49				
Average	0.46	0.54	A572	Millscale	1-1/8	0.21	
	(0.041)*	(0.048)*		A572 Average		0.22 (0.013)*	
Hydraulic bolt (3 tests)		0.55					
Organic Zinc (8 mils) plus Epoxy Topcoat (3 mils)	15/16	0.34	0.41	A514	Millscale ↓ Blasted ↑ A572	1	0.30
	15/16	0.38	0.47	A514		1	0.30
	1	0.31	0.38	A36		1	0.70
	1	0.33	0.40	A36		1	0.75
	1	0.24	0.30	A572		15/16	0.70
	1	0.33	0.39			15/16	0.61
	1-1/8	0.32	0.39			1	0.75
	1-1/8	0.34	0.42			1	0.77
	1-1/8	0.32	0.40	A572		1-1/8	0.63
	Average	0.32	0.40	A572		Blasted	1-1/8
	(0.039)*	(0.048)*		A572 Average		0.71 (0.069)*	
Hydraulic bolt (3 tests)		0.42					
Inor- ganic Zinc (3 mils)	1-1/8	0.52	--	A514	Blasted ↑ A514	1	0.61
	1-1/8	0.54	--	A514		1	0.62
	1	0.49	--				
	1	0.48	--				
	1	0.41	--				
	1	0.42	--				
	Average	0.48	--				
	(0.053)*						
Hydraulic bolt (3 tests)		0.55					

\*Standard deviation

extensometer (see Figure 14) was sensitive to  $\pm 0.0001$  in. (0.0025mm), the reliability was probably closer to four times this value. Evaluation of each connection's change in elongation made it apparent that some judgment would be required to make meaningful use of the results. First, any change  $\pm 0.0004$  in. (0.0102mm) or less was considered no change, and, therefore, neglected. Second, a few data which had experimental errors were discarded. This was determined by noting how the slip load of the particular sample varied from the other tests with the same surface.

Each group of specimens showed fairly consistent results within its sample without considering loss of clamping force (the three painted groups showed coefficients of variation of about 10 percent), so it would be expected that any loss in clamping force would be similar for all the bolts within the particular group. For example, in the organic zinc specimen, the ASC = 0.46 with a standard deviation of 0.041 without considering clamping force. When three of the data are eliminated as described above and are assumed unchanged, but the slip coefficient of the remaining five specimens is calculated considering the undivided losses which range up to 13.5 kips (60.0 kN), the ASC becomes 0.516 with a standard deviation of 0.107. This approach gives a coefficient of variation close to 20 percent. Consequently, it was decided to present the data assuming that each bolt has a reduction in force corresponding to the average of the sample.

In Table 26, the slip coefficients calculated on this basis are shown under the heading, Average Loss. For the organic zinc sample, the average slip coefficient becomes 0.54, because of the average loss of clamping force equal to 7.1 kips (31.6 kN) (15 percent of the initial clamping). The ASC is very close to the hydraulic bolt control specimen (3 tests) in which the ASC = 0.55. Similarly, the thickest coating tested, 8 mils of organic zinc plus 3 mils of epoxy topcoat, showed an average loss equal to 20 percent. The losses for the 3 mil inorganic zinc and the uncoated surfaces were too small (< 4 percent) to be reliable, so are not shown in the tables.

The average slip coefficient (ASC) for the organic zinc paint considering average losses of 20 percent, is within 5 percent of the control specimens. The bolted inorganic zinc specimens gave an ASC = 0.48, while the control specimens gave ASC = 0.55. Probably some of the difference is due to small losses in clamp forces which were not considered; the remainder is typical scatter within a small sample.

The millscale specimens gave slip coefficients close to the average of 0.34 published in Ref. 15. The results on A572 Grade 50 steel are at the low end of the data histograms [15] for millscale, where only 6 percent of the total sample is recorded. The six connections tested all came from the same heat of steel, so no broad conclusions can be reached. The blasted specimens showed uniform behavior almost independent of the yield strength. The A514 does show an ASC 13 percent below that for



A572 steel, but since there are only two samples the difference is attributed to experimental scatter. Earlier in this chapter it was shown by statistical analysis of the factorial experiment that A514 and A572 material were not significantly different in their slip coefficients.

### Full-Size Connections

Eleven full-size truss-type connections, as shown in Figure 44, were tested for the slip load. Compression load was applied by a test machine to the vertical W10x77 member, while the horizontal W10x77 rested on the base of the test machine. Four different joints were fabricated; after the first tests they were sand-blasted and reused twice. The purposes of the full-size tests were to provide slip data for comparison with the small slip tests, monitor any losses in clamping force due to compressive creep of the paint, and determine any difference between laboratory and fabricator installation techniques.

Eight of the connections were bolted in the laboratory by graduate students. Three different paint systems were applied, inorganic zinc primer, organic zinc primer, and organic zinc with an epoxy topcoat. All paints were the same type as those used in the factorial experiment, but in some instances the paints were from different lots. One sand-blasted connection was also tested.

Three sand-blasted specimens were bolted up by fabricators. Two connections were sent to Fabricators A and B, both of whom would be considered large fabricators handling steel fabrication for construction throughout the U.S. and some foreign countries. Through the cooperation of the engineering departments of these fabricators, assurances were made that no special techniques other than those which are shop practice would be used. The connection bolts were taken from a single lot and supplied to the fabricators. These bolts had been previously prepared with milled ends and countersunk holes as described in Chapter 2 in the section on bolt calibration. Each bolt was numbered and bolt length recorded before shipment to the fabricator so the clamping force could be determined after installation. Because of the special end condition of the bolts supplied, the true purpose of the installation was obviously known by the installers. The only instructions given to the installers was that the joint was a friction-type connection and bolts should be installed in the normal fashion for such connections.

A final specimen was connected using torque-controlled Lejune fasteners. These were installed in the laboratory by a field representative of the supplier using fasteners from a single lot. These calibration tests were performed to establish that the clamping force of the fastener was 42.7 kips.

In the following sections data collected on bolt installation forces and bolt shortening will be presented along with the slip test results on these connections and a comparison with the Bolt Spec.

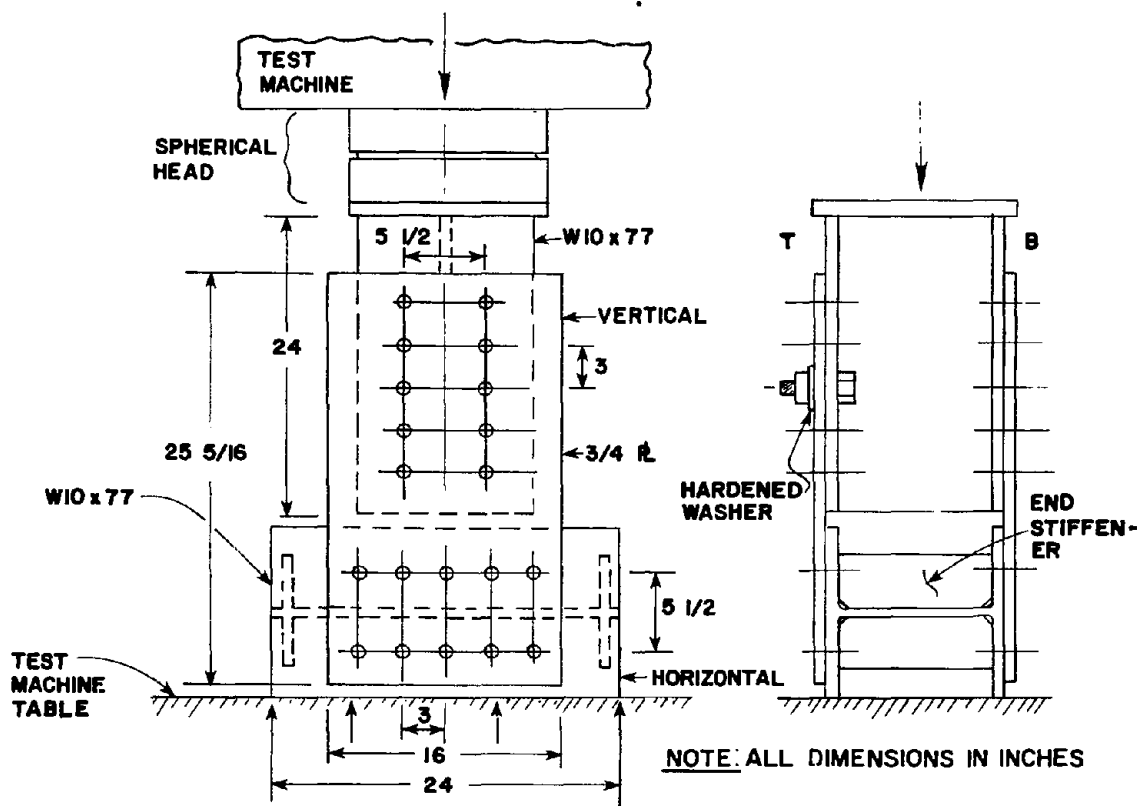
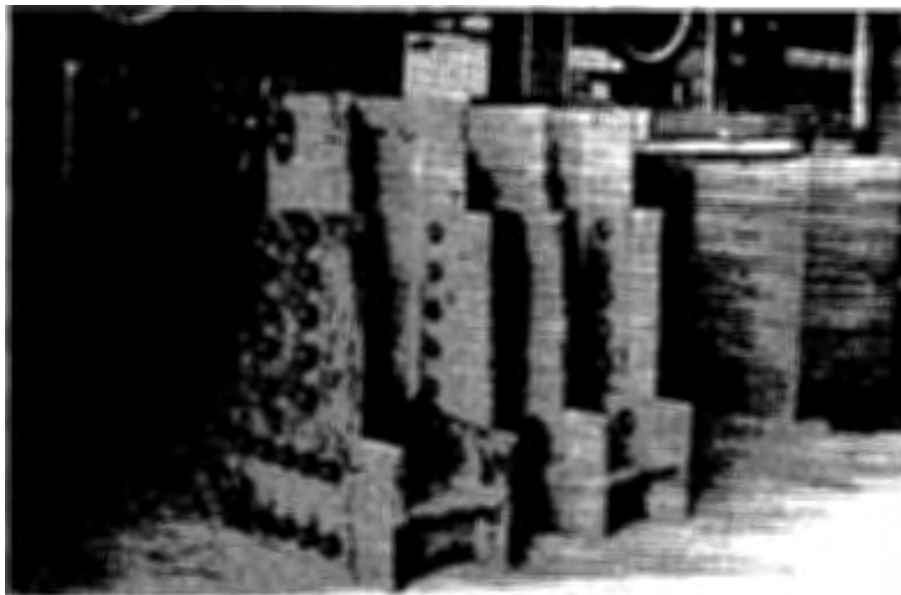


Figure 44. Full-size slip connection  
(1 in. = 25.4 mm)

Bolt Clamping Forces, Laboratory Connections. Each group of ten bolts in the connection was numbered and identified as shown in Figure 44; Vert (T), Horz (T), Vert (B), and Horz (B). In the connections tightened in the laboratory, three or four of the ten bolts in each group were specially prepared to monitor the bolt forces as discussed previously. Within the financial and time constraints of the project it was not practical to monitor all the bolts. The three or four bolts were widely dispersed within each ten bolt pattern so their response would be representative of the group.

The laboratory connections were used mainly to correlate with the small slip tests and to determine the magnitude of bolt relaxation due to paint creep. Therefore, it was desirous to keep scatter in the clamping force to a minimum. Bolts were installed to 3/4 turn from snug so all bolts would be in the flat plateau of the bolt-elongation response curve, as shown in Figure 45. Normal installation procedure for the grip length would have required 1/3 turn from snug [30]. During the installation, the bolts were first taken to 1/3 turn and bolt elongations recorded before tightening to the 3/4 turn level. All bolts in a group were snugged and some resnugged before each bolt was tightened to the desired level.

Histograms of bolt elongation were developed for the 12 or 16 bolts in each connection. Two typical plots are shown in Figures 45 and 46, along with the bolt calibration curves. Separate calibrations were conducted for standard 15/16 in. holes (24mm) and the oversize 1-1/16 (27mm) holes. The clamping force data at 1/3 turn are summarized in Table 27.

Table 27. Measured clamping force for 1/3 turns  
(1 kip = 4.45 kN, 1 in. = 25.4 mm)

Coating	Size of Hole (in.)	Number of Bolts Measured	Maximum Torqued Tension		Col. (5) 39 kips	Installed Bolt Tension	
			Strength (kips)	Mean Tension 1/3 turn (kips/bolt)		(kips/bolt)	Col. (7) 39 kips
(1)	(2)	(3)	(4)	(5)	(6)	(7)	(8)
Organic Zinc	15/16	32	52.0	47.8 (0.85)*	1.22	51.7	1.33
Organic Zinc	1-1/16	16	54.6	46.2 (1.00)	1.18	52.5	1.35
Or. Zn.+Epoxy	15/16	16	52.0	47.7 (0.40)	1.22	51.5	1.32
Inorg. Zinc	15/16	24	52.0	47.1 (0.90)	1.21	51.5	1.32
Inorg. Zinc	1-1/16	12	54.6	45.6 (1.50)	1.17	52.0	1.33
Sand-blasted	15/16	16	52.0	46.4 (3.50)	1.19	51.3	1.32
				Average	1.20		

\*Standard deviation

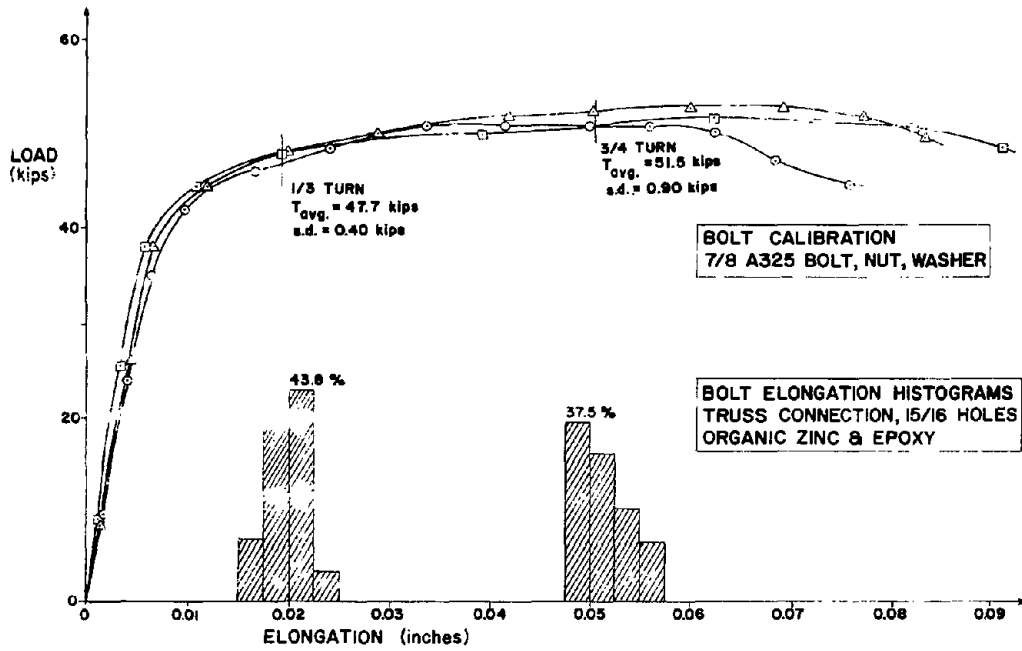


Figure 45. Bolt force histograms and calibrations  
(1 kip = 4.45 kN, 1 in. = 25.4 mm)

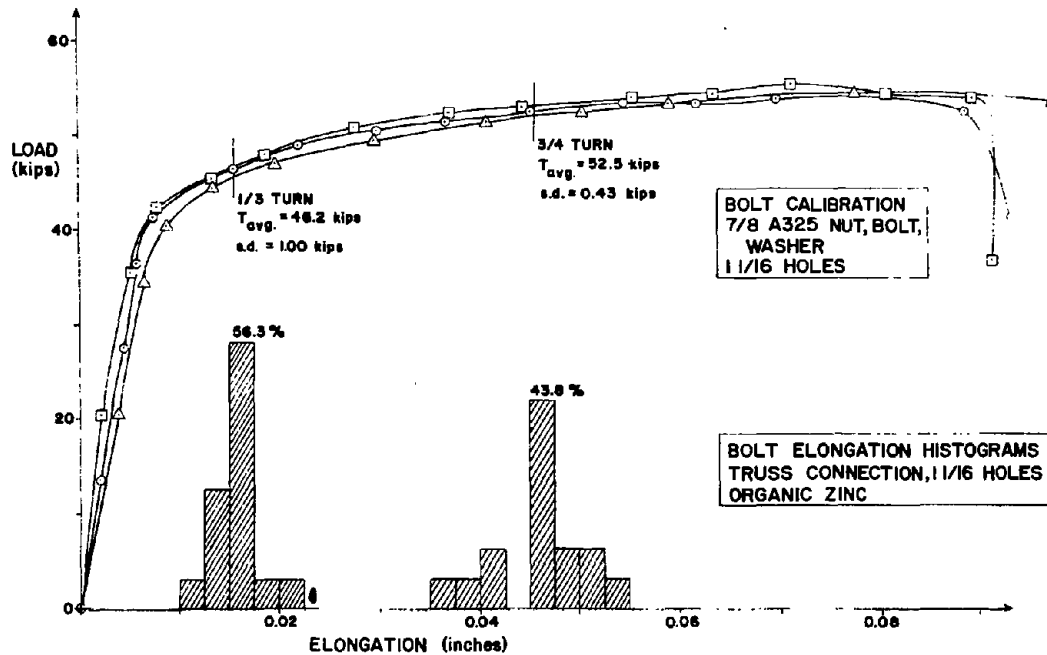


Figure 46. Bolt force histograms, oversize holes  
(1 kip = 4.45 kN, 1 in. = 25.4 mm)

The average was 20 percent of the minimum specified. The standard deviation is quite small, except for the sand-blasted connection. This greater scatter was due to improper initial snugging; the bolts were not checked for looseness after the initial snug. As expected, the installed bolt tension shown in Col. (7) of Table 27 showed very little scatter because of the installation method (3/4 turn).

About fifteen minutes after the bolts were installed, a new set of bolt elongation data was obtained to determine if any immediate bolt relaxation could be detected. The inorganic zinc-rich specimens were then stored under no load for two weeks and elongations again measured just prior to the slip test. Connections with organic zinc paint were monitored each week for two weeks. The histograms of bolt elongation for each paint and hole size are given in Figures 47 through 51. There is a large scatter in the data, some of which is due to experimental sensitivity. The bolt elongation data should be reliable to  $\pm 0.0003$ . The histograms take all the data for a joint, or, in the case of replicates, two joints together.

In Table 28, the bolt relaxation is summarized for each ten bolt group within the connection. Measured paint thickness on the faying surface is also presented to determine if there is any experimental correlation between the paint thickness and creep. No correlation is evident, mainly because the measured bolt shortening is rather small and the experimental sensitivity, 0.0003 in. (0.01 mm), corresponds to 2 kips (8.9 kN). For all painted surfaces except the organic zinc with epoxy topcoat, the apparent measured shortening is close to the experimental sensitivity. The shortening that does take place occurs within the first week after bolting.

Bolt Clamping Forces, Fabricator Connections. All forty bolts in each of the connections for Fabricators A and B were machined to monitor the bolt elongation using the C-frame extensometer. A new lot of bolts was used for this portion of the program. The calibration curves for three 7/8 A325 bolts (22mm) are given in Figures 52 and 53, along with the histograms of the measured elongations. The connections had sand-blasted surfaces but they were not sand-blasted at the same time as the laboratory sand-blasted specimens discussed in the previous section. Fabricator A developed 23 percent greater clamping force than Fabricator B. The average clamping force developed by Fabricator B did not reach the minimum specified 39 kips (174 kN).

The following items were observed during the installation process:

- (1) The connection was not brought to the snug position.
- (2) The bolt head was not prevented from turning.
- (3) Wrenches were not calibrated for the bolts provided, even though the installation method was sort of calibrated wrench.
- (4) One wrench had no adjustment for controlling torque.
- (5) The bolts were installed by "sound". The operator could "tell" when they were tight enough.

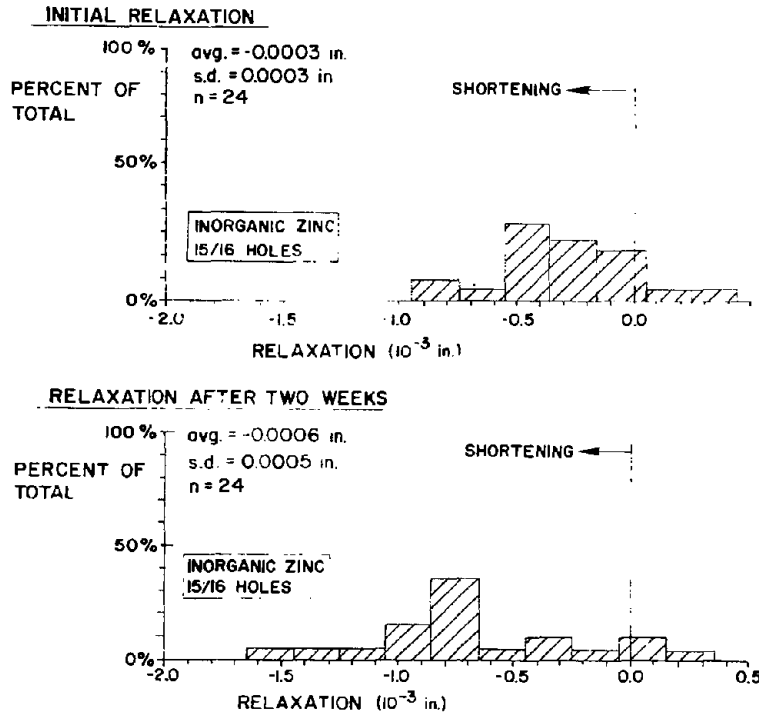


Figure 47. Bolt relaxation histograms, inorganic zinc, 15/16 holes (1 in. = 25.4 mm)

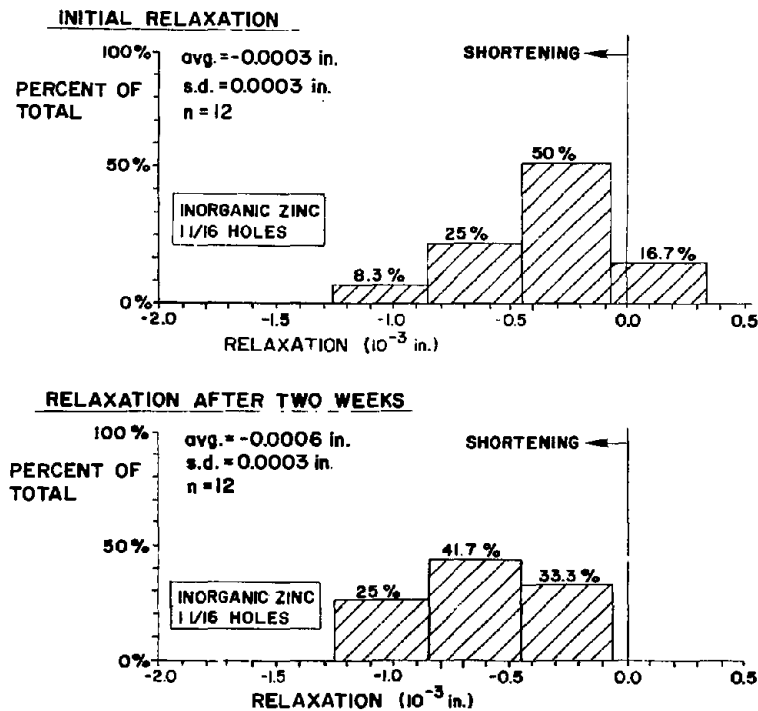


Figure 48. Bolt relaxation histograms, inorganic zinc, 1-1/16 holes (1 in. = 25.4 mm)

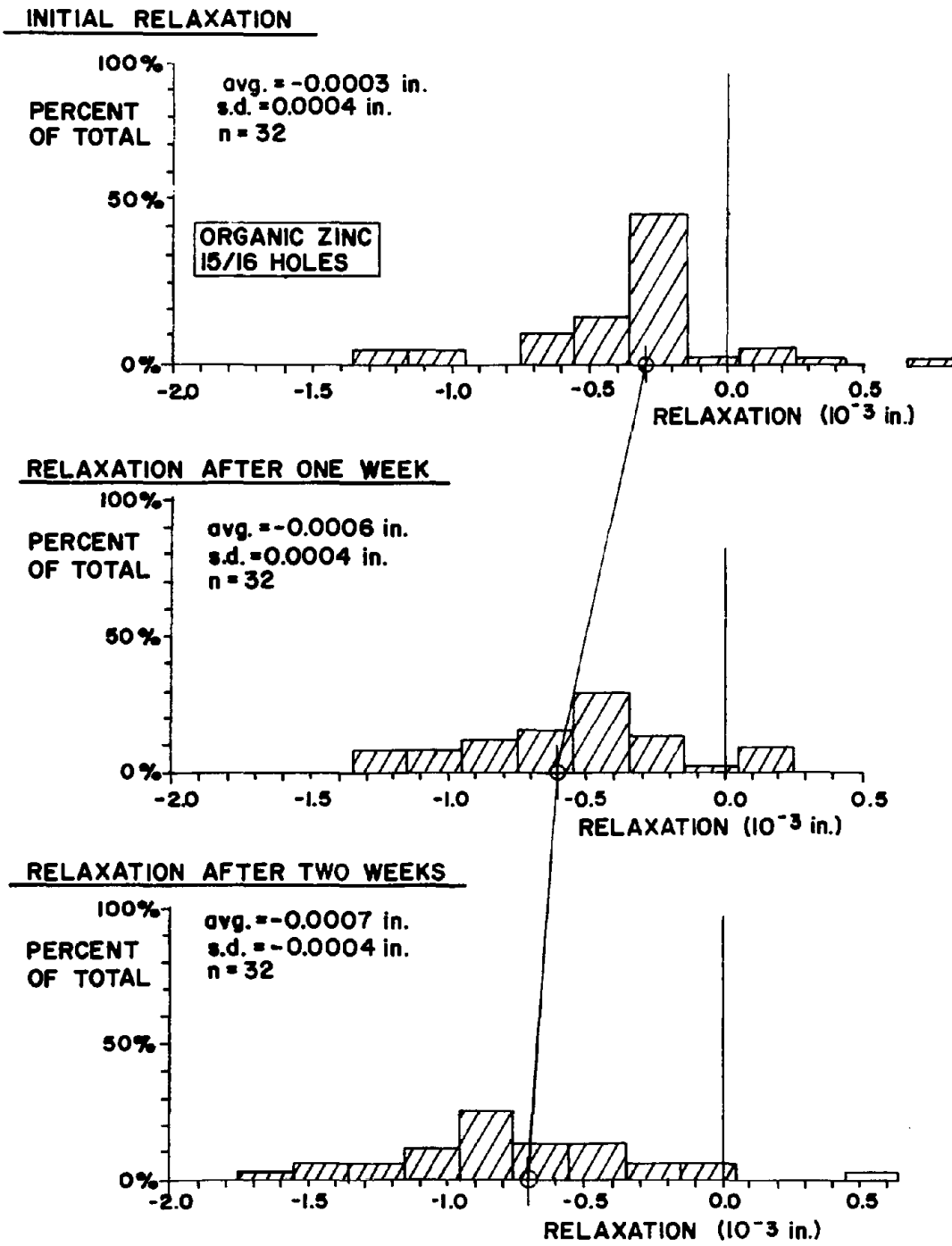


Figure 49. Bolt relaxation histograms, organic zinc, 15/16 holes (1 in. = 25.4 mm)

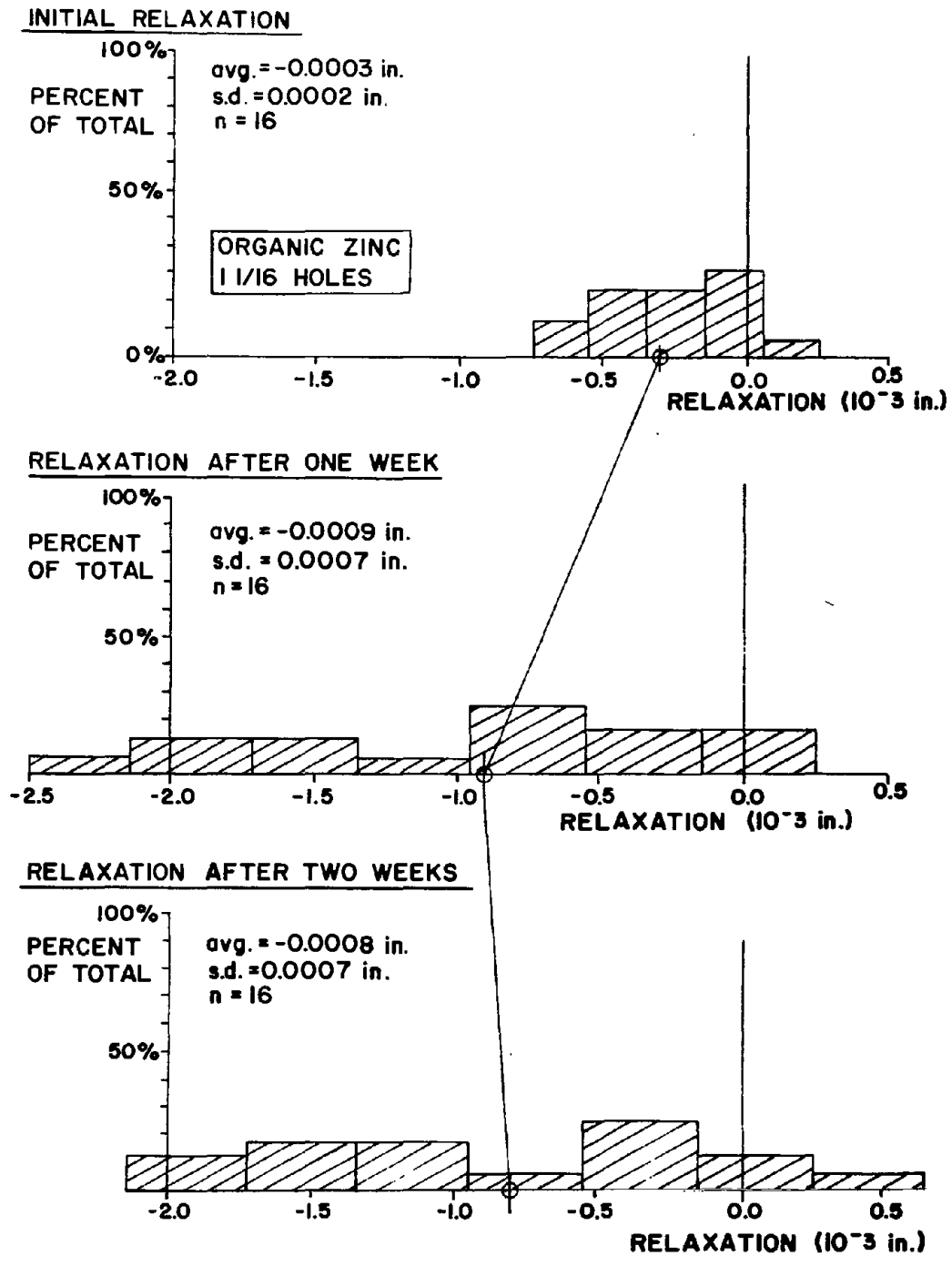
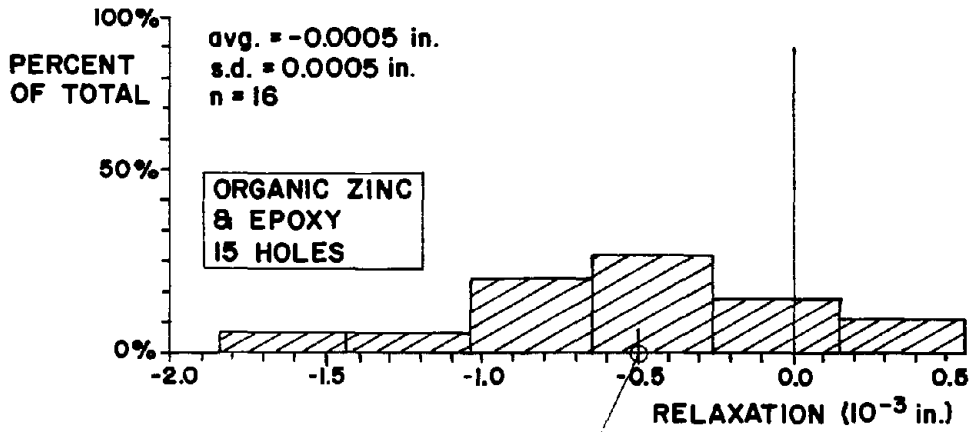


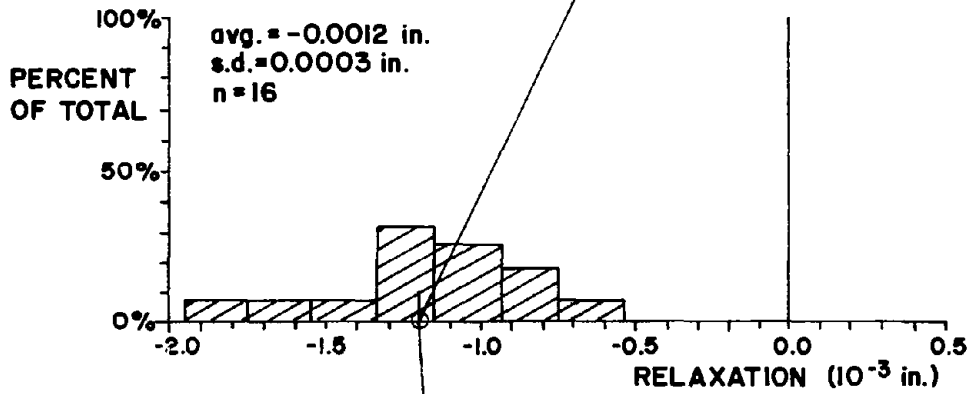
Figure 50. Bolt relaxation histograms, organic zinc, 1-1/16 holes (1 in. = 25.4 mm)



**INITIAL RELAXATION**



**RELAXATION AFTER ONE WEEK**



**RELAXATION AFTER TWO WEEKS**

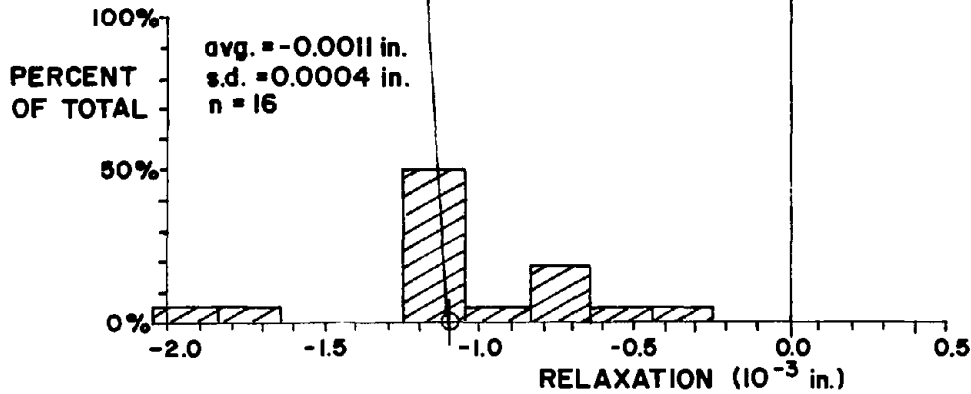


Figure 51. Bolt relaxation histograms, organic zinc + epoxy  
(1 in. = 25.4 mm)

Table 28. Paint thickness and bolt shortening data  
(1 mil = 0.001 in. = 0.025 mm)

Test No.	Contact Surface Hole Size (in.)	Paint thickness and bolt shortening averages for each zone (mils)				Average Paint Thickness Each Specimen (mils)	Average Bolt Shortening (In. $\times 10^3$ )
		Member	Vert(T)	Horz(T)	Vert(B)		
1	Inorganic Zinc	PL	2.9	2.9	6.3	5.9	3.6
		WF	1.9	3.9	2.7	3.1	
	15/16		0.5	--	1.0	--	0.8
2	Inorganic Zinc	PI	5.2	3.5	2.9	5.2	3.1
		WF	2.2	1.7	2.5	2.2	
	15/16		0.6	1.1	0.3	0.7	0.7
3	Inorganic Zinc	PL	4.1	3.0	2.3	2.1	3.1
		WF	2.4	3.4	3.3	4.4	
	1-1/16		0.6	0.4	0.9	0.5	0.6
4	Organic Zinc	PL	4.1	3.7	4.6	4.4	4.2
		WF	3.9	3.8	4.5	4.9	
	15/16		1.2	0.7	0.9	0.8	0.9
5	Organic Zinc	PL	4.5	3.8	4.4	4.6	4.4
		WF	5.1	4.0	4.1	4.8	
	15/16		0.8	0.6	0.6	0.8	0.7
6	Organic Zinc	PL	4.9	3.9	4.0	3.7	4.2
		WF	4.7	3.7	4.4	4.7	
	1/16		1.3	0.7	0.9	0.5	0.8
7	Or. Zinc + Epoxy	PL	3.8+2.4	3.6+3.1	5.2+2.1	3.7+2.3	4.1 + 2.1
		WF	4.0+1.9	4.1+2.0	4.3+1.6	4.1+1.5	
	15/16		1.4	1.2	1.1	0.6	1.1

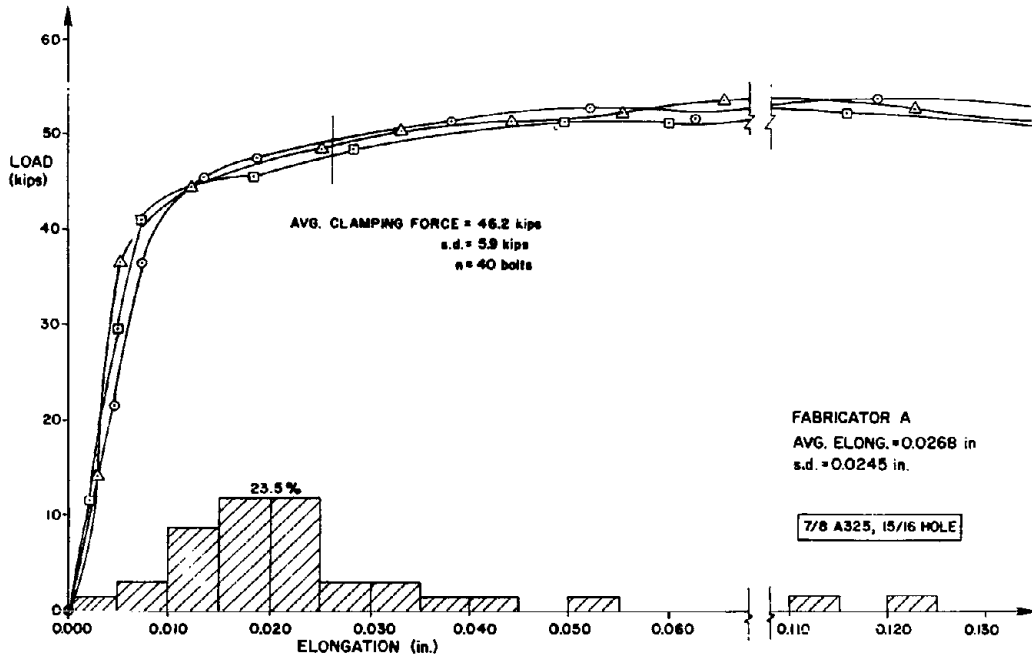


Figure 52. Bolt tightening histograms, Fabricator A

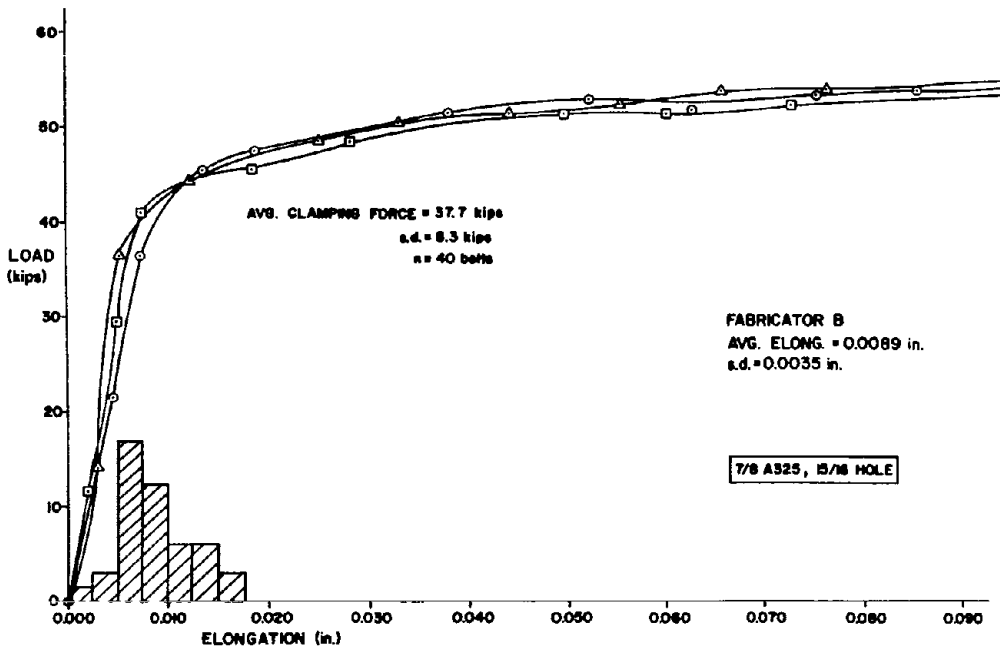


Figure 53. Bolt tightening histograms, Fabricator B

- (6) There was a general unawareness of the Bolt Specification, and especially the required tightening procedure.

The Lejune fasteners installation followed the Bolt Specification. Bolts were first snugged with a small impact wrench and then the special wrench installed the bolts starting from the center of a bolt pattern and working out towards the ends. Because the bolt has a twistoff end, no method was readily available to determine the actual installed clamping forces. It will be assumed that the clamping force is the same as that developed at twistoff in the bolt calibration, 427 kips (190 kN).

Slip Tests. The connections were loaded in a 600 kip (2670 kN) test machine and slip of the vertical member and side splice plates monitored by linear potentiometers, as shown in Figure 54. The load-slip response was monitored on two X-Y recorders. Each test connection provided two independent slip loads, slip on both vertical bolts and slip on the horizontal bolts. It is also possible for slip to occur with one vertical group and one horizontal group. The results of the eleven full-size tests are given in Table 29. In Col. (7) of the table, the symbol V refers to slip of the vertical W10x77 and H means the gusset plates have slipped at the horizontal W10x77. V-H means the slip occurred in one vertical group of bolts and the horizontal group on the opposite side.

In Test 8, the load in the connection with forty bolts reached the capacity of the machine without the occurrence of slip. The specimen was unloaded and two bolts (No. 1 and 2 in Figure 44) were removed from both sides of the connection. Although there were only 16 bolts connecting the vertical member to the plates, the first slip occurred on a diagonal (V-H) at 533 kips (2370 kN), which had 18 bolts in the slip plane. Further loading could not produce the second slip load so the specimen load was reduced and an additional bolt, No. 5, removed from the horizontal row. The slip load for the 17 bolts in the slip load was 542.

The theoretical slip load in Col. (8) was determined by the following equation:

$$\text{Theo. slip load} = \text{S.C.} \times (\text{initial clamping force} - \text{loss}) \times \text{No. of bolts}$$

The allowable load is based on the 1978 Bolt Specification. When slip control specimens were not tested, the average slip coefficient was taken from Ref. 16. The control slip coefficients shown in Tests 1 through 7 are averages from three hydraulic bolt control specimen tests. The ratio in Col. (11) represents the comparison between the small slip test and the full-size connection. Column (12) is a measure of the factor of safety, but recall that the clamping force is higher than usual because of the 3/4 turn tightening procedure adopted. If the slip load is directly related to the clamping force, then the maximum load would have been less if the recommended 1/3 turn approach was used. For example,

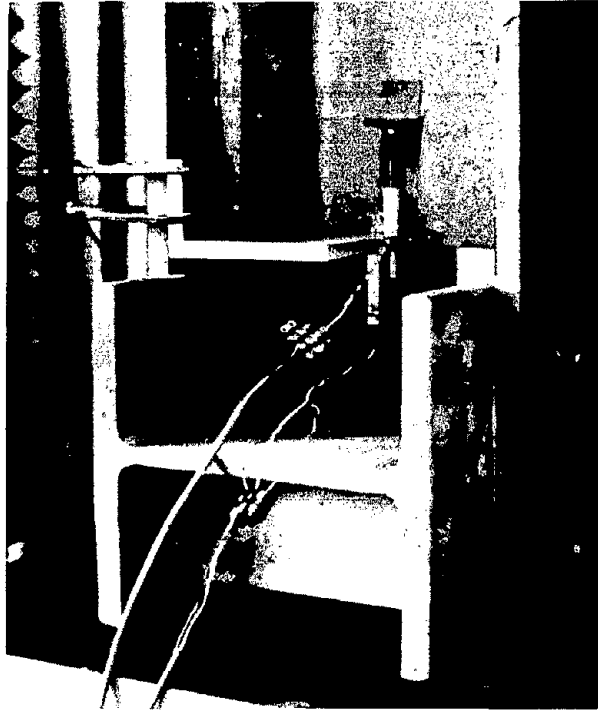


Figure 54. Slip gages for truss connections

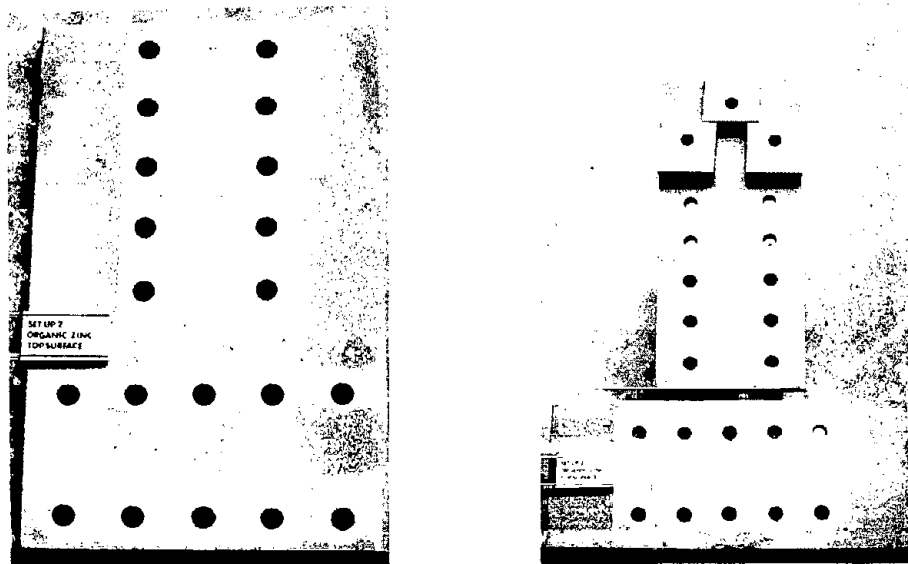


Figure 55. Contact area for full-size connection

Table 29. Test results, full-size specimens

Test No.	Contact Surfaces (Control slip coefficient)	Hole Size (in.)	Avg. paint thickness (mils)	Avg. Installed Clamping Force/bolt (kips)	Avg. Loss in Clamping Force/bolt (kips)	Slip Test Load (kips)	Theo. Slip Load (kips)	Allow. Load (kips)	Col. 7 Col. 8	Col. 7 Col. 9
(1)	(2)	(3)	(4)	(5)	(6)	(7)	(8)	(9)	(10)	(11)
1	Inorganic Zinc (S.C. = 0.55)	15/16	4	51.4	5	V 466 H	513	354	0.91	1.32
2	Inorganic Zinc (S.C. = 0.55)	15/16	3	51.5	4	V 446 H 446	525 525	354 354	0.85 0.85	1.26 1.26
3	Inorganic Zinc (S.C. = 0.55)	1-1/16	3	52.0	4	V-H 434 H-V 489	531 531	300 300	0.82 0.92	1.47 1.63
4	Organic Zinc (S.C. = 0.37)	15/16	4	51.8	5	V 445 H 499	346 346	252 252	1.29 1.44	1.77 1.98
5	Organic Zinc (S.C. = 0.37)	15/16	4	51.6	4	V 438 H 470	352 352	252 252	1.24 1.34	1.74 1.87
6	Organic Zinc (S.C. = 0.37)	1-1/16	4	52.5	5	V 393 H 462	352 352	216 216	1.12 1.31	1.82 2.13
7	Organic Zinc+Epoxy Topcoat (S.C. = 0.24)	15/16	4 + 2	51.5	7	V 229 H 242	214 214	--- ---	1.07 1.13	---- ----
8	Blasted- Laboratory (*ASC = 0.52)	15/16	-	51.3	-	V/H (18)**533 H/V (17)**542	480 453	298 281	1.11 1.20	1.78 1.93
9	Blasted-Fabricator A (*ASC = 0.52)	15/16	-	46.2	-	H 454 V 511	480 480	330 330	0.94 1.06	1.38 1.55
10	Blasted-Fabricator B (*ASC = 0.52)	15/16	-	37.7	-	V 288 V 356	392 392	330 330	0.73 0.91	0.87 1.08
11	Blasted - Lejune	15/16	-	42.7	-	V-H 413 H-V 463	444 444	330 330	0.93 1.04	1.25 1.40

\*Average from Ref. 16.

\*\*Number of bolts.

Test No. 1 would have a factor of safety of  $1.32 \times (47.1/51.4) = 1.21$ . No values of allowable load are shown for the epoxy topcoat since the Bolt Specification does not address the paint category.

Specimens with coated surfaces were disassembled upon completion of the test. A typical surface is shown in Figure 55. The significant contact zone was confined to a small area around the hole similar in size to the small compression specimen. This reinforces the premise that the slip coefficient from the small specimens can predict slip load in large structures.

Discussion of Full-Size Tests. The comparison between test and theory given in Col. (10) of Table 29 is quite reasonable except for the organic zinc tests which have been significantly underestimated. This may be due to some unrepresentative control slip coefficients. The average of three control organic zinc primer slip coefficients was 0.37. In Ref. 16, only 7 slip coefficients out of 106 fall below this level. If the average organic zinc slip coefficient of 0.464 as reported in Ref. 16 is used, the theoretical slip load becomes 434 kips (1933 kN), which is in good agreement with the tests.

The factor of safety for the inorganic zinc specimen is low (see Col. 11, Table 29). In fact, if the bolts had been installed by the turn-of-nut method using 1/3 turn from snug, the average factor of safety for the 6 inorganic zinc tests would be 1.25. This average is consistent with the factor of safety against the mean derived by Fouad [16] using the results in Ref. 15. Fouad found that the factor of safety was only 1.24 for inorganic zinc, because a 10 percent probability of slip criteria was used to develop the Bolt Specification with no allowance for a factor of safety against the mean of the data.

The results from connections bolted by the fabricators pointed out the shortcomings of using only laboratory data to determine average slip loads. Consideration must be given to those factors which can reasonably be expected to occur in practice. The Lejune bolts performed satisfactorily. They developed a clamping force 12 percent above the minimum specified and with a slip coefficient of 0.52, close to the 0.49 published by Fisher [15], resulting in a factor of safety of 1.25. This is actually consistent with the current Bolt Specification which has low factors of safety against the mean data for certain surfaces, as will be shown in the next section.

These full-size tests showed that a control sample larger than three should be used to develop the slip coefficients. Also, in the organic zinc with epoxy topcoat which had a thickness of 6 mils, the loss in clamping force due to paint creep was significant (> 10 percent). This is consistent with the data discussed in the previous section on tension slip tests, and also the creep tests by others [6,42].

The Bolt Specification requires a 15 percent reduction in allowable stress when oversize holes are used in the outer plies of a friction connection. This is due to a reported reduction in clamping force when turn-of-the-nut method is used to install the bolt, because of head dishing and local compression of the plates. The data for 1/3 turn shown in Table 27 gives only a 3 percent reduction in clamping force, which is insignificant. There is no reduction at the installed tension (in fact there is a slight increase) because a 3/4 turn was used.

### Recommendations

In the full-size tests, it was shown that in some instances, the factor of safety against slip is less than 1.45, even though the bolts are properly tightened and the slip coefficient is reasonably close to the value assumed in the development of the Bolt Specification. This is to be expected because Fouad [16] has shown that the Bolt Specification has low factors of safety for some surface coating, as shown in Table 30. Column (5) in the table is calculated as follows:

$$S.C. \times 1.13 \times \text{Min. specified clamping force} \div \text{Area} = \text{Shear Stress}$$

Table 30. Safety factor for different surface treatments  
(1 ksi = 6.9 MPa)

Surface Treatment	Slip Coeff.*		Specs Allowable Shear Stress (A325) ksi (4)	Theo. Shear Slip Stress (A325) ksi (5)	F.O.S. (6)
	Avg.	Std. Dev.			
(1)	(2)	(3)			
Blast-cleaned	0.493	0.074	27.5	36	1.31
Organic zinc-rich paint	0.350	0.035	21.0	26	1.22
Inorganic zinc-rich paint	0.500	0.050	29.5	37	1.24
Vinyl primer	0.270	0.023	16.5	20	1.20

\*Values recommended by Fisher and Struik.

The Bolt Specification relies on a clamping force 13 percent higher than the minimum specified, which is typical of the calibrated wrench tightening method [15]. Even with this reliance, the factors of safety are as low as 1.20. This situation occurs because only a 10 percent probability of slip concept was used to develop the Bolt Specification [30]. The Bolt Specification for friction-type shear connections is reproduced as Table 31. There is no specified factor of safety against the mean. It



Table 31. Allowable working stress, ksi, based upon surface condition of bolted parts, for friction-type shear connections

Class	Surface Condition of Bolted Parts	Standard Holes		Oversize Holes and Short Slotted Holes		Long Slotted Holes	
		A325	A490	A325	A490	A325	A490
A	Clean mill scale	17.5	22.0	15.0	18.5	12.5	15.5
B	Blast-cleaned carbon and low alloy steel	27.5	34.5	23.5	29.5	19.5	24.0
C	Blast-cleaned quenched and tempered steel	19.0	23.5	16.0	20.0	13.5	16.5
D	Hot-dip galvanized and roughened	21.5	27.0	18.5	23.0	15.0	19.0
E	Blast-cleaned, organic zinc rich paint	21.0	26.0	18.0	22.0	14.5	18.0
F	Blast-cleaned, inorganic zinc rich paint	29.5	37.0	25.0	31.5	20.5	26.0
G	Blast-cleaned, metallized with zinc	29.5	37.0	25.0	31.5	20.5	26.0
H	Blast-cleaned, metallized with aluminum	30.0	37.5	25.5	32.0	21.0	26.5
I	Vinyl wash	16.5	20.5	14.0	17.5	11.5	14.5

Source: Reference 30, Table 2a.

is the authors' opinion that a dual criteria, considering the mean value and the distribution of data (probability of slip) must be used to develop a sound design specification.

In the 1966 Bolt Specification, the allowable bolt shear stress of 15 ksi (103 MPa) for millscale surfaces was based on a  $k_s = 0.35$ , the minimum specified clamping force, and a factor of safety<sup>s</sup> of 1.51. In building structures, there has been almost twenty years of satisfactory connection performance using this stress level. Data collected since then give an average  $k_s$  for millscale = 0.336 [15], so that the factor of safety using the 1966 stress level would be 1.45. In 1976, the Bolt Spec increased the allowable stress to 17.5 ksi (121 MPa), mainly on the basis of laboratory data which indicated that the clamping force for calibrated wrench tightening would be typically 13 percent higher than the minimum specified.

In the authors' opinion, the possible increase above the minimum specified clamping force should not be considered in the development of design recommendations for the following reasons:

- (1) The statistics which indicate higher than minimum specified clamping have typically been developed from laboratory data, with the bolts tightened carefully by researchers. This may not be representative of actual field installation by fabricators and erectors.
- (2) Much of the turn-of-nut data was based on one-half turn from snug, but current specifications would permit many of these bolts to be tightened to one-third turn, resulting in a lower clamping force.
- (3) Tension control techniques such as load indicator washers produce results closer to the minimum specified clamping force which should be acceptable.
- (4) Losses in bolt clamping force due to paint creep, approximately 10 percent for thickness between 4 to 6 mils.

A factor of safety of 1.45 with the minimum specified clamping and the mean  $k_s$  from the tests reported herein is used to develop the design recommendations along with a probability of slip concept discussed below.

Friction connections should only be specified when slip is objectionable to the usefulness of the structure. Important instances would be reversed loading and oversize and slotted holes. Under such circumstances, the authors would recommend a much lower probability of slip, say 1 percent, instead of 10 percent currently in use. Table 32 shows the allowable slip coefficients for different probability of slip and a factor of safety of 1.45 against the mean for the coating studied in the factorial experiment. Other levels of probability of slip are shown for comparison. The table follows the format of the Bolt Specification in

Table 32. Allowable slip coefficients

Surface Treatment	Overall Average Slip Coeff.	Allowable Slip Coeff. based on a probability of slip			Allowable Slip Coeff. FOS=1.45
		10%	5%	1%	
Sandblasted	0.521	0.421	0.392	0.339	0.359
Organic zinc-rich primer	0.464	0.385	0.362	0.319	0.320
Organic zinc-rich primer with epoxy top coat	0.276	0.236	0.224	0.202	0.190
Inorganic zinc-rich primer with vinyl top coat	0.510	0.436	0.415	0.374	0.352
Inorganic zinc-rich primer--80% zinc	0.618	0.577	0.563	0.533	0.426
--75% zinc	0.507	0.492	0.486	0.470	0.350
-- 0% zinc	0.276	0.271	0.270	0.265	0.190
Vinyl primer	0.193	0.171	0.165	0.151	0.133
All vinyl system	0.195	0.174	0.165	0.143	0.139

Table 33. Design Recommendations for Slip-critical Shear Connections--Uncoated Surfaces and Paints Tested Herein

Class	Slip Coef.	Range Slip Coef.	Surface Treatment	Allowable Shear Stress	
				A325	A490
A	0.22	0.19-0.30	A588 millscale, epoxy topcoat, vinyl primer <sup>1</sup>	10	12
B	0.33	0.31-0.37	Other millscale, phenoxy-base organic zinc <sup>2</sup>	15	18
C	0.40	0.38-44	Epoxy-base organic zinc	18	22
D	0.47	0.45-0.53	Phenoxy-base organic zinc <sup>3</sup> , inorganic zinc (75% zinc), sandblasted, vinyl topcoat	21	26
E	0.56	>0.54	Inorganic zinc (80% zinc)	25	31

(1) Not recommended for sustained loading; see Chapter 4

(2) One brand of phenoxy-base organic zinc that satisfies the State of California Spec (90% zinc)

(3) One brand of phenoxy-base organic zinc that has 80% zinc

that there is a category for each type of paint.

The research summarized in this chapter indicates that the current AASHTO Specification for allowable bolt shear stresses in connections with painted faying surfaces is not reliable. The current format of Table 1.7.41C2 of the AASHTO Specification which gives allowable stresses for 9 classes of surface treatment should be changed for the following reasons. First, within a paint category, say organic zinc, the products vary widely with respect to their frictional characteristics ( $0.31 > S.C. < 0.46$ ). There are obviously other organic zincs which may fall outside the current bounds. Second, the variations which occur even for a particular coating do not justify three significant figures. It is, therefore, suggested that the friction shear stress table be arranged as a function of slip coefficient, not particular painting groups. Five groups are suggested in Table 33. The allowable stresses would be modified by factors for paint thickness, oversize holes, etc. These aspects will be considered in more detail in the last chapter. The proposal presented above will also require the development of a standard classification test which could be run by the paint manufacturers themselves to determine what category a particular produce will fit. Questions related to curing time, time before assembly, etc., all have significant effects on slip resistance. Paint manufacturers must address these problems in order to get a paint classified. A draft of such a standard test is contained in the Appendix.

#### 4. CREEP OF COATED SPECIMENS

The relative movement of the plates in a bolted joint under a sustained static load is an important characteristic of a bolted friction joint. A friction joint is used in applications where joint deformation is to be limited. The friction joint is idealized in design as a joint which undergoes no displacement until it reaches its slip load. Small elastic deformation in the connected material will cause small displacements prior to slip, but these are small relative to the displacements which occur at slip. A friction joint subjected to sustained loading below the slip load may exhibit creep deformation. The creep deformation may be of such a magnitude that the joint no longer satisfies the design assumption of no deformation prior to reaching the slip load.

A study conducted by the Jet Propulsion Laboratory in Pasadena, California [23] investigated sustained loading behavior of numerous connections with galvanizing and other surface coatings. They concluded that all of the coating systems tested exhibited a steady state rate of slip for the duration of the test once movement was initiated. The slip rate projected for the life of the structure would result in significant displacements at the bolted joint. They also noted that the factor of safety against slip, based on short-term loading, does not apply to cases of sustained loading. On the basis of these test results, the use of organic zinc-rich paints and galvanized coatings to structures with low sustained loads has been limited [5].

Evidence in this study will be analyzed and compared with previous tests in order to achieve the following objectives:

- (1) Determine if creep studies should be required prior to approval of use of a particular coating system.
- (2) Determine the major factors affecting creep behavior.
- (3) Establish design recommendations.

#### Experiment Design

The tests performed in this study consist of a series of shear specimens subjected to long-term loading. All specimens are A572 Grade 50 material and designed as a double shear, butt splice connected with one 7/8 in. (22mm) diameter high-strength bolt. The specimen configuration was chosen for simplicity in testing and in order to obtain good correlation with results from the compression slip tests accomplished in another phase of this project.

The basic variables investigated were the paint system, paint thickness, clamping force, and shear load. Four different paint systems

were investigated. These consisted of inorganic zinc with vinyl topcoat, organic zinc, organic zinc with epoxy topcoat, and a vinyl primer. The two paint thicknesses were "normal" and "thick", based on current practices in structural applications. In order to determine the influence of the clamping force of the bolt on slip behavior, two types of bolts were selected for the tests: ASTM A325 bolts and ASTM A490 bolts. This provided two significantly different clamping forces.

The experiment design, as indicated below, provides for a total of forty-eight specimens, with three replicate specimens for each condition.

#### Experiment Design

<u>Coating Thickness</u>	<u>Coating 1</u>	<u>Coating 2</u>	<u>Coating 3</u>	<u>Coating 4</u>
Normal	3	3	3	3
Thick	3	3	3	3

No. of Specimens =  $3 \times 4$  (coating systems)  $\times 2$  (thickness)  $\times 1$  (steel)  $\times 2$  (clamping forces) = 48 specimens

Four control specimens were included to provide a base for comparison of results. They consisted of two blasted specimens and two inorganic zinc coated specimens. One blasted and one inorganic zinc specimen were assembled with A325 bolts and the other two with A490 bolts.

#### Experimental Procedures

Bolt Calibrations. In order to achieve and maintain consistent clamp loads throughout the test, a number of bolt calibrations were performed. It was determined that the most practical method of achieving the desired result was to control lot uniformity and to calibrate a limited number of bolts from each lot. All bolts, both A325 and A490, were from the same lots, respectively. The calibrations were performed by using bolt elongations as an indicator of the load. The normal force of the bolts was determined from a load versus elongation calibration curve. This method is one of several bolt calibration techniques used by previous investigators [31,13], and was chosen as the most efficient method of determining typical behavior of bolts stressed into the inelastic range. The details of the method are given in Chapter 2.

All A325 bolts were calibrated with an A325 load-indicating washer within the grip length. All A490 bolts were calibrated with a standard quenched and tempered A325 flat washer under the turned element with an A490 load-indicating washer at the opposite end. All bolts were machined flat on each end and were center-drilled with a 1/8 in. (3mm) 60° counter-sink drill. All bolts were used in their "as received" condition, i.e., no special cleaning was performed nor were any lubricants applied to the bolts.

Results of each calibration were plotted on a load versus elongation curve. The results for each bolt are shown in Figures 56 and 57. Utilizing the curves developed from three to four tests, from each respective lot, the behavior of the remainder of the bolts was approximated. Tightening the bolts beyond their yield point, i.e., on the "plateau" of their respective load deformation relationships, provided for a convenient and effective method of duplicating and maintaining the appropriate clamping force from specimen to specimen. As indicated in Figures 56 and 57, a specified elongation range was selected for each respective type of bolt within which a particular clamping load on the specimen could be assured. By requiring an elongation of 0.04 in. to 0.05 in. (1 to 1.3 mm) for the A325 bolts, it could be assured within 5 percent that the clamping load on the specimen was 45 kips (200 kN). Likewise, by requiring 0.03 in. to 0.04 in. (0.8 to 1 mm) for A490 bolts, it was assured with the same accuracy that each specimen had a clamping load of 68 kips (303 kN).

Difficulty did occur initially in attempting to predict the behavior of the A325 bolts. Considerable scatter of the results existed in the load versus elongation data for these bolts. Initially, standard high-strength A325 nuts were used, but these failed to perform consistently. In most cases, the nut would strip prior to reaching ultimate capacity of the bolt. On the other hand, by utilizing a 2H nut this problem was avoided, thus reducing the scatter and providing more consistent results. The 2H nuts were used on all the test specimens and in all the calibration tests.

Load-Indicating Washer Calibration. A brief study of the behavior of load-indicating washers was performed in order to establish their value in measuring clamping load on a specified bolt. Two grades were examined, i.e., those designed for use with A325 bolts and those designed for use with the A490 bolts.

The testing utilized the "hydraulic bolt" used in the slip test and described in Chapter 2. This apparatus allowed load to be applied to the washer with the use of the hydraulic ram, while the applied load was measured by the load cell.

Load stages were in stages up to 45 kips (200 kN) for the A325 washers (specified clamping load = 39 kips [174 kN]), and in stages to 55 kips (245 kN) for the A490 load-indicating washers (specified clamping load = 49 kips [218 kN]). Washer gap readings were taken at approximately the third points around the washer at each load stage, utilizing a feeler gage capable of reading to 0.001 in. (0.025 mm). Readings were taken immediately after reaching the prescribed load. The gap was taken as the average of the three readings. The results were plotted on a load versus gap curve, and are provided in Figures 58 and 59.

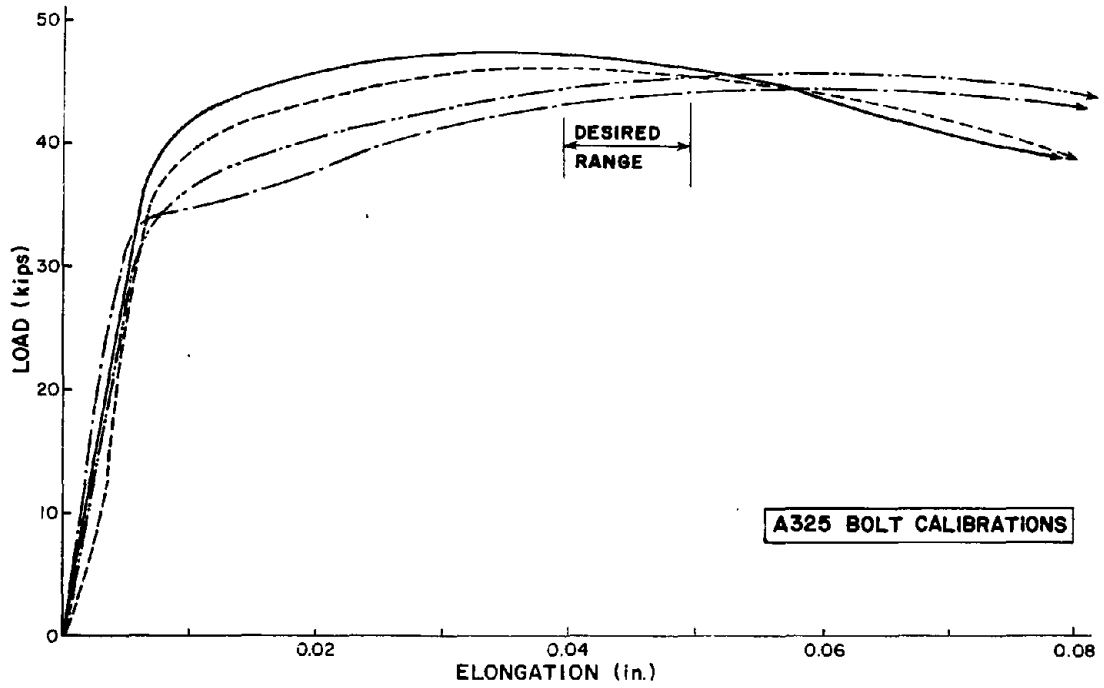


Figure 56. A325 bolt calibrations (1 kip = 4.45 kN, 1 in. = 25.4 mm)

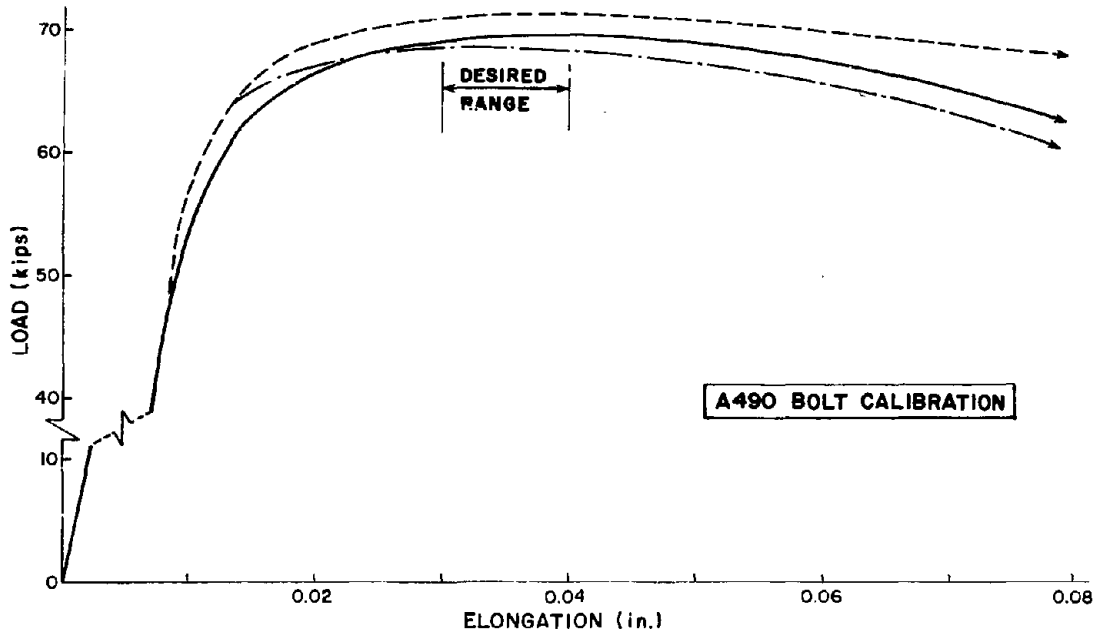


Figure 57. A490 bolt calibrations (1 kip = 4.45 kN, 1 in. = 25.4 mm)



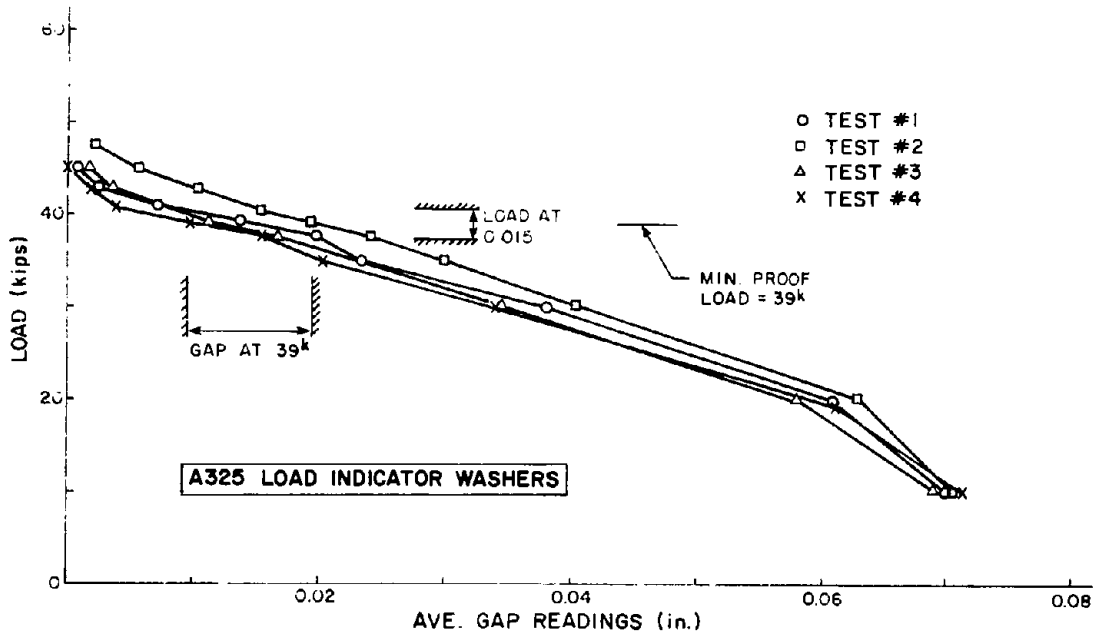


Figure 58. A325 load-indicator washer calibrations  
 (1 kip = 4.45 kN, 1 in. = 35.4 mm)

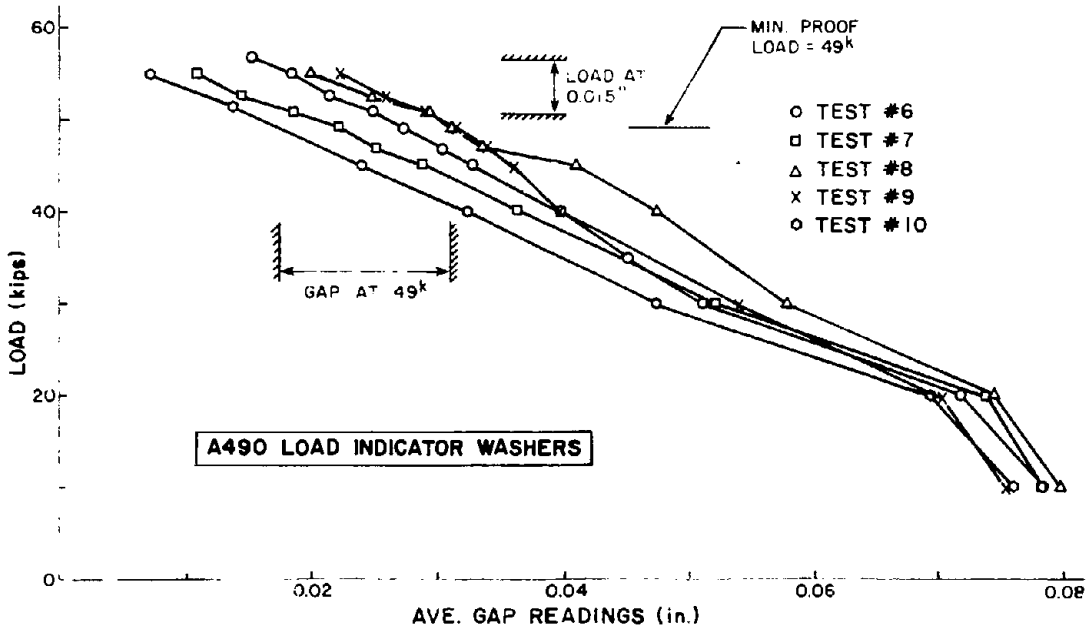


Figure 59. A490 load-indicator washer calibrations  
 (1 kip = 4.45 kN, 1 in. = 25.4 mm)

The manufacturer's gap reading for the minimum specified proof load is 0.015 in. (0.38mm). This gap reading was assumed to be appropriate for our tests, since the 2H nuts used against the washer had an average hardness of rockwell C27, which is comparable to the hardness requirements for A325 bolts. From the curves representing the A325 washers, it is apparent that merely relying on this predicted gap reading would not assure that the proof load has been reached. On the other hand, the A490 washers tested indicated that for a gap of 0.015 in. (0.38mm), there is some confidence that the designated proof load for this bolt has been reached. Note the gap scatter bands at minimum proof loads for each type of washer shown on the two figures. These curves show representative behavior of a total of seven and eight tests for the A325 and A490 washers, respectively. These data seem to indicate that further study of the behavior of load-indicating washers is warranted. Additionally, it would indicate that by merely reaching the manufacturer's predicted gap reading may tend to give a false sense of security to the user in field applications. Also, it was observed that at all load stages deformation of the load-indicating washer was not uniform throughout. For this reason, three readings were taken and the average of the three was used as the appropriate gap reading. Some of the three readings varied drastically, leading to the conclusion that if only one reading is taken, it will not indicate the actual load on the bolt.

It is for the above reasons that the load-indicating washers were used only as an indicator of the bolt load, and the bolt elongation was used for the actual determination of the bolt clamping force. It should be noted that, since the clamping loads were considerably above the proof load for each bolt, the gap readings in most cases were zero at the termination of the assembly procedure.

Specimen Fabrication. All specimens were cut from A572 Grade 50 bar stock. Each specimen consisted of three plates from the same bar, each 7 in.  $\times$  4 in.  $\times$  5/8 in. (178 mm  $\times$  102 mm  $\times$  16 mm). The dimensions were selected to match the width and thickness of the static compression slip tests run in conjunction with this study of creep behavior, and to allow the specimens to be connected in series. Compressive static slip behavior of control specimens was measured to establish the slip load. Each plate was center-drilled with two 15/16 in. (24mm) diameter holes, 1-1/2 in. (38mm) from each end. The plates were connected with one high-strength 7/8 in. (22mm) diameter bolt, tightened to a predetermined elongation and arranged such that other specimens could be connected in a pinned series simulating a chain. Figure 60 is a schematic of the chain-type arrangement with the hatched portion designating one specimen.

The specimens were painted using the same procedures used in the static slip tests. Table 34 gives the average paint thickness of the of the plates used in each specimen. The second letter of the specimen designation is the code for the clamping force. The letter "L" specimens were used with A325 bolts and the letter "H" with A490 bolts. All

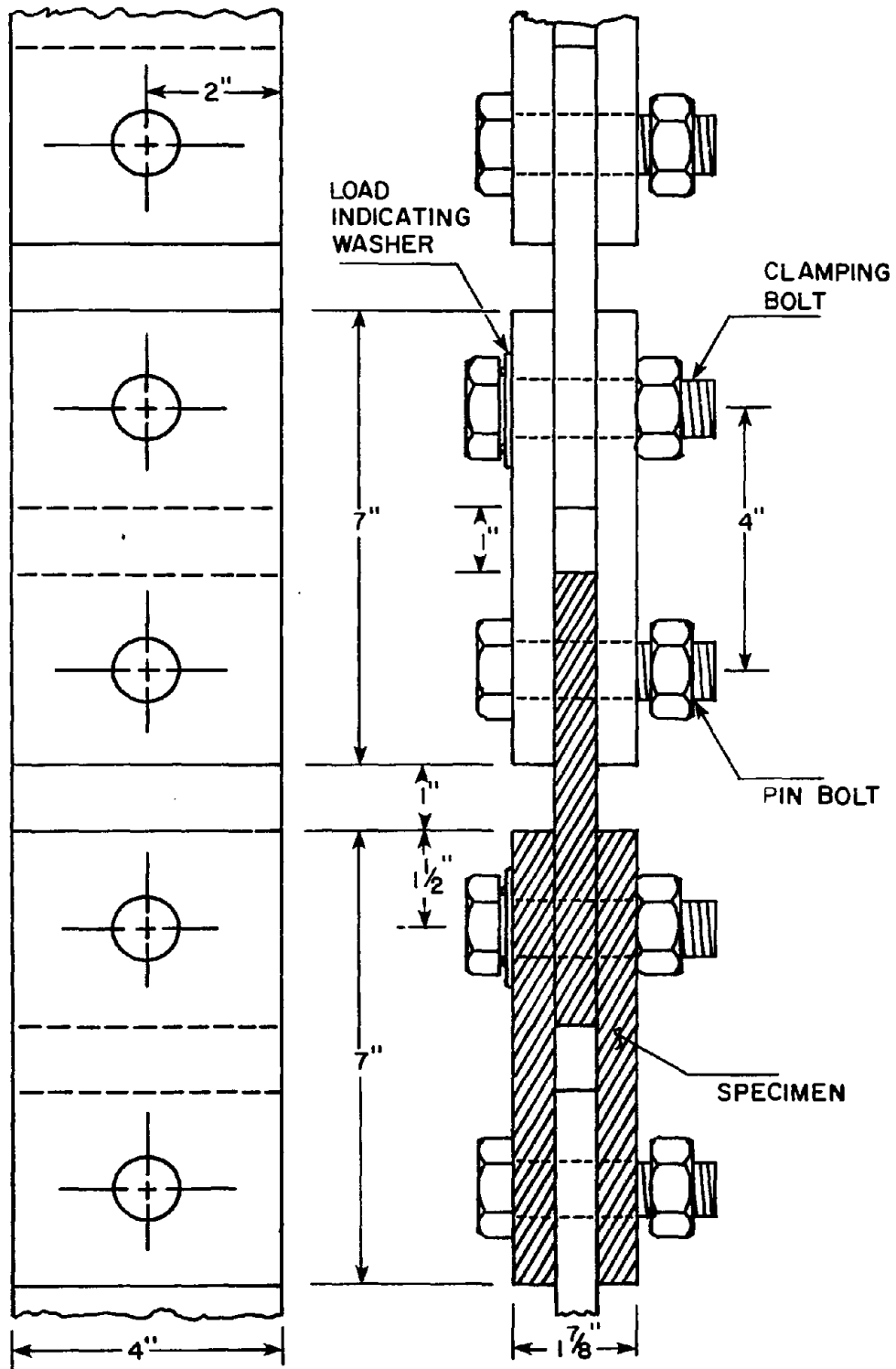


Figure 60. Creep specimens in series  
(1 in. = 25.4 mm)

Table 34. Average faying surface coating thickness for creep specimens (mils)

<u>Inorganic Zinc with Vinyl Topcoat - Normal</u>						
Specimen	24BHVK5	25BHVK1	23BHVK4	21BLVK3	22BLVK4	20BLVK2
Outer Plate	8.7	8.4	11.8	7.8	9.5	9.5
Center Plate	10.0	9.6	8.2	8.3	9.2	9.5
Outer Plate	9.5	9.1	9.0	9.2	9.4	9.6
Outer Plate	8.6	8.2	10.8	9.0	9.2	9.5
<u>Inorganic Zinc with Vinyl Topcoat - Thick</u>						
Specimen	22BHV3	20BHV1	21BHV2	24BLV6	20BLV9	23BLV5
Outer Plate	13.6	12.1	12.2	11.6	12.9	12.0
Center Plate	13.8	14.5	11.5	13.2	11.6	12.2
Outer Plate	14.0	14.2	12.6	13.8	12.9	13.5
Outer Plate	12.5	12.5	12.5	12.4	14.5	12.0
<u>Organic Zinc - Normal</u>						
Specimen	21BHZ4	22BHZ5	20BHZ5	22BLZ1	24BLZ8	23BLZ9
Outer Plate	6.6	6.1	7.1	6.8	7.0	6.8
Center Plate	6.0	6.2	5.4	5.9	6.5	6.2
Outer Plate	7.0	7.5	5.9	5.6	7.5	5.9
Outer Plate	6.0	6.0	7.0	5.3	6.2	8.5
<u>Organic Zinc - Thick</u>						
Specimen	23BHZK2	24BHZK1	25BHZK3	24BLZK3	20BLZK7	21BLZK8
Outer Plate	13.1	10.8	11.5	7.8	9.2	9.9
Center Plate	6.5	10.4	10.5	8.4	8.9	7.0
Outer Plate	6.8	11.8	7.8	8.5	7.4	7.1
Outer Plate	12.6	10.4	11.6	7.1	10.9	11.0
<u>Organic Zinc with Epoxy Topcoat - Normal</u>						
Specimen	22BHE10	24BHE9	20BHE8	22BLE9	21BLE7	24BLE10
Outer Plate	9.2	10.4	7.5	9.4	6.6	8.2
Center Plate	8.0	10.2	8.9	8.4	8.4	8.2
Outer Plate	8.1	9.8	9.2	8.5	6.6	8.4
Outer Plate	8.4	10.5	6.8	9.4	9.0	7.6
<u>Organic Zinc with Epoxy Topcoat - Thick</u>						
Specimen	21BHEK9	20BHEK4	23BHEK6	21BLEK10	25BLEK2	23BLEK1
Outer Plate	9.5	12.0	11.2	10.5	9.5	9.2
Center Plate	11.2	10.6	11.2	11.4	10.4	10.6
Outer Plate	10.0	11.1	11.8	11.2	10.8	9.5
Outer Plate	10.5	11.4	10.4	10.6	8.9	10.0
<u>Vinyl Primer - Normal</u>						
Specimen	23BHX3	24BHX7	22BHX8	23BLX7	24BLX4	20BLX6
Outer Plate	2.2	2.1	2.7	2.6	2.2	2.2
Center Plate	2.1	2.6	2.7	2.5	2.3	2.5
Outer Plate	2.2	2.4	2.8	2.6	2.4	2.5
Outer Plate	1.8	2.5	2.7	2.3	2.2	2.3
<u>Vinyl Primer - Thick</u>						
Specimen	21BHXX6	22BHXX6	20BHXX10	20BLXX3	21BLXX5	22BLXX2
Outer Plate	4.8	4.2	4.3	3.6	4.8	4.3
Center Plate	3.5	4.4	3.9	3.9	4.4	4.9
Outer Plate	4.5	4.2	3.6	3.9	3.6	4.5
Outer Plate	3.6	4.2	4.7	4.4	5.1	5.1

(1 mil = 0.001 in. = 0.03 mm)

specimens with a particular coating system were painted and bolted together at the same time.

Specimen Assembly. All creep specimens were bolted together in a double shear, butt splice configuration utilizing a pneumatic impact wrench. Each bolt with appropriate washers was slipped through the three plates and brought to a finger-tight position. The specimen was placed in a specially designed fixture to ease assembly and assure specimen alignment. The specimens were assembled in full bearing opposite the direction of actual loading, in order to allow the full 1/8 in. (3mm) range of slip. Initial bolt length measurements were taken. The bolt was then tightened in three to four stages utilizing turn of the nut to approximate the load and elongation measurements to check the load. It was determined from the bolt calibration curves that a clamping load of 68 kips (303 kN) for the A490 bolts could be attained with good repeatability if elongation ranged from 0.03 in. to 0.04 in. (0.8 to 1 mm). Likewise, a clamping load of 45 kips (200 kN) for the A325 bolts could be attained if elongations ranged from 0.04 in. to 0.05 in. (1 to 1.3 mm). The bolt loads were selected for ease of attainment of the load, such that a small change in elongation should not appreciably change the load. The specimens were then hung from the loading frame connected with bolts acting as pins in a chain-type configuration. Each chain consisted of thirteen specimens, all of which could then be subjected to the same tensile loading. Twelve specimens were painted with the selected coating, while the thirteenth was used as a control specimen.

Slip Gages. Two slip gages were welded to each specimen prior to assembling the chain. These gages consisted of two short pieces of 1/8 in.  $\times$  3/4 in.  $\times$  3/4 in. (3 mm  $\times$  19 mm  $\times$  19 mm) angle attached to each side of the specimen, as shown in Figure 61. One 1/2 in. (13mm) long angle was tack-welded to the center plate of the specimen. Another 1-7/8 in. (48mm) long angle was tack-welded to the outer plates. A small countersunk hole was drilled in each angle and a 5/32 in. (4mm) diameter ball bearing was mounted in the hole using epoxy. The gages were arranged to give positive readings as slip occurred. The gage length, the distance between measuring points on the ball bearings, was 0.67 in.  $\pm$  0.07 in. (17 mm  $\pm$  2 mm). Measurements were taken using a precision micrometer capable of reading to 0.0001 in. (0.0025 mm). The accuracy of these measurements varied slightly, due to improper alignment of the micrometer with the ball bearings. This experimental error was determined to be  $\pm$  0.0004 in. (0.01mm) from 140 sample measurements taken on specimens where no slip was occurring. The amount of slip was taken as the average change of the two gages on each specimen. By mounting the angles closely together, the effects of elastic joint elongation were negligible. The welding of these gages did not appear to affect the paint on the faying surfaces of the plates, as evidenced by the very small discoloration of the painted outer surfaces.

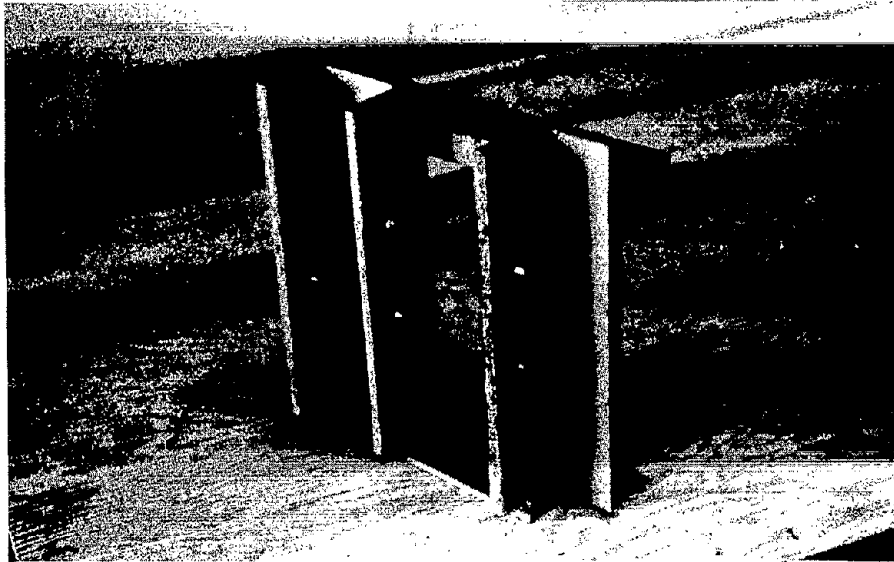
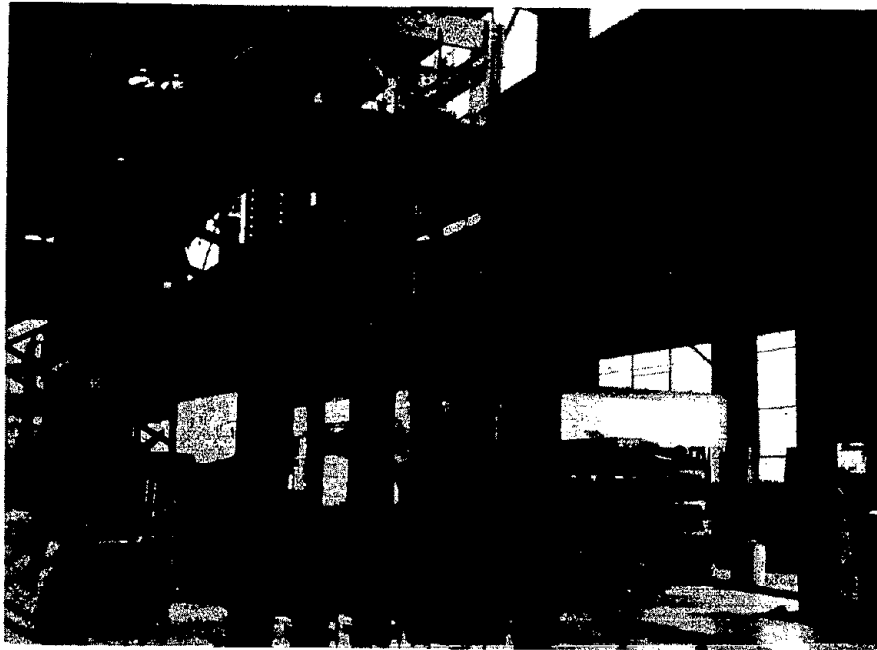


Figure 61. Slip gages

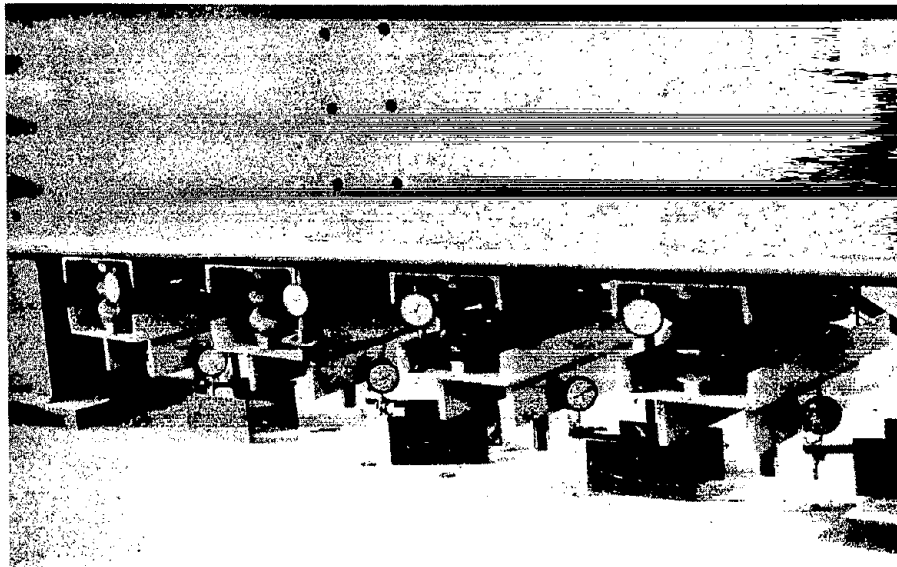
Loading Apparatus. A load frame (see Figure 62a) was designed and constructed with two primary objectives in mind: (1) the capacity should be sufficient to accept a large number of specimens, and allow for the variable loads to be applied, and (2) the apparatus should be capable of applying sustained loads over long periods. Provisions were made to accommodate four chains of specimens, each consisting of thirteen specimens. Two of the chains utilized A325 bolted specimens and two utilized A490 bolted specimens. Each chain was composed of two different coatings each of "normal" and "thick" paint thickness and one control specimen.

The most practical method of applying sustained loads with this design was with the use of springs, as shown in Figure 62b. These springs served to soften the system in order to maintain the load while small amounts of slippage occurred in the specimens. Each chain was loaded by four springs (two sets of large springs with smaller nested springs). Each set of two springs had a spring constant of approximately 14 kips per in. (2.45 kN/mm). This method of load application proved to be very satisfactory in maintaining the load  $\pm 280$  lbs (1.25 kN) and provided the capacity needed to produce loads causing slip to occur. The springs were contained in a bracket fabricated from C 9  $\times$  20 channel. Two dial gages capable of reading spring deflection to 0.001 in. (0.003 mm) were mounted within the bracket, one adjacent to each spring. A 1-1/4 in. (32 mm) diameter high-strength rod was inserted between the springs at the center of the bracket. This rod, as well as a similar rod attached to the top of the load frame, provided a means of applying tensile load to each chain. Each rod was fitted with a clevis-type device which was attached to the end specimens of the chain by a loose bolt. A device was fabricated for the top of the frame through which the top 1-1/4 in. (32 mm) rod could be suspended (see Figure 63). This device was designed to provide a means of applying the load to each chain by utilizing a hydraulic 60-ton ram with a load cell to indicate the precise load, and to allow the load to be locked in by tightening the nut shown below the load cell.

The specimens were connected with untightened pin bolts and hung vertically in the load frame. Once the desired load on the chain was attained, the deflection of the springs was noted on the dial gages. Then the nut at the top of the chain under the load cell and ram was tightened and the hydraulic ram was unloaded. Any creep that occurred in the specimens caused a change in the deflection of the springs. Each specimen chain was monitored such that any slight load reduction due to creep effects was limited to approximately 0.01 in. (0.25 mm) change in spring deflection, or about 280 lbs (1.25 kN). Any subsequent load adjustments were easily attained by inserting the hydraulic ram and load cell into the system and jacking in the desired load.



(a) Load frame



(b) Springs used to maintain loads

Figure 62 Specimen setup





Figure 63. Top support for specimen chain and load system

### Load Application and Specimen Deformation Measurement Procedures

Loading stages were determined by evaluating the static slip coefficient from the basic compression slip tests under short-term loading for each particular coating, results of which are tabulated in Table 35 [16]. The arrangement of the particular coatings was also a factor in determining the load stages. Each specimen chain consisted of twelve specimens, three with normal and three with thick coatings, of two different coating systems. The clamping force was the same for all specimens in one chain. An attempt was made to match up the coefficient of slip in order that all specimens of a particular chain would experience as near as possible the same percentage of their individual static slip loads at each load stage. Table 36 shows the arrangement of the specimens in the load chains. It was decided to apply load to each chain in several load stages, with the final load being that load which approximates a service load condition experienced in an actual structure. The specimens were closely monitored at each stage to establish if any creep behavior was taking place. The service load condition was established using the following relationship:

$$P_u = k_s m N \quad (2)$$

$$P_s = P_u / 1.5 = 67\% P_u \quad (3)$$

where  $P$  = slip load  
 $P^u$  = service load  
 $k$  = static slip coefficient measured in the control specimens  
 $m^s$  = number of slip planes = 2  
 $N$  = normal force  
1.5 = Factor of Safety against slip

The slip, service, and the allowable load, as specified in Ref. 30, are given in Table 37 for each coating system.

Load was applied to each chain of specimens as discussed previously. The level of loading stages was decided upon prior to load application, subject to revision in the event any creep behavior was detected. Once the particular load stage was reached, measurements were taken immediately on the slip gages with the precision micrometer, as shown in Figure 64. This was done in order to detect any instantaneous slip behavior. An additional reading was taken on each specimen after approximately 1 hr at the individual load stage. If no movement was detected, i.e., less than 0.0004 in. (0.012 mm) deformation experienced, the load was increased an additional increment and the procedure above was repeated. However, if movement was detected after 1 hr interval, the load remained at this level and slip was monitored frequently during the first week to ten days, and thereafter at less frequent intervals until no further slip was detected or the specimen had slipped "into

Table 35. Slip coefficients for short-term loading

Coating System	Normal		Thick	
	Thickness (mils)	$k_s$	Thickness (mils)	$k_s$
Inorganic Zinc w/Vinyl Topcoat	7.9/2.8	0.383	11.3/2.6	0.446
Mean: 0.429	7.4/2.4	0.391	11.8/2.8	0.405
Std. Dev.: 0.036	7.2/2.6	0.456	11.8/1.7	0.487
	7.5/2.7	0.444	12.5/2.0	0.418
Organic Zinc	6.0	0.560	7.7	0.582
Mean: 0.550	5.5	0.578	8.0	0.563
Std. Dev.: 0.030	6.1	0.573	8.0	0.516
	6.0	0.530	7.3	0.503
Vinyl Primer	2.7	0.196	3.8	0.211
Mean: 0.201	2.6	0.192	4.4	0.219
Std. Dev.: 0.017	2.3	0.197	3.8	0.221
	2.3	0.177	4.3	0.215
	2.4	0.170	3.7	0.210
			4.0	0.201
Organic Zinc w/Epoxy Topcoat	4.8/3.2	0.265	7.6/2.3	0.277
Mean: 0.269	5.1/3.2	0.289	9.5/2.5	0.317
Std. Dev.: 0.028	4.8/3.5	0.281	8.3/3.5	0.218
	5.2/2.6	0.282	8.3/2.4	0.284
	4.9/2.9	0.265	9.2/2.3	0.261
	4.9/2.7	0.219	8.4/3.4	0.266
Grade 50 Blasted				
Mean: 0.540				
Std. Dev.: 0.07				
No. of Tests: 36				

(1 mil = 0.001 in. = 0.03 mm)

Table 36. Creep specimen test arrangement

Load Chain No.	Bolt Type	Clamping Force (kips)	Painting Systems
1	A490	68	1) Organic zinc 2) Inorganic zinc with vinyl topcoat
2	A325	45	1) Organic zinc 2) Inorganic zinc with vinyl topcoat
3	A325	45	1) Organic zinc with epoxy topcoat 2) Vinyl primer
4	A490	68	1) Organic zinc with epoxy topcoat 2) Vinyl primer

(1 kip = 4.45 kN)

Table 37. Slip, service, and allowable loads

Coating	Ave. Slip Coeff.	A325 Bolt <sup>1</sup>			A490 Bolt <sup>2</sup>		
		Slip (kips)	Service (kips)	Allow. <sup>3</sup> (kips)	Slip (kips)	Service (kips)	Allow. <sup>3</sup> (kips)
Inorganic w/ Vinyl Topcoat	0.429	38.6	25.7		58.3	38.9	
Organic Zinc	0.550	49.5	33.0	25.2	74.8	49.9	31.3
Vinyl Primer	0.201	18.1	12.1		27.3	18.2	
Organic Zinc w/ Epoxy Topcoat	0.269	24.2	16.1		36.6	24.4	

(1 kip = 4.45 kN)

<sup>1</sup>A325 clamping force = 45 kips

<sup>2</sup>A490 clamping force = 68 kips

<sup>3</sup>RCSC Ref. 30

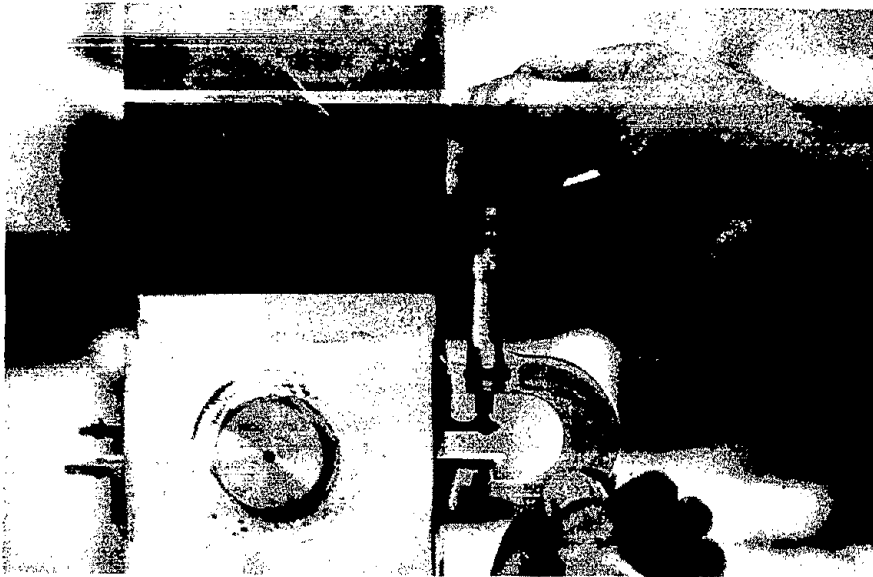


Figure 64. Precision micrometer measuring creep deformation

bearing". Once all noticeable slip had ceased, the load on a specific chain was increased again to a further load stage repeating the above-described procedures until the specimens either slipped into bearing or reached the prescribed service load condition. The specimens then remained at the service load condition indefinitely to determine if significant slip was occurring in any of the four coating systems.

Bolt elongation measurements were periodically made throughout the entire test to detect any effect of the coating, slip deformation, or other factors on the clamping load of the bolts. This measurement was accomplished using the same C-frame mounted dial gage that was used for the bolt calibration task described previously.

#### Creep Test Results

The four chains comprising the creep experiment were loaded for over one year. During this time the reading of the deformation of the specimens was taken periodically. Early evaluation of the data revealed that the rate of deformation decreased with time. Therefore, the frequency of reading could be decreased with time without the loss of significant information. Whenever the load of a chain was increased, the readings were taken on an hourly, then a daily, then a weekly, and finally a monthly basis. Table 38 summarizes the data for the four load chains. The blasted and inorganic control specimens contained in the chains did not exhibit any significant deformation during the duration of all the tests. The accuracy of the creep deformation reading is

Table 38. Summary of average total creep deformations

Chain No.	Load (kips)	Time at Load (hours)	$\frac{P^1}{P_s}$	Deformation		$\frac{P^1}{P_s}$	Deformation	
				Normal (mils)	Thick (mils)		Normal (mils)	Thick (mils)
				<u>Organic Zinc</u>		<u>Inorganic zinc w/vinyl</u>		
1	11.5	1106	0.23	0.6	1.0	0.30	66.0	66.0
	25.8	3408 2204	0.52	0.1	0.5	0.66	50.3	42.7
	40.8	5064	0.82	1.5	1.4	1.05	--	--
2	20.0	139	0.61	0.5	<0.4	0.78	101.4	79.9
	25.8	2981 2162	0.78	0.6	2.6	1.00	37.9	47.5
	27.0	5349	0.82	<0.4	<0.4	1.05	--	--
				<u>Organic Zinc w/Epoxy</u>			<u>Vinyl Primer</u>	
3	5.0	1103	0.31	<0.4	<0.4	0.41	0.8	4.8
	10.0	1464	0.62	<0.4	0.4	0.83	3.9	20.1
	10.4	4721	0.65	<0.4	<0.4	0.86	<0.4	0.5
	16.2	2811	1.01	47.6	21.2	1.34	77.3	49.0
4	5.0	1104	0.20	<0.4	<0.4	0.27	<0.4	2.4
	10.0	1633	0.41	<0.4	0.6	0.55	1.6	8.5
	15.7	4557	0.64	<0.4	<0.4	0.86	0.7	28.2
	24.4	2042	1.00	81.5	68.1	1.34	82.5	48.4

(1 mil = 0.001 in. = 0.03 mm, 1 kip = 4.45 kN)

<sup>1</sup>Applied load divided by service load

±0.4 mils (0.01 mm). The deformation in mils listed is the average deformation during the load stage of the three replicates for each condition.

The vinyl coatings, the primer and the topcoat, both exhibited large creep deformations at relatively low loads. The vinyl coatings showed a true creep behavior in the sense that the deformation occurred slowly with time with the rate of deformation decreasing with time. Figures 65 through 68 show the deformation of the inorganic zinc with vinyl topcoat for the first two load stages of Chains 1 and 2. All joints were essentially into bearing after the first load stage. Very little additional deformation occurred in the second load stage for these specimens. No further data were recorded for these specimens after approximately 2200 hrs of the second load stage.

Comparison of the data shown in Figures 65 and 66 indicates that the thicker coating crept at a faster rate. A deformation of 5 mils (0.1mm) occurred in the thick specimens after 1 hr of loading, while the normal coating reached this deformation after 10 to 20 hrs. The specimens in Chain 2, Figures 67 and 68, show a much faster creep rate. The ratio of the applied load to the service load,  $P_S$ , ( $P_S =$  slip load/1.5) is much higher for these specimens. The specimens in Chain 2 reached 5 mils of deformation almost immediately. The initial deformation rate for these higher loaded specimens is approximately 10 mils/hr. The rapid creep deformation of these specimens at loads much lower than maximum service levels based on their short-term static behavior was not expected. This same system had given very good results in the slip tests.

The experience of rapid creep with the vinyl topcoat led to the application of low initial loads to Chains 3 and 4. A load of 5 kips (22.3 kN) was applied initially to both chains. This was done to examine the creep behavior of the vinyl primer at low loads. This would allow investigation of the influence of paint thickness and clamping force upon the creep behavior to be examined before the bolts were in bearing. Figures 69 through 72 show the behavior of the vinyl primer specimens for an applied load of 5 kips. The normal thickness specimens in both chains exhibited very little deformation. The thicker coatings showed considerably more deformation. The total average deformation given in Table 38 for the thicker specimens was 4.8 and 2.4 mils (0.12mm and 0.06mm), respectively, for Chains 3 and 4. These observations, along with data for the next load stage of 10 kips (45 kN) confirmed that the rate of creep deformation was greater for the specimens with the thicker coating. The larger deformation which occurred in the specimens of Chain 3, which was assembled with the lower clamping force A325 bolts, indicated that the creep deformation rate was a function of the ratio of the applied load to the clamping force. This ratio is proportioned to the applied load divided by either the slip or service load. The ratio of the 5 kip (22.3 kN) applied load to service load was 0.41 and 0.27 for Chains 3 and 4, respectively. The total creep deformation was 4.8 and

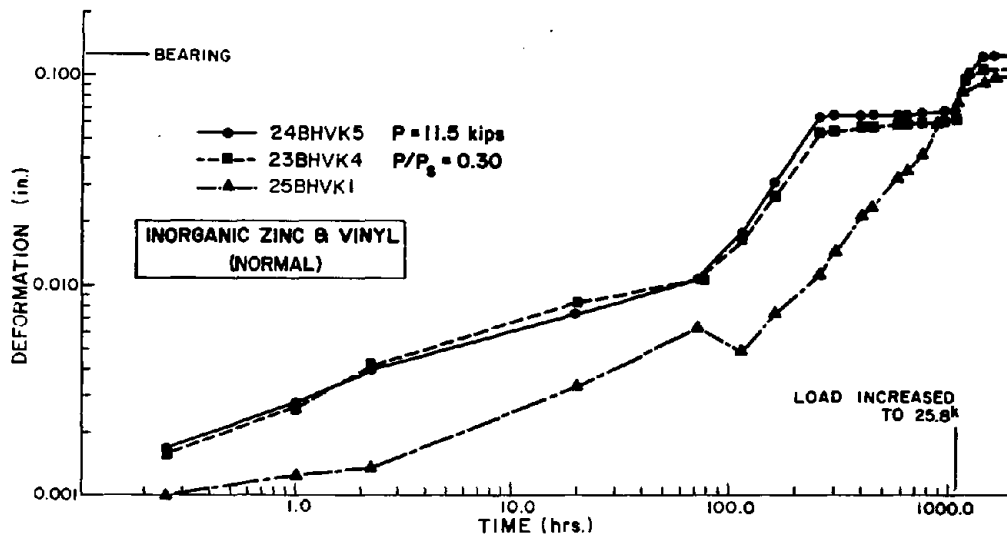


Figure 65. Inorganic zinc with vinyl topcoat (normal), Chain #1  
(1 in. = 25.4 mm, 1 kip = 4.45 kN)

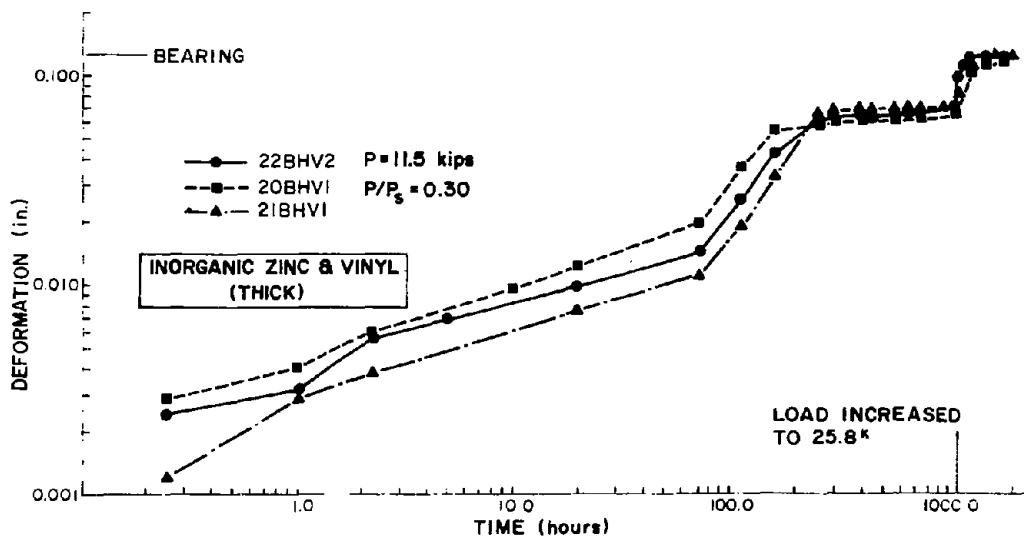


Figure 66. Inorganic zinc with vinyl topcoat (thick), Chain #1  
(1 in. = 25.4 mm, 1 kip = 4.45 kN)



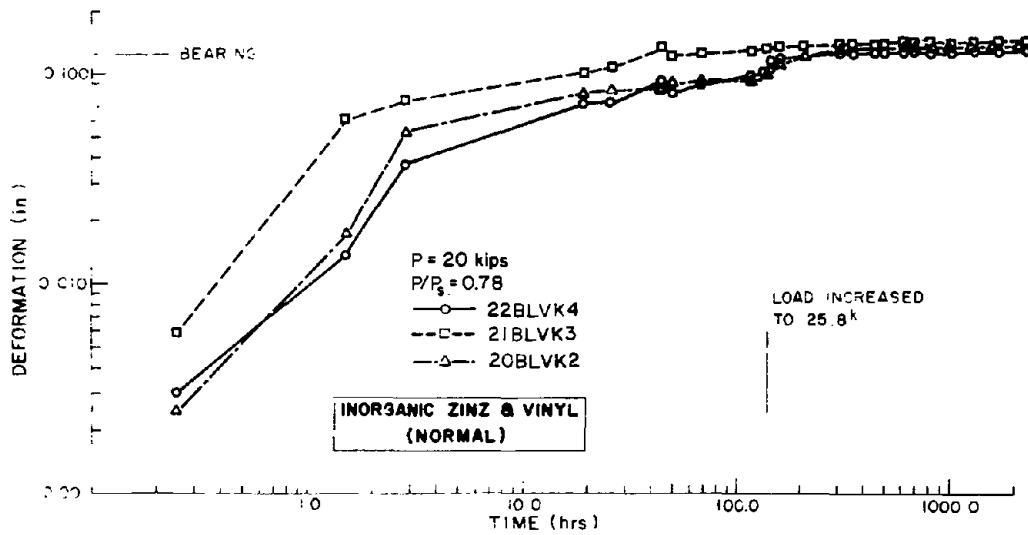


Figure 67. Inorganic zinc with vinyl topcoat (normal), Chain #2  
(1 in. = 25.4, 1 kip = 4.45 kN)

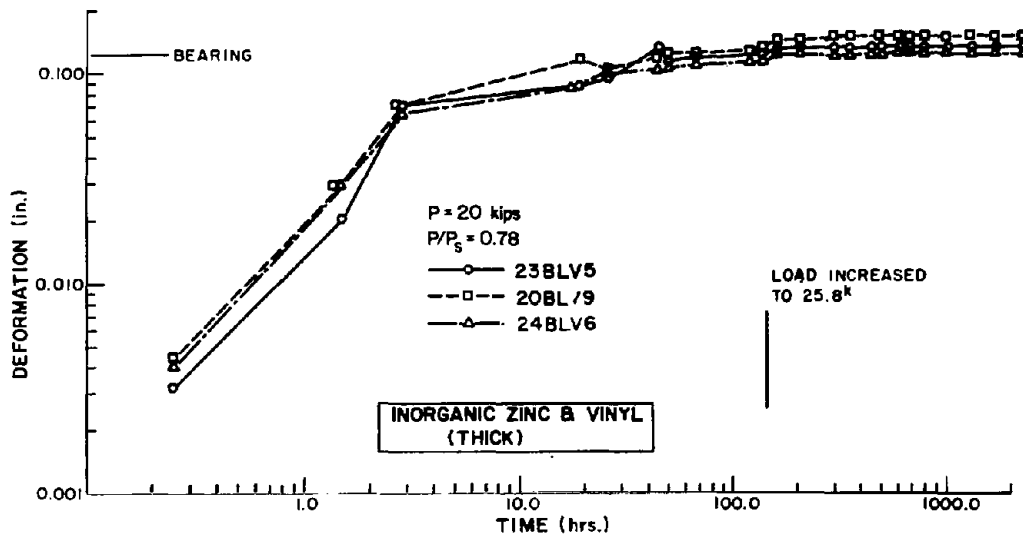


Figure 68. Inorganic zinc with vinyl topcoat (thick), Chain #2  
(1 in. = 25.4 in., 1 kip = 4.45 kN)

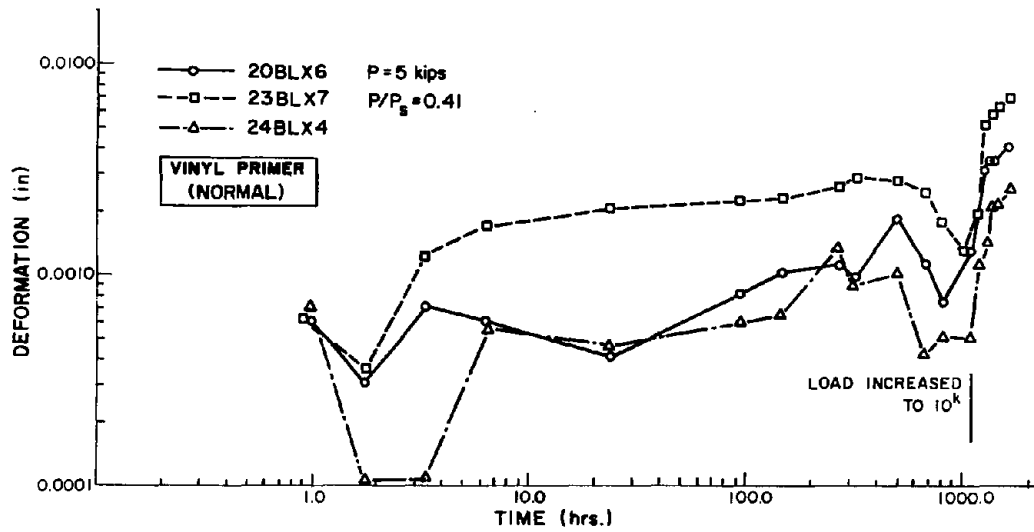


Figure 69. Vinyl primer (normal), Chain #3  
 (1 in. = 25.4 mm, 1 kip = 4.45 kN)

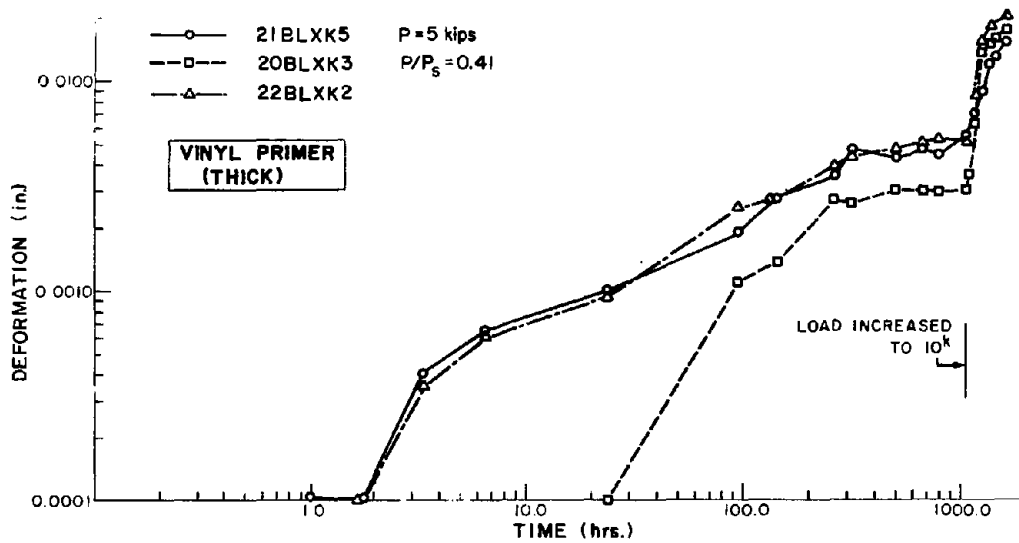


Figure 70. Vinyl primer (thick), Chain #3  
 (1 in. = 25.4 mm, 1 kip = 4.45 kN)

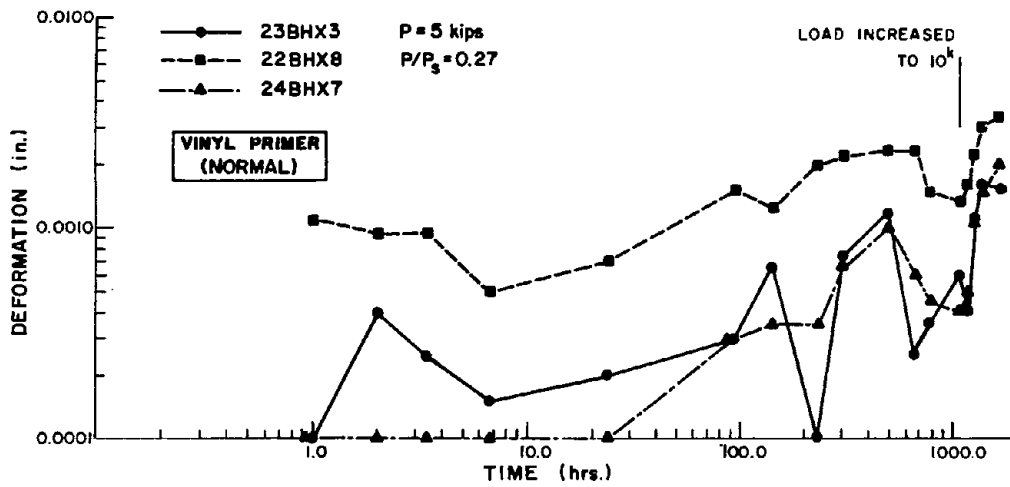


Figure 71. Vinyl primer (normal), Chain #4  
(1 in. = 25.4 in., 1 kip = 4.45 kN)

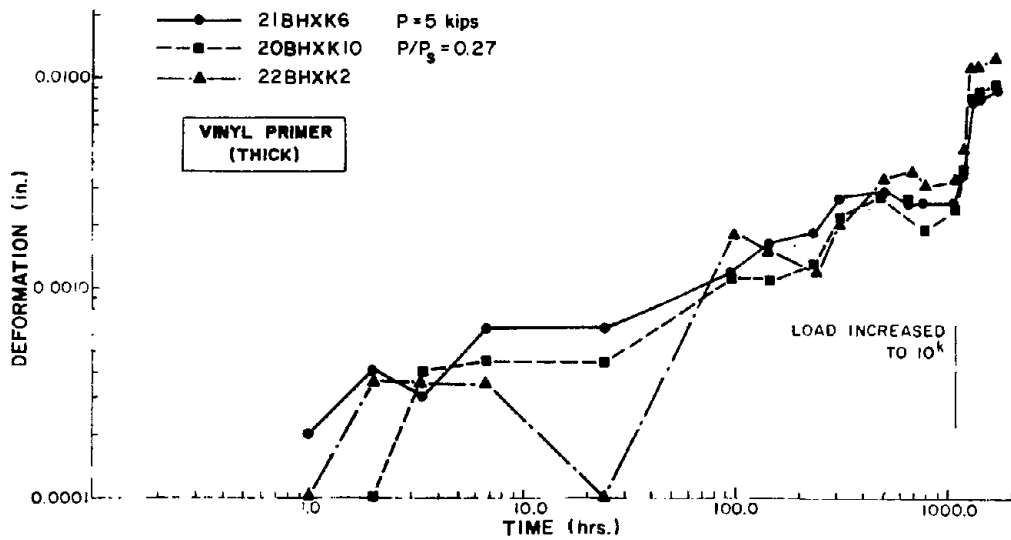


Figure 72. Vinyl primer (thick), Chain #4  
(1 in. = 25.4 mm, 1 kip = 4.45 kN)

2.4 mils (0.12 and 0.06 mm) for the thick coating specimens of these chains. This indicates almost a linear relationship between the load ratio and creep deformation. The 10 kip (44.5 kN) load stage data given Table 38 shows the same linear relationship.

The organic zinc specimens in Chains 1 and 2 exhibited very little deformation during the creep tests. The thicker coating specimens exhibited the largest deformations. The load on the organic zinc specimens in the final load stage were determined using the values of service level loads for A325 and A490 bolts with organic zinc paint calculated from the factorial experiment short-term slip tests performed at the same time of the creep tests. These tests indicated a mean slip coefficient of 0.45, which was used to redefine the service load level. The load levels are above the current specification values [30]. Figure 73 shows the creep deformation of two replicate specimens with thick coating of Chain 2 at a load level of 25.8 kips (115 kN). The gradual deformation of the specimens is seen. The third replicate exhibited erratic deformation readings. The total deformation of the third specimen was similar, 2.1 mils (0.05 mm). The behavior of the organic zinc was similar to the vinyl paints in that the rate of creep deformation decreased with time. The amount of deformation occurring in the specimens after 1000 hrs of testing was less than 0.5 mils (0.001 mm).

A general trend of decreasing creep rate for the vinyl and organic zinc coating is evident in the data presented in Table 38. The organic zinc specimens in Chain 2 and vinyl primer specimens in Chain 3 exhibited negligible deformations in the 27 kip (120 kN) and 10.4 kip (46.3 kN) loads, respectively. These loads were sustained for approximately 5000 hrs. They were preceded by slightly lower loads between 1464 to 2981 hrs. It is evident that the significant portion of the creep deformation occurred during the initial lower loading and little deformation occurred at the slightly higher loads.

In Ref. 23, the authors assumed the creep rate was constant. They measured the creep deformation after 1000 hrs and calculated a creep rate using the total deformation divided by 1000 hrs. This type of calculation for example would imply that the information for the normal vinyl primer in Chain 3 at load of 10.4 kips (46.3 kN) (see Table 38) would be 12.6 mils (0.32 mm). The actual measured value was less than 0.4 mils (0.01 mm). Extrapolating an assumed constant creep rate for a service life of a structure, 50 years or more, would be extremely inaccurate. In all the creep tests performed in this investigation, negligible creep occurred after 1000 hrs of testing.

An anomaly in the behavior of the organic zinc paint creep behavior was found from an experiment of the creep behavior of A588 steel [36]. A single organic zinc specimen was included in this outdoor test. The results are shown in Figure 74. The bolt stress of 12.5 ksi (86.1 MPa) corresponds to an applied load of 15 kips (67 kN). The specimen had a creep deformation of 20 mils (0.51 mm) after 200 hrs. This result did not correlate with the results of organic zinc just discussed. The

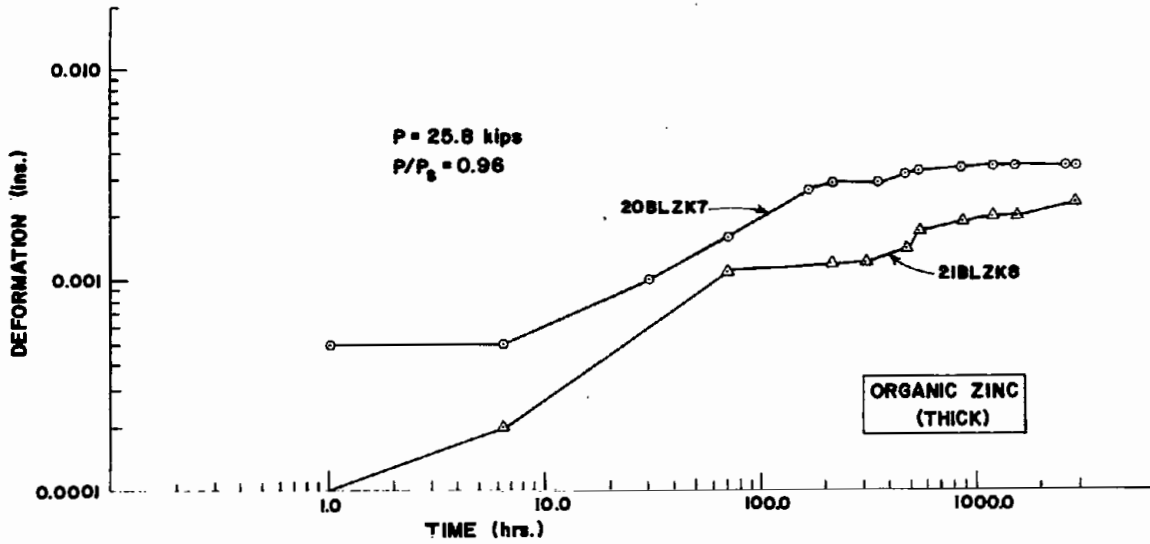


Figure 73. Creep of thick organic zinc, Chain #2  
 (1 in. = 25.4 mm, 1 kip = 4.45 kN)

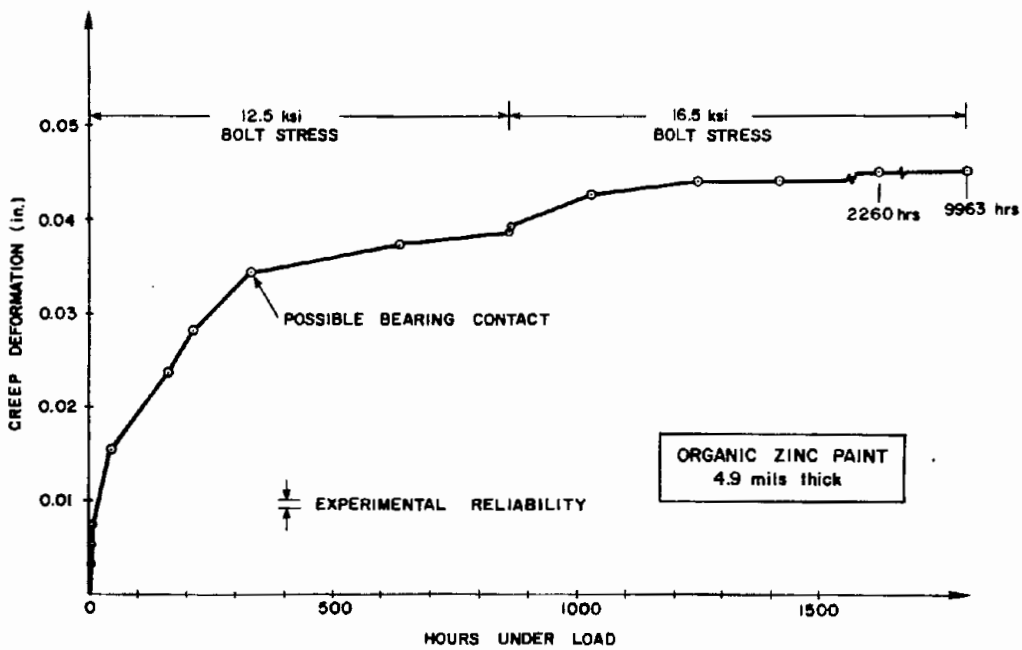


Figure 74. Creep-time response, organic zinc specimen,  
 outdoor test [36] (1 in. = 25.4 mm, 1 ksi = 6.89 MPa)

paint used was from the same manufacturer but from a different can. The specimen was tested outdoors. Possibly the higher temperature of the specimen may be responsible for the rapid creep at such a low load. While a single test result is not sufficient to develop broad recommendations or conclusions, it cannot be dismissed. Further creep tests should be conducted on specimens exposed to ambient conditions with organic zinc. In the meantime, organic zinc paint should be used with caution on the surfaces of connections with significant sustained loads.

The specimens in Chains 3 and 4 did not exhibit a creep-like deformation behavior. These specimens exhibited a sudden deformation which occurred normally within hours of an adjustment in the load in the chains. These adjustments were made when the load level was changed or when the load dropped below the desired level due to deformation of the specimens. The sudden deformation that occurred in the epoxy specimens produced an audible bang in the setup. The deformations occurred in the last load stages when the specimens were at their service loads. As shown in Table 38, prior to this last load stage no significant deformation occurred in the epoxy specimens.

#### Summary of Creep Test Results

The creep tests of the vinyl paints, vinyl primer and topcoat, indicate that before a coating system can be approved for use on friction joints, its creep characteristics must be determined. These vinyl paints exhibited good behavior in the static short-term slip tests. Their rapid creep behavior make them unusable for connections subjected to sustained loading. Because of their poor creep behavior, these coatings were not included in the fatigue tests described in the next chapter. The epoxy topcoat did not exhibit a steady creep behavior. The deformations were sudden but no less undesirable.

In general, the vinyls and organic zinc coatings exhibited the following characteristics in the creep tests:

- (1) Thicker coating showed more rapid and larger creep deformations.
- (2) The rate of creep decreased with time and was negligible after 1000 hours of loading.
- (3) The rate of creep increased with the ratio of the applied load to the static slip load of the joint.

Based on the results of this research, a tentative specification for the creep testing of coatings is given in the Appendix. Provisions are given for determining the allowable load of a coating based on a 1000 hr creep test. The anomalous behavior of the single outdoor organic zinc creep specimen indicates that creep testing at a temperature equal to the actual temperature of the steel in service may be necessary. Further research to determine the influence of temperature upon creep is needed to determine whether this is required.

It should be noted that Dusel, et al [42], in their study of organic zinc and vinyl coatings, concluded that creep tests must be performed to determine the suitability of a coating for friction connections. They recommend a creep test for 100 hrs and imply that this be performed above service load levels. They propose a 5 mil (0.15 mm) deformation the same as used in the test method proposed in the Appendix.

#### Bolt Relaxation Results

The elongations of the bolts used in the creep test specimens was monitored during the creep tests. The "C" frame used to measure the bolt elongation during installation was used in conjunction with two gage bolts. The two gage bolts, one A490 and one A325, were used to compensate for thermal expansion of the bolts and changes in the settings of the dial gage on the "C" frame. A gage bolt reading was taken before the measurement of the corresponding specimen bolts was made. The difference between the specimen bolt and gage bolt reading was compared with the previous readings. A decrease in the difference between two readings represents a shortening of the bolt. Assuming an elastic unloading of the bolt, the shortening implies a loss of bolt tension.

A loss in bolt tension can be caused by a relaxation in the bolt, relaxation being defined as a loss in load at constant deformation, or by compression creep, deformation under constant force, of the coating under the washers on the outside of the specimen and on the faying surfaces of the specimen. Since both creep and relaxation are limiting conditions and by definition cannot occur simultaneously, the bolt elongation values measured cannot be strictly interpreted as either phenomenon.

Table 39 gives a summary of the bolt elongation measurements. The accuracy of the results is estimated as 0.4 mils (0.01 mils). The A325 gage bolt was damaged during the test program. The results of the lower clamping force, 45 kips (200 kN), were continued for the duration of the test. However, examination of the data indicated that only data up to the time shown were valid. Consequently, the time duration for the A490 bolts is three times that for the A325 bolts. The data in Table 39 indicates two general trends. The amount of bolt relaxation was larger for thick coatings and for higher clamping force (A490 bolts). The difference in total time complicates the observations related to high clamping force and there are a few data that do not support both of these factors. The inorganic zinc and blasted control specimens showed negligible relaxation, less than 0.7 mils (0.02 mm), indicating that the measured shortening is due to compressive creep of the paint.

Figures 75 and 76 show the average bolt relaxation of the replicate specimens in each chain. The effect of clamping force is unclear for the results of Chain 3 and Chain 4 (Figure 76), vinyl primer and organic zinc with epoxy topcoat. The results in Figure 75 for Chains 1 and 2, inorganic zinc with vinyl and organic zinc, show a larger bolt

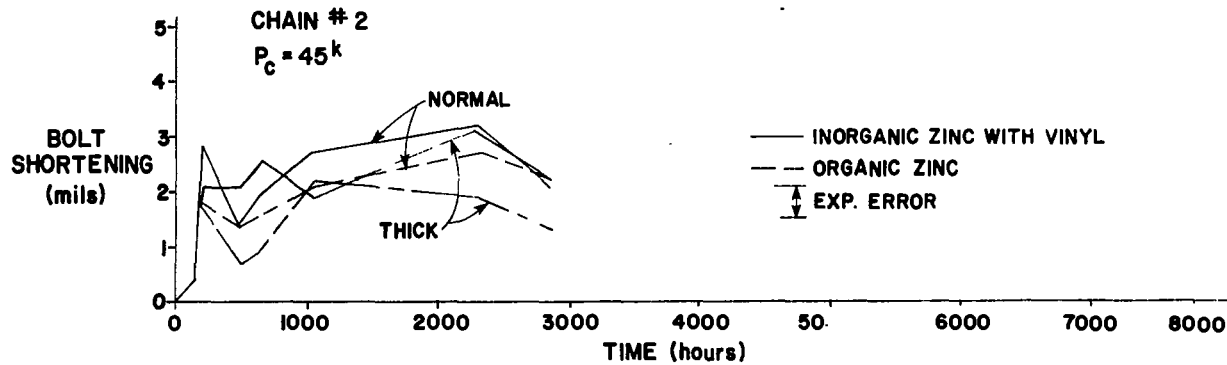
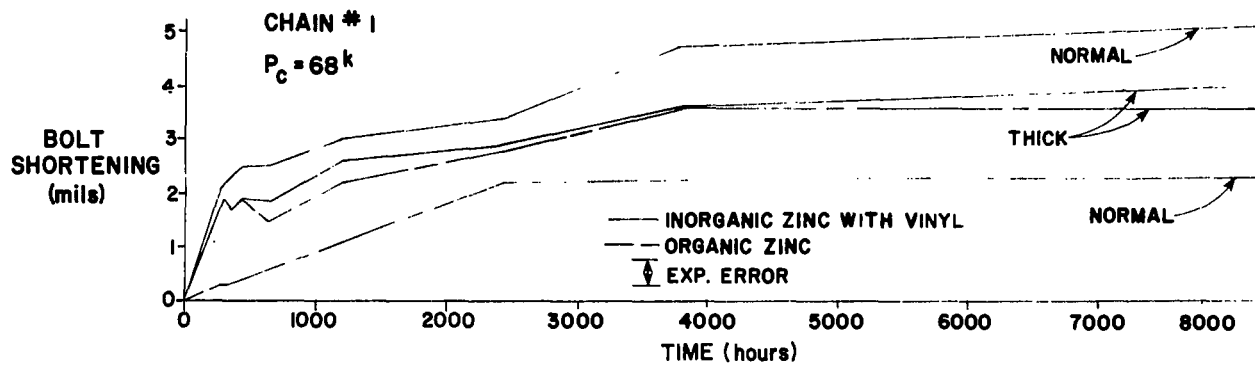


Figure 75. Average bolt shortening--inorganic zinc with vinyl and organic zinc  
 (1 mil = 0.01 in. = 0.03 mm)



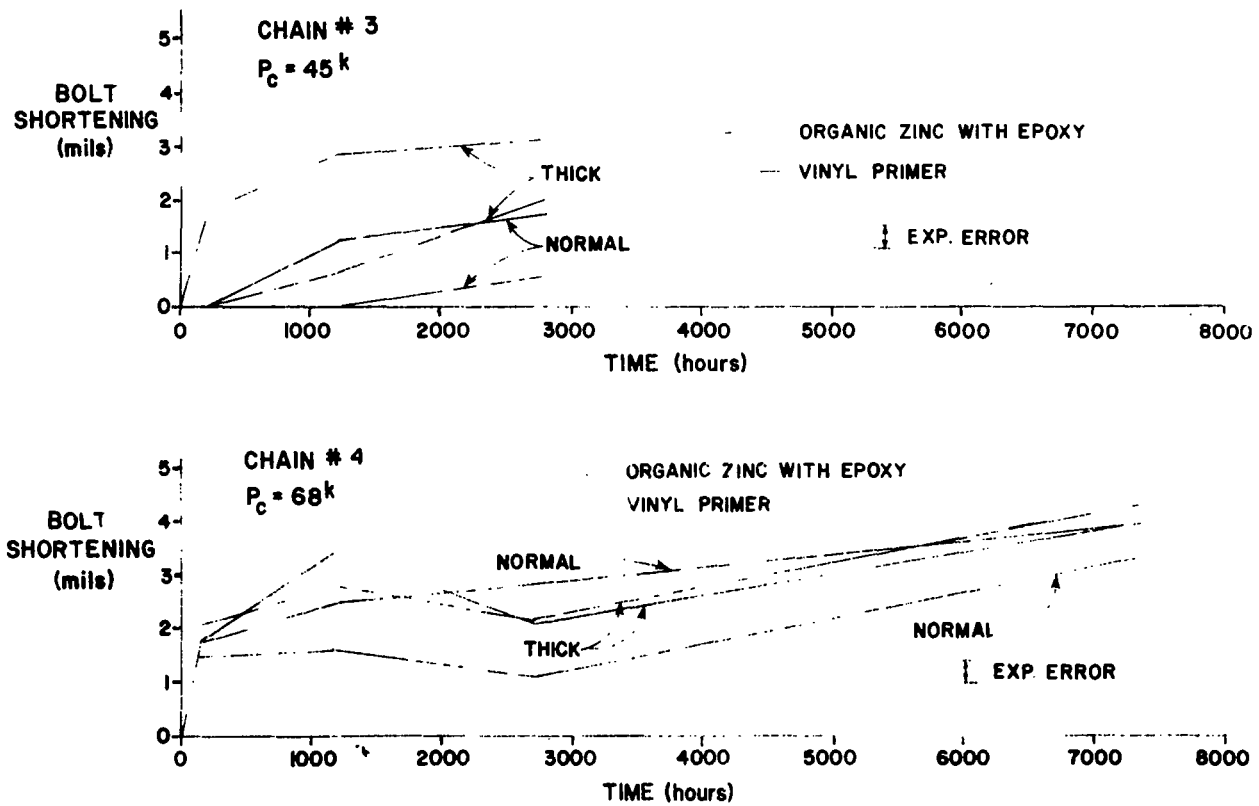


Figure 76. Average bolt shortening--vinyl primer and organic zinc with epoxy topcoat  
(1 mil = 0.001 in. = 0.03 mm)

Table 39. Average bolt shortening\* of creep specimens

Paint System	Coating Thickness	45 kips		68 kips	
		Shortening (mils)	Time (hrs.)	Shortening (mils)	Time (hrs.)
Organic Zinc	Normal	2.2	2850	2.3	8600
	Thick	1.3		3.6	
Inorganic Zinc with Vinyl Topcoat	Normal	2.1	2850	5.1	8600
	Thick	2.2		4.0	
Organic Zinc with Epoxy Topcoat	Normal	1.7	2720	4.0	7400
	Thick	3.1		4.0	
Vinyl Primer	Normal	0.5	2720	3.3	7400
	Thick	2.0		4.3	

(1 mil = 0.001 in. = 0.03 mm, 1 kip = 4.45 kN)

\*Estimated accuracy  $\pm 0.4$  mils.

deformation with the higher clamping force after 1000 hrs. The difference, however, is not larger.

The bolt shortening measured indicated a substantial loss in clamping force if the bolt is assumed to unload elastically. Examination of the bolt calibration curves, Figures 56 and 57, indicates that the elastic loading curves have a slope of about 5 kips/mil (876 kN/mm). The 3 to 5 mil (0.08 to 0.13 mm) shortening, when multiplied by this slope, corresponds to a 15 to 25 kip (67 to 112 kN) reduction in clamping force. This type of calculation neglects bolt force relaxation, which would increase the loss and assumes the bolt unloads elastically.

In order to determine the relationship between the bolt shortening measured and the loss in clamping force in the bolt, a series of separate experiments was performed. Plates,  $4 \times 4 \times 5/8$  in. ( $102 \times 102 \times 16$  mm) were painted on one side with a phenoxy-based organic zinc. The specimens were assembled as shown in Figure 77. Specimen Type 1 had a hardened washer between the painted surfaces to simulate the condition under the washers which occurred on the outer surfaces of the creep specimens. Specimen Types 2 and 3 had no hardened washer. These specimens were used to determine the condition on the faying surfaces of the creep specimens. Specimen 3 had a vinyl topcoat on the organic zinc. The force washer under the bolt head provided a bolt load indication separate of the bolt elongation. The force washer is a 1/2 bridge strain gage transducer designed to measure bolt forces. The units used

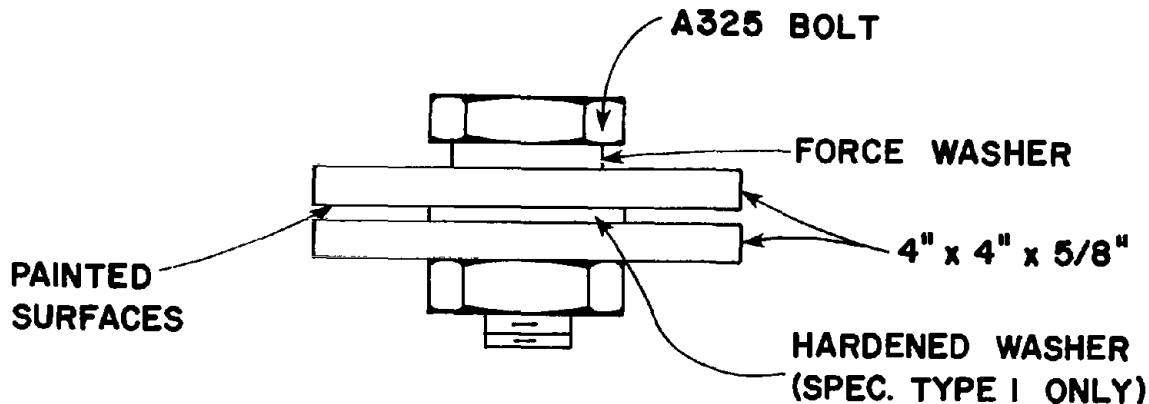


Figure 77. Bolt force reduction specimen  
(1 in. = 25.4 mm)

were individually calibrated. The washers were found to have a calibration significantly different from the manufacturers' calibration. The specimens were assembled using a pneumatic wrench. The specimens were stored in an air conditioned room for 50 days. Bolt elongation readings and force washer readings were taken periodically.

The results of the bolt force losses as determined by the force washers is given in Table 40. The percent loss in clamping force is similar for all specimens, about 6 percent. The majority of the loss for Specimens Type 2 and 3 occurred in the first 50 hrs. Specimen Type 1 showed approximately equal losses before and after 50 hrs. Figure 78 shows the results of Specimen 2-1 and also the losses based on bolt elongation. The relationship between bolt elongation and bolt force was determined by cycling bolts in the bolt calibration. The

Table 40. Compression creep tests

Specimen Type	Specimen No.	Average Coating Thickness (mils)	% Loss in Clamping Force	
			1200 hrs.	50 to 1200 hrs.
1 (Washer)	1-1	6.0	6.4	3.5
	1-2	5.8	7.3	2.8
2	2-1	6.2	6.0	1.5
	2-2	5.9	6.5	0.7
	2-3	5.8	5.0	1.8
3 (Vinyl Topcoat)	3-1	5.6+1.2	4.6	2.4
	3-2	6.0+1.3	5.9	1.3

(1 mil = 0.001 in. = 0.03 mm)

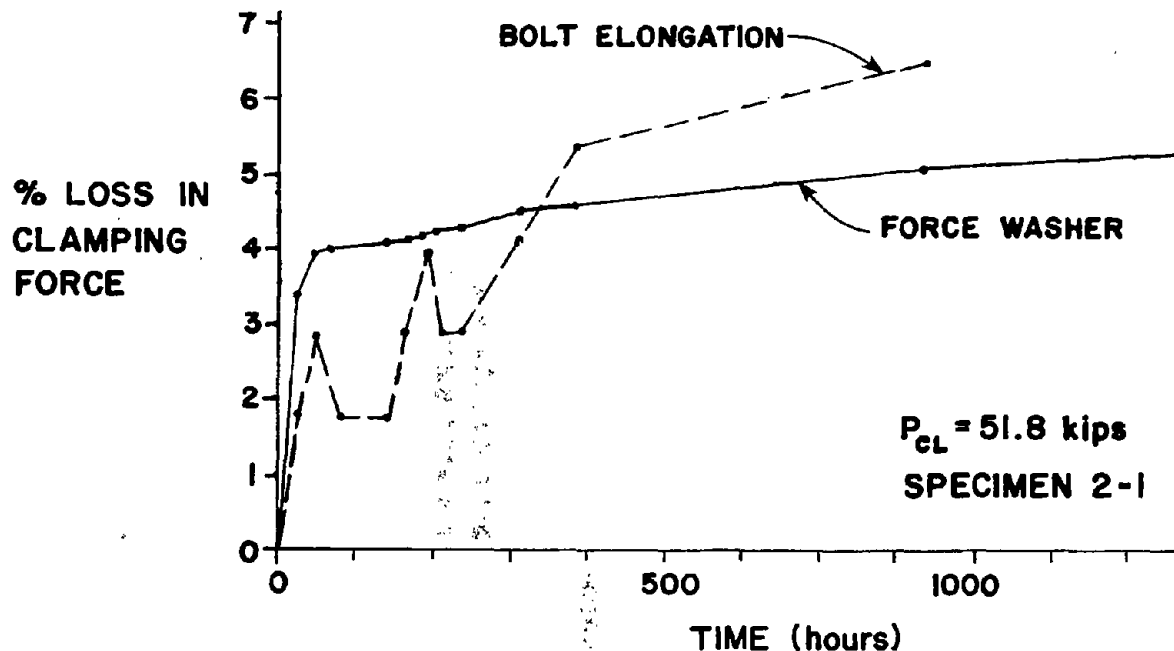


Figure 78. Specimen 2-1 bolt relaxation

results are shown in Figure 79. The cycling of the bolts was done by varying the hydraulic pressure in the calibrator with a hand pump. The results indicate the specimen unloaded in a linear elastic fashion with a slope of 6.1 kips/mil (1079 kN/mm) equal to the initial loading slope. The load calculated from the bolt shortening follows the trend of the force washer data but is very erratic. The erratic behavior is attributable to the experimental error in the bolt elongation measurements. The other specimens exhibited similar behavior and in general the loss in clamping force was overestimated, bolt force underestimated, by the bolt elongation measurements.

Post Creep Slip Tests

Tensile slip tests were performed on the creep test specimens. The results of the tests are given in Table 41. All specimens except the inorganic zinc with vinyl topcoat specimens were in full bearing. The measured creep deformation exceeded 0.10 in. (2.5 mm) in these specimens. Since the maximum slip deformation due to the hole clearances is 0.125 in. (3.2 mm), the specimens were judged to be in bearing. Visual observation of the specimens after disassembly confirmed the bolts were bearing against the holes.

The calculated slip loads were based on the slip coefficient measured in the control tests and initial clamping force. Examination of the

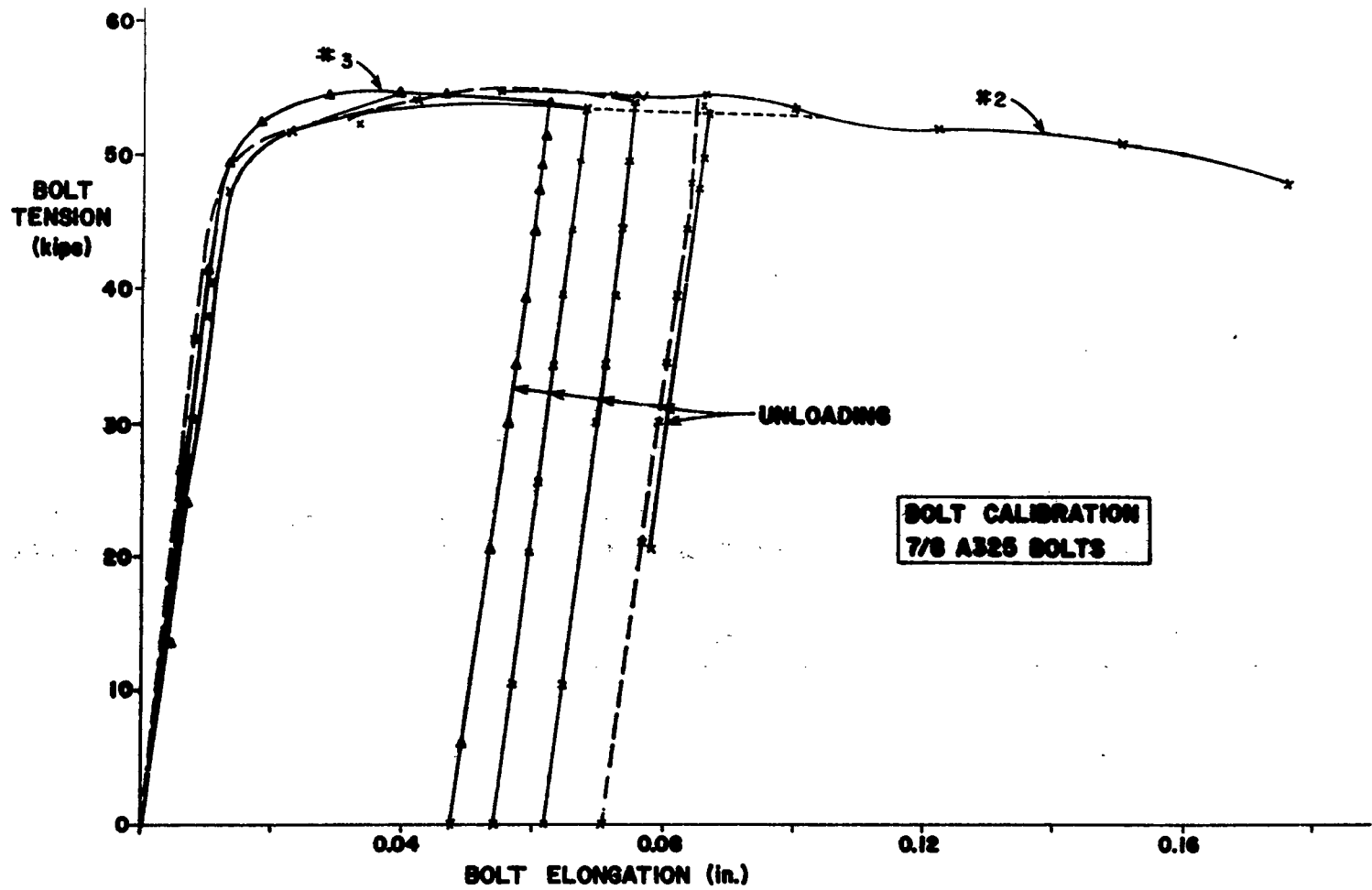


Figure 79. Unloading test of bolts (1 in. = 25.4 in., 1 kip = 4.45 kN)

Table 41. Post creep slip test results  
(1 mil = 0.001 = 0.03 mm, 1 kip = 4.45 kN)

Coating (Slip Coeff.)	Specimen	Initial Clamping Force (kips)	Average Coating Thickness (mils)	Measured Slip Load (kips)	Calculated* Slip Load (kips)	Meas. Calc.		
Organic Zinc ( $k_s = 0.55$ )	22BHZ5	68	6.4	54.5	74.8	0.73		
	21BHZ4	↓	6.4	58.7	↓	0.78		
	20BHZ5		6.4	58.7		0.78		
	25EHZK3		10.8	63.2		0.84		
	23BHZK2		10.3	59.4		0.79		
	24BHZK1		9.7	55.3		0.74		
	23BLZ9		45	6.9		48.1	49.5	0.97
	24BLZ8		↓	6.8		50.1	↓	1.01
	22BLZ1			5.9		52.1		1.05
	24BLZK3			7.9		47.9		0.97
	20BLZK7			9.1		49.7		1.00
	21BLZK8			8.8		49.1		0.99
Organic Zinc with Epoxy Topcoat ( $k_s = 0.27$ )	24BHE9	68	10.2	44.9**	36.6	1.23		
	22BHE10	↓	8.1	43.8**	↓	1.20		
	20BHE8		8.4	38.9**		1.06		
	21BHEK9		11.2	45.6**		1.25		
	23BHEK6		10.3	42.3**		1.16		
	24BHEK4		11.3	44.5**		1.22		
	21BLE7		45	7.6		29.2**	24.2	1.21
	22BLE9		↓	8.9		22.5**	↓	0.93
	24BLE10			8.1		21.1		0.87
	21BLEK10			10.9		18.9		0.78
23BLEK1	9.9	No data**		--				
22BLEK2	9.8	18.4	0.76					
Vinyl Primer ( $k_s = 0.20$ )	23BHX3	68	2.1	50.1**	27.3	1.83		
	22BHX8	↓	2.7	51.7**	↓	1.89		
	24BHX7		2.4	31.5**		1.15		
	21BHXK6		4.1	52.8**		1.93		
	20BHXK10		4.1	41.8**		1.53		
	22BHXK6		4.2	52.1**		1.91		
	20BLX6		45	2.4		28.1**	18.1	1.55
	23BLX7		↓	2.5		30.3**	↓	1.67
	24BLX4			2.4		31.7**		1.75
	21BLXK5			3.9		34.4**		1.90
20BLXK3	4.0	25.3**		1.40				
22BLXK2	4.7	35.5**	1.96					

\*Calculated slip load = initial clamping force × slip coefficient × 2.  
\*\*Creep deformation greater than 50 mils.

test results and inspection of the disassembled specimens revealed that a majority of the specimens were in either partial bearing or full bearing. Partial bearing occurs when the inner plate is bearing on the bolt. Further deformation requires that the bolt move relative to the outer plates. The two washer outer surface interfaces become additional slip planes, increasing the load required for further slip. Partial bearing occurs when the creep deformation exceeds 0.05 in. (1.3 mm). The specimens in either partial or full bearing are noted in Table 41. All of the organic zinc and three organic zinc with epoxy topcoat specimens were not in bearing. The remainder of the specimens judged to be in bearing had slip loads which exceeded the calculated slip loads. These higher figures are due to the bearing condition of the specimens. The only exception was Specimen 22BLE9, which had a slip load slightly below the calculated figure.

Four compression slip control specimens were painted along with the creep specimens for each coating and tested after completion of the creep test. These tests were done to determine the influence of time upon the slip coefficient. Unfortunately, the control specimens for the vinyl primer and inorganic zinc with a vinyl topcoat were lost in the 1-1/2 year period of storage. The tests of the organic zinc specimens gave a mean slip coefficient of 0.67 higher than the value of 0.55 measured in the control tests performed at the start of the creep tests, Table 35. The organic zinc with epoxy topcoat specimen gave a slip coefficient of 0.28, almost identical to the initial value of 0.27. The increase in the slip coefficient for the organic zinc follows the trend established in Chapter 3. These tests established that the slip coefficient increases with time in specimens left unbolted, but to a very limited extent after the specimens are bolted together. Such a large increase would not be expected in the bolted creep specimens.

The organic zinc specimen results were examined to determine whether the measured slip load could be correlated with the bolt shortening measured during the creep tests. Table 42 shows the results of that examination. The specimens shown all had A490 bolts installed. The slip load estimated using the bolt force estimated from the bolt shortening data is in good agreement with the measured slip loads. The average difference is 1 percent, with a scatter of plus 12 percent and minus 16 percent. The good agreement between the measured slip load and the slip load calculated using the bolt shortening data was encouraging until the A325 bolted specimens of the same coating were examined. The results for the organic zinc specimens with A325 bolts installed, clamping force = 45 kips (200 kN), shown in Table 41, indicated almost perfect agreement between the measured slip load and the slip load calculated using the initial clamping force. The measured bolt shortening in these specimens was essentially the same as the A490 bolted specimens. Consequently, in the A325 bolted specimens, the measured bolt shortening does appear to be an indication of a reduction of the clamping force. Similar results are reported in Ref. 42; a larger reduction in slip load was noted for bolts with larger clamping forces.

Table 42. Analysis of Chain #1 organic zinc post creep slip tests

Specimen	Average Coating Thickness (mils)	Bolt Shortening (mils)	Estimated Bolt Force <sup>1</sup> (kips)	Estimated Slip Load <sup>2</sup> (kips)	Measured Slip Load (kips)	<u>Estimated Measured</u>
22BHZ5	6.4	3.0	53.0	58.3	54.5	1.07
21BHZ4	6.4	1.6	60.0	66.0	58.7	1.12
20BHZ5	6.4	2.4	56.0	61.6	58.7	1.05
23BHZK-3	10.8	4.0	48.0	52.8	63.2	0.84
23BHZK-2	10.3	3.4	51.0	56.1	59.4	0.94
24BHZK-1	9.7	3.5	50.5	55.6	55.3	1.01
Average			53.1	58.4	58.3	1.01

(1 mil = 0.001 in. = 0.03 mm, 1 kip = 4.45 kN)

<sup>1</sup>Bolt force = 68 kips - 5k/mil × shortening

<sup>2</sup>Estimated slip load = estimated bolt force × 2 × 0.55.

#### Conclusions of Bolt Shortening and Post Creep Test Results

The loss of tension implied by the bolt shortening measurement is of concern in setting the allowable loads of friction connections. A loss in clamping force causes a proportional loss of friction capacity. Previous tests have shown that a rapid bolt tension reduction occurs immediately after tightening [15]. This rapid drop in tension normally occurs before the reading of a manual bolt calibration device. This reduction is consequently already incorporated into the bolt calibration curves. The measured bolt shortening and the loss of clamping force measured directly in the force washer experiments occurs over a longer period of time. In both the bolt shortening measured in the creep experiments and force washer measurement data, the reduction in bolt force occurred at a much slower rate and these rates correlated with one another. The majority occurred within 50 hours after tightening. Baldwin [6] has reported similar bolt force reductions in joints with painted surfaces. His results indicate even larger bolt force reductions than measured in the force washer experiments.

The correlation of the post creep slip tests of organic zinc with A490 bolt specimens to slip loads calculated from reduced clamping forces calculated from the bolt shortening measurements indicate that the bolt shortening measurements are a valid means of calculating bolt force reductions. The lack of correlation of the A325 bolted specimens with the same coating indicate that for these specimens the measured bolt shortening did not result in a reduction of bolt force. However, both Baldwin's [6] and the present force washer experiments indicate that a reduction of clamping force occurs due to compressive creep of the paint



both on the faying surface and under the bolt and nut or washer. The conflict in the conclusions from the data cannot be resolved. It does appear that in some coatings under high clamping forces a significant reduction in bolt clamping force can occur.

The proposed creep test method given in the Appendix addresses this problem by requiring the specimens be tested with A490 bolts and a slip test performed after completion of the creep test. The allowable load is to be determined based on the smaller load which produced no significant creep deformation (0.005 in. [0.13 mm] after 1000 hrs), the static short-term slip load, or the slip load measured after the creep test on the creep specimens. The latter requirement will, along with the requirements for a thick coating and A490 bolts, account for any loss in the clamping force upon the allowable load.

Additionally, consideration should be given to increasing the minimum installation tension required to 10 percent above the present values. The turn-of-the-nut method will normally give tension in excess of this value when the bolt assembly is in good condition [13]. Newer bolt tensioning methods such as load indicator washers and torque tension twist-off bolts can be calibrated to give any bolt tension value. Many times the manufacturers are setting these bolt tensions to the minimum bolt tension value specified. Setting the bolt tension to 10 percent above the minimum value will negate the reduction of clamping force due to compressive creep of the coating and also account for scatter in bolt clamping force. A similar approach is used in the Japanese specifications.

## 5. FATIGUE STUDY OF COATED BOLTED JOINTS

### Specimen Design and Testing Program

Fatigue tests were performed on specimens coated with organic zinc, organic zinc with an epoxy topcoat, and inorganic zinc. Vinyl base paints were not included in the fatigue tests due to their poor creep performance. In addition, a set of uncoated blast-cleaned specimens were included in the experiment design to allow direct comparison of the behavior of coated with uncoated specimens.

The object of the tests was to determine the influence of type of coating upon fatigue life, the slip performance of joints under cyclic loading, and the effect of the ratio of net area to gross area upon fatigue performance. Table 43 shows the experiment design used in the fatigue testing program. The stress ranges were based on the gross area of the specimen and selected to yield fatigue lives less than two million cycles of load. Two replicate specimens were tested at the principal stress ranges to determine the scatter in the test results. A total of twenty specimens was tested. The slip performance under cyclic loading was determined by measuring the slip of the specimens during the fatigue tests.

Table 43. Testing program

Stress Range	Organic Zinc	Organic Zinc/ Epoxy Topcoat	Inorganic Zinc	Blasted
20				1
25*		2	2	2
30		1	1	
35*	2**	2	2	2
40	1			
45*	2			

\*Principal stress range

\*\*Number of specimens

Four major factors were considered in the design of the specimen. First, it was necessary to have a slip load higher than the maximum applied load. This was done in order to simulate the usual design conditions where the maximum load permitted on a connection is a function of the slip load. Since the slip load is related to the clamping force of the bolts, ASTM A490 high strength bolts were used in all the joints to develop maximum slip loads. The variation of the slip coefficient of

the coatings was also taken into consideration in the determination of the specimen slip load.

Second, the main interest was to study high stress ranges in order to produce reasonably short fatigue lives. Third, a fluctuating tension load cycle was to be used in the tests. It was decided to have a minimum stress of 10 ksi (68.9 MPa) based on the gross area. These two factors led to the use of A514 steel with  $F_y = 100$  ksi (689 MPa), in order that the applied stresses would be of the order of normal allowable design stresses. This permitted a maximum allowable tensile stress of  $F_T = 53$  ksi (365 MPa) according to the AASHTO Specification based on the net area.

The fourth factor was to take in consideration the effect of the net and gross area which is a function of the geometry and size of the specimen. It was necessary to limit the size of the joints so that the expected failure load of the specimen would not exceed the maximum capacity of the fatigue testing equipment.

Two bolt arrangements were chosen to have different ratios of net to gross area. The specimen was a 3/8 in.  $\times$  7 in.  $\times$  21 in. (9.5 mm  $\times$  178 mm  $\times$  533 mm) plate connected with 7/8 in. (22mm) diameter A490 bolts, with a single row of four bolts on one side and a double row with two bolts per row on the other side.

Figure 80 shows an exploded view of the test specimen. Each specimen consisted of a single test plate, a pair of side plates at the top and bottom, and a set of filler plates. All surfaces of these plates had the same surface treatment, i.e., same coating or blast treatment. Figure 81 shows the assembled specimen and the location of LVDT used to monitor specimen slip during testing. The test specimen was inserted between the lap plates. The lap plates, pull plates, and their connection was designed to preclude fatigue failure. In order to increase the slip resistance between the lap plates and the side plates, filler plates were used which allowed two additional bolts to be used in the connection.

The gross area on the specimen plates was  $A_g = 2.63$  in.<sup>2</sup> (1697 mm<sup>2</sup>) and the net area was  $A_{net} = 2.25$  in.<sup>2</sup> (1452 mm<sup>2</sup>) for the single row pattern and  $A_{net} = 1.88$  in.<sup>2</sup> (1213 mm<sup>2</sup>) for the double row pattern. The net area was calculated using the hole diameter plus 1/16 in. (1.6 mm). All the specimens were saw-cut to length from 7 in. (178 mm) wide steel plates which had been flame-cut to this width by the supplier. Each specimen consisted of one 3/8 in.  $\times$  7 in.  $\times$  21 in. (9.5 mm  $\times$  178 mm  $\times$  533 mm) specimen plate, two 3/8 in.  $\times$  7 in.  $\times$  15 in. (9.5 mm  $\times$  178 mm  $\times$  381 mm) side plates, two 3/8 in.  $\times$  7 in.  $\times$  9 in. (9.5 mm  $\times$  178 mm  $\times$  229 mm) side plates, and two 3/8 in.  $\times$  7 in.  $\times$  2-3/4 in. (9.5 mm  $\times$  178 mm  $\times$  70 mm) filler plates, as shown in Figure 80. In order to assure that all the specimens and side plates were identical, templates were used in their fabrication. All the holes were first center-drilled with a

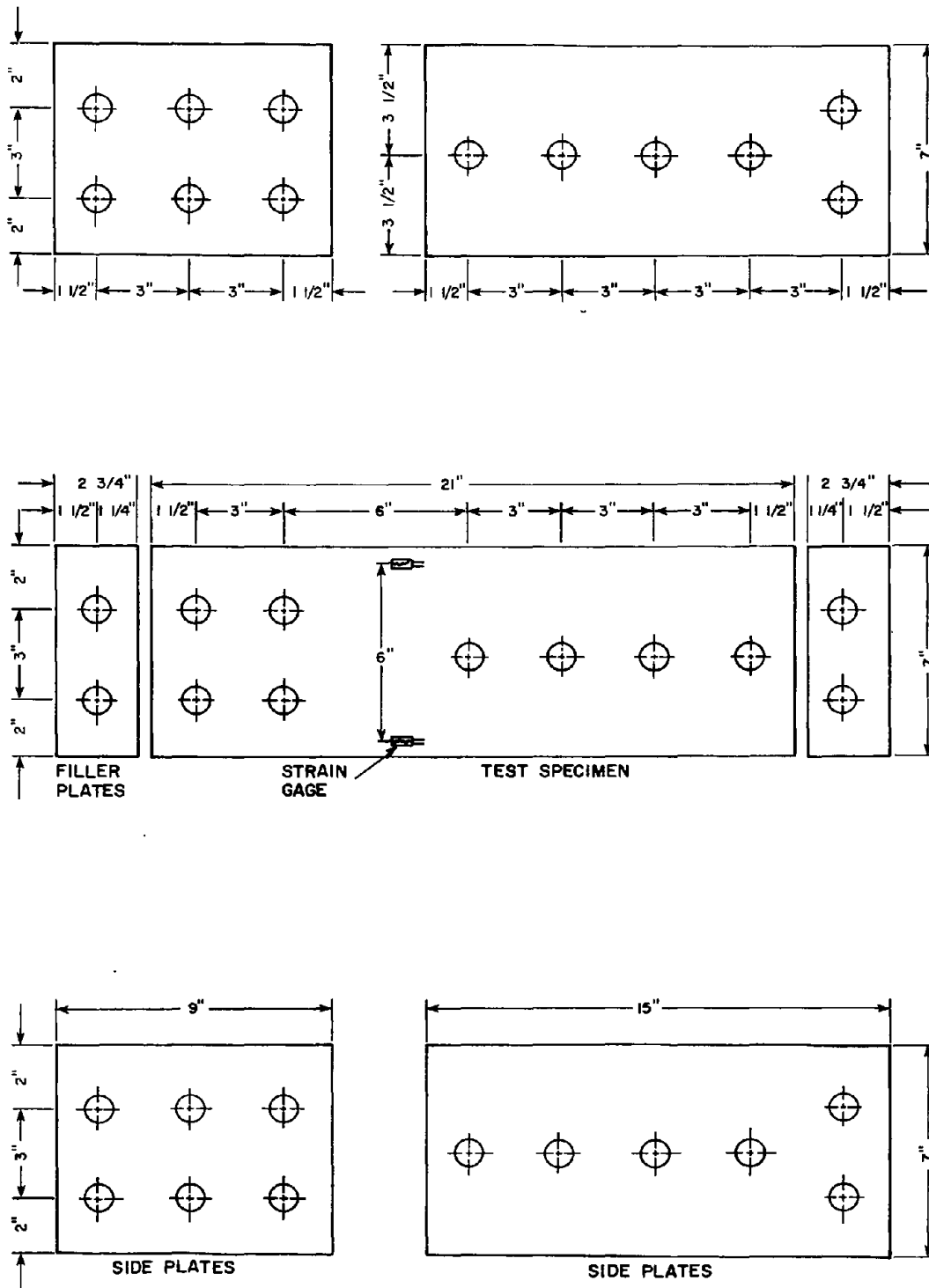


Figure 80. Specimen and plate dimensions  
(1 in. = 25.4 mm)

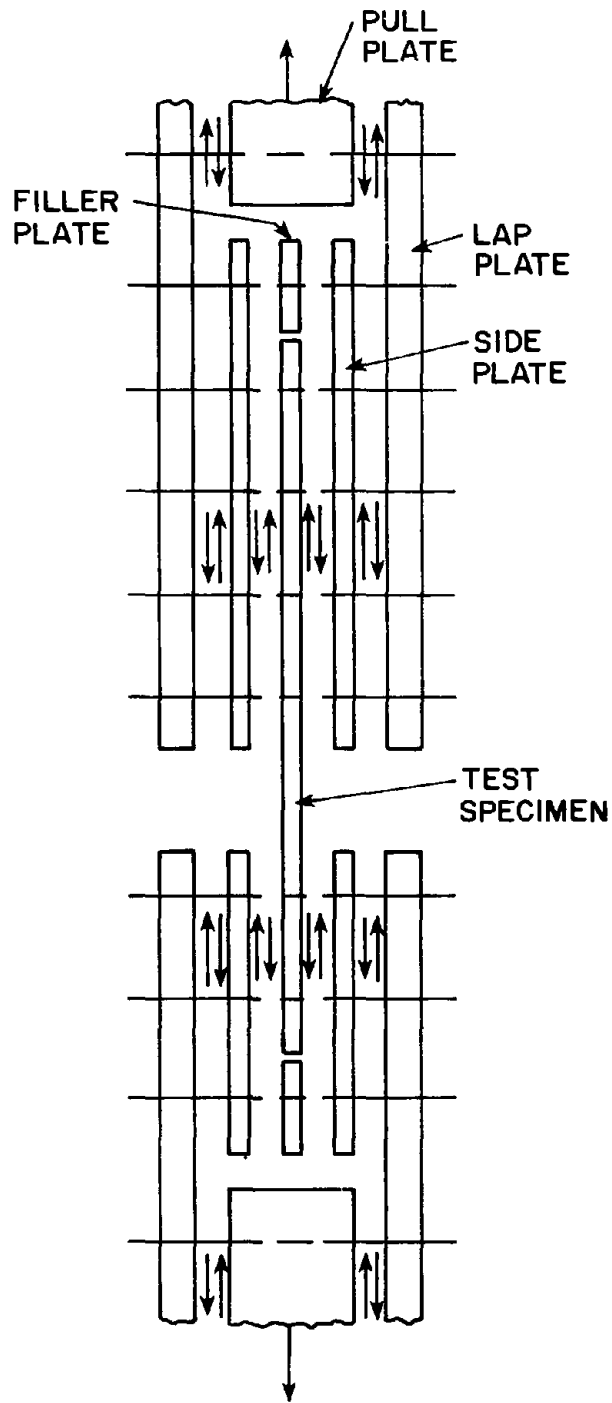


Figure 81. Shear force diagram

1/4 in. (6.4 mm) drill and then drilled to size with a 15/16 in. (24 mm) drill. The holes were reamed with a large tapered reamer to remove the burrs at the edge of the holes from the drilling operation.

### Test Equipment

A Riehle/Los Universal hydraulic self-contained single acting pulsator was used to supply the sinusoidal hydraulic pressure to the loading ram. The pulsator uses a constant pressure hydraulic pump to maintain the specified maximum load and a variable stroke large displacement piston to provide the fluctuating pressure. Two general purpose testing rams were connected to the pulsator. Each ram has 160 kips (712 kN) static load capacity and 120 kips (534 kN) dynamic load capacity. The testing frequency ranged from 4 to 8 Hz. Most of the testing was conducted at a frequency of 6 Hz. Figure 82 shows the test setup with the two loading rams and the specimen in the center.



Figure 82. Fatigue testing setup

## Instrumentation

The load in the specimen was monitored using strain gages applied to the specimen. Four 0.64 in. (16mm) gage length paperback 120 ohm strain gages were mounted on each specimen, two on each side. They were located 1/2 in. (12.7mm) from each edge of the specimen, as shown in Figure 80. They were attached using Eastman 910 cement.

The strain gages were connected to an amplitude measuring module. This module contains a high gain amplifier, a power supply for the strain gage, and a two-stage voltage comparator. The amplified strain signal is compared by the comparator circuits with two calibrated DC voltages corresponding to the desired maximum and minimum strains. The difference is displayed on an oscilloscope. The dynamic loads were set within 1 percent with the use of this system. The average of the four strain gages was used to establish the desired stress range.

Each specimen was loaded statically to the maximum stress at least three times before the cyclic loading was started. Strain gage readings were taken on all four gages during the static test. The average of all four strain gage readings was used to set the initial dynamic load settings on the pulsator.

The load was set to the maximum level and the pulsator was engaged. The stroke was then adjusted until the desired stress range was reached, as indicated by the average of the strain gage readings.

The pulsator contains a pair of limit gages which provided a means of sensing any change in pressure due to a crack in the specimen and stopping the pulsator. In addition, two micro-switches were mounted on the testing frame to limit the top crosshead movement. In the event of a failure of the specimen, the micro-switches would contact and automatically shut off the pulsator and displacement recorder.

In order to monitor the slip behavior of the joints during the test, two LVDT transducers were mounted on the specimen, as shown in Figures 83 and 84. The LVDT core rods were attached to a small aluminum angle glued between the test joints. The output of the transducers was connected to a strip chart recorder and monitored continuously during the fatigue test for most of the specimens. During the first two tests, the output of the transducers was connected to the amplitude measuring module. The chart recorder sensitivity used was 0.5 volts, which allowed displacements as small as 0.0005 in. (0.013mm) to be measured.

## Specimen Preparation

Painting. Painting was done using an air-pressure spray gun. A uniform and even coat was applied. Wet paint thickness was measured with a prong-type wet paint gage to control the final dry paint thickness. All the specimens, side plates, filler plates, and slip control

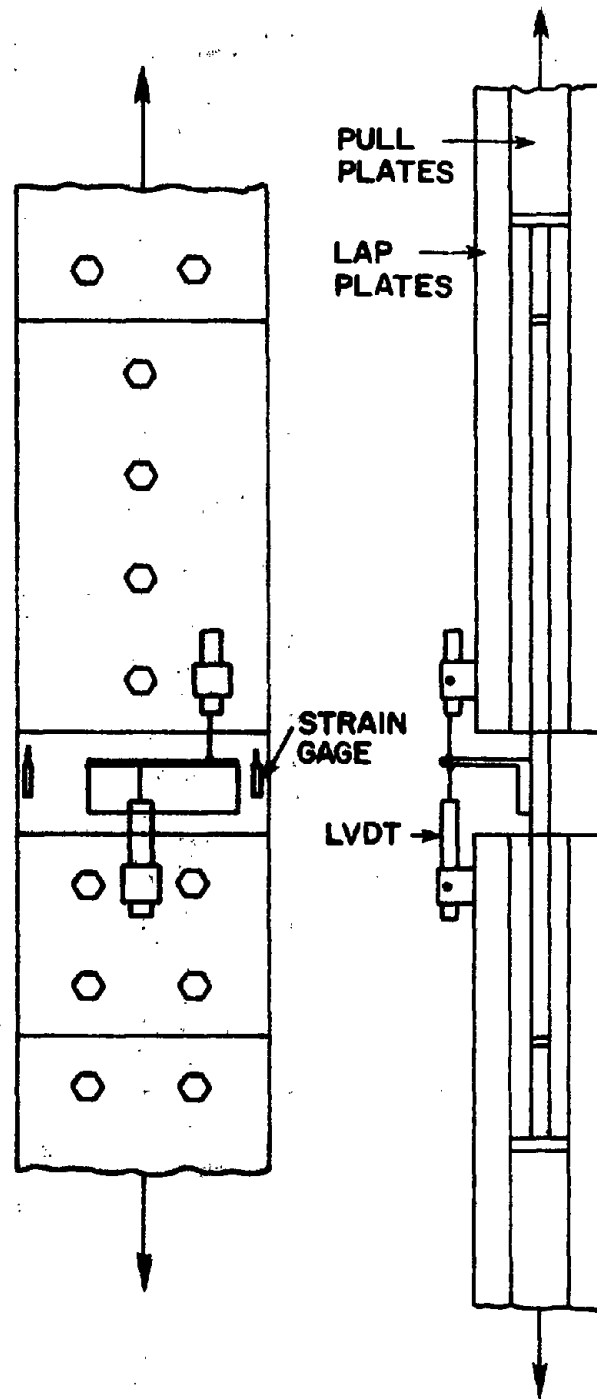


Figure 83. LVDT mount



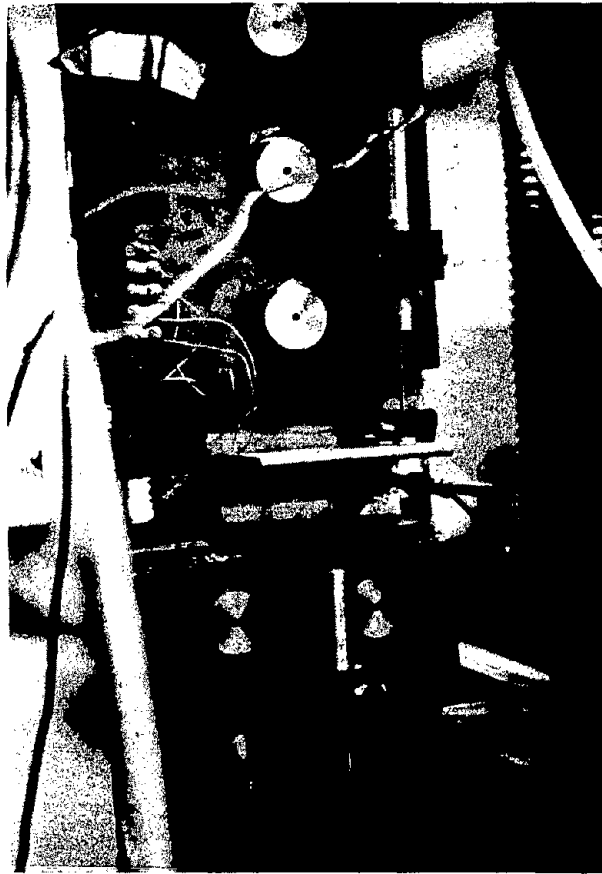


Figure 84. LVDT and strain gage mount

specimens from each coating system were painted at the same time.

All the specimens and plates were sandblasted prior to the painting. All were painted within 24 hours of the blasting operation. The painted plates were placed in a low humidity air conditioned room to cure. The inorganic zinc set was initially cured by using a water-soaked burlap over the specimens for a period of one day before they were placed in the air conditioned room, since this system requires an initial high humidity for proper curing.

Because the width of the plates was greater than the width of the paint spray pattern, it was necessary to overlap the paint coatings. Thus, the center band of the test specimens and the side plates had a slightly higher thickness than the edges. The dry paint thickness was measured utilizing a Mikrotest magnetic gage after each coat of paint. Usually, two coats of paint were applied one day apart. Table 44 gives the average paint thickness of each plate used in the testing program.

Table 44. Average paint thickness (mils)

Painting System	21" Specimen		15" Filler Plate		9" Filler Plate		2-3/4" Filler Plate		2-3/4" Filler Plate	
	Side A	Side B	Side A	Side B	Side A	Side B	Side A	Side B	Side A	Side B
Organic Zinc	8.5	7.9	7.5	7.0	7.2	6.9	7.8	6.6	7.0	9.1
	8.8	7.7	7.5	7.8	6.8	6.4	7.8	6.6	7.0	9.1
	8.0	8.8	7.0	8.0	7.3	6.8	10.3	9.3	9.6	8.1
	7.5	8.0	6.9	9.1	7.0	6.5	7.8	6.6	7.0	9.1
	9.6	7.6	7.2	7.0	7.5	7.0	7.8	8.5	8.3	9.3
Organic/Epoxy Topcoat	7.7	8.1	8.5	8.3	10.5	7.4	8.6	8.4	8.5	10.0
	3.9	8.9	5.4	4.4	4.7	3.5	6.3	8.3	6.7	5.7
Organic/Epoxy Topcoat	8.8	9.3	8.0	7.4	7.9	7.9	8.6	8.4	8.5	10.0
	4.0	3.9	4.9	3.5	4.0	4.8	6.3	8.3	6.7	5.7
Organic/Epoxy Topcoat	8.6	8.1	7.6	8.2	7.7	7.8	8.6	8.4	8.5	10.0
	6.9	4.7	2.5	5.5	4.0	4.7	6.3	8.3	6.7	5.7
Organic/Epoxy Topcoat	7.2	8.8	8.5	7.6	8.1	7.5	8.6	9.3	8.3	9.3
	4.9	5.2	3.7	3.0	4.0	4.7	7.1	7.3	9.1	5.6
Organic/Epoxy Topcoat	8.0	7.9	7.9	8.2	7.3	7.3	8.1	7.8	8.1	8.5
	4.0	4.7	5.1	4.6	4.7	2.5	3.8	4.3	6.3	8.3
Inorganic Zinc	3.6	4.6	2.6	3.3	3.2	3.6	3.6	3.8	3.1	3.9
	4.7	4.2	3.2	3.7	3.2	3.5	3.6	3.8	3.1	3.9
	3.8	3.4	4.9	5.2	4.2	4.1	3.6	3.8	3.1	3.9
	5.0	3.4	4.1	3.3	3.5	3.5	3.4	4.6	4.4	3.2
	5.1	4.0	4.3	4.0	4.2	3.0	3.5	3.0	3.8	4.1

(1 mil = 0.001 in. = 0.025 mm, 1 in. = 25.4 mm)

Bolt Calibration and Tightening Procedure. Four bolt calibrations (tensile load-bolt elongation relationship) were performed in order to determine the clamping force of the bolts used in each specimen. All the 7/8 in. (22mm) A490 bolts used in the specimens were from the same lot. Four of these bolts were selected randomly and calibrated. The bolt calibration procedure was the same as discussed previously. All the threads of the bolts and the turning surface of the nuts used in the calibration and in the specimens were lubricated with a high temp C5-4 anti-seize compound.

All the bolts in the test specimens were tightened to 1/3 of a turn past snug tight. Initial bolt elongation readings were taken with no load on the bolt. Each bolt was then tightened to a snug position which corresponded to the full strength of a man using an 18 in. (457mm) long wrench. The bolts were then impacted to 1/3 of a turn and a bolt elongation reading taken. The 1/3 of a turn was measured by a mark in the impact wrench.

Figure 85 shows a histogram of the actual bolt tension obtained on all the bolts used. The mean clamping force was 64.7 kips (288 kN) with a standard deviation of 2.0 kips (8.9 kN). The average bolt clamping force for the four bolts used in each test joint varied between 63.5 and 64.5 kips (283 and 287 kN). A value of 64 kips (285 kN) was used for all joints in calculating their slip loads. The minimum specified fastener tension is 49 kips (218 kN) [2].

#### Control Slip Tests

Three control compression-type slip tests were performed on each coating in order to obtain the slip coefficient of each type of paint system. The control slip specimens were fabricated from A572 Grade 50 steel plate which was nominally 5/8 in. (16mm) thick. The control slip specimens and test procedures were identical to those described previously. The average slip coefficients from the control specimens are given in Table 45. These results were used to establish the theoretical slip load of the full-size fatigue test specimens.

Table 45. Slip coefficients from control specimens

Painting System	Slip Coefficient
Organic Zinc	0.586
Organic Zinc/Epoxy	0.421
Inorganic Zinc	0.518

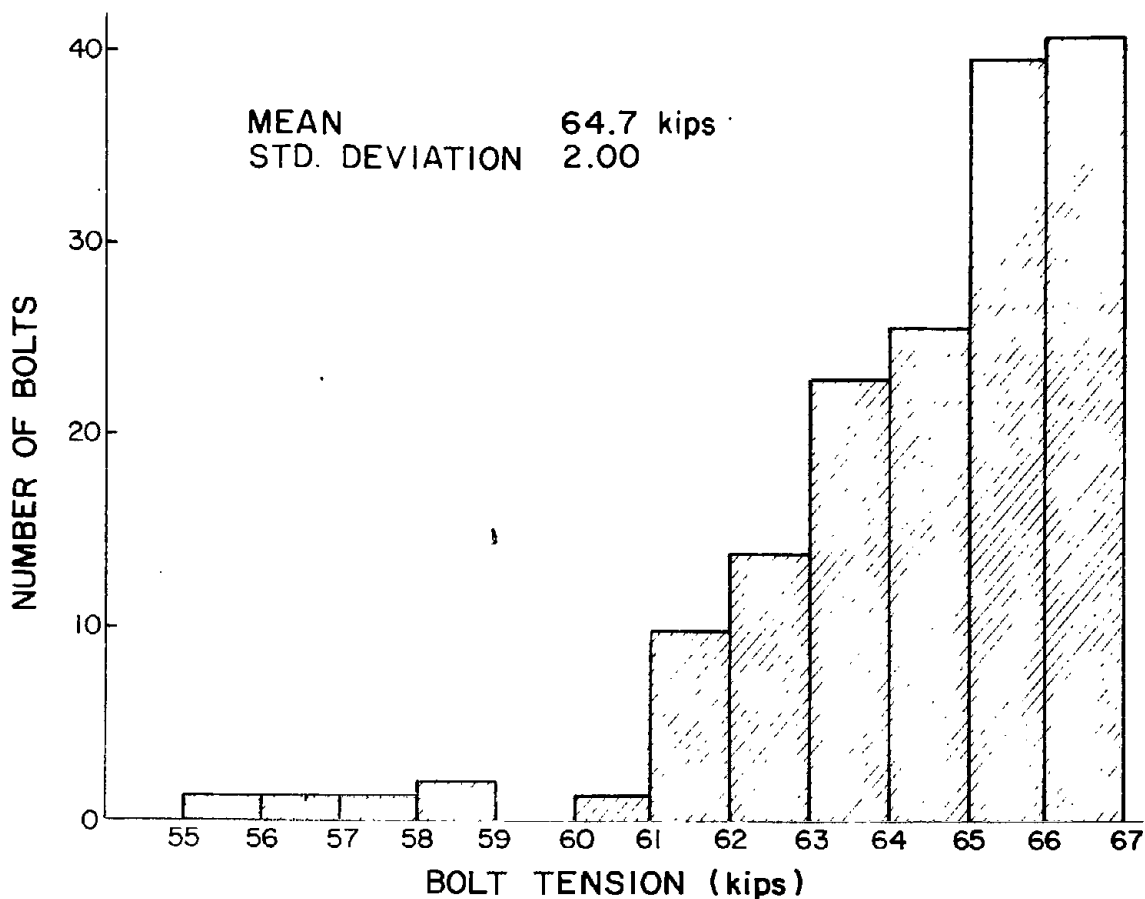


Figure 85. Bolt tension histogram of fatigue specimens  
(1 kip = 4.45 kN)

The slip coefficient for the control specimens with an organic zinc component was higher than the average found in the slip tests of this paint, but they were within the range of the measured values. The inorganic zinc control specimens gave results similar to the average found in the slip tests.

#### Test Results

Figures 86, 87, and 88 show typical failed test specimens. Figure 86 shows an organic zinc specimen that failed through the net area at the single hole pattern. Figure 87 shows an organic zinc with an epoxy topcoat that failed through the net area at the double hole bolt pattern. Figure 88 shows an inorganic zinc specimen that failed through the gross area.

Organic Zinc Fatigue Results. Five specimens were tested with organic zinc-rich primer. Two specimens were tested at 35 ksi (241 MPa) gross section stress range, two at 45 ksi (310 MPa), and one at 40 ksi

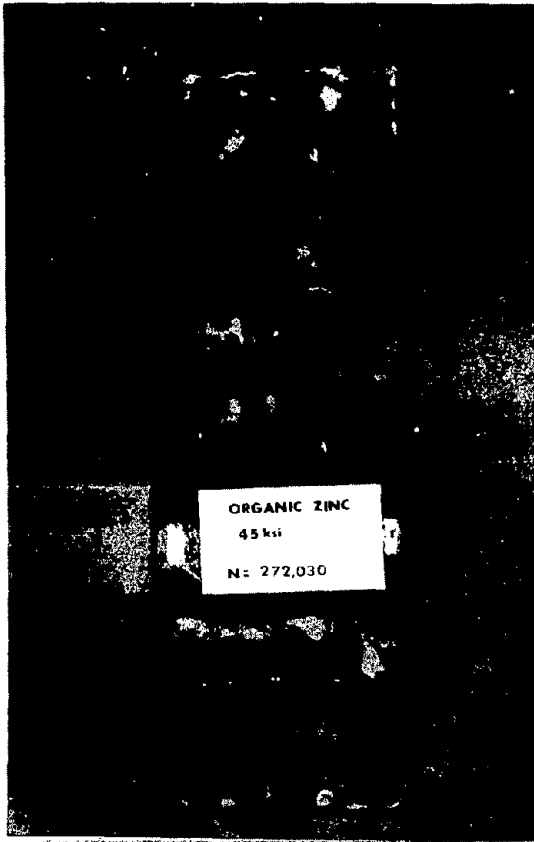
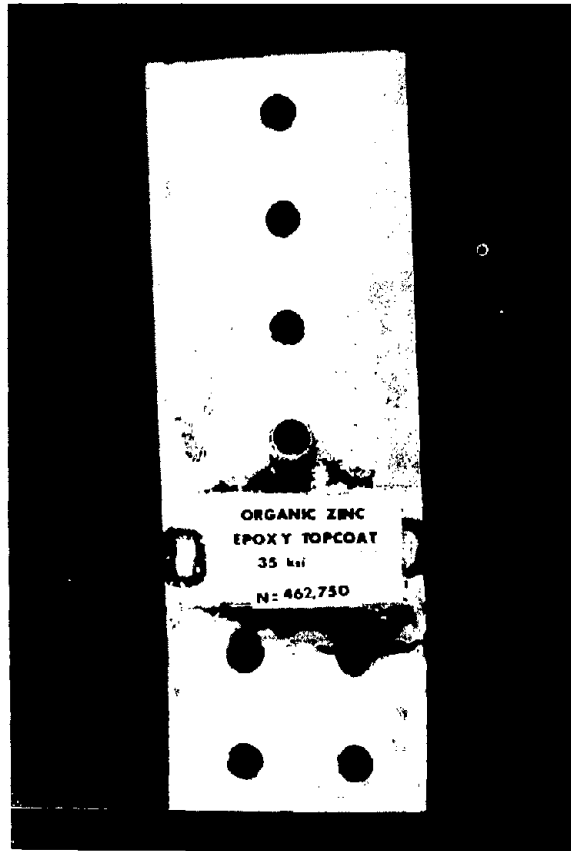


Figure 86. Organic zinc specimen  
(1 ksi = 6.89 MPa)

Figure 87. Organic zinc/epoxy  
specimen  
(1 ksi = 6.89 MPa)



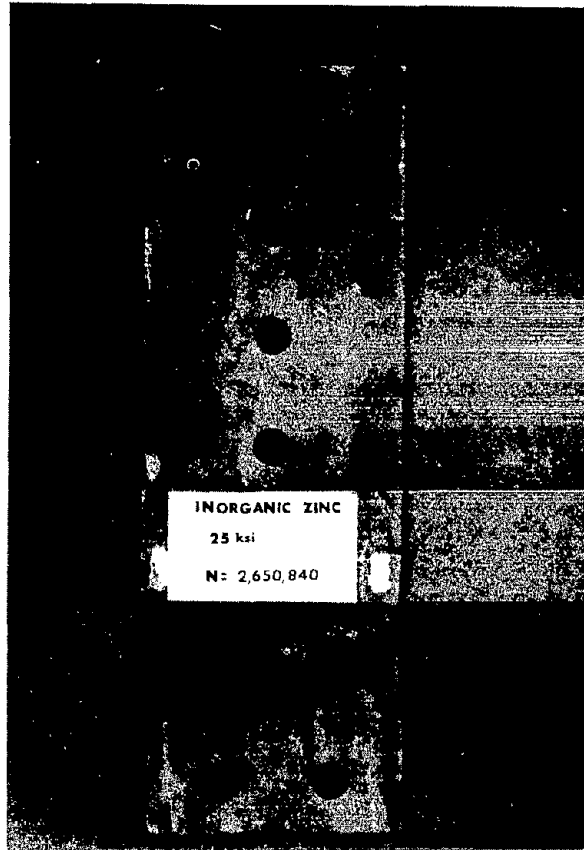


Figure 88. Inorganic zinc specimen  
(1 ksi = 6.89 MPa)

(276 MPa). Table 46 summarizes the results for the five organic zinc specimens. In the table,  $S_R$  is the stress range on the gross area in ksi. When failure occurred through the net section, the net section stress range in ksi is also given. The minimum gross section stress was 10 ksi (69 MPa) for all specimens.  $P_{max}$  is the maximum applied load in kips.

The average slip coefficient from the three control slip specimens was 0.586, which gives a slip load,  $P_{slip}$ , of 300 kips (1335 kN) based on the average measured clamping force<sup>slip</sup> of 64 kips (285 kN). The ratio of  $P_{max}$  to  $P_{slip}$  shows that all the tests were conducted at load levels less than 50 percent of the expected slip load.

Two other load levels,  $P_{allowable}$  and  $P_{spec}$ , are also given in Table 46 for reference. These loads can be considered as "service or allowable" loads.  $P_{allowable}$  is based on a service load slip coefficient,  $k_s = 0.31$ , established by using a factor of safety of 1.5 with the mean slip coefficient from the static slip test program

Table 46. Test results--organic zinc specimens  
(1 ksi = 6.89 MPa, 1 kip = 4.45 kN)

Specimen No.	$S_R$	Net Stress Range	No. of Cycles to Failure	Location of Failure	(d)		(a)	(a)	(b)	(b)	(c)	(c)
					$P_{max}$	Average Clamping Force	$P_{slip}$	$\frac{P_{max}}{P_{slip}}$	$P_{allowable}$	$\frac{P_{max}}{P_{allowable}}$	$P_{spec}$	$\frac{P_{spec}}{P_{max}}$
	(ksi)	(ksi)			(kips)	(kips)	(kips)		(kips)		(kips)	
1	35	.	2,678,250	None	118	64	300	0.39	121	0.98	125	0.94
2	35		2,285,340	None	118	64	300	0.39	121	0.98	125	0.94
3	45	52.5	117,180	Net Area Single	144	64	300	0.48	121	1.20	125	1.15
4	45	52.5	272,030	Net Area Single	144	64	300	0.48	121	1.20	125	1.15
5	40	46.7	256,860	Net Area Single	131	64	300	0.44	121	1.09	125	1.05

(a) Based on the control specimen,  $k_s = 0.586$ .

(b) Based on recommended values in Ref. 16,  $k_s = 0.31$ , and a clamping force = 49 kips.

(c) Based on specification (Class E) in Ref. 30,  $F_v = 26$  ksi

(d)  $P_{max} = A_G(S_R + 10 \text{ ksi})$

[16]. Using the service load slip coefficient and the minimum specified clamping force of 49 kips (218 kN) for a 7/8 in. (22mm) A490 bolt, the service load obtained is 121 kips (538 kN). The allowable load based on specification of the Research Council on Riveted and Bolted Structural Joints [30],  $P_{spec}$ , is 125 kips (556 kN) for an organic zinc-rich primer. The maximum loads in the fatigue experiment were close to or slightly above the recommended service load levels.

Specimens 1 and 2 at 35 ksi (241 MPa) gross stress range did not slip during the applied fatigue loading. The slip of these specimens was monitored using the voltage amplitude device. It was found that this method was not a convenient means of keeping a record of the data. However, the data available indicate that no slip occurred in either the top single row joint or the bottom double row joint. The maximum applied load was 118 kips (525 kN). The test load was 39 percent of the slip load calculated from the control specimens. The specimens experienced no failure after 2-1/4 million cycles.

Since Specimens 1 and 2 did not fail in fatigue, they were then loaded statically to determine the slip load. On Specimen 1, first slip was observed on the double row joint at  $P_{slip} = 241$  kips (1072 kN), which corresponds to a slip coefficient  $k_s = 0.471$ , based on an average clamping force of 64 kips (285 kN) per bolt. On this specimen the single row joint slipped at  $P_{slip} = 252$  kips (1121 kN) ( $k_s = 0.492$ ). On Specimen 2, the performance was similar; the measured slip loads on the double row and single row were  $P_{slip} = 242$  kips (1121 kN), respectively. The capacity measured after cycling represents 80 to 84 percent of the capacity estimated using the control specimens. The results are well within the scatter found in static tests. Consequently, the slip capacity of these joints was judged to be unaffected by the applied fatigue cycles.

Specimens 3 and 4 were tested at 45 ksi (310 MPa) gross stress range with an applied maximum load of 144 kips (641 kN), which was 48 percent of the slip load calculated from the control specimens. The slip of these specimens was measured using a Brush strip chart recorder. The range on this recorder was not appropriate to measure the total slip. However, it was observed that both joints on each of the specimens gradually slipped until they reached the limit of the recorder, approximately 1/16 in. (1.6 mm) slip. On both specimens, failure occurred through the net area on the single row bolt pattern. The stress range on the net area was 52.5 ksi (362 MPa). It was observed in Specimen 3 that heating and subsequent melting of the coating occurred, due to the rapid testing frequency of 6 Hz. The frequency on Specimen 4 was reduced to about 3 Hz and in this specimen no heating or melting was observed. Figure 87 shows Specimen 4 after failure.

The last specimen was tested at 40 ksi (276 MPa) gross stress range. The maximum applied load was 131 kips (583 kN), which was 44 percent of the slip load. On this specimen as well as in the rest of the



specimens tested, a Hewlett Packard strip chart recorder was used to measure the slip. On this specimen, both joints slipped gradually into bearing after 20,000 cycles. The slip measured on the single joint was 1/8 in. (3 mm). The slip measured on the bottom double joint was about 3/32 in. (2 mm). Failure occurred through the net area on the single row pattern joint.

Organic Zinc/Epoxy Topcoat Fatigue Results. Table 47 summarizes the test variables and results on the five fatigue specimens coated with organic zinc primer and an epoxy topcoat. The minimum stress for all specimens was 10 ksi (69 MPa) on the gross area. Three stress ranges were tested: 25 ksi (172 MPa), 30 ksi (207 MPa), and 35 ksi (241 MPa).

From the control specimens, an average slip coefficient of  $k_s = 0.421$  was obtained, which yielded a slip load of  $P_{slip} = 215$  kips (957 kN). This slip coefficient is higher than the average slip coefficient obtained from Fouad's tests [16]. His average slip coefficient was  $k_s = 0.276$ . The applied maximum fatigue load varied between 92 and 118 kips (409 and 525 kN), which is 43 to 55 percent of the slip load obtained from the control specimen.

Specimens 1 and 2 in this series were tested at 25 ksi (172 MPa) gross section stress range. Slip on these specimens was observed to be less than 1/32 in. (1 mm) after  $1 \times 10^6$  cycles. One of the specimens failed through the gross area. However, it was observed that this specimen had a notch on the edge from the burning operation. The second specimen experienced no failure after more than  $2 \times 10^6$  cycles.

A slip test was performed on Specimen 2. The single row joint slipped at a load of  $P_{slip} = 187$  kips (832 kN), which yields a slip coefficient of  $k_s = 0.365$ . The double row joint slipped at a load of  $P_{slip} = 181$  kips (805 kN), which yields a slip coefficient of  $k_s = 0.354$ .

The measured slip loads after fatigue cycling are between 84 and 87 percent of the value estimated from the control specimens. These percentage values are similar to those measured in the organic zinc specimens tested after fatigue cycling and well within the scatter of the static test results.

Two specimens were tested at 35 ksi (241 MPa) gross stress with a maximum applied load of 118 kips (525 kN), which is 55 percent of the slip load from the control specimens. Slip on these specimens occurred suddenly after 10,000 cycles of load had been applied. One of the specimens failed through the net area on the single row joint after 424,480 cycles. The net section stress range was 40.8 ksi (281 MPa). The second specimen failed through the double bolt pattern joint after 462,750 cycles at a net section stress range of 49 ksi (336 MPa), as shown in Figure 88.

Table 47. Test results--organic zinc/epoxy topcoat specimens  
(1 kip = 4.45 kN, 1 ksi = 6.89 MPa)

Specimen No.	S <sub>R</sub>	Net Stress Range	No. of Cycles to Failure	Location of Failure	(d)	Average Clamping Force	(a)	(a)	(b)	(b)	(c)	(c)
					P <sub>max</sub>		P <sub>slip</sub>	$\frac{P_{max}}{P_{slip}}$	P <sub>allowable</sub>	$\frac{P_{max}}{P_{allowable}}$	P <sub>spec</sub>	$\frac{P_{spec}}{P_{max}}$
	(ksi)	(ksi)			(kips)	(kips)	(kips)		(kips)		(kips)	
1	25		1,209,540	Notch on Gross Area	92	64	215	0.43	71	1.30	0	0
2	25		2,474,620	None	92	64	215	0.43	71	1.30	0	0
3	35	40.8	424,480	Net Area Single	118	64	215	0.55	71	1.67	0	0
4	35	45	462,750	Net Area Double	118	64	215	0.55	71	1.67	0	0
5	30	32	252,760	Net Area Double	105	64	215	0.49	71	1.49	0	0

(a) Based on the control specimen,  $k_s = 0.421$ .

(b) Based on recommended values in Ref. 16,  $k_s = 0.18$  and a clamping force = 49 kips.

(c) The specification does not allow this type of painting.

(d)  $P_{max} = A_G(SR + 10 \text{ ksi})$

The last specimen of this series was tested at 30 ksi (207 MPa) gross section stress range. The applied maximum load was 105 kips (467 kN), which is 49 percent of the slip load. A slip of about 3/32 in. (2 mm) was measured on both joints before 15,000 cycles of load had been applied. The specimen failed through the net area on the double bolt pattern at a net section stress range of 42 ksi (289 MPa).

Inorganic Zinc Fatigue Results. Five specimens coated with an inorganic zinc paint were tested in fatigue, as summarized in Table 48. Three stress ranges of 25 ksi (172 MPa), 30 ksi (207 MPa), and 35 ksi (241 MPa) were considered and the minimum stress in all specimens was 10 ksi (69 MPa). The maximum fatigue load levels were between 35 percent and 45 percent of the theoretical slip load,  $P_{slip} = 265$  kips (1179 kN).

At a stress range of 25 ksi (172 MPa), Specimens 1 and 2 both failed in fatigue through the gross section near the single row bolt pattern, as shown in Figure 88. The two specimens failed at  $1.53 \times 10^6$  cycles and  $2.65 \times 10^6$  cycles, respectively. Specimens 3 and 4 were tested at a 35 ksi (241 MPa) gross section stress range. In both cases, the fatigue failure occurred through the gross section near the double row bolt pattern joint. Specimen 5, at a 30 ksi (207 MPa) stress range, also failed through the gross section near the double row of holes. In all specimens, the total measured slip was less than 1/32 in. (1 mm).

Blasted Surface Fatigue Results. Table 49 summarizes the results from the five fatigue tests on blasted specimens with no paint on the faying surfaces. The tests were conducted at stress ranges of 20, 25, and 35 ksi (138, 172, and 241 MPa). The minimum stress for all specimens was 10 ksi (69 MPa). No slip control tests were conducted for these blasted specimens, so a slip coefficient of  $k_s = 0.50$  recommended by Fisher and Struik [15] was used. This yields a slip load of  $P_{slip} = 256$  kips (1139 kN), based on an average clamping force of 64 kips (285 kN)

In Specimens 1 and 2, tested at a 25 ksi (172 MPa) stress range, failure occurred through the gross section near the single row bolt pattern joint. No slip was observed on these specimens, which was typical for all the blasted specimens. Specimens 3 and 4 were tested at a 35 ksi (241 MPa) gross area stress range. The applied maximum load was  $P_{max} = 118$  kips (525 kN), which was 46 percent of the assumed slip load. In both tests, failure occurred through the gross section near the middle of the specimen. The final specimen was tested at a 20 ksi (138 MPa) gross area stress range. Failure occurred after  $2.61 \times 10^6$  cycles through the gross area near the single bolt pattern joint.

### Analysis of Results

Comparison with Previous Studies. Figure 89 shows the S-N plot for all the twenty specimens tested compared to Category B of the AASHTO

Table 48. Test results--inorganic zinc specimens  
(1 kip = 4.45 kN, 1 ksi = 6.89 MPa)

Specimen No.	$S_R$	Net Stress Range	No. of Cycles to Failure	Location of Failure	(d)	Average Clamping Force	(a)	(a)	(b)	(b)	(c)	(c)
					$P_{max}$		$P_{slip}$	$\frac{P_{max}}{P_{slip}}$	$P_{allowable}$	$\frac{P_{max}}{P_{allowable}}$	$P_{spec}$	$\frac{P_{spec}}{P_{max}}$
	(ksi)	(ksi)			(kips)	(kips)	(kips)		(kips)		(kips)	
1	25		792,620	Gross Area	92	64	256	0.36	161	0.57	166	0.55
2	25		862,120	Gross Area	92	64	256	0.36	161	0.57	166	0.55
3	35		200,240	Gross Area	118	64	256	0.46	161	0.73	166	0.71
4	35		350,550	Gross Area	118	64	256	0.46	161	0.73	166	0.71
5	20		2,813,680	Gross Area	79	64	256	0.31	161	0.49	166	0.48

146

(a) Based on recommended values in Ref.15,  $k_s = 0.50$ .

(b) Based on recommended values in Ref.16,  $k_s = 0.41$  and a clamping force = 49 kips.

(c) Based on specification (Class B) in Ref. 30,  $F_v = 34.5$  ksi.

(d)  $P_{max} = A_G(S_R + 10 \text{ ksi})$

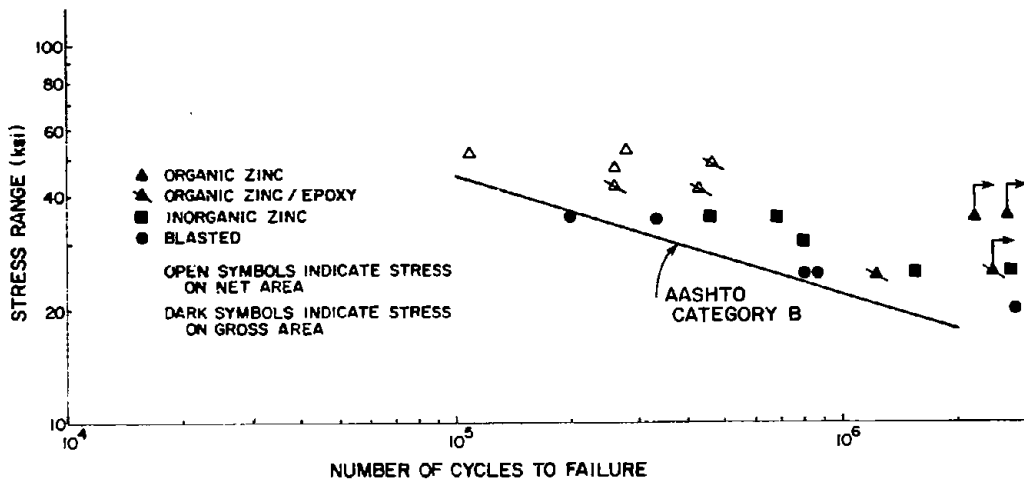


Figure 89. Fatigue test results (1 ksi = 6.89 MPa)

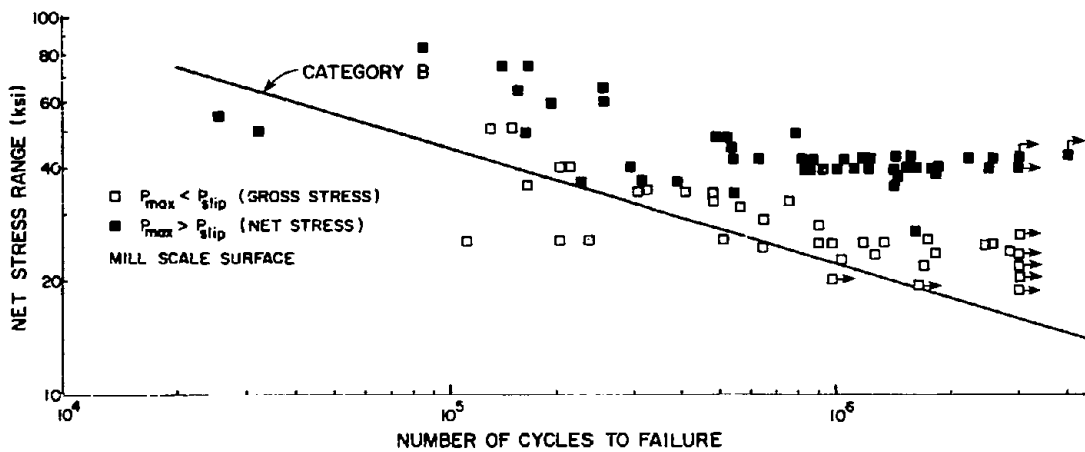


Figure 90. Previous fatigue test results (1 ksi = 6.89 MPa)

Table 49. Test results--blasted specimens  
(1 kip = 4.45 kN, 1 ksi = 6.89 MPa)

Specimen No.	$S_R$	Net Stress Range	No. of Cycles to Failure	Location of Failure	(d)	(a)	(a)	(b)	(b)	(c)	(c)	
					$P_{max}$	Average Clamping Force	$P_{slip}$	$\frac{P_{max}}{P_{slip}}$	$P_{allowable}$	$\frac{P_{max}}{P_{allowable}}$	$P_{spec}$	$\frac{P_{spec}}{P_{max}}$
	(ksi)	(ksi)			(kips)	(kips)	(kips)		(kips)		(kips)	
1	25		1,527,070	Gross Area	92	64	265	0.35	161	0.57	178	0.52
2	25		2,650,240	Gross Area	92	64	265	0.35	161	0.57	178	0.52
3	35		457,740	Gross Area	118	64	265	0.45	161	0.73	178	0.66
4	35		684,180	Gross Area	118	64	265	0.45	161	0.73	178	0.66
5	30		791,360	Gross Area	105	64	265	0.40	161	0.65	178	0.59

(a) Based on control specimens,  $k_s = 0.518$ .

(b) Based on recommended values in Ref. 16,  $k_s = 0.41$ , and a clamping force = 49 kips.

(c) Based on specification (Class F) in Ref. 30,  $F_v = 37$  ksi.

(d)  $P_{max} = A_G(S_R + 10 \text{ ksi})$

Specification [2]. The specimens are plotted on the gross area or net area, based on the location of the failure observed. On those specimens in which the joints slipped, failure occurred through the net area, either through the single row bolt pattern or the double row bolt pattern. If no slip was observed, failure occurred through the gross area. It can be observed that the painted specimens showed a better fatigue performance than the blasted uncoated specimens.

Figure 90 shows the results of previous studies [7,8,19] on fatigue specimens with a mill scale surface condition. The open symbol represents those specimens in which the applied maximum load was less than the slip load and is plotted based on the gross area stress range. The solid symbol indicates those specimens in which the applied load exceeded the slip load and were plotted based on the net area stress range. All the specimens are compared to Category B of the AAASHTO Specification. The open symbol test results which lie below the Category B fatigue specification line were subjected to maximum load levels within 5 percent of their calculated slip loads. It is likely that due to the variation of the slip load, the slip load was exceeded in these specimens. These specimens would lie above the Category B line if their stress range was calculated on the net area. In these studies it was observed that when the specimens slipped, failure was observed through the net area. On the other hand, when no slip occurred, failure was observed through the gross area.

Comparing both figures, it can be seen that the painted specimens showed an equal or better fatigue life than the specimens with a mill scale surface condition.

Analysis of Slip Behavior of Fatigue Specimens. The organic zinc and organic zinc with epoxy topcoat specimen tests at the highest load levels exhibited a decrease in the slip load under fatigue cycling. These specimens slipped before 25,000 cycles of load at maximum loads between 44 to 66 percent of the static slip loads. The failure of the specimens which slipped during the fatigue tests was through the net section of the specimens. The applied maximum loads of the organic zinc specimens which slipped were 44 percent and 48 percent of the slip load for the specimens tested at 40 and 45 ksi gross stress range, respectively. A similar behavior was observed on the long-run creep studies. The creep rate of organic zinc specimens increased gradually when the applied load was 55 percent of the short-term static slip load obtained from control specimens. In the organic zinc specimens (Specimens 1 and 2,  $P_{\max}/P_{\text{slip}} = 0.39$ ) that did not slip and did not fail in the fatigue tests did not exhibit a decrease in the static slip resistance when tested statically after fatigue cycling.

A similar correlation between the fatigue and creep test results was found for the organic zinc with an epoxy topcoat. The specimens were observed to creep suddenly at a load of 66 percent of the static

slip load in the creep tests. The fatigue specimens slipped when the maximum applied load was 49 and 55 percent of the slip load based on the control specimens. Specimen 2 ( $P_{\max}/P_{\text{slip}} = 0.43$ ), which did not fail in fatigue or exhibit any major slip in the test, did not exhibit a decrease in static slip load due to the fatigue cycles applied.

The applied maximum load on the organic zinc specimens which slipped exceeded the allowable load permitted by Table 2a of the Bolt Spec [30]. No values are given in the Bolt Spec for the organic zinc with an epoxy topcoat.

Using Fouad's recommended values [16], the allowable load was calculated for these specimens. His recommendation uses a factor of safety of 1.5 with respect to the mean test data. Tables 46 and 47 show the  $P_{\text{allowable}}$  calculated and the ratio of  $P_{\max}/P_{\text{allowable}}$ . It can be observed that in the organic zinc specimens and in the organic zinc with an epoxy topcoat that as long as this ratio is 1.0 or less, no slippage was observed in the specimens. In those specimens in which this ratio of  $P_{\max}/P_{\text{allowable}}$  exceeded 1.0, slippage occurred in the joints. This type of relationship,  $P_{\max}/P_{\text{allowable}}$ , is based on the allowable load permitted by the Bolt Spec [30].

In the inorganic zinc specimens as well as in the blasted specimens, no slippage occurred. All failures occurred through the gross section. In the inorganic zinc specimens, the maximum applied load was 45 percent of the slip load for the specimens tested at 35 ksi gross stress range. For all the specimens tested, the ratio of  $P_{\max}/P_{\text{allowable}}$  based on Fouad [16] and on the Bolt Spec [30] was less than 1.0, as can be observed in Table 48.

For the blasted specimens, a similar behavior was noted. The allowable load was calculated using Category B of Table 2a of the Bolt Spec [30]. The blasted specimens are compared to the specification values for low strength steels. No reduction in the slip coefficient for the A514 steel in the blasted condition was found in Ref. 16. The ratio of  $P_{\max}/P_{\text{allowable}}$  shown in Table 49, based on Fouad [16] and the Bolt Spec [30], does not exceed 1.0.

#### Summary and Conclusions of Fatigue Tests

The fatigue tests indicate that the application of a coating to the faying surface provides a fatigue life equal to or greater than the fatigue of an uncoated millscale or blasted surface. The existing Fatigue Category B of the AASHTO Specification provides a suitable lower bound to the fatigue data. The results of the current tests, as well as previous tests, indicate that the fatigue stress range should be based on the gross area for specimens which do not slip in testing and on the net area for specimens which slip during the fatigue test. Uncoated



specimens slip during the fatigue testing when the maximum applied load is 90 to 95 percent of the static slip load [7,8,15]. The specimens coated with organic zinc and organic zinc with an epoxy topcoat tested in the current study slipped during the fatigue tests when the maximum load was about 50 percent of the calculated static slip load. These two coating systems also were observed to slip under creep type loadings at roughly the same percentage of the slip load.

Specimens tested at a lower stress range and corresponding lower maximum load of the same two coatings did not slip and produced excellent fatigue performance. When the maximum load was about 40 percent of the slip load, the specimens of these coatings not only did not slip, but also showed negligible decrease in static slip capacity after over  $2 \times 10^6$  cycles of fatigue loading. Therefore, it appears that satisfactory fatigue life, resistance to slip during fatigue cycling, and no degradation of slip performance due to fatigue is obtainable if the maximum applied load is below the load at which a coating exhibits no creep deformation.

The correlation between the loads at which the coatings exhibited creep deformation and slippage in the fatigue tests had not, to the authors' knowledge, been previously reported. The slippage of the fatigue specimens produced failure through the net section. The result was a reduction in the fatigue strength. This reduction in fatigue strength deserves consideration in setting maximum design allowable slip load and also the testing required to determine the suitability of a coating for structures subjected to fatigue loading. The maximum design load should be less than the load at which creep is observed in long-term creep tests. This requirement, based on the correlation between creep and fatigue behavior observed in the present study, may be a means of eliminating the slippage of the joint during fatigue loading. It should be noted in setting the design loads, that slippage occurred in the fatigue specimen at a lower percentage of the static short-term slip load than that which caused creep deformation to occur.

It appears that the creep behavior of a joint must be established as well as its static short-term slip behavior before it is used in structures subjected to fatigue. It is recommended, based on this study and the creep results in Ref. 26, that creep tests be performed on paints at the recommended service level (see Section 4 of Appendix A). Fatigue tests at the same maximum load level could be performed instead of the creep tests. Paints which do not exhibit significant creep deformation would be expected to not slip during fatigue loadings below the maximum design loads.

These recommendations are based on the assumption that the slippage which occurred in the fatigue specimens was caused by the maximum load exceeding a certain percentage of the static short-term slip load. The experiment design does not allow the effects of load range and maximum load to be separated. The correlation found with the creep tests

suggests that the maximum load is the important variable. It is recommended that further tests be performed to determine whether the slippage occurred due to the maximum load (as assumed in the preceding discussion) or the load range.

## 6. SPLICE CONNECTIONS WITH UNDEVELOPED FILLERS

### Introduction

If two members of unequal depths are to be spliced, filler plates are added to the thinner member to produce equal depths, as shown in Figure 91. Splice plates are then used to connect the members and load is transferred between the main members through shear in the bolts. Filler plates are also used where connections are made between rolled sections of the same depth but with different flange or web thickness.

There are two types of filler plates that may be used in a bolted splice joint. The first type usually has the same dimensions as the splice plate and is connected only by bolts going through the splice plates and main member, as shown in Figure 91a. These are called loose or undeveloped fillers because they are assumed to carry no net axial load. The bolts in this type of connection are used only to transfer load between the main structural members through the splice plates. If the filler plate is longer than the splice plate and is bolted to the main member outside the splice plate, then it is considered a developed filler (Figure 91b). A filler is developed when a uniform stress pattern occurs across the combined filler plate and main member areas [2,3]. This stress is defined as the load carried by the main member divided by the combined areas of the filler plates and main member [2].

The American Association of State Highway and Transportation Officials (AASHTO) specification [2] allows undeveloped fillers of any thickness to be used in friction-type connections. However, if the bolted joint is designed as a bearing-type joint, then undeveloped fillers are limited to a maximum thickness of 1/4 in. (6mm). Fillers thicker than 1/4 in. (6mm) must be developed and no more than two plies of filler plate may be used to achieve this thickness without prior approval. The American Institute of Steel Construction (AISC) specification [3] has similar requirements, except there is no restriction on the number of plies used to obtain filler thickness.

Shear Strength of A325 Bolts. Shear tests on A325 bolts have been mostly double shear tests without fillers [15,34] so that there is little bending or bearing deformation of the fixtures. Therefore, the ultimate load is controlled solely by the shear strength of the bolt and the bolt is loaded as shown in Figure 92a. The shear planes through the bolt occur at the contact of the splice plate and the main structural member.

The use of undeveloped fillers, which carry no stress, would create an idealized separation in the loading pattern, as shown in Figure 92b. This loading pattern would occur after the bolt is completely in bearing with no friction present. The separation of the loading gives the bolt more space to deform or bend. As filler

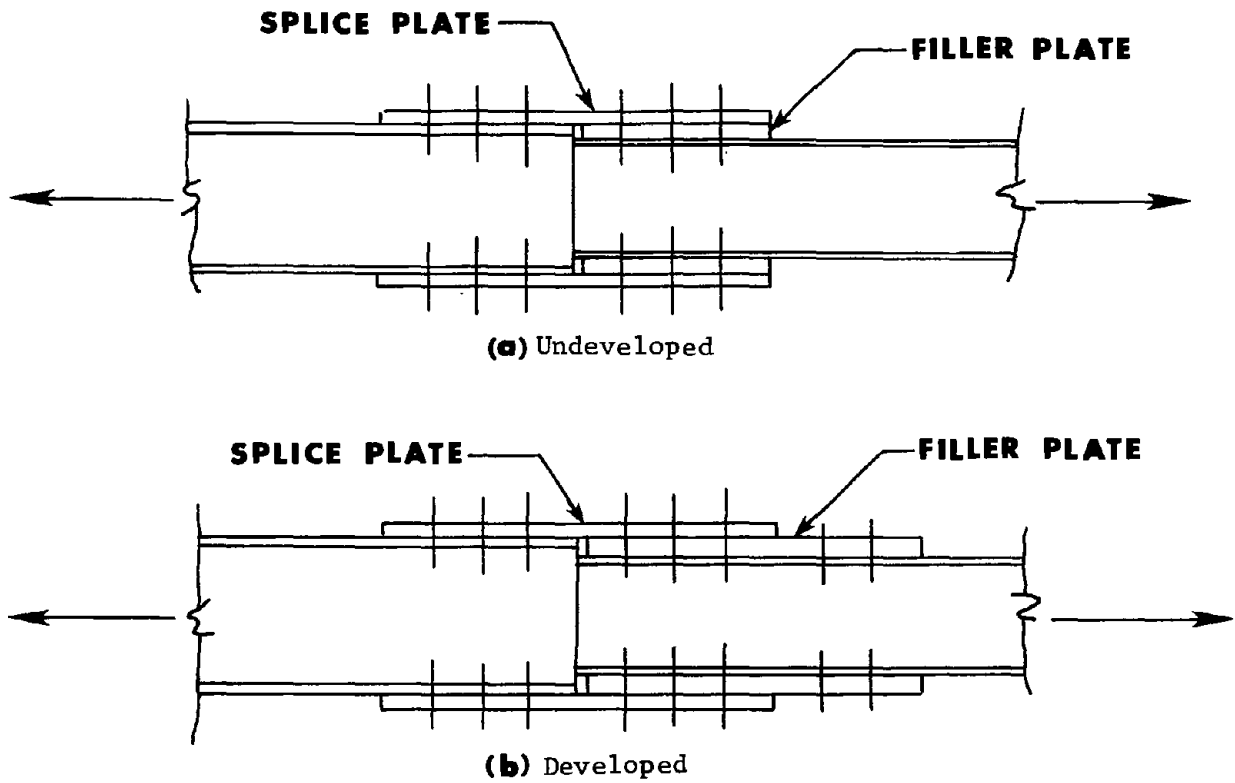


Figure 91. Filler plates

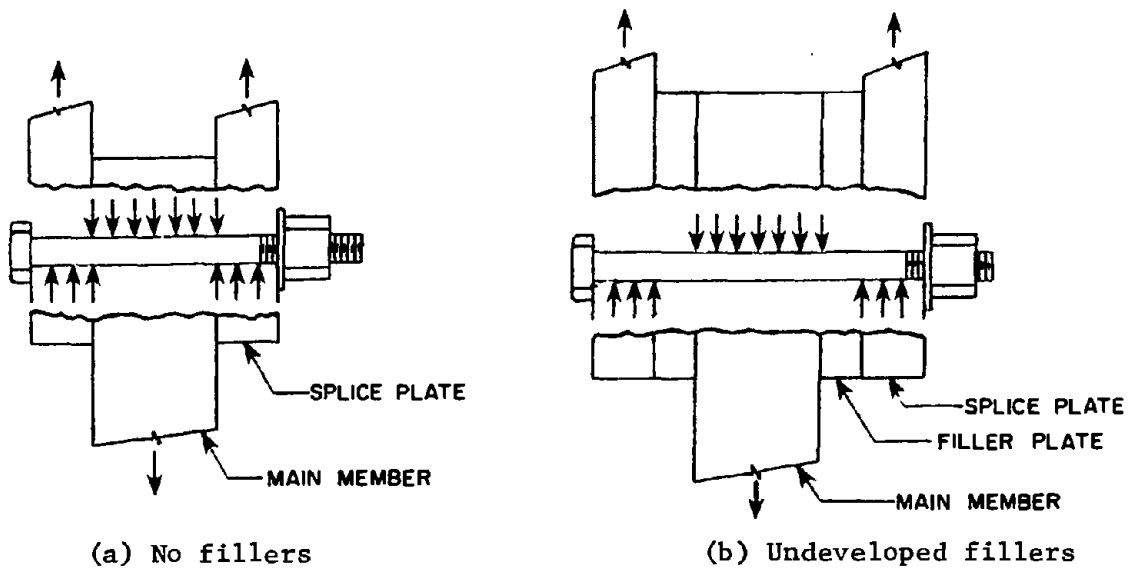


Figure 92. Idealized loads on bolts

thickness increases this load separation also increases and the joint becomes more flexible, with a probable lower strength due to bolt bending. An undeveloped filler composed of many plies will offer the least resistance to bending of the bolts as the filler plates can move relative to one another. A solid undeveloped filler probably offers some resistance to bolt bending within the filler thickness, but the filler is still free to move and would carry no net axial stress when no friction is present. The shear plane in the case of undeveloped fillers is not defined and could practically occur anywhere between the splice plate and the structural member.

Objective and Scope. The influence of grip length, joint length, and initial tension on shear strength of bolts has been investigated [15]. A few tests have recorded the influence of filler plates on slip load [37]. However, no tests were found that investigated either the influence of developed or undeveloped fillers. Fisher and Struik [15] suggest that if undeveloped fillers are used, then they are permissible if no large scale bending occurs in the bolt. However, no criterion was presented to define the limits of filler thickness or bending. Also, no tests were found that would lead to the 1/4 in. (6mm) and two-ply limitation on fillers given in the AASHTO specification discussed earlier.

With no information available on ultimate strength of bolted splice specimens using developed or undeveloped fillers, the joints which will produce the largest deformations and lowest ultimate loads were selected to be tested. Filler plates of lower strength steel than the splice plates and main members would also increase the flexibility of the joint. Therefore, undeveloped fillers of lower strength steel were used with the test specimens. The test specimens were designed to force the failure into the bolt where the influence of undeveloped fillers would be the most pronounced. Filler plate thickness from 0 to 0.75 in. (19mm) was the main variable considered and one multi-ply specimen was also tested. All tests were loaded to ultimate. Slip loads for three of the test assemblages were also investigated. The slip loads are presented only for assemblages that used identical filler plates and surface conditions.

### Splice Connection Tests

Test Specimen. The bolted splice specimen is shown in Figure 93. It consisted of two central pull plates made of A514 steel along with splice plates of A514 steel and filler plates made from A36 steel. The 2 in. (51mm) thick pull plates and the 1 in. (25mm) thick splice plates were designed to force the failure into the bolts. The fillers used on the upper plate were fully developed by one bolt. Undeveloped fillers were placed on the lower pull plate to match the upper member. Bolt spacing was 3 in. (76mm) on center and 1-1/2 in. (38mm) from the ends of the plates. A325 bolts with a 7/8 in. (22mm) diameter were used in the 15/16 in. (24mm) diameter drilled holes.

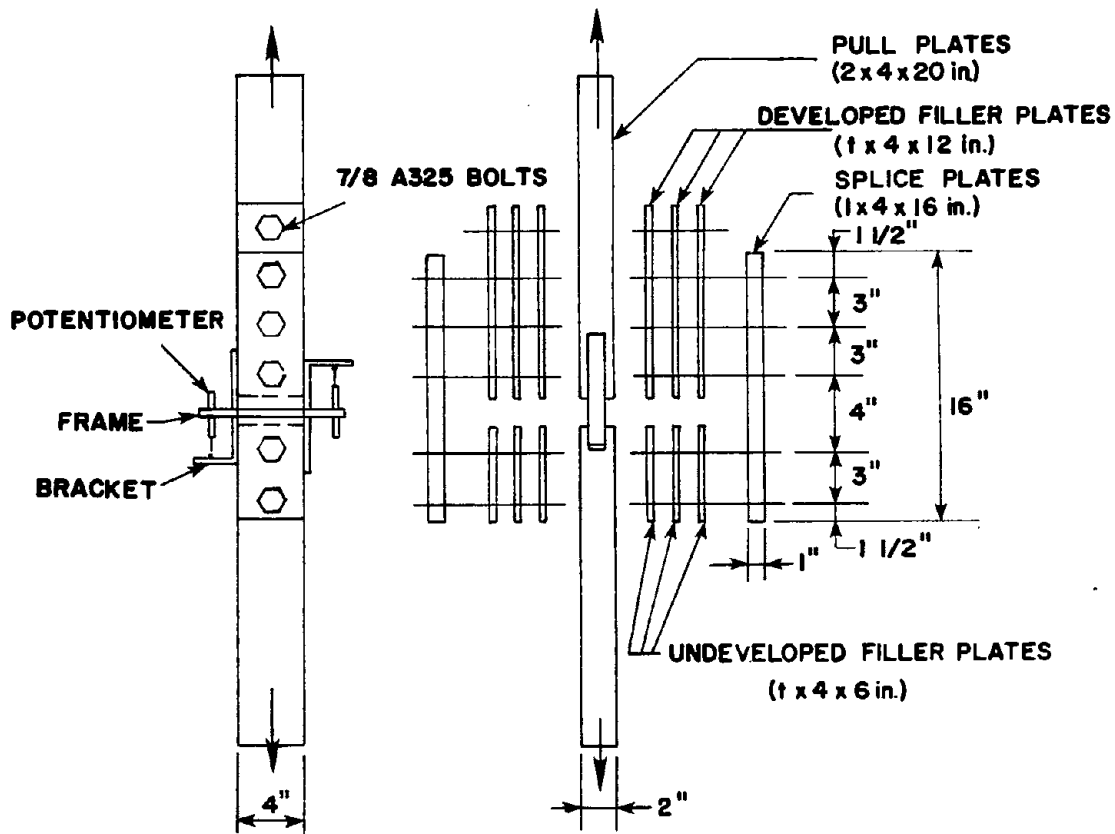


Figure 93. Test specimen and instrumentation (1 in. = 25.4 mm)

The pull plates, splice plates, and the 0.25 in. (6.4mm) filler plates all had a clean millscale finish. The 0.075 in. (1.9mm) fillers had a rust coating which was removed by wire brushing. The solid 0.75 in. (19mm) plate had been sandblasted about eight months prior to testing and stored under cover with no noticeable surface corrosion.

The test specimens were assembled with bolt threads coated with an anti-seize lubricant. The bolts were tightened one-half turn past snug-tight according to the turn-of-nut method [30]. Bolt elongations were recorded so that the clamping force could be determined from the bolt calibration curves.

The testing program consisted of two replicate tests of five different specimen assemblages. The combinations used were no-fillers and fillers of thicknesses of 0.075 in. (1.9mm), 0.25 in. (6.4mm), and

0.75 in. (19mm). Two types of filler assemblages were used to get the 0.75 in. (19mm) thickness. One was by using a single plate and the other used three plates of 0.25 in. (6.4mm) thickness, each as shown in Figure 93. All other tests used a single filler plate to achieve the desired thickness. The filler thickness is defined as the thickness of all fillers on one side of the joint.

Bolt Properties. Three lots of 7/8 in. (22mm) A325 bolts were used and are designated A, B, and C according to their length of 5-1/2 (140mm), 5-3/4 (146mm), and 6-3/4 in. (172mm), respectively. Calibration tests were completed on each lot to characterize the strength of the bolts in direct tension, torqued tension, and single shear. The detailed procedures and discussion of results are given in Ref. 18.

The bolt calibration curves (torqued tension) were developed as outlined in Chapter 2 and are given in Figure 94. The mean values from these tests for ultimate tension and shear strength in each lot are given in Table 50. The single shear strength for both the gross area and threaded area of the bolt was developed using the test fixture shown in Figure 95. The torqued tension strength given as a percentage of the measured direct tension test for lots A, B, and C are 85 percent, 78 percent, and 86 percent, respectively. The average ratio of ultimate shear stress on the gross area to the ultimate direct tensile stress on the tensile stress area is 0.60, which is close to the average of 0.62 reported by others [15].

Table 50. Mean ultimate bolt capacity in kips  
(1 kip = 4.45 kN)

Bolt Lot	Torqued Tension	Direct Tension	Single Shear	
			Threaded Area	Gross Area
A	49.0	57.6	37.1	46.0
B	44.3	56.8	36.1	45.3
C	55.7	64.9	41.8	49.6

Test Results. Two potentiometers attached to the test joint as shown in Figure 93 monitored the displacement between the splice plate and the pull plate for both the two-bolt and three-bolt groups as tension load was applied. A typical response is shown in Figure 96 for the specimen with three 0.25 in. (6.4mm) fillers. As expected, the two-bolt group slipped first and exhibited more deformation to failure compared to the three-bolt group. As the load-transfer mechanism shifts from friction to bearing, the load-deformation curve slope decreases as localized yielding occurs in the bolts. Figure 97 shows the test specimen after localized yielding has started. The two-bolt group

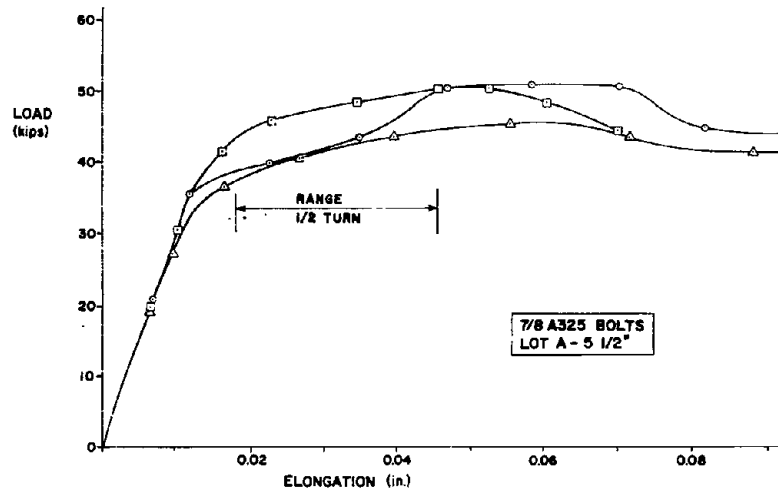
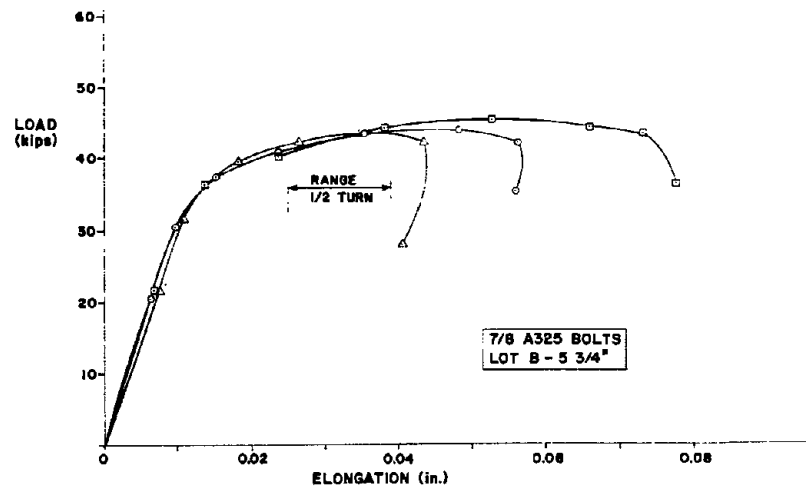
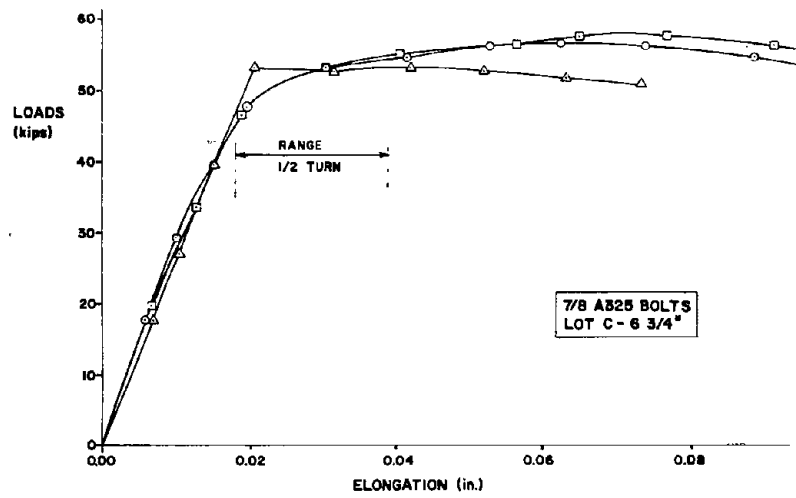


Figure 94. Torqued tension tests (1 in. = 25.4 mm)  
(1 kip = 4.45 kN)



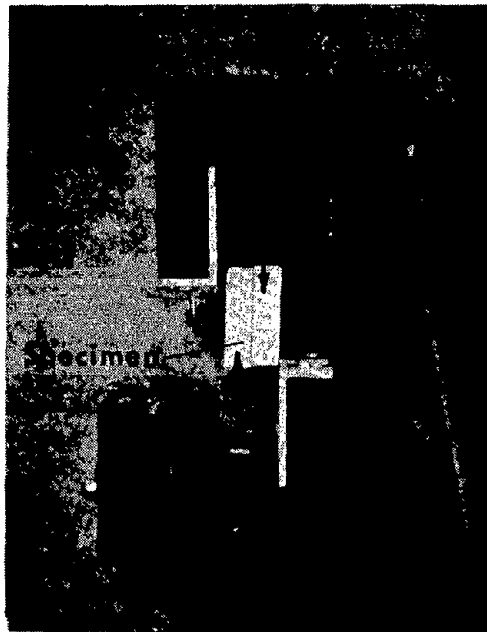


Figure 95. Single shear test

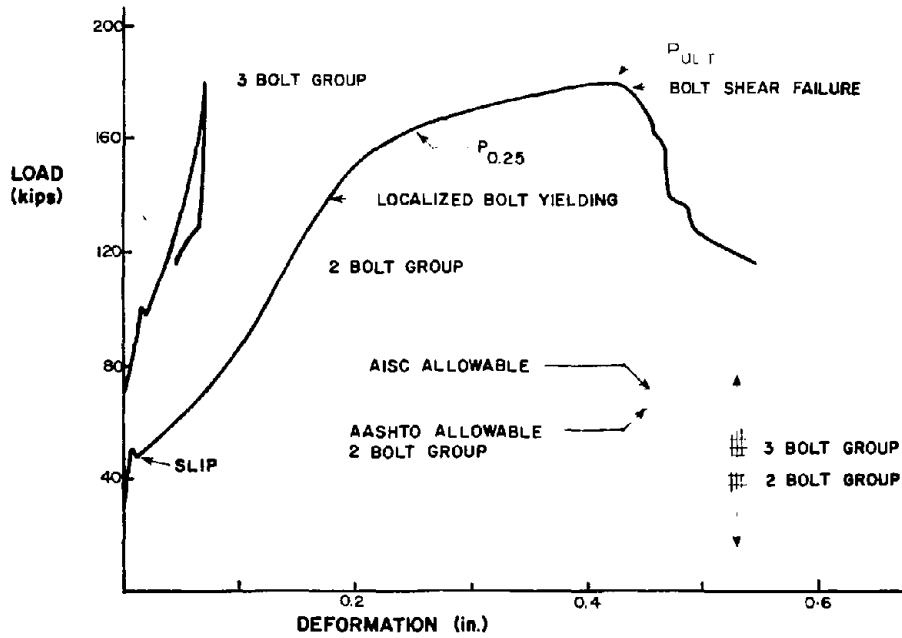


Figure 96. Load-deformation for 3 × 0.25 in. fillers  
(1 in. = 25.4 mm, 1 kip = 4.45 kN)

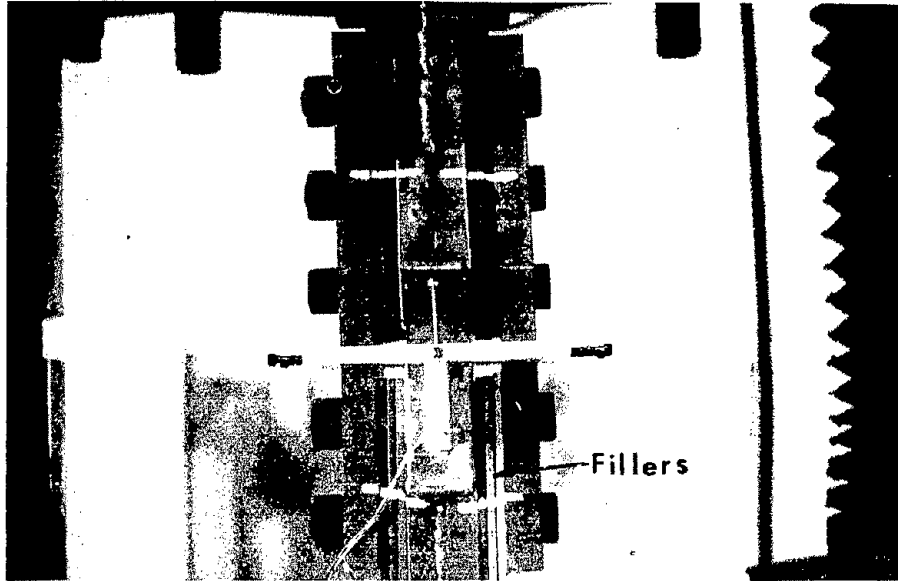


Figure 97.  $3 \times 0.25$  in. (6.4mm) fillers--intermediate load

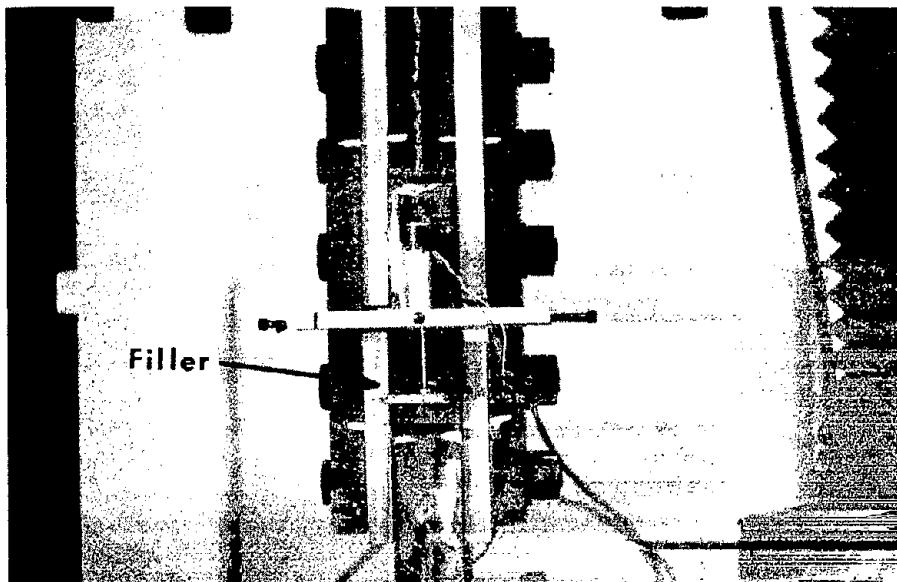


Figure 98. 0.75 in. (19mm) fillers--intermediate load

white markings show a distinctive step pattern while the three-bolt group shows relatively little movement. In the stepped pattern the filler plate next to the pull plate has moved the most, with the filler plate next to the splice plate moving the least. As the load approaches ultimate, the slope of the load-deformation curve for the two-bolt group becomes very flat. Failure occurred by one or both bolts shearing through the shank.

In an effort to reduce the amount of deformation caused by the relative movement of the three 0.25 in. (6.4mm) filler plates, a solid 0.75 in. (19mm) filler plate was also used. Figure 98 shows the solid 0.75 in. (19mm) filler specimen after localized bolt yielding. The filler plate shows little movement with respect to the splice plate, with most of the deformation occurring between the filler and pull plates. Figure 98 is typical of the slip pattern of test specimens with one filler plate.

The load-deformation curves for all ten specimens are given in Ref. 18. The replicate specimens showed very little scatter. There was usually some difference between replicates in the initial portion of the curves due to variations in clamping force. However, once the bolts went into bearing, there was little difference. The average curve for each type of filler arrangement is shown in Figure 99, where the test load has been nondimensionalized by the shear strength of the bolt group,  $P_{\text{shear}}$ . This should eliminate the influence of different bolt lots in comparing test results. A sheared bolt from the two-bolt group of each type of specimen is presented in Figure 100. The splices show increased flexibility as the filler thickness increases. There is also a decrease in ultimate load with this increased flexibility. The 0.75 (19mm) and  $3 \times 0.25$  in. (6.4mm) filler specimens have a flatter curve towards ultimate load than the other specimens. These thicker fillers allow more bending in the bolt.

The 0.75 in. (19mm) filler shows only slightly improved performance over the  $3 \times 0.25$  in. (6.4mm) filler at all stages of loading. After slip, the solid plate filler showed approximately 0.2 in. (5mm) less deformation than the three-ply filler throughout the load history. The 0.75 in. (19mm) filler offered more resistance to bolt bending than the three-ply filler. One reason why greater improvement was not observed was that a significant local bearing deformation occurred in the solid filler plate. This deformation occurred on the side of the filler next to the pull plate where the majority of movement occurred, as shown in Figure 98. The similarity between the two tests can be seen by comparing the failed bolts for the  $3 \times 0.25$  (6.4mm) and 0.75 in. (19mm) fillers in Figure 100. The use of a solid filler plate of a higher strength steel may improve the behavior by reducing the amount of bearing deformation.

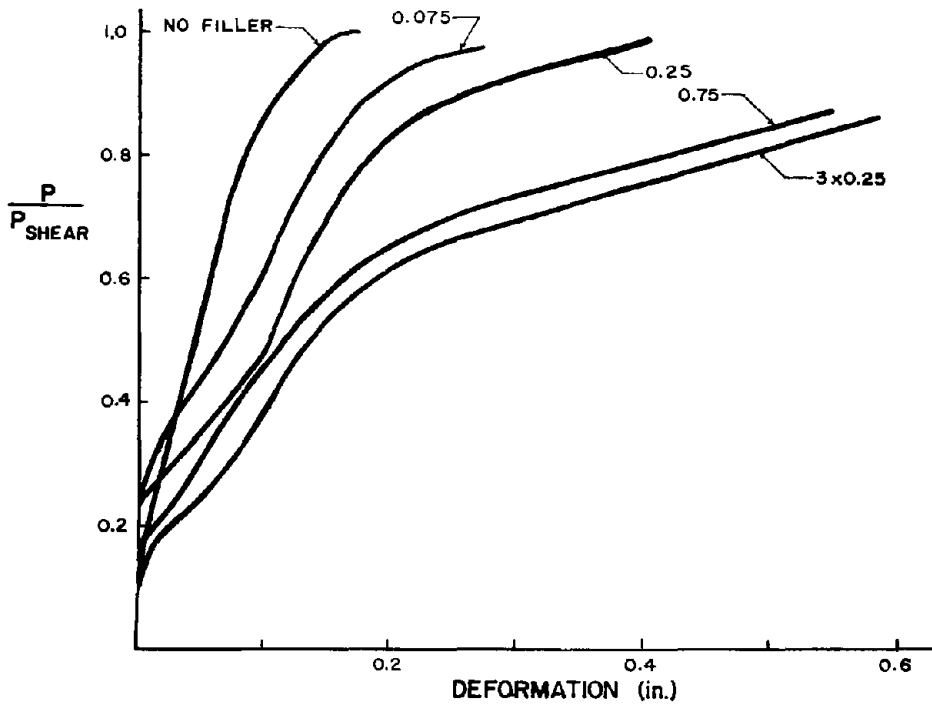


Figure 99. Summary of filler tests

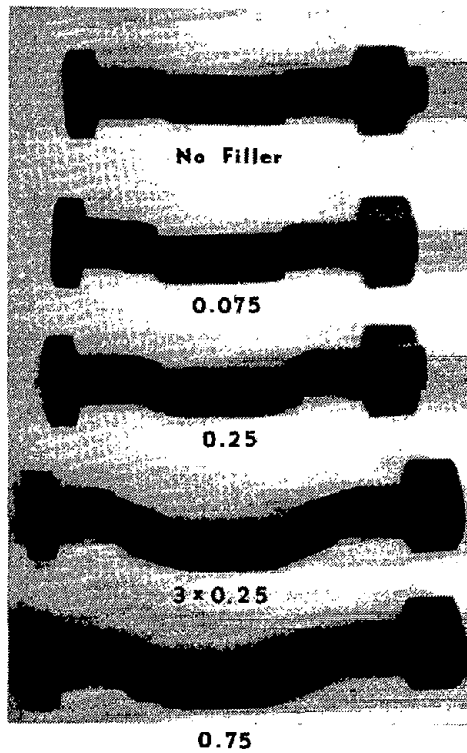


Figure 100. Bolts after test failure

## Test Discussion

Slip Loads. Slip loads were determined for the tests using the 0.25 in. (6.4mm) filler plates, since all the plates in contact including the splice plates and the pull plates had the same type of surface, namely clean mill scale. The measured average clamping force for the two bolts in the connection are given in Table 51, along with the measured slip loads and experimental slip coefficients. Previous test results indicate a slip coefficient of approximately 0.33 for millscale surfaces [15]. The slip coefficients for the test specimens without a filler compare well with the average presented above.

Table 51. Slip loads (1 in. = 25.4 mm, 1 kip = 4.45 kN)

Filler Thickness (in.)	Average Clamping Force (kips)	Slip Load (kips)	Slip Coefficient
No filler	44.5	52	0.35
	43.3	62	0.30
0.25	43.6	44	0.25
	43.5	50	0.29
3 × 0.25	53.4	41	0.19
	51.8	32	0.16

The addition of the 0.25 in. (6.4mm) filler plates resulted in a reduced slip coefficient for the test specimens. The reduction in the average slip coefficients was 16.7 percent. Lee and Fisher found that undeveloped rectangular fillers reduced the average slip coefficient by 20 percent [37]. They also noted that varying the thickness of the filler plate up to 1 in. (25mm) had no influence in reducing the slip coefficient any further. The test results presented in Table 51 show a lower slip coefficient for the 3 × 0.25 in. (6.4mm) than for the 0.25 in. (6.4mm) fillers. Consequently, although single filler plates up to 1 in. (25mm) thickness may reduce the slip coefficient by 20 percent, it appears that multiple fillers may reduce the slip coefficient even further.

The slip characteristics of the three-bolt groups were not distinctive and it was difficult to establish a slip load for the bolt group. Therefore, slip coefficients could not be accurately established.

Ultimate Loads. The ultimate failure loads,  $P_{ult}$ , and deformations at maximum load for the ten tests are summarized in Table 52. The ratio of ultimate load to bolt shear strength,  $P_{ult}/P_{shear}$  is also given.

Table 52. Splice test summary (1 in. = 25.4 mm,  
1 kip = 4.45 kN)

Filler Thickness (in.)	Bolt Lot	Failure Loads (kips)	Maximum Deformation (in.)	P <sub>0.25</sub> (kips)	$\frac{P_{ult}}{P_{shear}}$	$\frac{P_{0.25}}{P_{shear}}$
No filler	A	190.1	0.160	190.1	1.033	1.033
		178.9	0.190	178.9	0.972	0.972
0.075	A	174.6	0.280	172.6	0.949	0.938
		183.8	0.270	183.0	0.999	0.994
0.25	B	178.9	0.400	164.0	0.985	0.903
		180.2	0.415	163.5	0.992	0.900
3 × 0.25	C	169.9	0.585	130.0	0.856	0.655
		172.6	0.580	134.0	0.870	0.675
0.75	C	177.3	0.565	140.5	0.896	0.708
		170.8	0.527	139.0	0.861	0.701

The no filler test assemblage average for  $P_{ult}/P_{shear}$  is 1.002 with the average maximum deformation being 0.175 in. (4.44 mm). The ultimate load to shear load ratio indicates that the test without fillers could be considered a double shear test since the single shear strength of the bolts accurately describes the ultimate load of the specimen. There appears to be little, if any, splice plate prying, since the tension specimen tests compare very well with the single shear tests. The average maximum deformation of the no filler test specimens is also very close to the maximum deformations of a single bolt in double shear of 0.19 in. (4.83mm) [34].

The test specimens maintained 98.8 percent of their shear strength for fillers with 0.25 in. (6.4mm) thickness. This percentage reduced to 87.8 percent and 86.3 percent for the 0.75 in. (19mm) and 3 × 0.25 in. (6.4mm) fillers, respectively. Based on these data, the thickness limit of 0.25 in. (6.4mm) in the AASHTO and AISC specifications will ensure the development of the full bolt shear strength. However, thicker fillers could be permitted, since the strength reduction for thickness up to 0.75 in. (19mm) is quite modest.

The three-bolt group was subjected to loads up to 66 percent of ultimate load. The deformations of the three-bolt group with developed fillers were less than the two-bolt groups, but the measurements only extend to the ultimate load of the two-bolt group. At the two-bolt group ultimate, the bolts in the three-bolt group showed no failure or distress with some slight permanent deformations.

Deformation-Limited Loads. The factors of safety for the specimens are all above 2.0 and all the test specimens appear to have satisfactory ultimate loads. However, with the thicker fillers there is an increase in joint flexibility and an increase in maximum deformation. This maximum deformation can be detrimental to the usefulness of a structure or structural member. Figure 99 shows that for the latter part of the load-deformation curve for the 0.75 in. (19mm) fillers there is a large increase in deformation with a relatively small increase in applied load. To obtain the last 20 percent of the load, the amount of deformation must be doubled. Therefore, the test specimen's useful strength may be restricted by the amount of deformation permitted.

Other researchers have used deformation limits as the basis for defining maximum useful loads. The useful load is defined as the smaller of either the maximum test load or the load at a specified deformation. Perry found in his research on bearing failures of splice plates that a deformation of 0.25 in. (6.4mm) rendered most of his specimens useless due to extensive buckling [29]. Specimens that had not undergone large scale buckling achieved 80 percent of their ultimate load at 0.25 in. (6.4mm) and required an additional 0.75 in. (19mm) of deformation to reach the ultimate load. Based on these observations, the load characteristics,  $P_{0.25}$ , at a deformation of 0.25 in. (6.4mm) will be evaluated.

The load at 0.25 in. (6.4mm) of deformation,  $P_{0.25}$ , for each specimen tested appears in Table 52. The average of the nondimensional loads plotted against filler thickness appears in Figure 101, along with the nondimensional ultimate and allowable loads. The deformation-limited loads show a steady reduction in useful load with filler thickness. Deformation causes the useful load for 0.25 in. (6.4mm) fillers to be less than the ultimate load achieved. Therefore, while the AISC and AASHTO specifications appear to provide adequate factors of safety based on ultimate loads, the specifications may allow significant deformations. Table 53 presents the factors of safety for the specimens with the deformation-limited loads. Up through the 0.25 in. (6.4mm) thickness the factors of safety maintain a satisfactory level for these compact two-bolt connections. At 0.75 in. (19mm), the factors of safety would be unsatisfactory.

Table 53. Factors of safety for deformation-limited loads  
(1 in. = 25.4 mm)

Specification	Filler thickness (in.)				
	No Filler	0.075	0.25	0.75	3 × 0.25
AASHTO	2.8	2.7	2.5	2.0	1.8
AISC	2.5	2.4	2.2	1.8	1.7

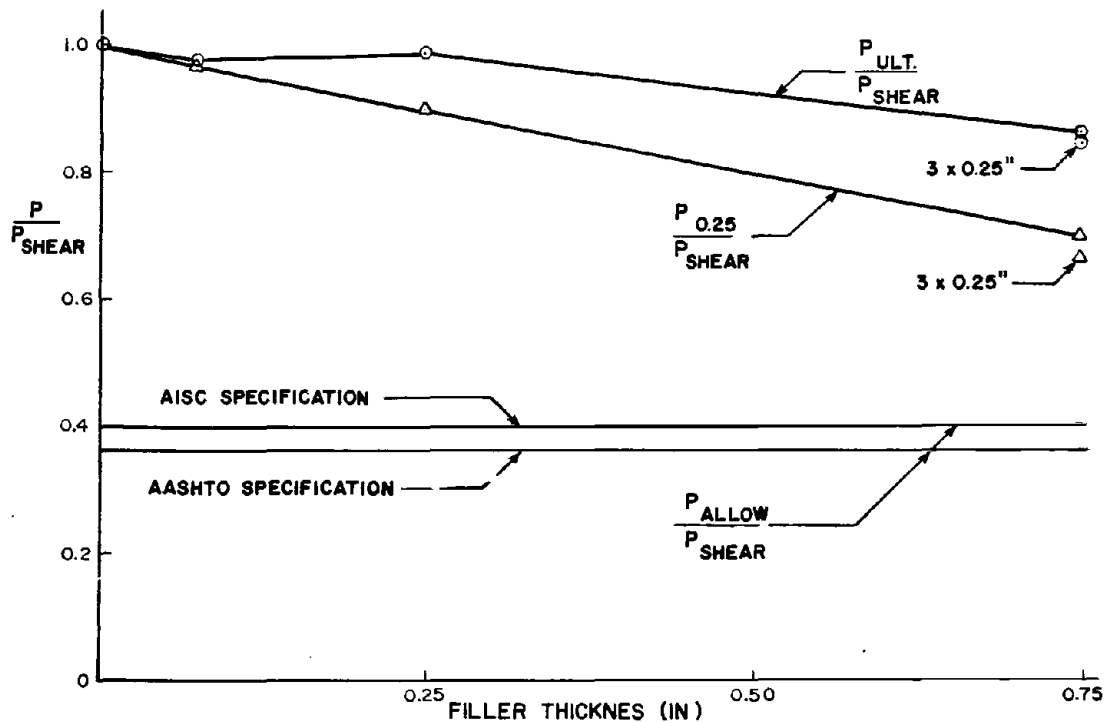


Figure 101. Effect of filler thickness on shear capacity  
(1 in. = 25.4 mm)

#### Design Recommendations

For  $t_u \leq 0.25$  in. (6.4mm), Table 53 shows that the factor of safety is adequate, even considering the deformation limit. However, the tests reported herein are on short compact connections, and it is well-known that the shear strength of bolted joints is affected by joint length. As shown in Figure 5.47 in Ref. 15, for joint lengths up to 50 in. (1270mm), the joint length effects will not reduce the factor of safety below 2.0. Beyond this length, both AASHTO and AISC require a 20 percent reduction in allowable bolt shear strength, which enables the factor of safety to be maintained at levels greater than 2.0 up to joint lengths of 90 in. (2290mm) [15].

The length effects described above are based on theoretical and experimental evidence on joints without undeveloped fillers. The use of undeveloped fillers causes greater joint deformations. As shown in Figure 101, the deformation limit of 0.25 in. (6.4mm) would require a 10 percent reduction in allowable shear stress if  $t_u$  was 0.25 in. (6.4mm). Combining this 10 percent reduction with the joint length effects of Ref. 15 would indicate that joint lengths would have to be kept below 30 in. (760mm) to keep the AASHTO factor of safety acceptable. When the joint length is greater, the allowable bolt shear stress should



be reduced by 20 percent. It may be questionable to directly combine the filler flexibility effect and the joint length effect, but this approach is recommended until tests on long joints with undeveloped fillers are conducted.

For compact joints, undeveloped filler thickness greater than 0.25 in. (6.4mm) could be permitted based on the test evidence reported herein. Current allowable bolt shear strength in AASHTO would be modified by the factor  $1 - 0.4 t$ , which is the slope of the straight line through the data in Figure 101. However, it is recommended that such a modification not be implemented until tests on longer joints are undertaken.

### Summary

Ten tests were conducted on bolted splice connections with undeveloped fillers of varying thicknesses and plies. The major findings were:

(1) The addition of an 0.25 in. (6.4mm) undeveloped filler plate reduced the slip coefficient by 16.7 percent.

(2) Multi-ply undeveloped fillers reduce the slip coefficient by a greater degree than single ply filler plates.

(3) Increasing the thickness of undeveloped fillers allows more bending in the bolts, which results in increased deformation at maximum load and decreased ultimate load.

(4) The difference in ultimate loads and maximum deformations between the 0.75 in. (6.4mm) and  $3 \times 0.25$  in. (6.4mm) fillers was negligible. The difference between the solid and multi-ply filler would probably be greater if the filler plates had been of a higher strength steel, as less bearing deformation would have occurred in the solid filler.

(5) The AASHTO and AISC specifications have conservatively limited undeveloped fillers to a thickness of 0.25 in. (6.4 mm) when based on ultimate loads. But because of increased deformations, it is recommended that a short joint be limited to a 30 in. (760mm) rather than the current 50 in. (1270mm) when undeveloped fillers are used.

## 7. BEARING CRITICAL SPLICE CONNECTIONS

### Introduction

General. The two types of bolted shear connections used are friction-type connections and bearing-type connections. As their names imply, friction-type connections rely on frictional resistance between the connected parts induced by the clamping forces in their bolts and these connections have been discussed in Chapters 3, 4, and 5. Bearing-type connections rely on the bearing strength of the connected parts and the shear strength of their bolts. Friction connections must also be checked for bearing strength of the connected material, since the factor of safety against slip is 1.45 or less. Once slip is overcome, the forces are transmitted by the bolts bearing on the connected plate material, so the bearing strength must be checked to maintain at least a factor of safety of 2.0 against ultimate.

Present specifications for the design of bolted connections require consideration of four failure modes: bolt shear, end tearout, bearing, and net section failure. The plate bearing stress  $f_p$  for the connections shown in Figure 102 is calculated as

$$f_p = \frac{P}{n d t} \quad (4)$$

where  $n$  is the number of bolts,  $d$  is the bolt diameter, and  $t$  is the thickness of the plate. According to Ref. 15, bearing failure will occur when  $f_p = 3.0F_u$ , where  $F_u$  is the ultimate tensile strength of the material.

End tearout, shown in Figure 102b, occurs when the shear stress along the two shear planes shown reaches  $0.70F_u$ . Net section failure, shown in Figure 102c, occurs when the net section stress equals the tensile strength of the steel.

The ultimate limits described above assume that they are not interdependent. In this chapter, the interaction of bearing stress and net section stress is explored experimentally by tests on bearing-type shear connections.

Previous Work. In much of the early work on bearing stresses in bolted plates, a term bearing ratio (BR) defined as

$$BR = \frac{\text{bearing stress}}{\text{net section tensile stress}} \quad (5)$$

was used to describe the test conditions and boundary between net section tensile failure and bearing failure. In a connection using a fairly wide thin plate and a single row of a few fasteners, the net section stress will be small compared to the bearing stress for a given load. Thus, the BR will be high and a bearing failure will be expected. Conversely, for the same load  $P$ , as the plate width decreases the net section stress will increase, resulting in a low BR and a probable net section tensile failure.

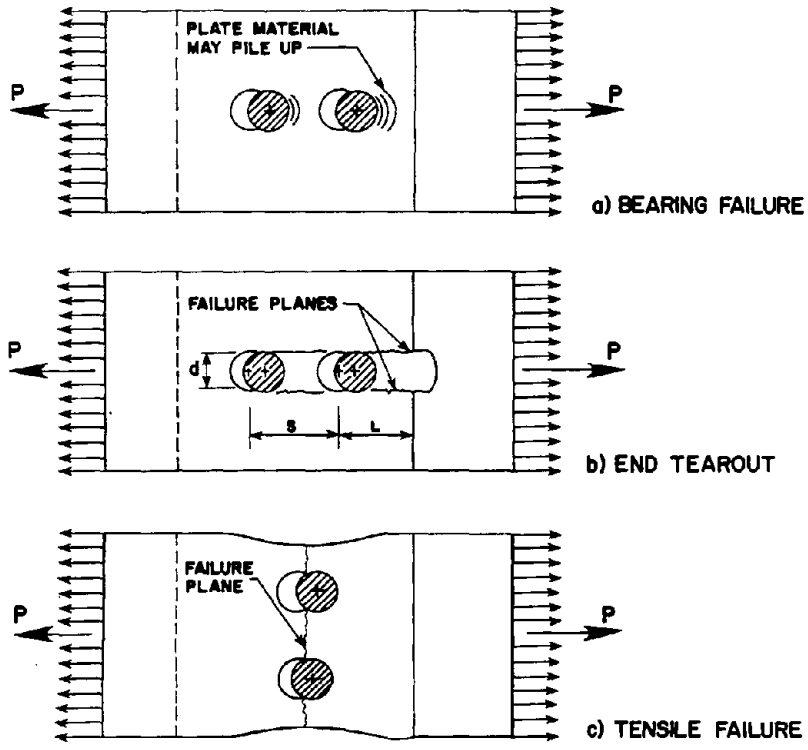


Figure 102. Plate failure modes in bolted lap splices

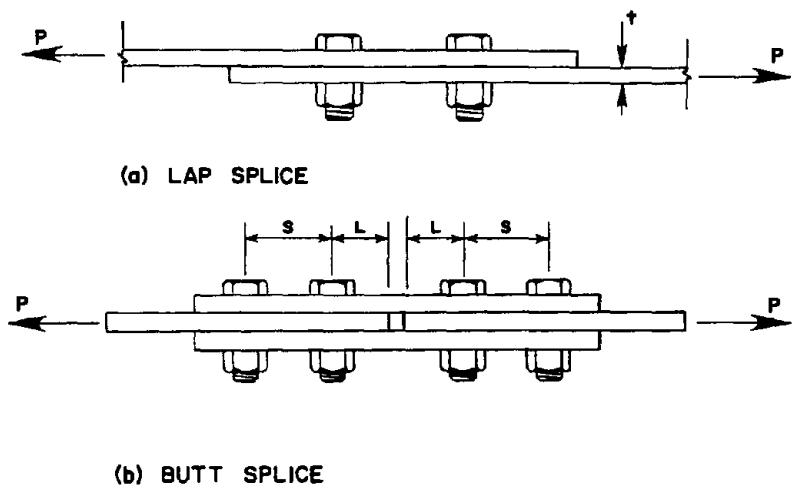


Figure 103. Connection types for bearing tests

Research performed between 1959 and 1961 at the University of Illinois and reported by Jones [21] indicated that connections with a bearing ratio less than 2.25 would fail as net section failures. Bearing would be no problem.

Jones [21] reported that German research in 1931 on riveted symmetrical butt splices failing their inside pull plates found the bearing stress could go as high as  $3.21F_u$ . The Illinois work [25] cited above reported three principal series of tests called 49x, 50, and 51. Bearing ratios in the 49x Series were no larger than 2.5, high enough to observe a behavioral change from net section failure, but not high enough to define an ultimate bearing stress. The 50 Series failed the outside splice plated in tests similar to the 49x Series and the 51 Series failed the webs of built-up I beams. A maximum bearing ratio of 2.75 was used and a corresponding bearing stress of  $2.5F_u$  prevented an upper limit on ultimate bearing stress from being defined. Regardless of the possible additional bearing capacity available, a behavioral bearing limit of  $2.25F_u$  was suggested as being more appropriate than a strength limit. This limit precluded serious connection deformations [21].

Research for the American Iron and Steel Institute (AISI) Specifications for light gage steel connections was presented in 1956 by Winter [35]. The research related connection geometry and net section stress at failure, but did not make a direct comparison of bearing stress and net section stress at failure. Bearing stress limits were treated strictly as functions of the ratio between plate edge distance and bolt diameter,  $L/d$ , reaching a maximum possible bearing stress of  $4.8F_y$ , the yield strength of the material. For the steel properties in Winter's tests,  $4.8F_y$  equals  $3.2F_u$ , the original German limit on bearing stress. All of Winter's conclusions were based on tests of bolted lap splice connections. Washers were used under all bolt heads and all bolts were torqued to a hand tight condition. The 1980 AISI Specification still uses essentially the same limits and design procedures recommended by Winter in 1956.

The 1976 Bolt Specification has adopted a design recommendation which is similar to the AISI design procedure, based on the research by Fisher, Struik, and Wittermans [12,15]. An ultimate bearing stress of  $3.0F_u$  is the criterion for bearing failure with bearing-stress-induced end tearout shown in Figure 102 limited by  $F_u L/d$ . The 1978 AISC and 1979 AASHTO design procedure have adopted these recommendations using factors of safety of 2.0 and 2.2, respectively. Net section failure and bearing failure are treated independently. Bearing stress limits in previous editions of these specifications were based on the Illinois work where the  $2.25F_u$  limit on bearing stress was recommended. In the new approach, bearing failure is no longer considered to result from excessive deformations. Munse's original research [25] on which the bearing stress limit of  $2.25F_u$  was based showed connections with bearing ratios of 2.75 capable of reaching bearing stresses at failure of  $2.5F_u$ , yet the deformations at a bearing ratio of 2.25 were severe enough to constitute

failure. This indicates that the deformations of the connections tested by Fisher, Struik, Wittermans, and Winter required to reach a bearing stress of  $3.00F_u$  may be quite large; no actual deformation data are reported.

An additional observation of the tests presented by Fisher, Struik, and Wittermans is that all of the tested specimens were symmetrical butt splices which failed their inside pull plates. No specimens which failed their outside splice plates were tested. Basing bearing stress limits on test specimens constrained to planar deformations may be unconservative. Lateral confinement is described best by examining a symmetrical butt splice shown in Figure 103. The thick splice plates prevent the main pull plates from deforming out-of-plane and also prevent plate material from piling up adjacent to the bolt when bearing stresses are high. If the butt splice test specimen was designed such that failure occurred in the splice plates, the plate material could deform out-of-plane. Presently, design specifications do not distinguish between confined and unconfined plates. Actual connections such as lap-spliced columns, moment connections, or gusseted truss connections have very little constraint. All the research has considered standard round holes. It is assumed that slotted holes have the same bearing strength as round standard holes.

Gaylord and Gaylord [17] present the most complete look at net section behavior. Their approach, discussed in detail later, considers plate and hole geometry, but only within the constraint of bearing ratios less than  $2.25F_u$ .

Objectives. In light of the discussion of the research presented in the previous section, thirty symmetric lap splices with bearing ratios of 0.5 to 3.5 were tested. The program had four main objectives. To study connections with minimal out-of-plane constraint symmetric butt splices were tested with their outside splice plates designed to fail. Additionally, tests were run with the connecting bolts torqued to their maximum clamping force and also torqued only to a snugged condition to study the effect of bolt preload on the bearing strength. A test series was planned with slotted holes instead of round holes in the splice plates to determine the effect of type of hole. The final objective was to reexamine the criteria used to define failure in bolted connections. If excessive deformations in a connection limit the usefulness of a structure or cause the members it connects to fail, then a deformation limit must be chosen which will permit the connected members to reach their ultimate capacities. To meet this objective, extensive load versus deformation data were collected.

### Test Program

Test Variables. The main test variables studied are bearing ratio, bolt tension, and bolt hole dimensions. Two additional variables studied were the result of a need for additional information after beginning the

original test series. They were material behavior and end distance in the splice plates. Two heats of steel were used to fabricate the test specimens, and the end distance was varied in the splice plates when the original test specimens showed some unanticipated behavior to be discussed later.

Specimens. A typical test specimen is shown in Figure 104. It is a symmetric butt splice designed to fail its splice plates. The pull plates were made of 2 in. (51mm) A514 steel and the splice plates were nominal 1/4 in. (6mm) A36 steel plate. One in. diameter (25mm) A498 bolts were used to resist the double shear stresses. Splice plates with round holes were fabricated in nominal widths of 2, 4, 6, 7, and 8 in. (51, 102, 152, 178, and 203 mm). Splice plates with slotted holes were fabricated in nominal widths of 5, 7, 8, and 9 in. (127, 178, 203, and 229 mm). One 8 in. (203mm) wide specimen and one 6 in. (152mm) wide specimen were fabricated with 3 in. (76mm) end distances. All other splice plates had 6 in. (152mm) and 9 in. (227mm) end distances,  $L_2$  and  $L_1$ , respectively, in Figure 104, to avoid any possibility of end tearout failures. The dimensions of the specimens with short end distances are shown in parentheses. Actual dimensions of each tested specimen are given elsewhere [29]. Thirty connections were fabricated and tested; each had the two and three bolt arrangement shown in Figure 104. There were actually fifteen connections with varying parameters, but each connection was replicated to provide a measure of the experimental scatter.

Assembly. The test specimens were first loosely assembled with hand-tightened bolts. A490 high strength bolts were used in the assembly as a precautionary measure against bolt shear failure and washers were used only under the nut. The Bolt Specification [30] required that washers be used under both the nut and bolt head when using A490 bolts with A36 steel to avoid deforming the steel. This requirement was neglected to simulate more typical structural joints which use A325 or A307 bolts. Also, in eleven of the fifteen specimens prepared, the bolts were only tightened to the snug position to simulate lower strength bolts. The allowable bearing stresses given in design specifications are applicable to all bolted construction, not just high-strength bolts. In assembling the test specimens with slotted holes, bar washers were not used. Bar washers are generally necessary in slotted hole applications to provide adequate bearing area for the torqued bolt heads and nuts. Since the bolts were only torqued to a snugged condition in the slotted hole specimens, bar washers were omitted to provide a better view of the bearing deformations occurring in the vicinity of the bolt holes. Hardened washers were used under the bolt heads and nuts in the slotted hole specimens to keep the bolt from pulling through the slot during testing.

The assembled specimens were then hung from an overhead hoist to put the bolts into nominal bearing and all of the bolts were torqued to a tight condition. On the specimens which required fully torqued bolts, the nuts were then given an additional one-half turn. The tension in the bolts was monitored by measuring the elongation of each bolt and using a

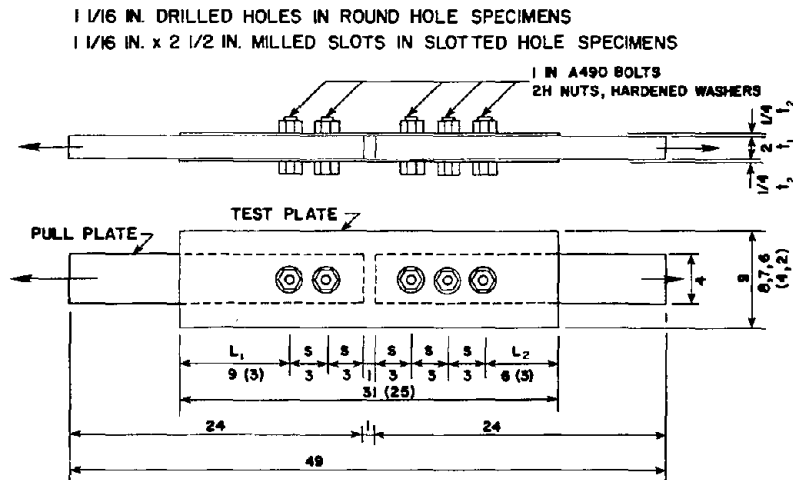


Figure 104. Bearing critical test specimens

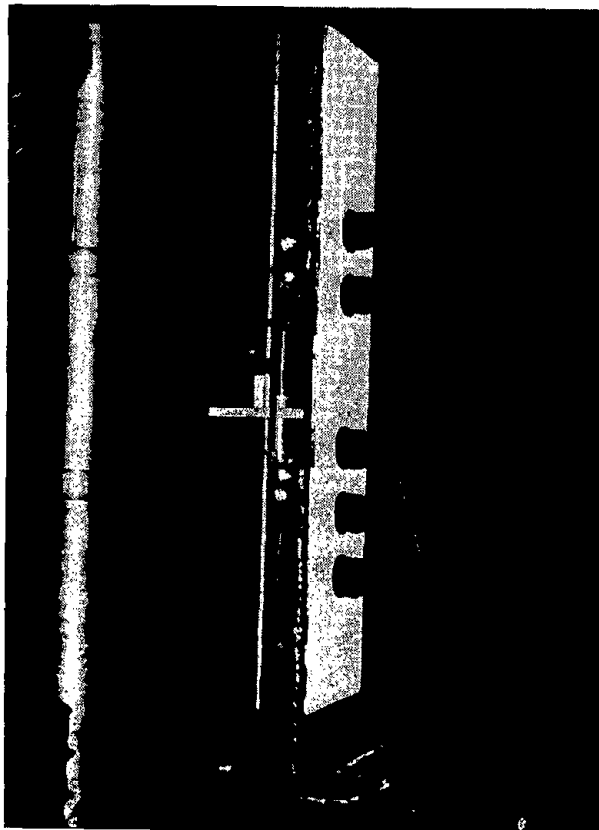


Figure 105. Test setup

bolt calibration curve, as discussed in Chapter 2. This bolt load monitoring provided a verification that the bolts were fully torqued, and also provided information required to compute the frictional slip coefficients for the test specimens. The assembled specimens were then placed in a universal load machine, whitewashed to detect yield patterns, instrumented with deflection measuring potentiometers, marked to get a double check on the deflection measured by the potentiometers, and tested. Figure 105 shows an assembled test specimen prior to testing.

Measurements. Deflection measuring potentiometers were attached to both the two-bolt group and the three-bolt group. Each potentiometer was attached to an X-Y plotter along with a load output load from the universal testing machine. Two load vs. deflection graphs were generated for each test. The plotted deflections were verified by measuring the relative motion between slip marks on the splice plates and the pull plates. After the specimens were disassembled, the actual hole elongations were measured as a final check. Overall distortion patterns were monitored by photographing a square grid drawn on one of the splice plates in each test at various load stages.

All specimens were tested at the same load rate as the tension coupons used to obtain material properties. In each test loading was stopped two to four times for taking photographs, making measurements, and recording observations on the behavior of the splice plates. Each test was stopped as soon as an ultimate load was reached to avoid destroying the specimens.

Material Properties. Three ASTM standard tension coupons were fabricated from each heat of A36 steel plate and tested. A sample stress vs. strain graph is shown in Figure 106 along with a plot of the average behavior of steel heats 1 and 3. The results of the actual coupon tests are given in Table 54. The graph and the actual results show that the

Table 54. Material properties

Coupon	Yield Strength (ksi)	Tensile Strength (ksi)	Percent Elongation	Percent Area Reduction
Heat 1-1	40.8	60.9	47.0	53.9
Heat 1-2	40.6	51.0	46.9	57.7
Heat 1-3	40.4	60.9	43.8	56.1
Average	40.5	60.9	45.9	53.8
Std. Dev.	0.1	0.0	1.8	2.3
Heat 3-1	47.2	65.2	48.3	49.0
Heat 3-2	49.7	64.9	48.8	56.3
Heat 3-3	47.0	65.1	45.8	49.8
Average	48.0	65.1	47.4	51.7
Std. Dev.	1.2	0.1	1.4	4.0

(1 ksi = 6.89MPa)



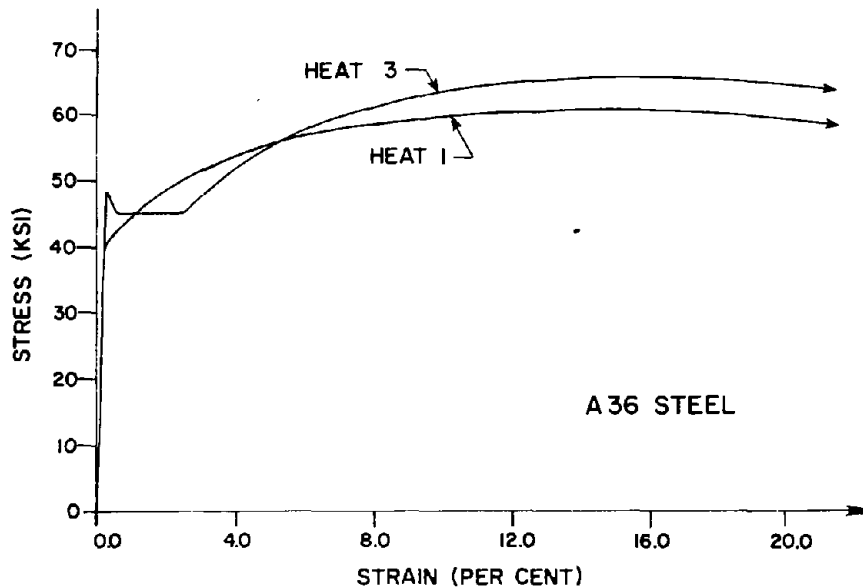


Figure 106. Steel stress-strain curves

two steels differ slightly. Heat 1 has a slightly lower yield and ultimate strength than Heat 3, and Heat 3 has a yield plateau where Heat 1 is slightly strain-hardened. With such slight differences in behavior between the two steels, test specimens fabricated from either steel can be compared directly but in subsequent sections the results will be non-dimensionalized by  $F_u$  of the particular steel for more reliable comparisons.

The measured splice plate thicknesses are 0.244 in. (6.20mm) and 0.261 (6.63mm) for Heats 1 and 3, respectively.

Notation. A typical test specimen designation is 8-H1-1. the "8" represents the nominal width of the splice plates in inches. The "H1" represents the steel heat from which the splice plates were fabricated, and the "1" indicates that this test specimen is the first in the series of two replicates. The designation shown above also indicates that the bolts are torqued only to a snug tight condition, bolt holes are round, and failure is controlled by the two-bolt group. A specimen named 8-H1-1C indicates that the specimen is identical to the previously described specimen except that the bolts are fully torqued. If the splice plates failed in the three-bolt group (or the information catalogued under a given name is for the behavior of its three-bolt group), the name is appended with a parenthetic message. 8-H1-1C(3) is now the full designation of the example test specimen. Splice plates with slotted holes have an "S" appended to the nominal width index. An example of a specimen with a slotted hole is 6S-H3-2.

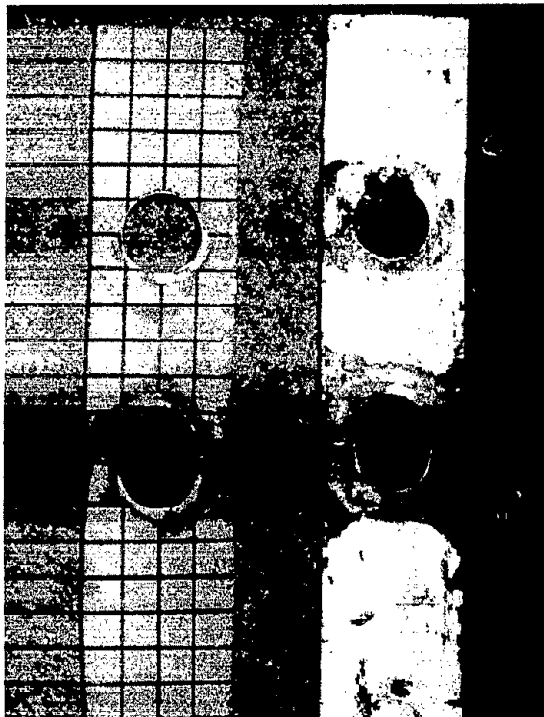
Deflections. The plate deformations which were measured over a 4 in. (102mm) gage length included the combined effects of plate elongation due to stresses on the gross cross section over a 3 in. (76mm) length, plate elongations over a 1 in. (25mm) long net section, local bearing deformation, and slip. During assembly, the connection was supported in a manner so that at least one bolt of each group was in bearing to minimize slip deformation. Since the holes in each splice plate were drilled separately, they did not line up perfectly, so some slip was recorded in most tests. To help examine specimen behavior and determine the failure mode by a method other than visual inspection of the splice plates, a computer model was used to separate the total measured specimen deformation into bearing deformation and cross section elongation components.

The computer model defined total specimen deformation as the relative displacement between the clamping point of the potentiometer on the splice plate and the pull plate. The total specimen deformation was further defined to consist of only cross section elongation over the 4 in. (102mm) zone and bearing deformation; slip was neglected. Cross section elongation was computed at various load stages assuming uniform stress distributions in the net and gross sections and using an approximate stress-strain relationship which was a fit to the measured response. Bearing deformation was computed by subtracting the computed cross section elongation from the total deformation measured by the potentiometers. An evaluation of this separation technique indicated the results were reliable within  $\pm 0.1$  in. (2.5mm) [29].

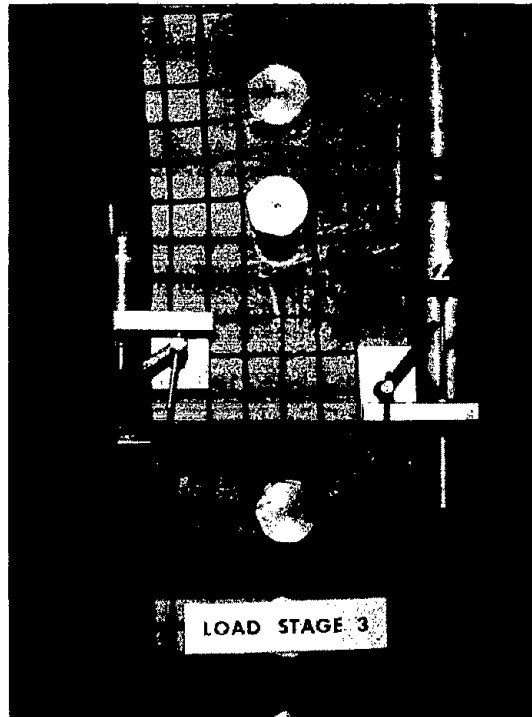
### Test Results

Failure Modes. The two basic failure modes examined are net section tensile failure and bearing failure. Net section failure occurs when the stress through the net section of the outside splice plates reaches the tensile strength of their material. Net section failure is characterized by uniform cross section distortion ("necking") and fracture of the metal along the net cross section (Figure 107a). Bearing failure occurs when the plate material in contact with the bolts undergoes excessive deformation due to bearing stress and begins to tear (Figure 107b). Net section failure and bearing failure are both characterized by an eventual loss in load-carrying capacity of the outside splice plates. The two are distinguished from each other by the type of deformations they exhibit. Visual examination of the grids drawn on one splice plate in each test shows net section failure to be characterized by uniform grid distortion, while bearing failure is characterized by localized distortion of the grid along the centerline of the bolts.

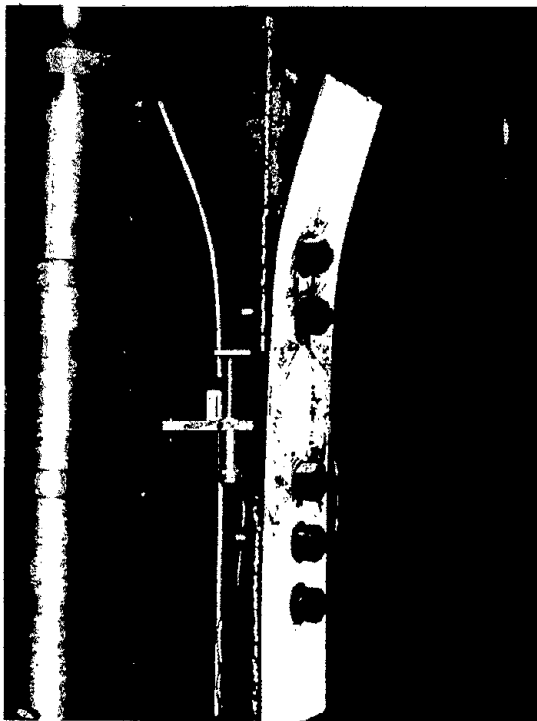
Two observed failure modes which occur before the maximum net section stress or bearing stress of a test specimen can be reached are buckling of the splice plates (Figure 107c) and excessive deformation. Splice plate buckling is dependent on connection details such as the number of columns of bolts and lateral restraint of the splice plate yet constitutes



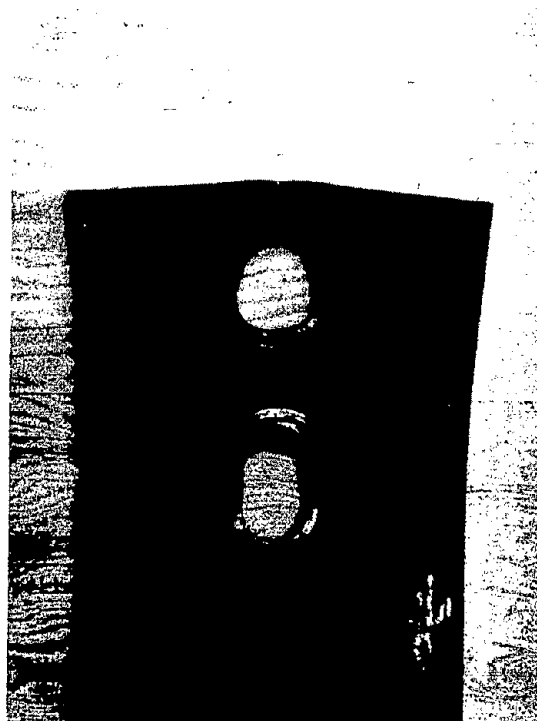
(a) Net section failure



(b) Bearing failure

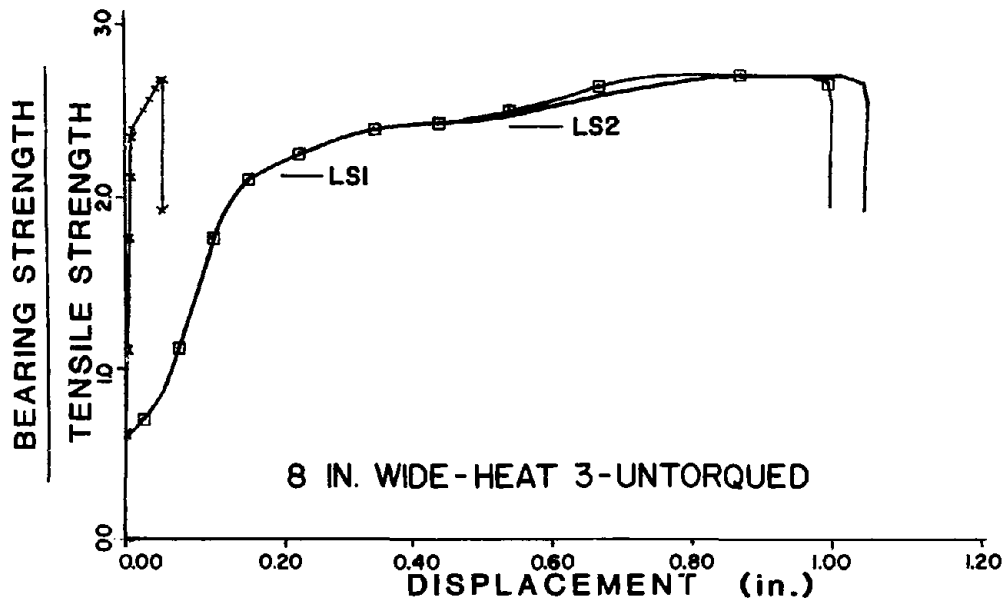


(c) Plate buckling



(d) End tearout

Figure 107. Failure modes



— TOTAL DISPLACEMENT (IN.)  
 × CROSS SECTION ELONGATION (IN.)  
 □ BEARING DEFORMATION (IN.)

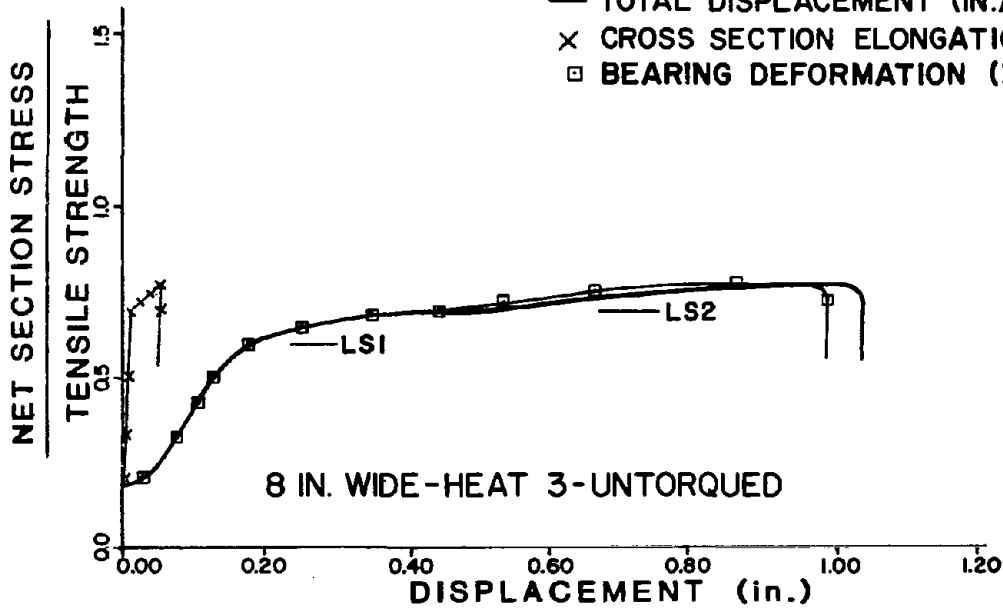


Figure 108. Stress-displacement curves, Test 8-H3-1  
 (1 in. = 25.4 mm)

a connection failure because such a grossly deformed connection is both unserviceable and can interfere with the performance of nearby structural and nonstructural elements. Excessive deformation in a connection is a defacto failure mode. Although a connection may have additional load capacity at a certain deformation level, the connection has failed if the effectiveness of the structural members it connects or the structure itself have been reduced.

The final failure mode to be discussed is end tearout. End tearout, shown in Figure 107d, is caused by the bolts in a connection tearing the end of the splice plate before the net cross section capacity or the bearing stress capacity can be reached. End tearout was considered only in two test specimens which were designed specifically to allow this failure mode. All other test specimens were designed to preclude end tearout as a possible failure mode by maintaining sufficient end distance.

The experimental load-deflection relationship and the separation of the deformation into bearing and elongation components are given for each specimen in Ref. 29. The replicates are not presented because they gave identical results. Stress vs. deflection relationships representing the various observed behavioral modes are presented herein for Specimens 8-H3-1, 6-H1-1, 8S-H3-1, 6S-H3-1, 6-H3-2, and 8-H3-2. These tests represent bearing failure in splice plates with round holes, net cross-sectional failure in splice plates with round holes, bearing failure in splice plates with slotted holes, net cross-sectional failure in splice plates with slotted holes, end tearout failure, and an attempted end tearout failure, respectively. The differences between test specimens with fully torqued bolts and test specimens with snugged bolts are discussed later.

For each test, two plots are provided, bearing stress vs. displacement and net section stress vs. displacement. In each case, the stress is nondimensionalized by the tensile strength of the material. In all cases, the responses are for the two-bolt group. Typical behavioral phenomena are cited at various load stages.

Bearing Failure in Splice Plates with Round Holes (Test 8-H3-1, Figure 108. Load Stage 1 corresponds to the "elastic" limit of the behavior of the splice plates. Approximately 20 percent additional load will be gained through 500 percent additional displacement. At this load level, virtually no distortion is visible in the grid and the steel above the bolts has yielded. The first signs of instability are observed; the splice plates are pulling away from the pull plates. This behavior is defined as "buckling".

Load Stage 2 shown corresponds to the yielding of the net cross-sectional area of the splice plates shown. At this point the cross section elongation begins making a noticeable contribution to the displacement. Severe bearing deformations are visible in the splice plate

and the amount of buckling would present a serious problem in an actual connection.

Load Stage 3 corresponds to load failure. Extensive yielding occurs but the cause of load failure is the excessive bearing deformation shown. A tear in the splice plate occurred above the lower bolt in the two-bolt group. Since the net cross-sectional area only reached 75 percent of its tensile capacity, the mode of failure is classified as bearing. Failure occurred at a bearing stress of  $2.67F_u$ .

Net Section Failure in Splice Plates with Round Holes (Test 6-H1-1, Figure 109). In the "elastic" range corresponding to Load Stage 1, all of the displacement results from bearing deformations and the splice plates only show slight local yielding above the bolts in the two-bolt group.

Load Stage 2 corresponds to yielding of the net cross section shown and the onset of buckling. The splice plate grid still shows no distortion and only a slight amount of bolt movement. Bearing deformation is still the major source of displacement, but elongation of the cross section is increasing rapidly.

Load Stage 3 corresponds to slight necking and extensive yielding. Cross section elongation is beginning to dominate the displacement and the buckling of the splice plates is sufficient to render the connection useless. If Load Stage 4 takes place, a 10 percent increase in load causes a 100 percent increase in displacement to generate a net cross section failure.

Failure shown is the result of the splice plates reaching the steel's tensile strength before the bearing stress reached the previous stress level limit of  $2.67F_u$ , attained in Test 8-H3-1 (Figure 108). A classic net section failure<sup>u</sup> occurred. Failure in this specimen is defined using an ultimate load criterion, but because of the extreme deformations in the splice plates the connection is already useless at a lower load.

Bearing Failure in Splice Plates with Slotted Holes (Test 8S-H3-1, Figure 110). Load Stage 1 is in the elastic range of the load vs. displacement curve as was true for the previous two tests. But the behavior differs substantially from the behavior of the specimens with round bolt holes. The plate between adjacent holes acts as a "beam" and most of the deformation appears to be the result of bending in this beam, as shown in Figure 111a. The local yielding which occurs above the bolt holes is similar to the yielding in the test specimen splice plates with round holes and a similar bearing ratio. Buckling and net cross section yielding occurred simultaneously. The drop in load shown at this stage is the result of net cross section yielding. The beam formed by the two slots had a plastified zone in its middle from bearing stresses and the net cross section yielding plastified the end restraints of the beam. This

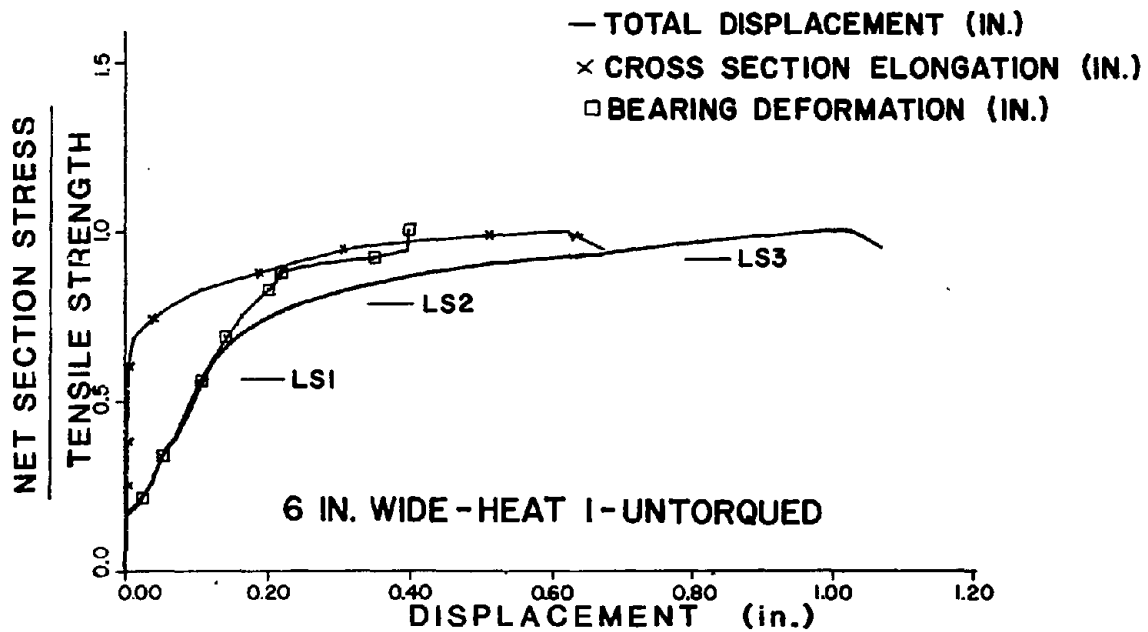
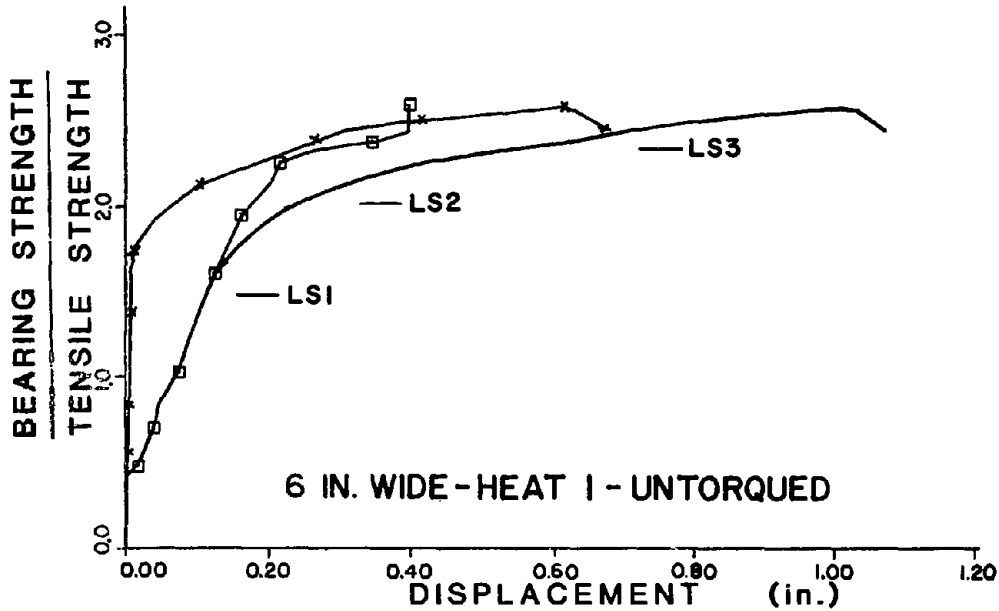


Figure 109. Stress-displacement curves, Test 6-H1-1  
(1 in. = 25.4 mm)

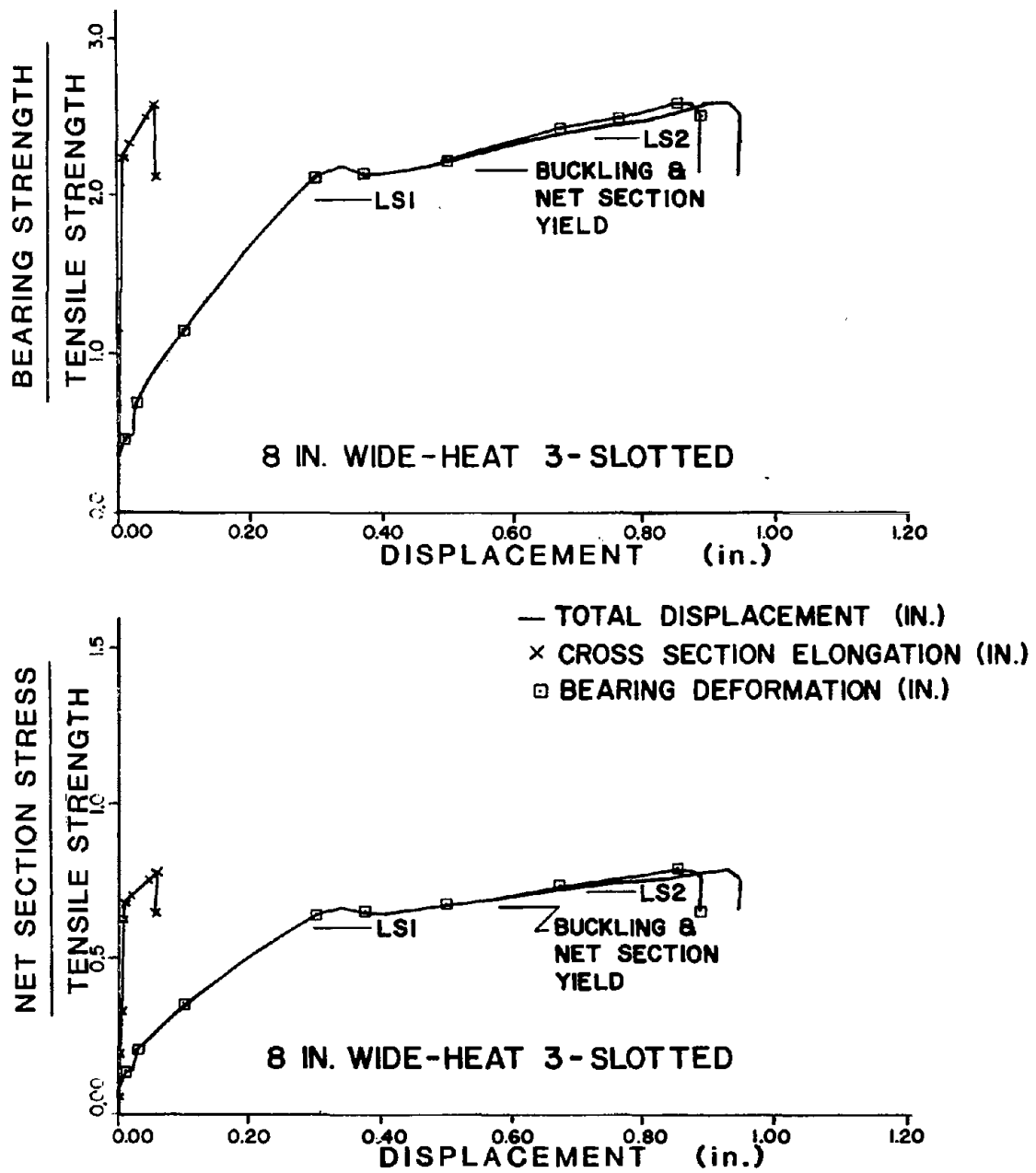
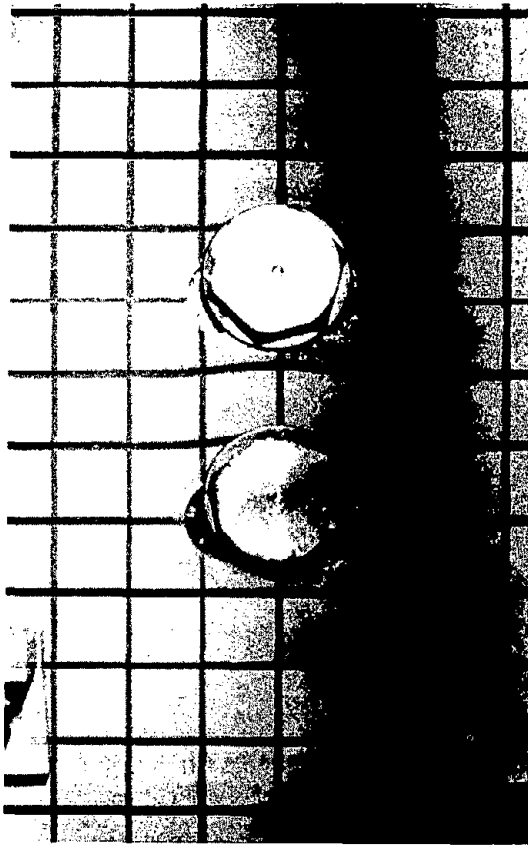
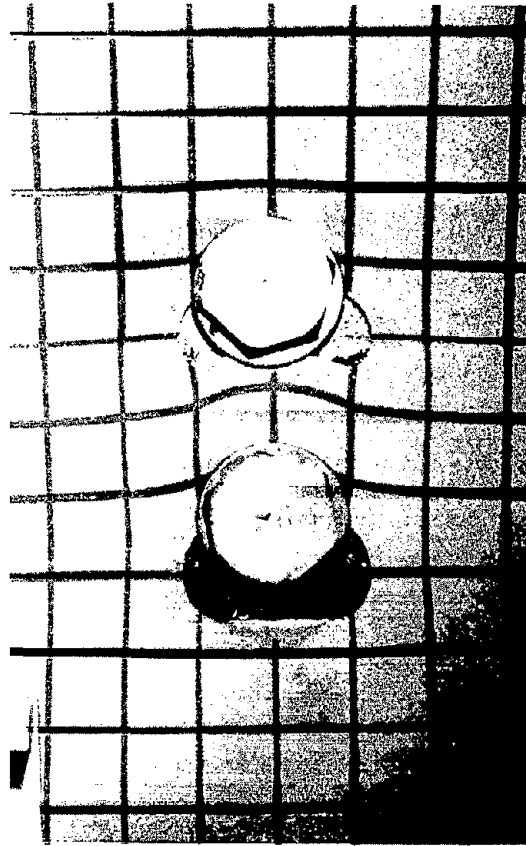


Figure 110. Stress-displacement curves, Test 8S-H3-1  
(1 in. = 25.4 mm)





(a) Load Stage 1



(b) Load Stage 2

Figure 111. Bearing deformation at slotted holes, Test 8S-H3-1

classic beam failure by a plastic analysis approach displaces without an increase in load until the steel begins to strain harden.

Load Stage 2 is shown in the range where the test specimen continues to pick up additional load due to strain-hardening of the "beam" and bearing capacity above the top bolt in the two-bolt group. The extent of the deformation and yielding are shown in Figure 111b. Notice that all of the deformation is very localized around the two bolts.

Load Stage 3 corresponds to load failure of the splice plates. And, as with previous tests, splice plate buckling is very serious by this load stage. Cross section elongation does not add any substantial displacement in this type of failure because the gross cross section does not yield. Since the failure resulted principally from excessive bearing deformations, the failure is categorized as a bearing failure, although the failure does not precisely fit the definition of bearing failure. All test specimens with slotted holes and nominal widths of 8 in. (203mm) and 7 in. (178mm)

displayed this same type of behavior. Figure 110 shows that failure occurred without reaching either of the theoretical limits,  $1.0F_u$  and  $3.0F_u$  for net section stress and bearing stress, respectively.

Net Section Failure in Splice Plates with Slotted Holes (Test 6S-H3-2, Figure 112). This test specimen, discussed as a net section failure in splice plates with slotted holes, not only shows a net cross section failure, it shows how net cross section tensile capacity can be reduced by the effects of interacting bearing stresses.

Load Stage 1 is in the "elastic" range of the load vs. displacement curve and no significant deformations are observed.

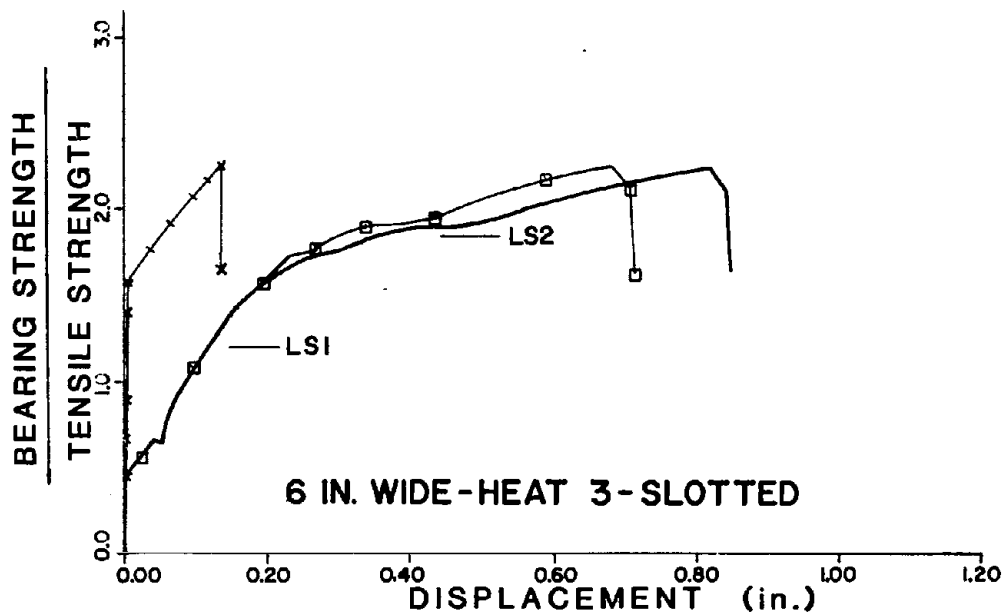
Load Stage 2 corresponds to net cross section yielding and buckling. The bearing stresses have not plastified the "beam" as described in the previous section, although the yielded net cross section has plastified the ends of the "beam". Without the three plastic hinges necessary to fail the beam, the splice plates continue to carry additional load.

Load Stage 3 corresponds to load failure. The "beam" has reached a plastic mechanism, but the beam bending deformations are not as pronounced as for the splice plates with slotted holes which were bearing failures. The grid markings showed the net cross section necking, classic tensile strength failure distortion patterns, and a crack forming across the net cross section in Figure 113a. Buckling of the splice plates occurred before the ultimate load was reached. While this test specimen was primarily a net cross section failure, the bearing stresses were high enough to cause the net cross section to fail at 92 percent of its tensile capacity. The condition of the first bolt in the three-bolt group in Figure 113b shows similar deformation patterns to the two-hole group which also justifies this failure as primarily a net section failure.

End Tearout Failure in Splice Plates with Round Holes (Test 8-H3-2, Figure 114). As was discussed previously, the reason for testing this specimen and the following specimen was to see whether splice plates with standard end distances exhibited the same buckling behavior as splice plates with long end distances. The modified test specimen is shown in Figure 104 with dimensions in parenthesis referring to these two special tests.

Load Stage 1 corresponds to the extensive yielding around and between the bolt holes. Comparing this load vs. displacement curve with the load vs. displacement curve for the bearing failure in splice plates with round holes (Figure 108) shows that the shortened end distance provides a less stiff connection.

Load Stage 2 is past net cross section yielding and the start of buckling. The buckling is not as pronounced as in the test specimens



- TOTAL DISPLACEMENT (IN.)  
 □ CROSS SECTION ELONGATION (IN.)  
 ○ BEARING DEFORMATION (IN.)

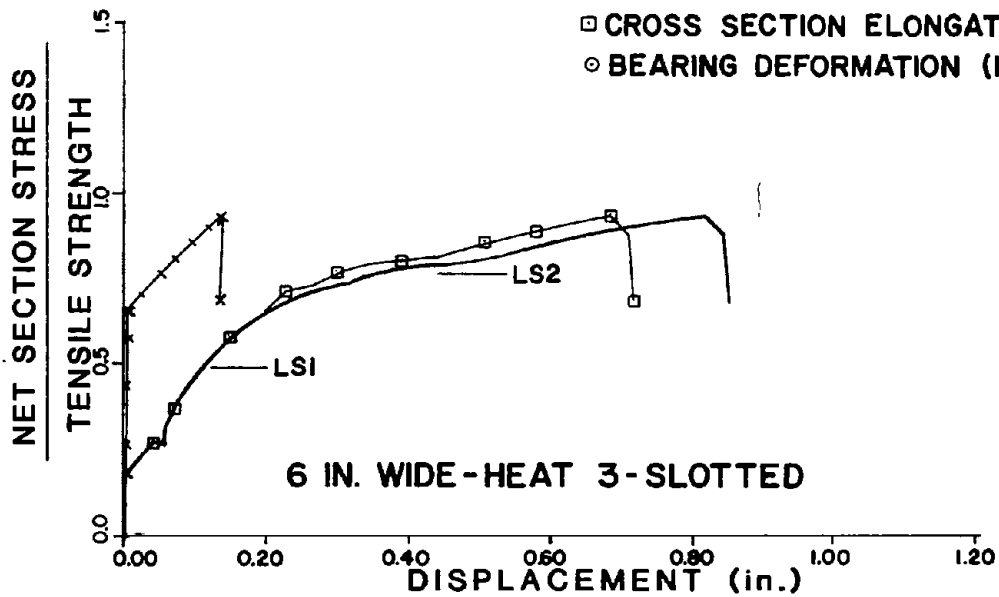
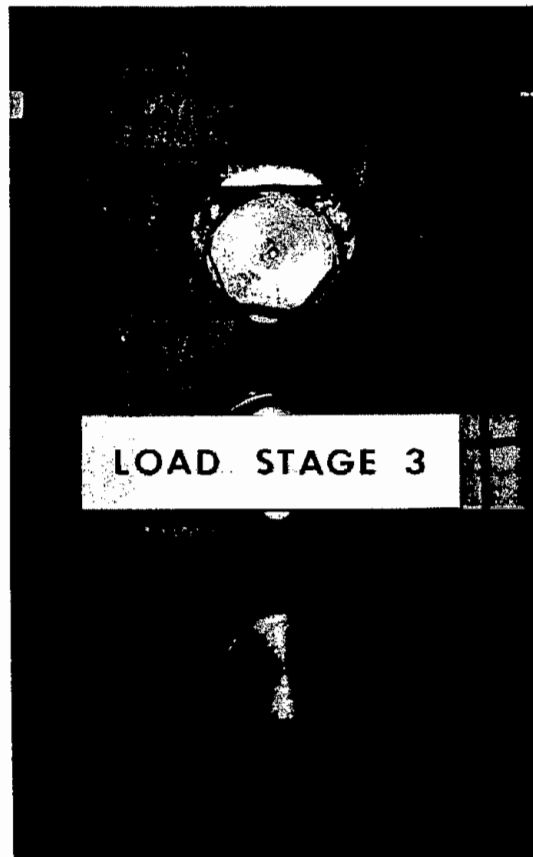


Figure 112. Stress-displacement curves, Test 6S-H3-2  
 (1 in. = 25.4 mm)



(a) Two-bolt group



(b) Three-bolt group

Figure 113. Net section failure, slotted holes, Test 6S-H3-2

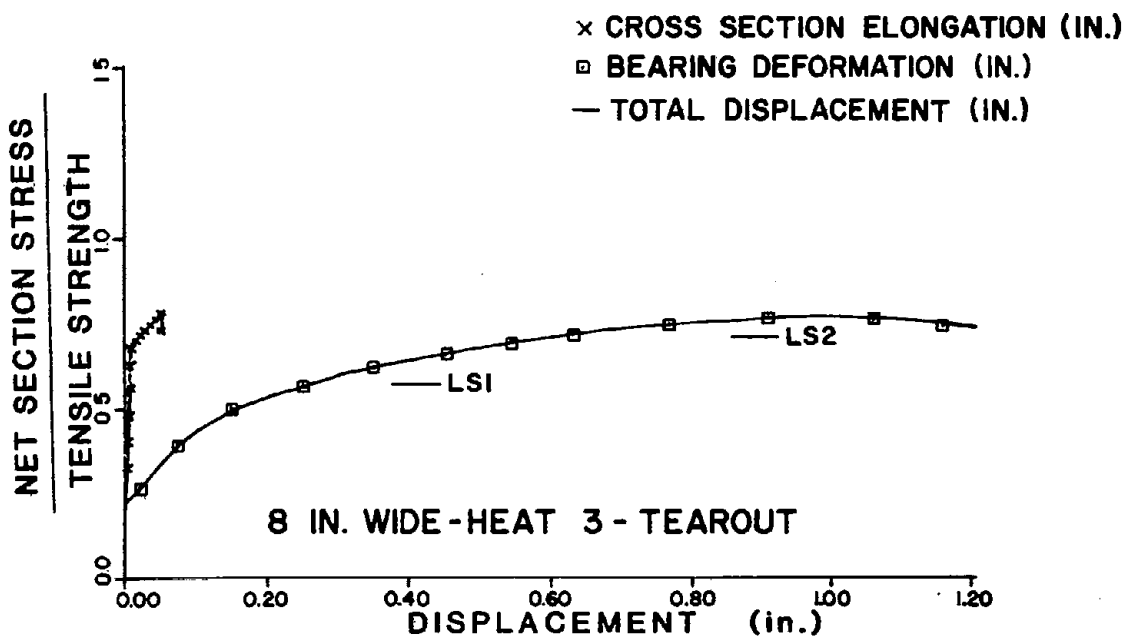
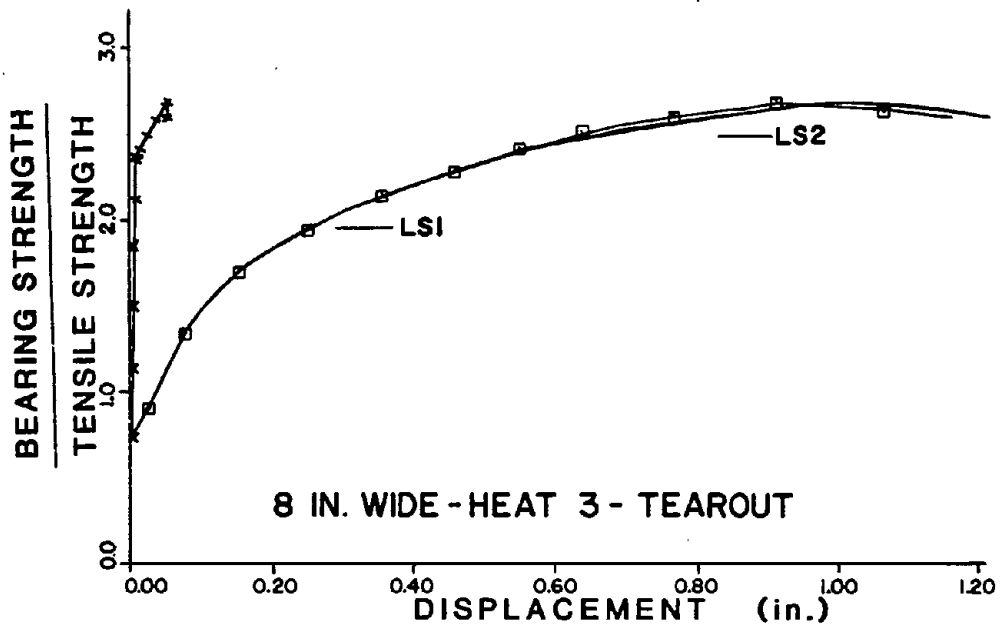
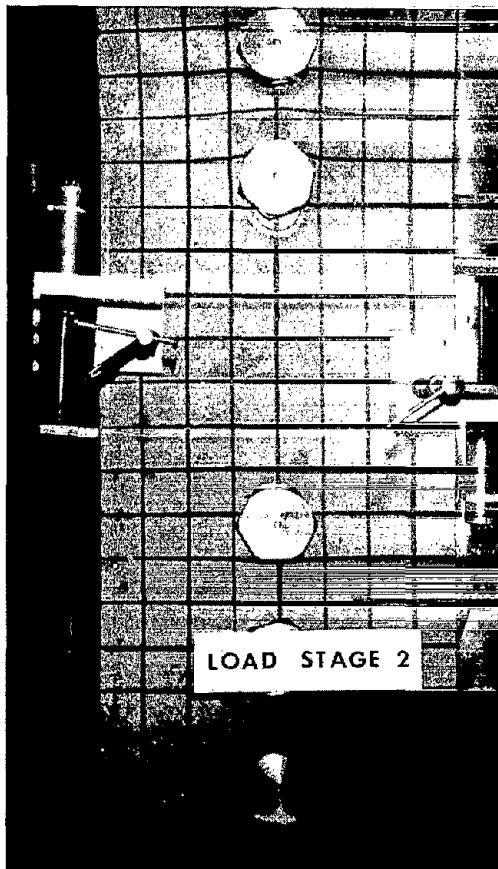
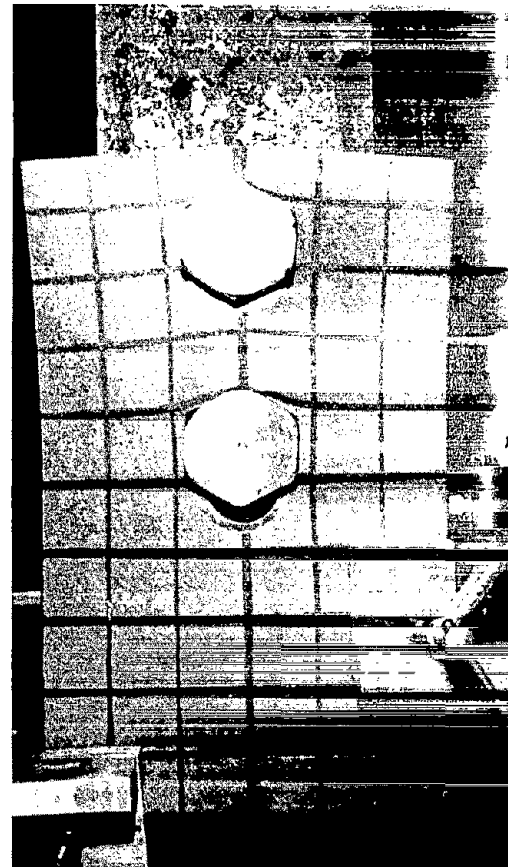


Figure 114. Stress-displacement curves, Test 8-H3-2  
 (1 in. = 25.4 mm)



(a) Test 8-H3-2



(b) Test 6-H3-2

Figure 115. Effect of short edge distance, Load Stage 2

with long end distances, but its presence was obvious during the test. The significant deformations at Load Stage 2 are evident in Figure 115a.

Load Stage 3 corresponds to load failure. The short end distance provides far less restraint against end tearout than the long end distance used in most other test specimens. At failure the splice plates have widened and necked down ahead of the two-bolt group as the bolts pushed through to the end of the plates. In spite of the lack of restraint, the splice plates exhibit a classic bearing failure.

End Tearout Failure in Splice Plates with Round Holes (Test 6-H3-2, Figure 116). This specimen was tested for the same reasons as the previous end tearout failure. The difference between these two tests is that the previous test used splice plates which originally exhibited a bearing failure with long end distances, while the splice plates in this type specimen with long end distances exhibited a net cross section failure. Their respective bearing ratios are 3.5 and 2.5.

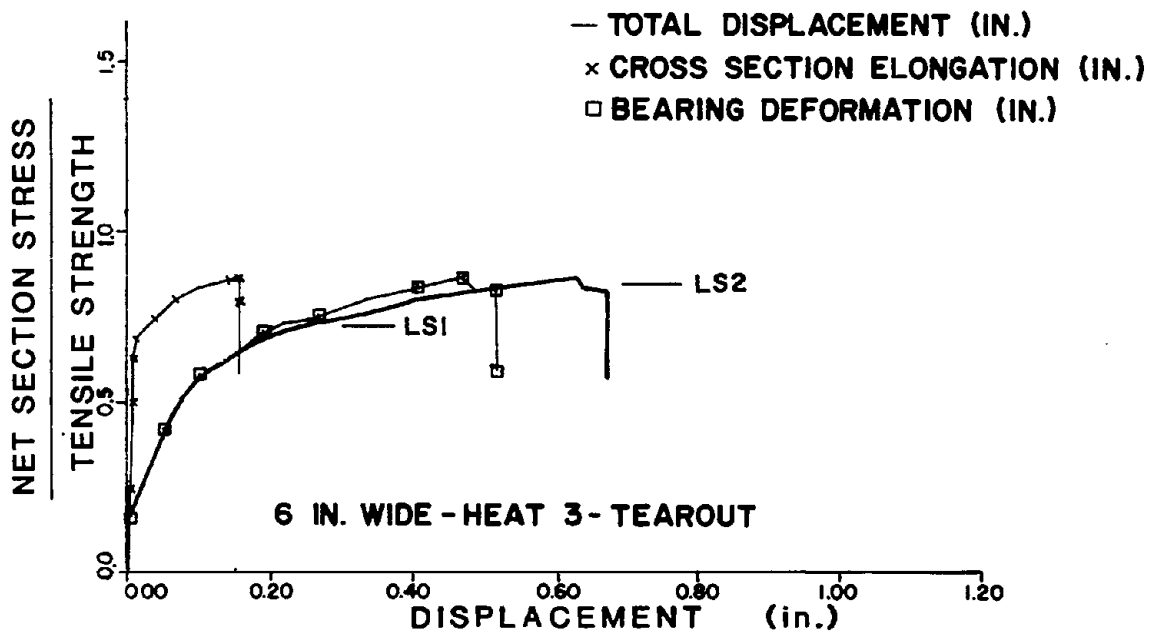
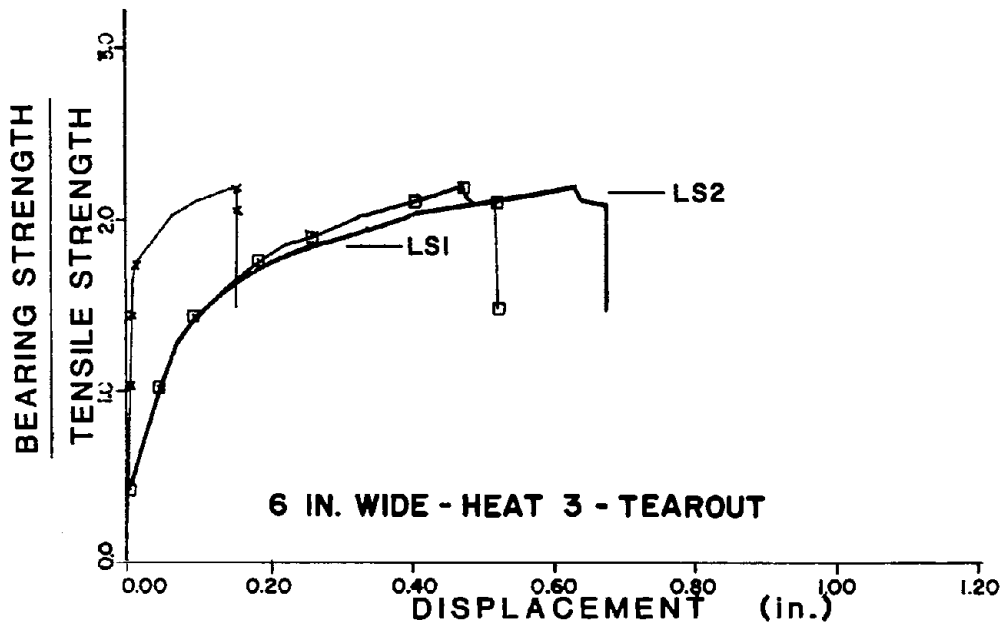


Figure 116. Stress-displacement curves, Test 6-H3-2  
 (1 in. = 25.4 mm)

At Load Stage 1, the net cross section has yielded and extensive yielding above the bolts in the two-bolt group is the result of bearing stresses. No buckling is visible at this load stage.

Load Stage 2, shown in Figure 115b, corresponds to the same widening of the splice plates as occurred in the previous end tearout failure. The load vs. displacement curve is similar to the curve for the net cross section failure specimen with the long end distance (Figure 108) to this point. Up to Load Stage 1 bearing deformations had dominated the splice plate behavior, but from Load Stage 1 to Load Stage 2, cross section elongation became prominent.

Load Stage 3 corresponds to load failure at 85 percent of the net cross section's tensile capacity. Large bearing deformations are shown in Figure 116 and the necking and fracture associated with end tearout were observed.

Slip Loads. In the tests with the A490 bolts torqued by turn of nut, a slip load was discernible in some of the connections. The mill-scale surface of A36 steel from Heat 1 gave a slip coefficient of 0.217 (s.d. = 0.034) for five data using the two-bolt group and 0.210 (s.d. = 0.012) for four slip loads of the three-bolt group. The overall S.C. for the 9 slip loads give a slip coefficient of 0.214 (s.d. = 0.025), which is much lower than the average of 0.34 given in Ref. 15. Since these data are only for one steel heat, no broad conclusion can be drawn. It must be noted, however, that almost all data on millscale surfaces developed during this project (four different heats and steel strengths) showed value of slip coefficient less than the mean published value.

### Analysis of Results

In this section various parameters will be studied by comparing the nondimensionalized plots of bearing stress and net section stress. It is shown in Ref. 29 that even though two different heats of steel are used, comparison of the test results are valid when nondimensionalized.

Effects of End Distance. End distance, shown as L in Figure 117, is the distance from the centerline of the bolt nearest the end of a splice plate or pull plate to the end of the plate. For all 8, 7, and 6 in. (203, 179, and 152 mm) wide plates the end distance was 9 in. (228 mm). For all 4 in. (102 mm) and 2 in. (51 mm) wide plates, the end distance was 3 in. (76 mm). For all tests, the pitch, shown as s in Figure 104, was 3 in. (76 mm), and the bolt diameter was 1 in. (25 mm). According to research by Struik [15] which examined test specimens failing by either end tearout or bearing failure, a lower bound is defined by the relationship  $L/d = F_p/F_u \leq 3.0$ . This relationship was derived from tests on one-bolt symmetric butt splices failing in their inside splice plates. End tearout is also affected by the material's bearing strength which is a function of splice plate



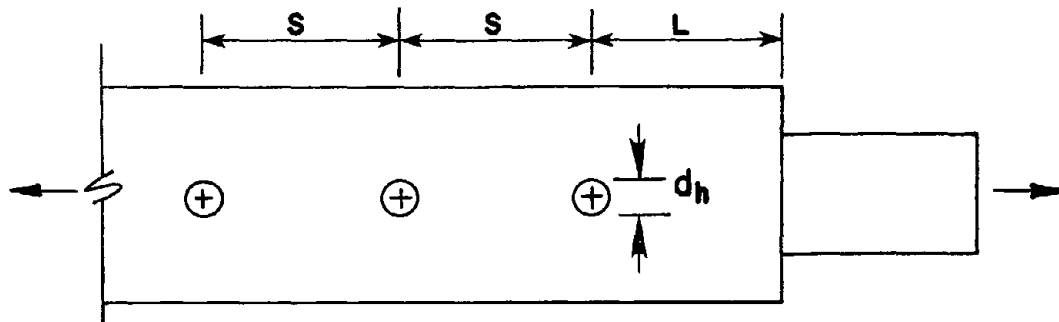


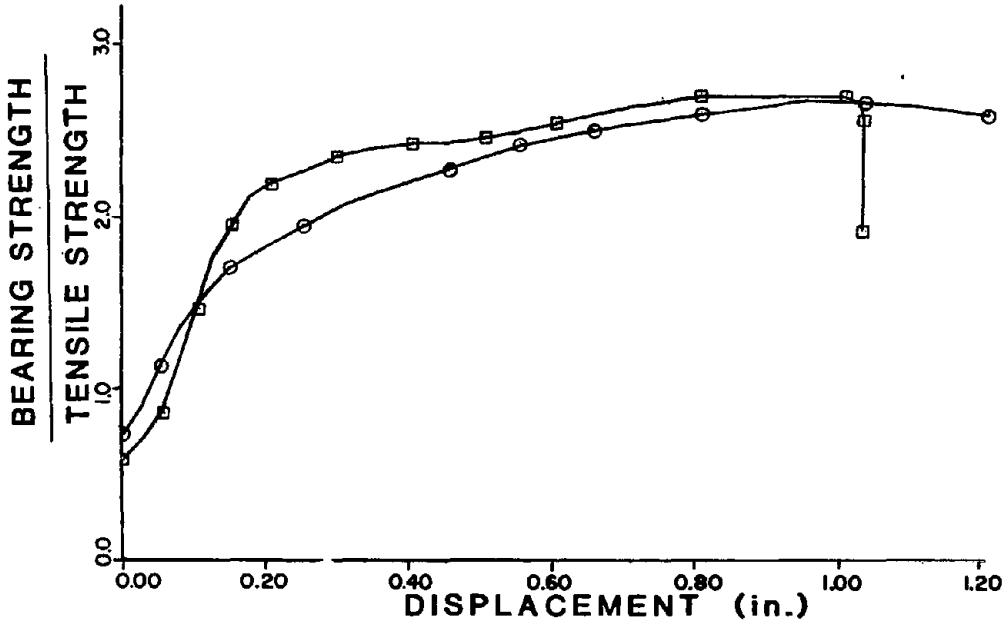
Figure 117. End tearout model

restraint. Connections with bolts torqued to a snugged condition fail at a 20 to 30 percent lower bearing stress, a tearout, than connections with bolts torqued to their full capacity [12].

End tearout can be computed by assuming the bolt shears along two planes through the plate, beginning at the edge of the bolt and continuing to the end of the plate, as shown in Figure 117. Expanding this idea to multiple bolt connections gives excellent correlation with test results. Specimen 8-H3-2 had a theoretical failure load of 170 kips (756 kN) and an actual failure load of 178 kips (792 kN). The difference between the two loads is 5 percent. Specimen 6-H3-2 had a theoretical failure load of 144 kips (641 kN) and had an actual failure load of 146 kips (650 kN). The difference between the two loads is 2 percent. This close correlation between the predicted failure load and actual failure load supports the model developed by Struik.

The relationship between test specimens with long end distances and short end distances is made by comparing Specimen 8-H3-1 with Specimen 8-H3-2 and Specimen 6-H3-1 with Specimen 6-H3-2. Specimens 8-H3-1 and 8-H3-2 were identical except for their end distances. Specimen 8-H3-1 had an  $L/d$  ratio equal to 9 and failed at bearing stress of 2.57 times the tensile strength of the material. Specimen 8-H3-2 had an  $L/d$  equal to 2.5 and failed at a bearing stress of 2.62 times the tensile strength of the material. Figure 118 compares the response of these two specimens. Their behavior is essentially identical except that the short end distance specimen is not as stiff as the specimen with the long end distance. Specimens 6-H3-1 and 6-H3-2 are compared in Figure 119. As with the 8 in. (203 mm) wide specimens, their behavior is virtually the same except that the specimen with the short end distance fails at a lower load. As discussed previously, the additional end distance reduced deflections.

The intent of this section was to show that excessive end distance in the splice plates of the test specimens did not adversely influence the general behavior of the test specimens. As an addition, the method of computing end tearout resistance based on allowable bearing stress will also be discussed. End tearout can be computed very accurately



□ 8 IN. WIDE - HEAT 3 - UNTORQUED (L=9)  
 ○ 8 IN. WIDE - HEAT 3 - TEARCUT (L=3)

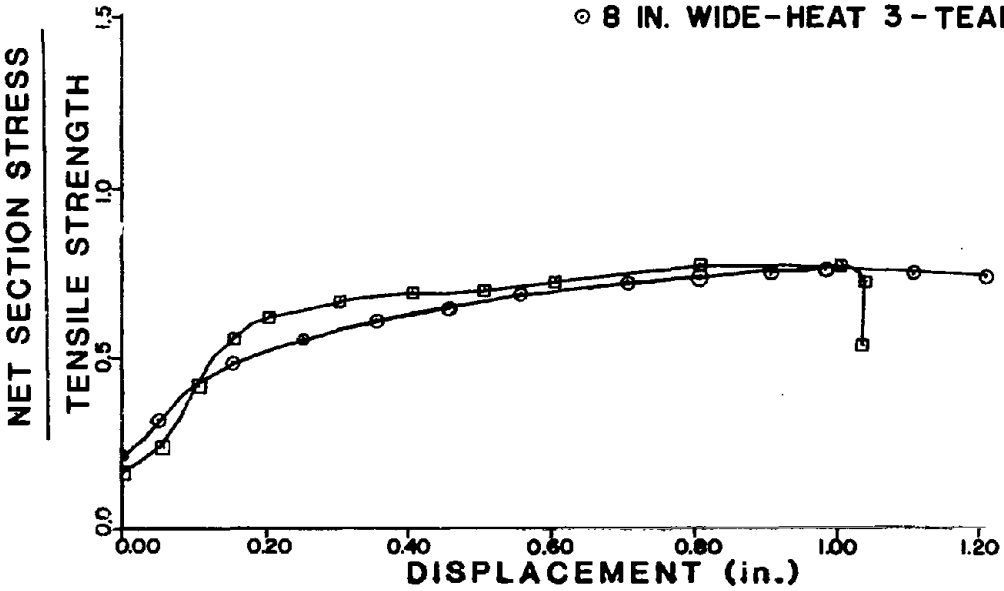
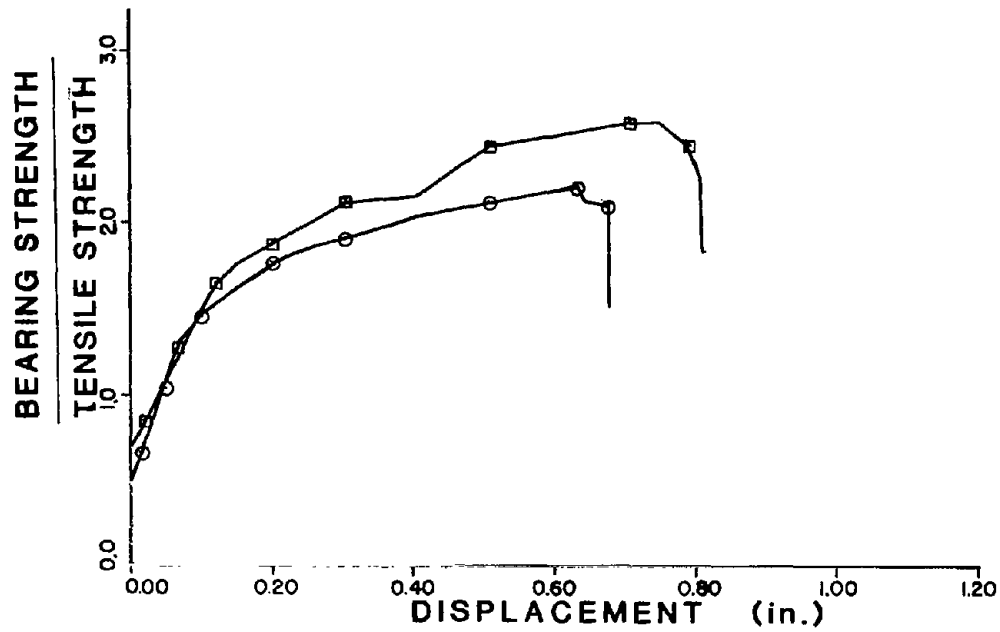


Figure 118. Effect of end distance, 8 in. wide plates  
(1 in. = 25.4 mm)



□ 6 IN. WIDE - HEAT 3 - UNTORQUED (L=9)  
 ○ 6 IN. WIDE - HEAT 3 - TEAROUT (L=3)

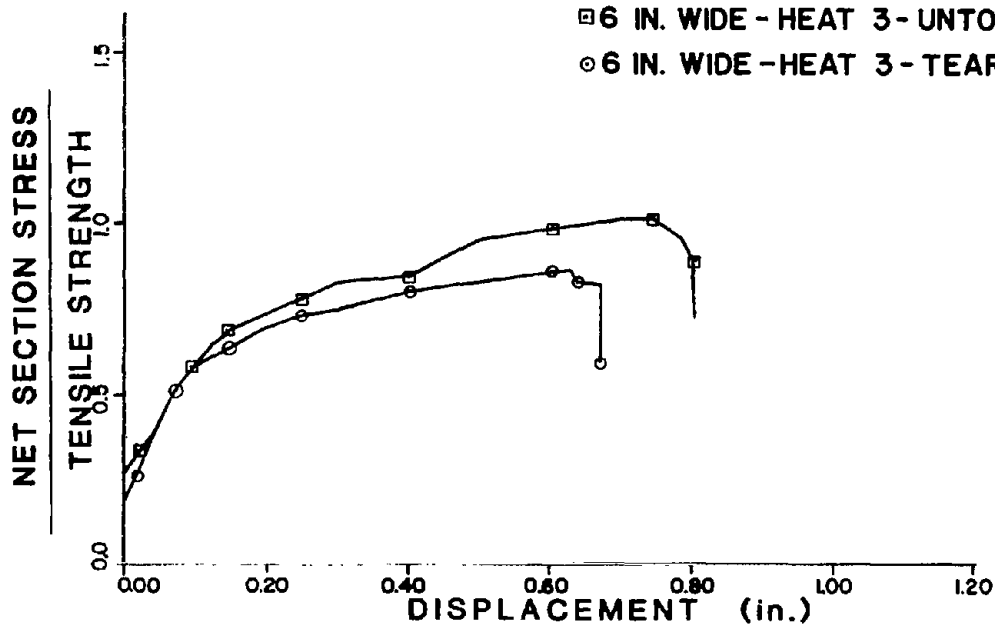


Figure 119. Effect of end distance, 6 in. wide plates  
(1 in. = 25.4 mm)

by the shear plane approach; however, it does not consider deformation levels required to reach load failure. Stress limits can be used effectively to limit deformations as well as end tearout.

Effects of Connection Geometry. Various dimensionless parameters have been used to categorize the behavior of bolted connections. The previous section discusses how  $L/d$  is a valid dimensionless parameter for determining end distance and bolt spacing. When discussing net cross section efficiency,  $g/d$  is a good indicator of behavior [17], but only within certain constraints, as will be shown later in this section. The bearing ratio of a bolted connection is the dimensionless parameter which best describes the overall behavior of a bolted connection. The bearing ratio, BR, is defined as bearing stress,  $f_b$ , divided by net section stress,  $f_t$  (see Eq. 5). The bearing ratio<sup>P</sup> accounts for the ratio of net cross-sectional area to gross cross-sectional area. Further discussion and comparison of specimens with similar BR are given in Ref. 29. It is concluded that connections with different geometries but similar BR behave in a similar manner.

Effects of Bolt Clamping Force. Figure 120 shows the general behavioral differences between connections with fully torqued bolts and connections with bolts torqued only to a snug tight condition. The torqued specimen continues to pick up load without additional displacement until the friction is overcome. Once the specimen has slipped, the load quickly peaks and the specimen fails. The snugged specimen behaves similarly, except that its slip load is below its net section load, so its failure occurs basically when the tensile capacity of the net cross section is reached. When failing the outside splice plates of a symmetrical butt splice, the ultimate capacity is independent of the clamping force in the bolts, except when the slip load is greater than the ultimate tensile strength. Tests with a 2 in. (51mm) wide plate (BR = 0.475) show a significant increase in capacity (40 percent and 70 percent above the ultimate net section tensile capacity for Tests 2-H1-1C and 2-H1-2C, respectively) because of friction force.

A more important aspect of the effects of clamping force is shown in Figure 121, a comparison of torqued and snugged bearing failures, and Figure 122, a comparison of torqued and snugged net cross section failures. In both comparisons the test specimens failed at virtually identical ultimate loads. What is important is the initial portions of the load vs. displacement curves. The curves for the specimens with untorqued bolts show much more displacement for a given load than specimens with torqued bolts. This initial lack of stiffness in untorqued specimens will become a critical factor when failure is defined as a displacement limit in later sections of this report.

Effects of Slotted Holes. At ultimate load the slotted hole specimens have the same capacity as the round hole specimens. In the presentation of results in a previous section, it was noted that the behavior of slotted hole specimens is different from the behavior of

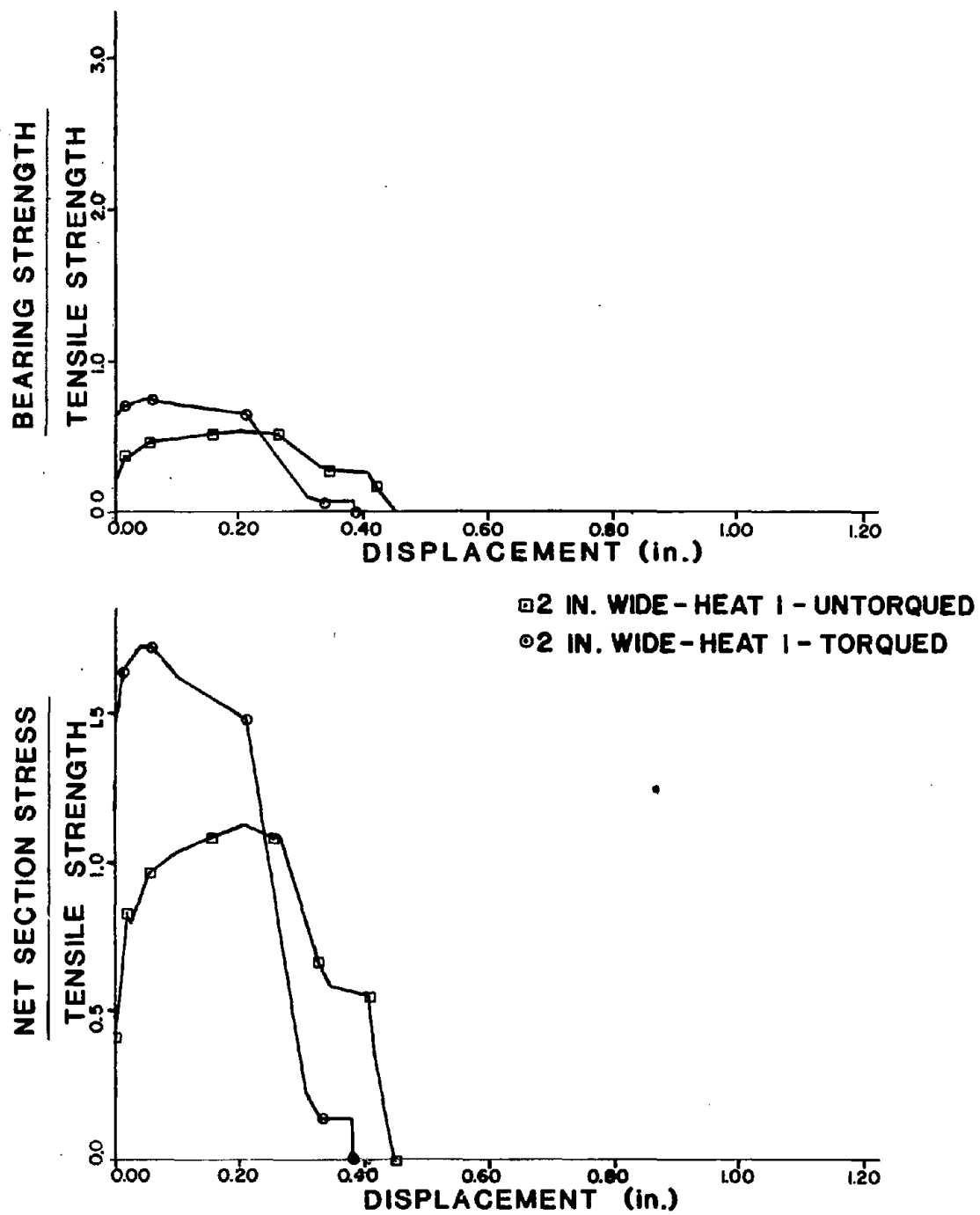


Figure 120. Effect of clamping force, 2 in. plates  
 (1 in. = 25.4 mm)

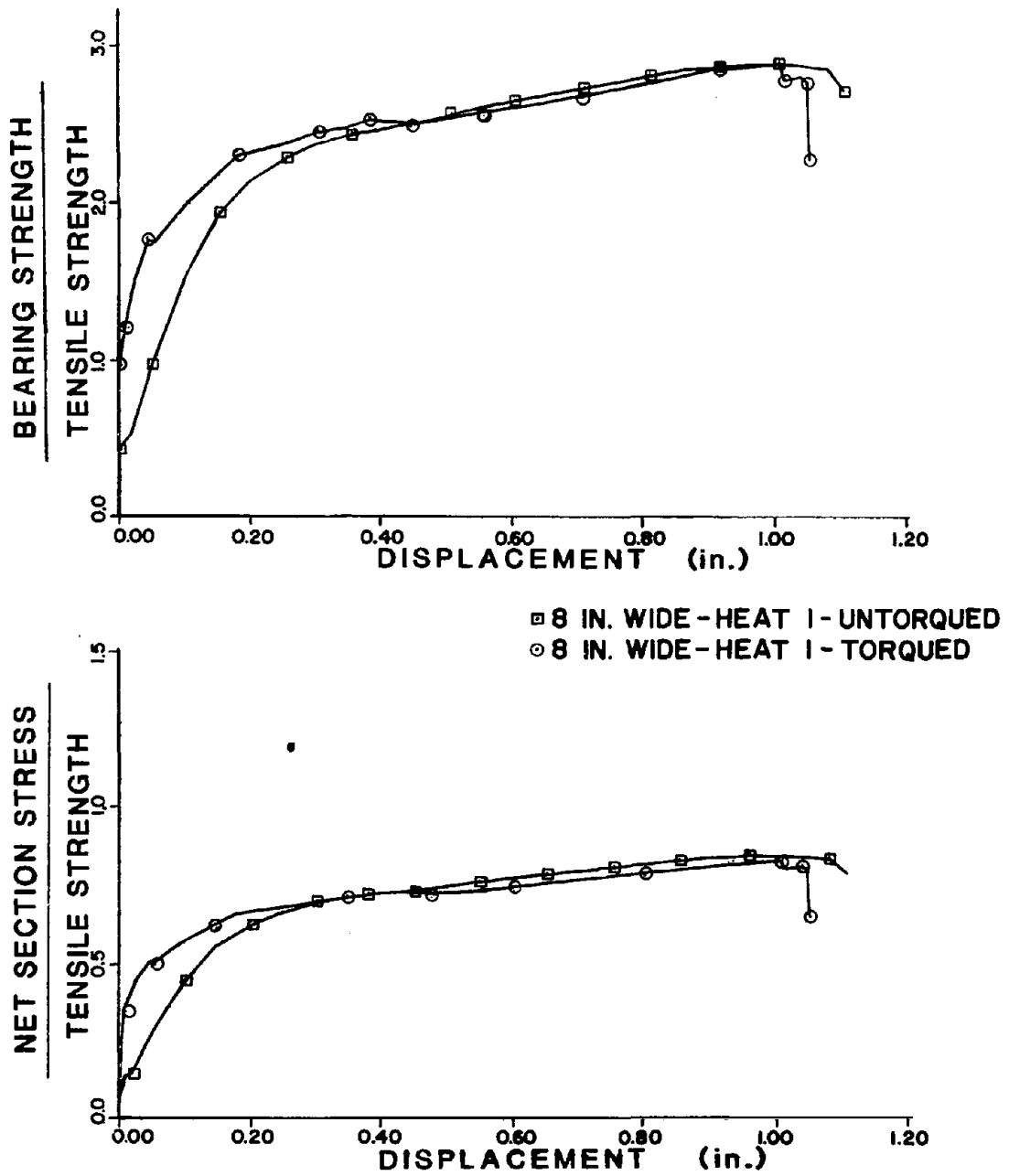
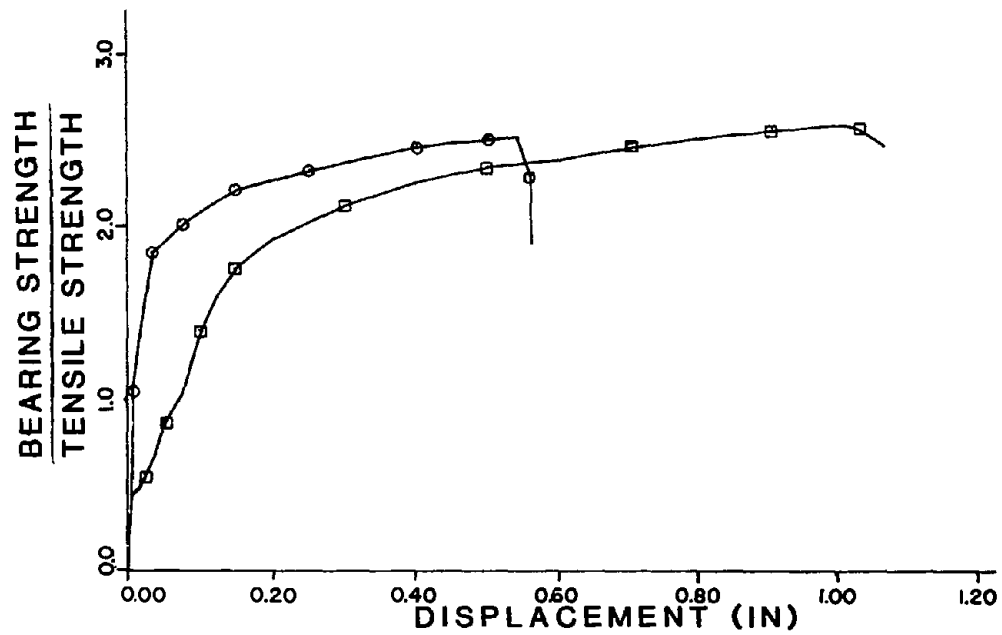


Figure 121. Effect of clamping force, 8 in. plates  
(1 in. = 25.4 mm)



□ 6 IN. WIDE - HEAT 1 - UNTORQUED  
 ○ 6 IN. WIDE - HEAT 1 - TORQUED

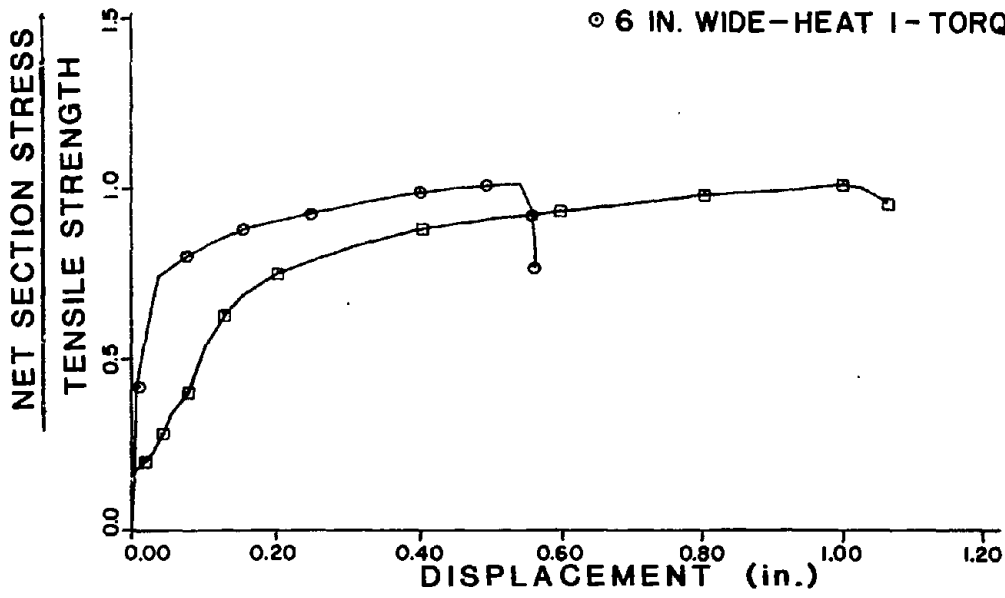


Figure 122. Effect of clamping force, 6 in. plates  
(1 in. = 25.4 mm)

round hole specimens of similar bearing ratios. Figure 123 compares the load vs. displacement behavior of slotted hole specimens vs. round hole specimens for a bearing failure. In the comparison, the slotted hole specimen shows considerably more displacement per load than the round hole specimens with only a small difference in ultimate load. This difference in ultimate load is the result of the slotted hole specimens having slightly lower bearing ratios than the round hole specimens. For the same bearing ratio, slotted hole specimens have the same ultimate load capacity as round hole specimens. But, as will be discussed later in this report, slotted hole specimens have much less capacity than round hole specimens when deflection limits are used as failure criteria. Comparison of 6 in. (152 mm) wide and 4 in. (102 mm) wide specimens, which had combined bearing and net section failure and net section failure, respectively, showed similar reductions for slotted holes [29].

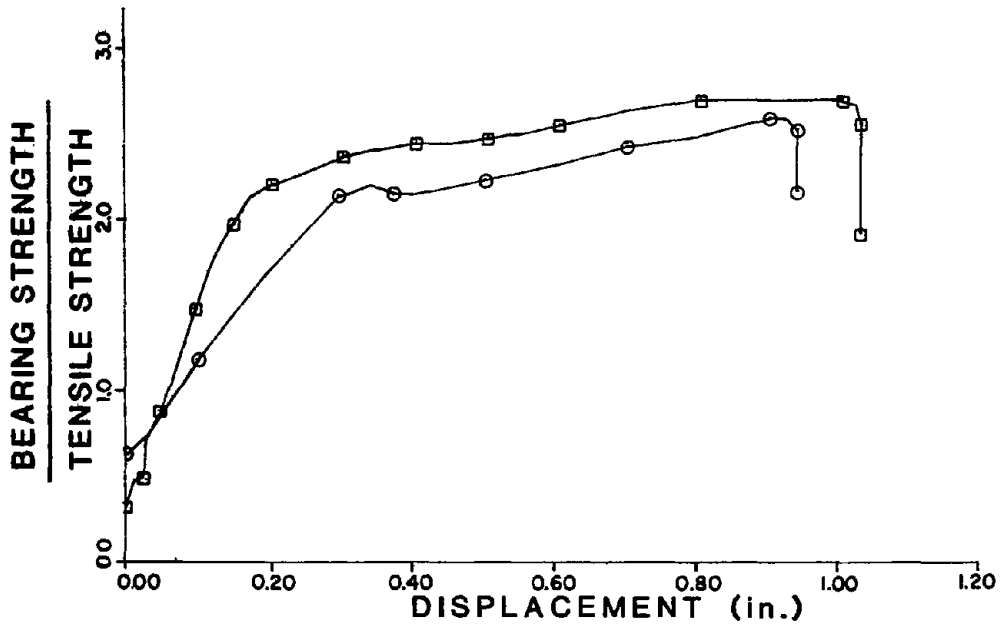
Analysis of Failure Criteria. A summary of the test data for all specimens is given in Table 55. Replicates are not shown because the data are almost a direct duplicate. In some instances results are given for the three-bolt group, identified in the test number by (3), when significant behavior occurred. The maximum load from the test is shown in Col. (5). In addition, the load on the load-displacement curve corresponding to a deformation of 0.25 in. (6.4 mm) is also shown and will be discussed later.

The test data from Table 55 are presented in Figures 124, 125, and 126. Each figure contains two plots of the same data. The left axis plots net cross section stress divided by  $F_u$  versus the specimen bearing ratio. A line through the data plotted in this fashion in Figure 124 is almost horizontal at a net section stress/ $F_u$  and is labeled Net Section Stress Curve. The right axis plots bearing stress divided by  $F_u$  versus the specimen bearing ratio. A plot of the data with these two axes corresponds to the solid curve labeled Bearing Stress Curve.

Figure 124 shows the theoretical tensile strength curve developed by Gaylord [17] and the bearing stress limit. Current recommendations from the AISC and AISI with factor of safety removed are also given for comparison with the test results.

An important problem is inherent with both the Gaylord and Gaylord and the AISI Specification net cross-sectional stress equations. Both rely on the ratio  $g/d$ . In Ref. 19 it was shown that connections with different geometries but similar bearing ratios behaved similarly. The ratio  $g/d$  is not the same as the bearing ratio. If Figures 124, 125, and 126 relied on  $g/d$  instead of bearing ratio, the data would be scattered across the plots. Using bearing ratio instead of  $g/d$ , the data from tests run by Munse [25] on full-scale connections plot on the two solid curves in Figure 124. Munse's connections had a wide variety of configurations and geometries and failed restrained as well as unrestrained plates. The AISI Specification does account for the





□ 8 IN. WIDE - HEAT 3 - UNTORQUED  
 ○ 8 IN. WIDE - HEAT 3 - SLOTTED

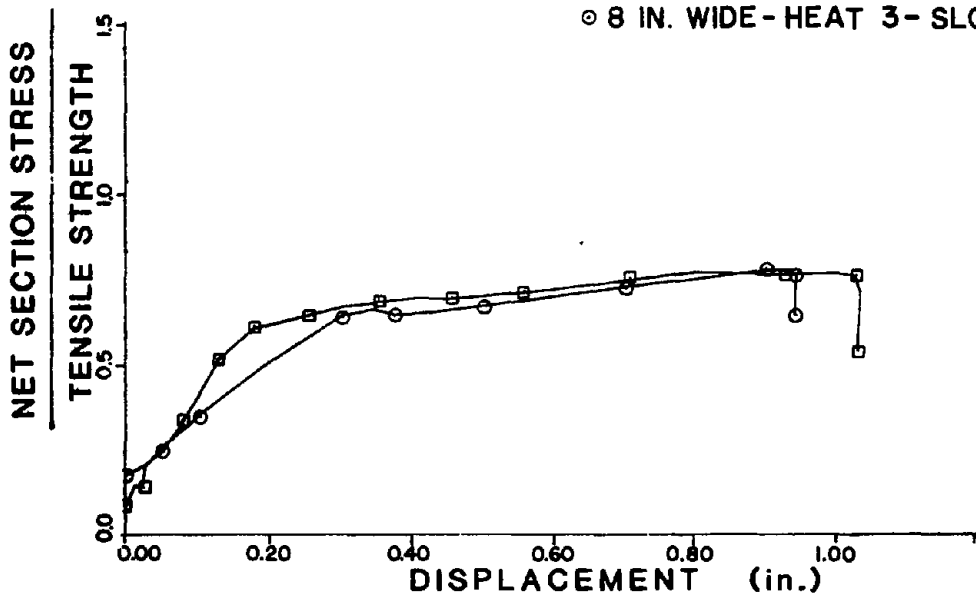


Figure 123. Effect of slotted holes, 8 in. wide plate  
(1 in. = 25.4 mm)

Table 55. Summary of bearing tests

Test No.	Bearing Ratio (Eq. 5)	Type of Failure*	$P_{0.25}$ (kips)	$P_u$ (kips)	(Net Ten. Stress) <sub>.25</sub> $F_u$	(Net Ten. Stress) <sub>u</sub> $F_u$	(Bearing Stress) <sub>.25</sub> $F_u$	(Bearing Stress) <sub>u</sub> $F_u$
(1)	(2)	(3)	(4)	(5)	(6)	(7)	(8)	(9)
8-H1-2	3.46	2	133.77	168.65	0.658	0.829	2.255	2.842
6-H1-1	2.53	1	119.2	151.8	0.780	0.993	2.008	2.558
6-H1-2(3)	1.65	0	132.9	145.0	0.905	0.988	1.493	1.629
6-H1-2	2.48	1	113.1	145.0	0.771	0.988	1.906	2.444
4-H1-1	1.48	0	85.2	88.4	0.965	1.001	1.436	1.489
4-H1-1(3)	0.99	0	90.15	92.7	1.021	1.049	1.013	1.041
2-H1-1	0.471	0	29.2	30.4	1.055	1.095	0.493	0.512
8-H1-1C	3.49	2	139.4	169.3	0.671	0.815	2.349	2.853
6-H1-1C	2.48	1	136.0	148.2	0.919	1.001	2.293	2.497
4-H1-2C	1.490	0	91.7	92.2	1.025	1.030	1.546	1.554
2-H1-2C	0.475	0	--**	42.7	--**	1.686	--**	0.720
8-H3-1	3.51	2	150.6	179.9	0.634	0.757	2.238	2.672
8-H3-2	3.51	3	129.7	178.3	0.547	0.752	1.923	2.649
7-H3-1	3.01	2	151.5	173.1	0.737	0.842	2.252	2.572
6-H3-1	2.51	1	131.7	172.4	0.767	1.003	1.958	2.562
6-H3-2	2.50	3	123.0	146.1	0.718	0.854	1.827	2.171
8S-H3-1	3.32	2	127.3	172.7	0.568	0.771	1.891	2.566
7S-H3-1	2.83	2	119.2	168.2	0.621	0.876	1.721	2.499
6S-H3-1	2.41	2	115.1	150.6	0.707	0.926	1.710	2.328
4S-H3-1	1.36	0	84.2	91.2	0.911	0.987	1.251	1.356

\*Code for Types of Failure

(1 kip = 4.45 kN)

0 Net Section

1 Mixed Mode

2 Bearing Failure

3 End Tearout

\*\*Did not slip until net section failure.

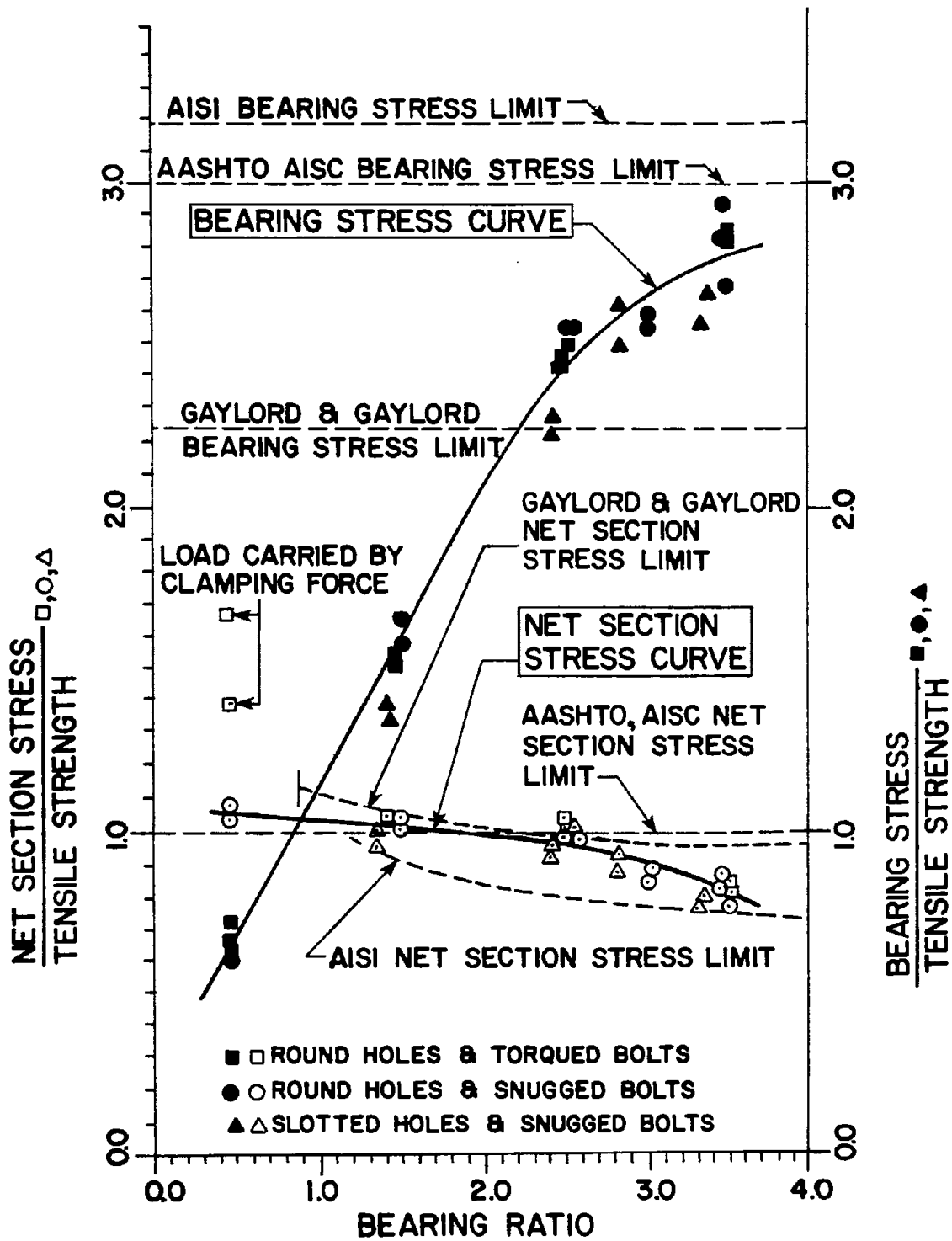


Figure 124. Test data at ultimate load

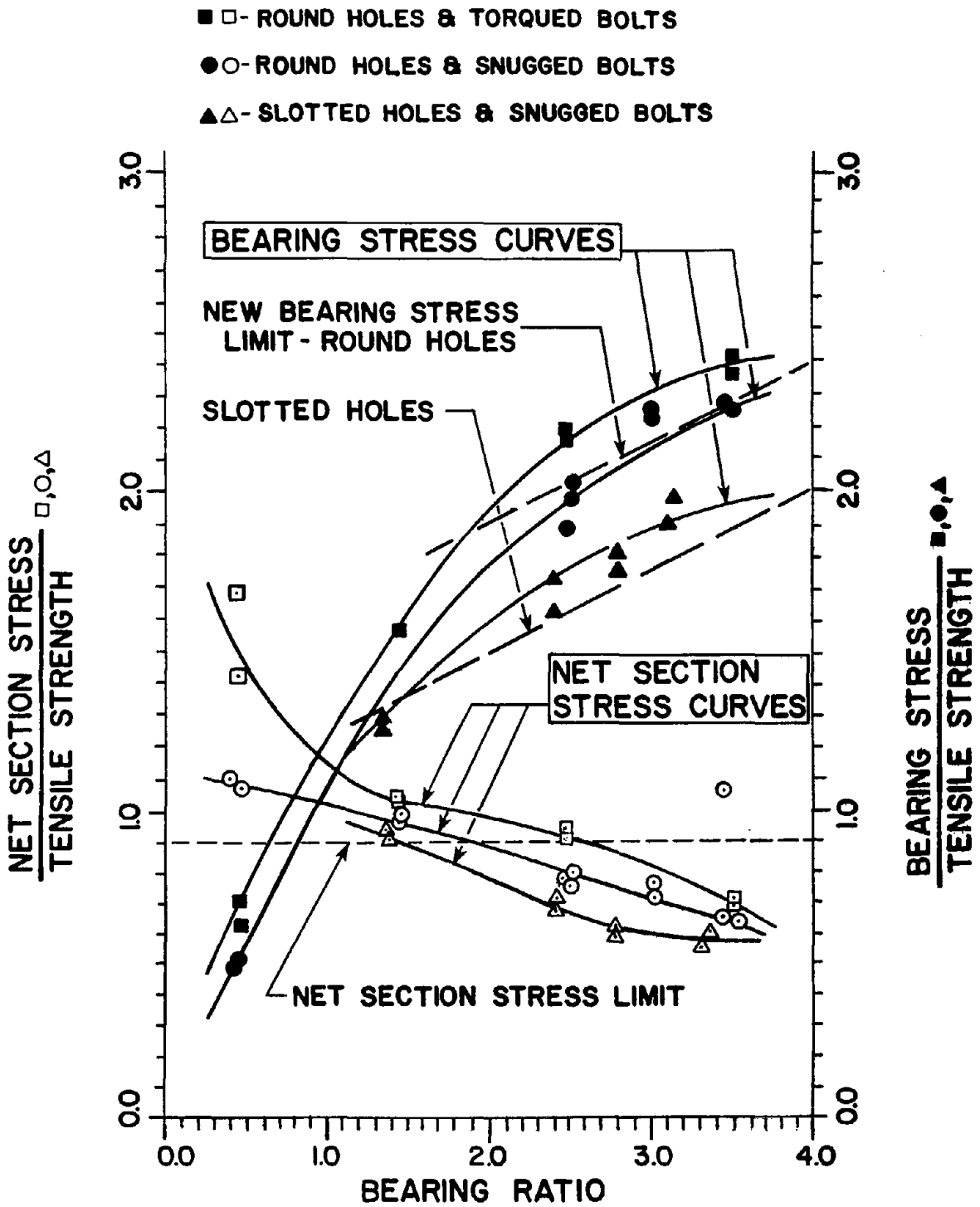


Figure 125. Test data at 0.25 in. total deflection (1 in. = 25.4 mm)

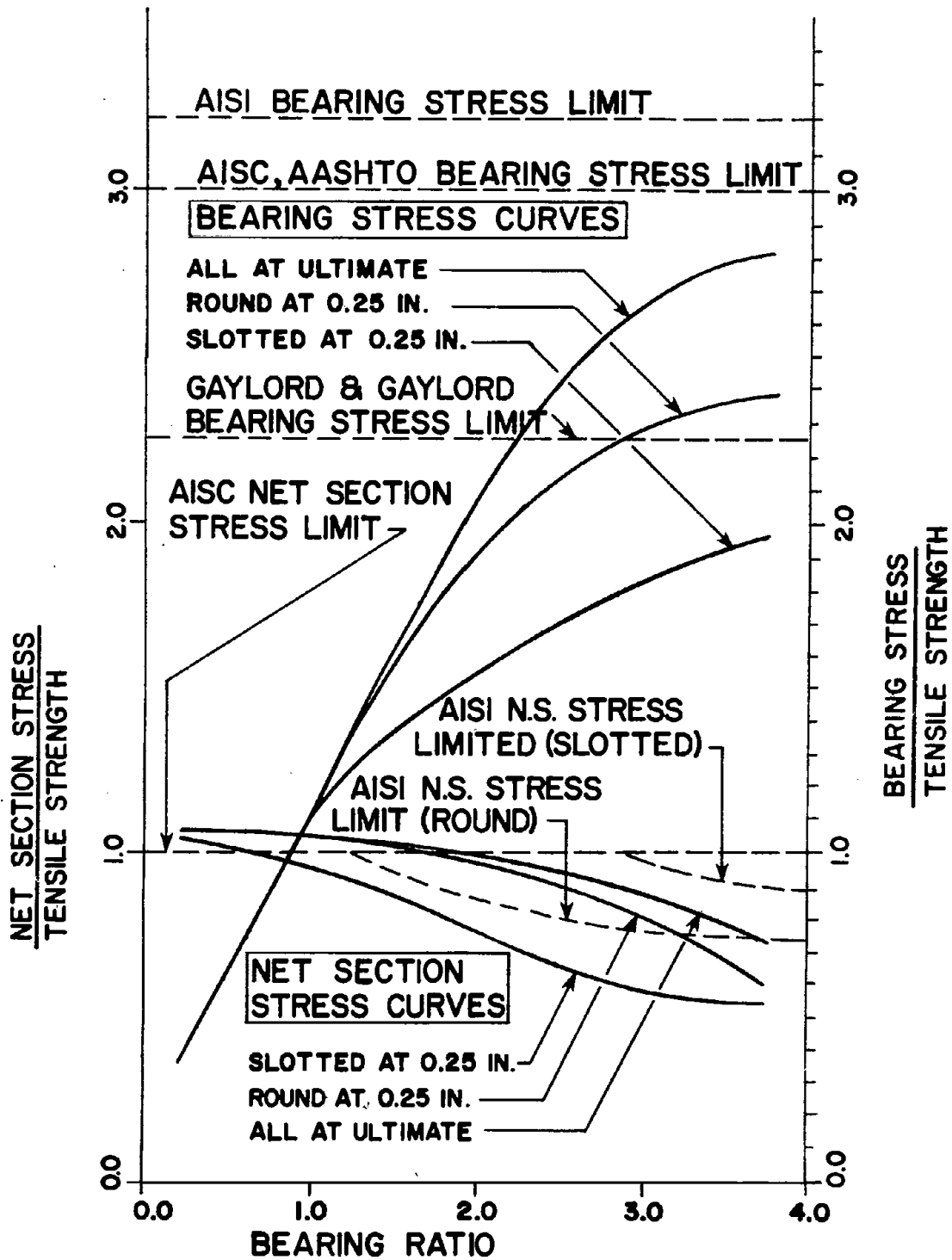


Figure 126. Comparison: ultimate load vs. 0.25 in. deflection  
(1 in. = 25.4 mm)

number of rows of bolts but it does not account for anything other than rectangular patterns of round bolt holes. If the AISI curve was plotted for specimens with one row of slotted holes, it would be shifted so far to the right on Figure 124 that it would be essentially the straight line used by the AISC. This same shift would occur for the Gaylord and Gaylord curve.

As long as a connection fails at a load which is greater than or equal to its predicted failure load, the connection design is safe. In Figure 124 the test curves are two views of the same data. For a given bearing ratio, as long as one of the test curves is above its assumed limit (bearing limit or tensile limit), the connection is safe. At a bearing ratio of 3.5 the net cross section stress curve is below the predicted Gaylord and Gaylord curve. Specimens at this bearing ratio failed in bearing before they reached their net cross-sectional capacity as predicted by Gaylord and Gaylord. Recognition must be given to the fact that the Gaylord and Gaylord curve is valid for  $g/d$  greater than 2.67 and that the curve is principally used for examining cross sections with low bearing ratio below 2.25. In its applicable range, the Gaylord and Gaylord net cross section stress limit is accurate within 5 percent. The bearing ratio limit is used to preclude the possibility of bearing failures by limiting bearing stress to  $2.25F_u$  [25]. This limit ignores additional bearing capacity in connections with bearing ratios greater than 2.25.

The AISI limits bearing failures by limiting net section stresses. In Figure 124, all of the test specimens failed at loads above their predicted failure loads according to the AISI Specification. If the test specimens had used only one row of bolts instead of two, the AISI net cross section stress curve would be the same as the AISC, AASHTO net cross section stress curve and the test curve would not be any different. Over half of the test specimens would have failed below their AISI Specification predicted failure load. Extrapolating the experimental data curves to bearing ratios above 4.0 would show the bearing stress curve becoming horizontal at a bearing stress ratio of 2.9 and a net cross section stress curve slowly working its way to a net cross section stress ratio of 0.4 at a bearing ratio of 5.0. This experimental behavior shows that in general the AISI Specification is unconservative in its load predictions for connections with bearing ratios above 2.25.

The relevance of the test results presented in this report towards light gage steel connections is verified by Winter's own research [35]. Winter's data base used in formulating his recommendations to AISI included test specimens fabricated from sheet steel 0.186 in. (4.72 mm) thick. The specimens tested for this report were fabricated from 0.25 in. (6.35 mm) thick sheet steel.

The AISC-AASHTO Specifications limits on bearing stress and net cross section stress shown in Figure 124 are unconservative above a bearing ratio of 2.25. The experimental net section stress ratio curve is less than 1.0 and the experimental bearing stress ratio curve does not reach the value of 3.0. At a bearing ratio of 3.0, the experimental bearing stress ratio curve is approximately 7 percent below the AISC-AASHTO predicted value of 3.0 and maximum error between these codes and the experimental curves shown in Figure 124 is not more than 15 percent, however.

Munse's data plots directly on the solid curves shown in Figure 124. Munse noticed that connections with bearing stresses greater than  $2.25F_u$  did not fail across their net cross sections and suffered serious deformation. To avoid this behavior, Munse recommended a bearing stress limit at this level. Winter [35] tested lap splice connections using snug tight bolts with washers under both the bolts and the nuts. He recorded bearing stresses as high as  $6.0F_u$ . His mean value for pure bearing stress failures was  $3.2F_u$ . Research by Chong and Matlock [10] was identical to Winter's, except that they did not use washers under their bolts or nuts and they used lighter gages of steel. Their limiting bearing stresses were  $1.9F_u$  and their limiting net cross section stresses were different from Winter's.

The one variable that follows the variations in bearing stress recommendations in the various research efforts is restraint of the failure surfaces. Connections such as symmetric butt splices with fully torqued bolts can withstand high bearing stresses in their inside pull plates, while symmetric butt splices which fail their outside splice plates can withstand lower bearing stresses. Lap splices using thin steel gages and no washers can withstand only very low bearing stresses because of their total lack of out-of-plane restraint against plate deformations. In light gage steel connections, washers provide relatively high amounts of restraint since their thickness is about the same as the plates they contact.

Bearing stress limits could better match experimental results if they considered actual connection restraint conditions. Typical bolted connections such as flange splices and column splices do not have the same amount of restraint as the inside pull plates of symmetric butt splices. The restraint provided in typical connections reported herein is more similar to the connections tested by Munse. A bearing stress limit based on ultimate load should be approximately  $2.0F_u$  for structural connections. The one remaining problem is connections with bearing ratios between 2.25 and 4.0, where bearing stress and net cross section stress interact to reduce bearing capacity from its ultimate limit. This problem will be discussed shortly.

### Deflection Limits as a Failure Criterion in Bearing

In the previous section failure loads were discussed simply in terms of the maximum load a test specimen carried regardless of how distorted, buckled, or yielded the specimen was at the ultimate load. As was discussed in an earlier section, restrained connections begin buckling at net connection yield. A cursory examination of the load sequences in the tests reported herein shows that at 0.25 in. (6.4 mm) displacement, the effectiveness of the connections was significantly reduced. The connections were severely buckled and the load vs. deflection curve was virtually flat. The low bearing ratio test specimens which were not subjected to any substantial bearing deformations had almost reached their ultimate loads. Undergoing an additional 0.75 in. (19.0 mm) displacement for a 20 percent increase in load is not realistic. For practical purposes, the connections had failed at 0.25 in. (6.4 mm) displacement.

The thirty connection failures presented in this report do not provide a sufficient data base on which 0.25 in. (6.4 mm) displacement can be justified as a failure criterion. But the load vs. deflection curves presented by Winter [35], Chong and Matlock [10], Struik and Wittermans [12], and Munse [25] are very similar to the load vs. deflection curves presented in this report. The initial portions of all of the load vs. deflection curves display a nearly vertical "elastic" range. Then they all quickly flatten, giving each curve an "elastoplastic" appearance. In all of the tests the connections had plastified before reaching 0.25 in. (6.4 mm) displacement. Also, at this displacement the connections had reached 80 percent of their ultimate loads. In the light gage tests of the lap splice connections, failure occurred at up to 0.75 in. (19.0 mm) displacement, and Munse measured displacements at failure of 0.50 in. (12.7 mm) in his large-scale specimens with high bearing ratios. Considering the test results of other researchers, a data base of several hundred tests exists in which 100 to 300 percent increase in displacement over 0.25 in. (6.4 mm) were required to gain 20 percent more load capacity.

Defining failure as a deflection limit is not without precedent. Gross cross section yielding of a steel truss tension member is considered to be a load limit but it is actually a deflection limit. Since bearing-type connections have very little capacity after 0.25 in. (6.4 mm) deflection, a connection deflection limit of 0.25 in. (6.4 mm) is recommended for use as a limit on bearing capacity.

The examination of load vs. deflection curves from a broad range of test specimens and some deflection limits presented in Ref. 29, the truss example, and the beam example show that using a deflection limit of 0.25 in. (6.4 mm) as a definition of connection failure is not realistic. Figure 125 presents the same test results as Figure 124, using the same format but considering connection failure to be defined



at 0.25 in. (6.4 mm) deflection. In this plot the differences in behavior of connections with torqued bolts, snugged bolts, and slotted holes is apparent. This separation of the data into three curves is a result of the differences in the initial stiffness of the three types of test specimens. The torqued specimens have the highest failure loads. The snugged specimens show about a 10 percent decrease in capacity from the torqued specimens due to the loss of out-of-plane restraint. This loss is approximately the same as the loss Struik and Wittermans experienced between their torqued test specimens and their untorqued test specimens at 0.25 in. (6.4 mm) deflection [12]. The slotted hole test specimens show approximately a 20 percent decrease in capacity below the torqued specimens, due to the varied stiffness of slotted holes.

Figure 125 shows more than the relative behavior differences between torqued, snugged, and slotted hole test specimens when 0.25 in. (6.4 mm) deflection is considered to be failure. It shows that net cross section failures and bearing failures follow similar patterns to the ultimate load curves in Figure 124, except that failure occurs at approximately 20 percent lower stresses. Figure 126 makes a direct comparison between failure defined as ultimate load and failure defined as 0.25 in. (6.4 mm) deflection. The format of the figure is the same as Figure 124 but the curves shown are for ultimate load for all specimens, 0.25 in. (6.4 mm) deflection for round hole specimens and 0.25 in. (6.4 mm) deflection for slotted hole specimens. Comparing the deflection limit curves to the predicted failure loads according to the AISC-AASHTO Specification, the AISI Specification, and Gaylord and Gaylord's recommendations shows that the predicted loads are unconservative for all round hole specimens with bearing ratios greater than 2.0 and for all slotted hole specimens with bearing ratios greater than 1.0. For failure defined as 0.25 in. (6.4 mm) deflection, more realistic capacity predicting criteria are required.

Figure 125 presents a set of failure criteria (shown dashed) using 0.25 in. (6.4 mm) deflection as a definition of failure. The predictions are based on always using fully torqued bolts in connections and bar washers where required on connections with slotted holes to get the maximum amount of connection stiffness. Connections which fail by approaching the tensile strength of their net cross sections can have their deflection limited to 0.25 in. (6.4 mm) by limiting net cross section stress to  $0.9F_u$ . Round hole connections which fail by approaching their bearing stress capacity can have their deflection limited to 0.25 in. (6.4 mm) by limiting bearing stress to  $2.4F_u$ . Similarly, connections with slotted holes should limit bearing stress to  $2.0F_u$ . Between these two limits are connections whose net cross section and bearing stresses are both high enough to cause failure below these limits. These connections are ones with bearing ratios between 2.0 and 4.0. (Using ultimate load as failure, this range is 2.25 to 4.0.) Failure in this range has more of an appearance of being a bearing failure than a net cross section failure, so a linearly varying limit on allowable bearing stress  $F_p$  is recommended, as follows, using a factor of safety of 2.0:

$$F_p = 1.2F_u (0.5 + 0.125 BR) \quad \text{round holes} \quad (6)$$

and

$$F_p = 1.0F_u (0.5 + 0.125 BR) \quad \text{slotted holes} \quad (7)$$

The range of bearing ratios for which the slotted hole equation is valid is from 1.5 to 4.0. A complete set of recommended limits is shown in Figure 125 with the factor of safety removed.

### Conclusions and Recommendations

Thirty bolted symmetrical butt splices with outside splice plates being the weakest portion of the connection were tested to examine the interaction of tensile and bearing stresses. The load vs. deflection characteristics were measured and the test results were compared to the research used for formulating the bearing stress limits in the Bolt Specification. Figure 127 represents a summary of the load-deflection behavior for the 8 in. plates. The use of the ultimate load as a basis

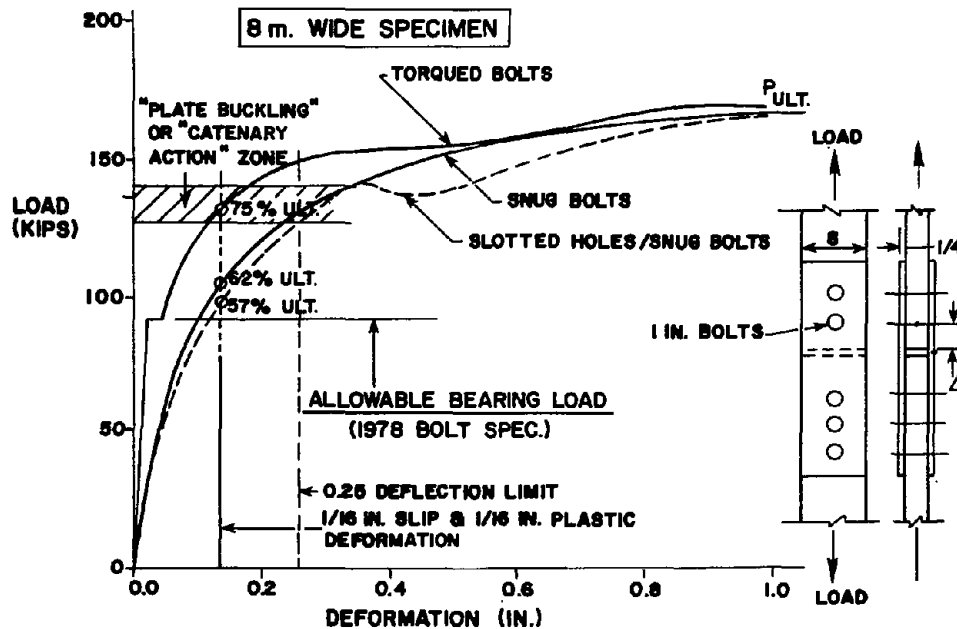


Figure 127. Typical load-deflection behavior

for design is examined and it is recommended that a deflection limit be used to define bearing strength. It was found that the factors of safety against bearing failure of an unconfined plate is less than 2.0 based on ultimate strength.

Conclusions. The results of the tests are summarized by the following conclusions:

1. When computing distances to avoid end tearout, the relationship

$$f_p / F_u = L/d \text{ with } f_p = \text{bearing stress limit}$$

is conservative as long as the bolt pitch,  $g$ , of the rows of bolts perpendicular to the line of force is greater than or equal to the end distance,  $L$ . Excessive end distances are not detrimental to connection strength.

2. Connection behavior can be described by a connection's bearing ratio,  $BR$ , defined by Eq. 5, where connections with similar bearing ratios behave similarly regardless of connection geometry.

3. Fully torqued bolts provide 10 percent greater capacity over snugged bolts for failure defined as 0.25 in. (6.4 mm) displacement. No increase in capacity is seen when failure is defined as an ultimate load except in low bearing ratios where the connections can behave as friction connections.

4. Slotted hole specimens have the same ultimate load capacity as round hole specimens with the same bearing ratios. Slotted hole specimens are less stiff than round hole specimens.

5. When failure is defined as a connection's ultimate load, Gaylord and Gaylord [17] give the most accurate net cross section stress failure predictions. These predictions are valid only for connections with round holes. Assuming failure when the net cross section stress equals the ultimate tensile strength is also sufficiently accurate and much simpler.

6. Bearing stress failure is highly dependent upon the amount of lateral confinement provided to the material being stressed. Fully restrained surfaces such as the inside splice plates of symmetrical butt splices tested by Struik and Wittermans [12] with fully torqued bolts reach ultimate load at bearing stresses of  $3.0F_u$  to  $3.5F_u$ . Unrestrained surfaces such as the outside splice plates of symmetrical butt splices reported herein or the light gage lap splices tested by Chong and Matlock [10] reach ultimate load at bearing stresses of  $2.0F_u$  to  $2.8F_u$ .

7. Using 0.25 in. (6.4 mm) deflection as a definition of failure, the tensile bearing strength of connections with typical amounts of restraint can be predicted by the following procedure:

#### Round Hole Connections

$$0.0 < BR \leq 2.0 \quad :: F_t = 0.9F_u$$

$$2.0 < BR \leq 4.0 \quad :: F_p = 2.4F_u (0.5 + 0.125 BR)$$

$$4.0 < BR \quad :: F_p = 2.4F_u$$

#### Slotted Hole Connections

$$0.0 < BR \leq 1.5 \quad :: F_t = 0.9F_u$$

$$1.5 < BR \leq 4.0 \quad :: F_p = 2.0F_u (0.5 + 0.125 BR)$$

$$4.0 < BR \quad :: F_p = 2.0F_u$$

Recommendations. The following are the recommended design specification changes:

1. The research on restrained connections in structural steel and restrained and unrestrained connections in light gage steel should be reevaluated with respect to bearing ratio and considering 0.25 in. (6.4 mm) deflection as a definition of failure. Transition equations for bearing ratios between 2.0 and 4.0 similar to those in Conclusion 7 should be formulated.

2. Connections with low bearing ratios should be tested to examine the effect of friction load on the tensile capacity of the connections for both restrained and unrestrained designs.

3. No substantial behavior differences exist between light gage steel and structural steel bolted connections. The design procedure should be made to be identical for all steel connections.

## 8. Summary and Comments

The extensive research program undertaken revealed that coatings applied to bolted joints can increase their slip resistance. In general, coating the faying surface, or other forms of surface treatment such as blast-cleaning, reduces the scatter in the slip performance of a bolted joint relative to the uncontrolled condition of a millscale surface. Therefore, it is the authors' recommendation that coating of the faying surfaces of bolted joints be encouraged when the steel itself must be painted. Not only will more uniform and, in some cases, better slip performance be obtained, but lower cost structures will result from the reduction of fabrication costs due to the elimination of the masking of faying surfaces. The maintenance cost of the structure will also be reduced by the elimination of the unprotected edges at the periphery of a joint which cause early coating failures.

The factorial experiments using the small compression specimens in which the clamping force was held constant during the test produced the following conclusions:

- (1) Paint thickness did not significantly change the slip coefficient of the coatings.
- (2) Hole size did not alter the slip coefficient of the coating.
- (3) The magnitude of the clamping force did not change the measured slip coefficient of the coating.
- (4) The type of steel on which the coating was applied did not change the slip coefficient of the coating.
- (5) The elapsed time between painting and testing influenced the slip coefficient of some coatings. Longer times, called curing time, produced higher slip coefficients. The increase in slip coefficient with time after assembling of a joint was small.
- (6) Hard coatings, such as the powdered epoxy coating, did not produce slip coefficient large enough to provide a usable value for design.
- (7) The slip coefficients of organic zinc paints is not a single value but depends on the type of organic vehicle employed in the coating. Perhaps a similar behavior would be suspected with other generic paint categories.

The fatigue tests of coated surfaces showed that the fatigue strength of bolted joints with coated faying surfaces was equal to or greater than the fatigue performance of uncoated surfaces. Two coatings exhibited gradual slippage during the fatigue tests when subjected to the larger stress ranges and maximum stresses. These same coatings exhibited creep deformation under sustained static loading. The

slippage in the fatigue tests occurred at such high levels of stress range it is of little concern in most structures. The correlation with creep performance indicates that by incorporating a creep performance criterion into the requirements for a coating it should eliminate this behavior in structures.

The creep tests performed in this study revealed that for some coatings the creep deformations can be considerable. The large and rapid creep deformation of the vinyl coatings indicate that short-term slip tests alone cannot be used to determine whether a coating is suitable for use on slip critical bolted joints. The creep tests also produced the following conclusions:

- (1) The amount and rate of creep deformation was proportional to the ratio of the applied shear load to the slip load.
- (2) The rate of creep deformation was not constant and was negligible after 1000 hours of loading.
- (3) Thicker coatings exhibited, in general, larger creep deformations than thinner coatings.
- (4) The slip load after creep testing was less than predicted using the initial value of the slip coefficient of the coating and the clamping force. The reduction in slip load correlated with the reduction in bolt length measured for the A490 bolted specimens. Other experiments showed that the bolt length changes corresponded to a reduction in bolt force (clamping force).
- (5) The measured changes in bolt length were larger for the thicker coatings and the change in bolt elongation decreased with time.

The tests of large truss-type joints and the tension specimens showed that the behavior of these specimens could be reliably predicted using the small single bolt compression specimens. In addition, important data were gathered concerning the reductions of clamping force found in the creep specimens. In all of these tests, significant reduction in the clamping force of the bolts was found for some coatings. The reduction in clamping force was the most significant behavior found in these tests. Neglecting this reduction in clamping force which is due to the compressive creep of the coating on the faying surface, and under the head of the bolt and nut, can lead to unconservative design values for the allowable load for slip critical connections.

Further information concerning the clamping force of bolts installed using the turn-of-the-nut procedure and the procedures utilized by the individuals actually tightening bolts in actual fabrication resulted from the full-size truss joint tests. The joints tightened in the research laboratory indicated that tightening to 1/3 of a turn

past snug tight produced a clamping force 20 percent in excess of the minimum specified, but not as high as the average 1/2 turn data (35 percent) given in Ref. 15. The joints tightened by the fabricators indicated considerable variation in clamping force. The variation is much larger than found in the published literature. As a consequence of these data, it is the authors' opinion that the minimum specified bolt tension be used in setting the allowable loads for slip critical connections. Also, the use of oversize holes did not result in a significant reduction in clamping force for the 7/8 in. (22 mm) A325 bolts installed using 1/3 turn from snug. Current specifications imply a 15 percent reduction.

The bearing tests performed indicated that large deformations occur before reaching the ultimate load. The current specification provisions which are based on ultimate capacity allow significant bearing deformation to occur at service load. Using a deformation limit for capacity results in an allowable bearing stress of  $1.2F_u$  for standard holes and  $1.0F_u$  for slotted holes. The deformation in slotted holes was much larger than in standard holes and results in the 20 percent lower capacity. Using these allowable bearing stress values allows the reduction in bearing capacity with increased plate tension found in the tests to be safely ignored in design. Tightening of the bolts is recommended for bearing joints because the joints are stiffened by reducing bearing deformation.

The tests on filler plates indicate that the present AASHTO design provisions related to undeveloped fillers are satisfactory except possibly for long bolted joints. It is recommended that the definition of a long joint be reduced from 50 in. (1270 mm) to 30 in. (762 mm) when undeveloped fillers are used.

The results of the numerous slip tests performed on coated surfaces indicate that many variables influence the performance of a coating. It is impossible to associate a slip coefficient and consequently a design allowable stress for a coating without actually performing tests on the coating. This presents a dilemma for specification writing. Two possible approaches could be taken to solve this dilemma. One approach would be a continuing research program to test all paints presently used or anticipated for use on steel structures. This never-ending research would be very costly. A second approach, which in our opinion is the better approach, is to require that manufacturers test their paint to determine its suitability for use on the faying surfaces of slip critical joints. This approach requires that a method of testing be available which addresses the variables found to be important in this research study. A draft of a testing specification is included in Appendix A. Based on the outcome of these tests on a paint product, a coating would be placed into a classification. The table below gives the allowable shear stress and minimum slip coefficient for each suggested category.

Class	Slip Coef.	Range Slip Coef.	Allowable Shear Stress--Slip Critical Connections (ksi) (1 ksi = 6.89MPa)	
			A325	A490
A	0.22	0.19-0.30	10	12
B	0.32	0.31-0.37	15	18
C	0.40	0.38-0.44	18	22
D	0.48	0.45-0.53	21	26
E	0.55	>0.54	25	31

The values of allowable shear stress are for connections in which relative movement between the plates making up a joint is critical. These joints are termed slip critical. Joints that would fall into the category of slip critical would be joints with oversize holes, slotted holes in the direction of applied stress, and joints subjected to reversal of load. The minimum factor of safety against the mean slip load using the allowable stresses in the table is 1.45, using the minimum specified clamping force. The test procedure in Appendix A also ensures that the creep deformation of the coating at service loads is not excessive and that the loss in clamping force in the bolts does not lower the slip load below the minimum associated with each classification. The testing also ensures that at most the probability of slip of the joint is 1 percent at the 75 percent confidence level. These requirements are only required in slip critical joints. Other joints should be designed on the basis of the shear capacity of the bolt and not the shear capacity based on slip of the connection.

Recommendations for changes in the present AASHTO Specification are given in Appendix B.



#### REFERENCES

1. Allan, Ronald N., and Fisher, John W., "Behavior of Bolted Joints with Oversize or Slotted Holes," Report No. 318.3, Fritz Engineering Laboratory, Lehigh University, Bethlehem, Pennsylvania, August 1967.
2. American Association of State Highway and Transportation Officials, Standard Specification for Highway Bridges, Twelfth Edition, Washington, D.C., 1977.
3. American Institute of Steel Construction, Specification for the Design, Fabrication, and Erection of Structural Steel for Buildings, New York, November 1978.
4. American National Standards Institute, Unified Inch Screw Threads (UN and UNR Thread Form), The American Society of Mechanical Engineers, New York, ANSI B1.1-1974.
5. American Society for Testing and Materials, High Strength Bolts for Structural Steel Joints, Including Suitable Nuts and Plain Hardened Washers, ASTM Designation A325-70a, Philadelphia, Pennsylvania, 1970.
6. Baldwin, James W., Jr., and Murphy, Dwayne D., "Loss of Bolt Tension in Steel Bridges," Missouri Cooperative Highway Research Program 77-2, Final Report, Department of Civil Engineering, University of Missouri, Columbia, Missouri, January 1978.
7. Birkemoe, P. C., Meinheit, D. F., and Munse, W. H., "Fatigue of 514 Steel in Bolted Connections," Journal of the Structural Division, ASCE, ST10, October 1969, pp. 2011-2030.
8. Birkemoe, P. C., and Srinivasan, R., "Fatigue of Bolted High Strength Structural Steel," Journal of the Structural Division, ASCE, March 1971, pp. 335-350.
9. Chesson, E., Jr., "Bolted Bridge Behavior during Erection and Service," Journal of the Structural Division, ASCE, Vol. 91, ST6, June 1965, p. 57.
10. Chang, Ken P., and Matlock, Robert B., "Light Gage Steel Bolted Connections without Washers," Journal of the Structural Division, ASCE, Vol. 181, ST7, July 1975.
11. Crawford, S. F., and Kulak, G. L., "Eccentrically Loaded Bolted Connections," Journal of the Structural Division, ASCE, Vol. 97, ST3, March 1971, pp. 765-783.

12. deBack, J., and de Jona, A., "Measurements on Connections with H.S.F.G. Bolts, Particularly in View of the Permissible Arithmetical Bearing Stress" (a condensed version of Reports 6-66-1 by J. H. A. Struik and 6-67-5 by S. Wittermans), Report 6-68-3, Stevin Laboratory, Delft University of Technology, Delft, The Netherlands, 1968.
13. Eaves, L. D., "Influence of Thread Lubrication on the Behavior of High Strength Bolts," MS thesis, The University of Texas at Austin, August 1978.
14. Fisher, J. W., Bridge Fatigue Guide, American Institute of Steel Construction, New York, May 1977
15. Fisher, J. W., and Struik, J. H., Guide to Design Criteria for Bolted and Riveted Joints, John Wiley & Sons, Inc., New York, 1974.
16. Fouad, F. H., "Slip Behavior of Bolted Friction-Type Joints with Coated Contact Surfaces," MS thesis, The University of Texas at Austin, January 1978.
17. Gaylord, E. H., Jr., and Gaylord, C. N., Design of Steel Structures, McGraw-Hill, New York, 1972.
18. Hansen, M. A., "Influence of Undeveloped Fillers on Shear Strength of Bolted Splice Joints," MS thesis, The University of Texas at Austin, March 1980.
19. Hansen, N. G., "Fatigue Strength of High Strength Steels," Journal of the Structural Division, ASCE, ST3, March 1959, pp. 51-71.
20. Hechtman, R. A., Young, R. D., and Savikko, E. R., "Slip of Joints under Static Loads," Proceedings, American Society of Civil Engineers, Vol. 80, September 1954.
21. Jones, J., "Effect of Bearing Ratio of Static Strength of Riveted Joints," Journal of the Structural Division, ASCE, Vol. 82, ST6, November 1956.
22. Laffitte, A., "Fatigue Behavior of Friction-Type Joints with Coated Faying Surfaces," MS thesis, The University of Texas at Austin, May 1979.
23. Lobb, V., and Stoller, F., "Bolted Joints under Sustained Loading," Journal of the Structural Division, ASCE, Vol. 97, ST3, March 1971, p. 905.
24. Moss, D. S., "High Strength Friction Grip Bolted Joints--Effects After One Year of Weathering under Load," Transport and Road Research Laboratory, Supplementary Report 499, Crowthorne, Berkshire, England, 1979.

25. Munse, W. H., "The Effect of Bearing Pressure on the Static Strength of Riveted Connections," Bulletin 454, Engineering Experiment Station, University of Illinois, Urbana, Illinois, 1959.
26. Nanninga, M. G., "Creep Behavior of Friction-Type Joints with Coated Faying Surfaces," MS thesis, The University of Texas at Austin, January 1978.
27. Nishimura, Akira, "Scattering of Slip Loads of High-Strength Bolted Joints," Proceedings of JSCE (in Japanese), No. 187, March 1971, pp. 37-47.
28. Office of Research and Experiments of the International Union of Railways (ORE), "Coefficient of Friction of Faying Surfaces Subjected to Various Corrosion Protective Treatments," Report No. 2, ORE, Utrecht, The Netherlands, June 1967.
29. Perry, W. C., "Bearing Strength of Bolted Connections," MS thesis, The University of Texas at Austin, 1981 (in preparation).
30. Research Council on Riveted and Bolted Structural Joints of the Engineering Foundation, Specification for Structural Joints Using ASTM A325 or A490 Bolts, AISC, New York, April 1978.
31. Rumpf, J. L., and Fisher, J. W., "Calibration of A325 Bolts," Journal of the Structural Division, ASCE, Vol. 89, ST6, December 1963, p. 215.
32. Steel Structures Painting Council, Steel Structures Painting Manual, Vols. 1 and 2, Pittsburgh, Pennsylvania.
33. Vitelleschi, Silvio, and Schmidt, Lewis C., "Damping in Friction Grip Bolted Joints," Journal of the Structural Division, ASCE, Vol. 103, ST7, July 1977.
34. Wallaert, J. J., and Fisher, J. W., "Shear Strength of High Strength Bolts," Journal of the Structural Division, ASCE, Vol. 91, ST3, June 1968, pp. 99-125.
35. Winter, G., "Tests on Bolted Connections in Light Gage Steel," Journal of the Structural Division, ASCE, Vol. 82, ST2, March 1956.
36. Yura, J. A., Frank, K. H., and Cayes, L., "Friction-Type Bolted Connections with A588 Weathering Steel," Final Report, Part 1, Federal Highway Administration Report No. FHWA/RD-81/147, Washington, August 1980.
37. Lee, J. H., and Fisher, J. W., Bolted Joints with Rectangular or Circular Fillers, Fritz Engineering Laboratory Report No. 318.6, Lehigh University, Bethlehem, Pennsylvania, June 1968.

38. Bendigo, R. A., Hansen, R. A., Rumpf, J. L., "Long Bolted Joints," Journal of the Structural Division, ASCE, Vol. 89, ST6, December 1963, pp. 187-213.
39. National Cooperative Highway Research Program Report 74, "Protective Coatings for Highway Structural Steel," Washington, D.C., 1969.
40. Clifton, J. R., Beeghly, H. F., and Mathey, R. G., "Nonmetallic Coatings for Concrete Reinforcing Bars," Report No. FHWA-RD-74-18, National Bureau of Standards, Washington, D.C.
41. State of California, "Standard Specifications," Department of Transportation, Sacramento, California, January 1978.
42. Dusel, J. P., Jr., Stoker, J. R., and Nordlin, E. F., "The Effects of Coatings Applied to Contact Surfaces of High-Strength Bolted Joints in Slip Behavior and Strength of Joints," Final Report No. FHWA-CA-TL-6610-77-34, California Department of Transportation, Sacramento, California.
43. Natrella, Mary G., Experimental Statistics, National Bureau of Standards Handbook No. 91, Washington, D.C., August 1963.

## APPENDIX A

### Draft Testing Specification to Determine the Design Slip Coefficient for Coatings Used in Bolted Joints

#### 1.0 General Provisions

##### 1.1 Purpose and Scope

The purpose of the testing procedure is to determine the design classification of a coating for use in high-strength bolted connections. The testing specification is designed to ensure that the coating has at a maximum a 1% probability of slip at the 95% confidence level and a factor of safety of at least 1.45 against the mean for its design classification. The testing specification ensures that the creep deformation of the coating due to both the clamping force of the bolt and the service load joint shear are such that the coating will provide satisfactory performance under sustained loading.

##### 1.2 Definition of Essential Variables

Essential variables define the variables which, if changed will require retesting of the coating to determine its design slip classification. The essential variables are given below. The relationship of these variables to the limitation of application of the coating for structural joints is also given.

The time interval between application of the coating and the time of testing is an essential variable. The time interval must be recorded in hours and any special curing procedures detailed. The coatings are qualified for use in structural connections which are assembled after coating for a time equal to or greater than the interval used in the test specimens. Special curing conditions used in the test specimens will also apply to the use of the coating in the structural connections. Curing at room temperature, 60° to 80°F, with a relative humidity of 20 to 80% is not considered to be a special curing procedure.

The coating thickness is an essential variable. The maximum average coating allowed on the bolted structure will be the average thickness rounded to the nearest whole mil of the coating used on the creep test specimens minus 2 mils.

The composition of the coating, including the thinners used, and its method of manufacture are essential variables. Any change will require retesting of the coating.

##### 1.3 Retesting

A coating which fails to meet the creep or the post-creep slip test requirements given in Section 4 can be retested in accordance with the methods in Section 4 at a lower classification, lower slip coefficient, without repeating the static short-term tests specified in Section 3. Essential variables must remain unchanged in the retest.

## 2.0 Test Plates and Coating of the Specimens

### 2.1 Test Plates

The test specimen plates for the short-term static tests are shown in Figure 1. The plates are 4 × 4 in. (102 × 102 mm) plates, 5/8 in. (16 mm) thick, with a 1 in. (25 mm) diameter hole drilled 1-1/2 in. ± 1/16 in. (38 mm ± 1.6 mm) from one edge. The specimen plates for the creep specimen are shown in Figure 2. The plates are 4 × 7 in. (102 × 178 mm), 5/8 in. (16 mm) thick, with two 1 in. (25 mm) holes, 1-1/2 in. ± 1/16 in. (38 mm ± 1.6 mm) from each end. The edges of the plates may be milled, as rolled, or saw cut. Flame cut edges are not permitted. Cold rolled plates may be used. The plates should be flat enough to ensure that they will be in reasonably full contact over the faying surface. Any burrs, lips, or rough edges should be filed or milled flat. The arrangement of the specimen plates for testing is shown in Figures 2 and 3. The plates are to be fabricated from a steel with a minimum yield strength between 36 to 50 ksi (248 to 345 MPa).

### 2.2 Specimen Coating

The coatings are to be applied to the specimens in a manner consistent with the actual intended structural application. The method of applying the coating and the surface preparation should be given in the test report. The specimens are to be coated to an average thickness 2 mils (0.05 mm) greater than average thickness to be used in the structure. The thickness of the total coating and the primer, if used, shall be measured on the contact surface of the specimens. The thickness should be measured by any nondestructive technique allowed by the Steel Structures Painting Council, e.g., a magnetic gage. The thickness of the coating should be measured at a minimum of four locations on each contact surface. The overall average thickness from the three plates comprising a specimen is the average thickness for the specimen. This value should be reported for each specimen. The average coating thickness of the three creep specimens will be calculated and reported. The average thickness of the creep specimen minus two mils rounded to the nearest whole mil is the maximum average thickness of the coating to be used in the faying surface of a structure.

The time between painting and specimen assembly is to be the same for all specimens within ±4 hours. The average time is to be calculated and reported.

The two coating applications required in Section 3 are to use the same equipment and procedures.

## 3.0 Compression Slip Tests

The methods and procedures described herein are used to determine experimentally the slip coefficient (sometimes called the coefficient of friction) under short-term static loading for high-strength bolted connections. The slip coefficient will be determined by testing two sets of five specimens. The two sets are to be coated at different times at least one week apart.

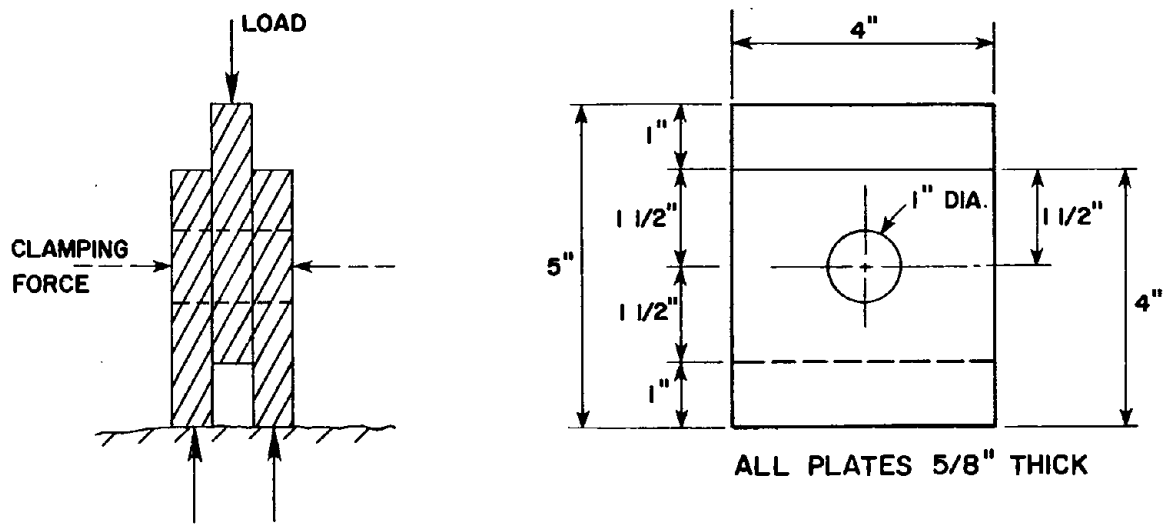


Figure 128. Compression test specimen

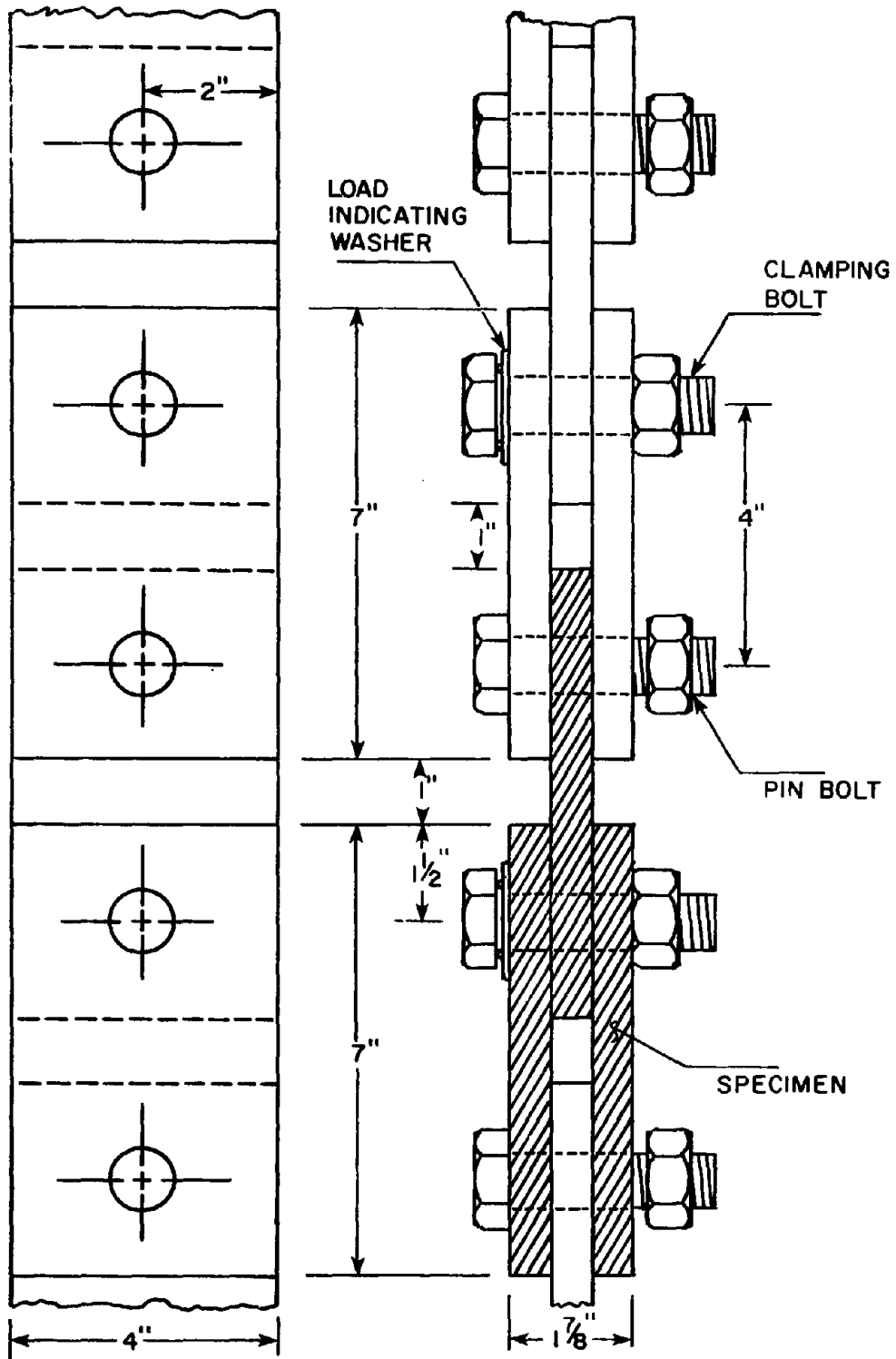


Figure 129. Creep test specimens



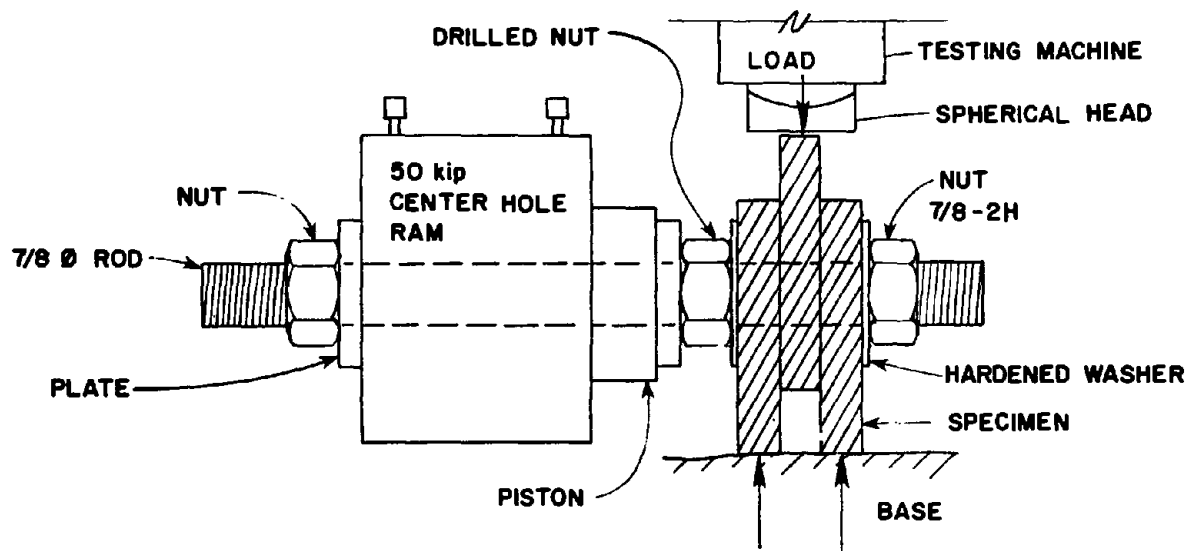


Figure 130. Test setup

### 3.1 Test Setup

The test setup shown in Figure 3 has two major loading components, one to apply a clamping force to the specimen plates and another to apply a compressive load to the specimen so that shear is applied to the faying surfaces.

Clamping Force System. The clamping force system consists of a 7/8 in. (22 mm) diameter threaded rod which passes through the specimen and a centerhole compression ram. A 2H nut and hardened washer is used at both ends of the rod. Between the ram and the specimen is a specially fabricated 7/8 in. (22 mm) 2H nut in which the threads have been drilled out so that it will slide with little resistance along the rod. When oil is pumped into the centerhole ram, the piston rod extends, thus forcing the special nut against one of the outside plates of the specimen. This action puts tension in the threaded rod and applies a clamping force to the specimen which simulates the effect of a tightened bolt. If the diameter of the centerhole ram is greater than 1 in. (25 mm), additional plate washers will be necessary at the ends of the ram. The clamping force system must have a capability to apply a load of at least 49 kips (219 kN) and maintain this load during the test with an accuracy of  $\pm 1\%$ .

Compressive Load System. A compressive load is applied to the specimen until slip occurs. This compressive load can be applied by a compression test machine or compression ram. The machine, ram and the necessary supporting elements should be able to support a force of 90 kips.

The compression loading system should have an accuracy of 1.0 percent of the slip load.

### 3.2 Instrumentation

Clamping Force. The clamping force must be measured within 0.5 kips (2.2 kN). This may be accomplished by measuring the pressure in the calibrated ram or placing a load cell in series with the ram.

Compression Load. The compression load must be measured during the test. This may be accomplished by direct reading from a compression testing machine, a load cell in series with the specimen and the compression loading device, or pressure readings on a calibrated compression ram.

Slip Deformation. The relative displacement of the center plate and the two outside plates must be measured. This displacement, called slip for simplicity, should be the average which occurs at the centerline of the specimen. This can be accomplished by using the average of two gages placed on the two exposed edges of the specimen or by monitoring the movement of the loading head relative to the base. Deflections can be measured by dial gages or any other calibrated device which has an accuracy of 0.001 in. (0.02 mm).

### 3.3 Test Procedure

The specimen is installed in the test setup as shown in Figure 3. Before the hydraulic clamping force is applied, the individual plates should be positioned so that they are in, or are close to, bearing

contact with the 7/8 in. (22 mm) threaded rod in a direction opposite to the planned compressive loading to ensure obvious slip deformation. Care should be taken in positioning the two outside plates so that the specimen will be straight and both plates are in contact with the base.

After the plates are positioned, the centerhole ram is engaged to produce a clamping force of 49 kips (219 kN). The applied clamping force should be maintained within  $\pm 0.5$  kips (2.2 kN) during the test until slip occurs.

The spherical head of the compression loading machine should be brought in contact with the center plate of the specimen after the clamping force is applied. The spherical head or other appropriate device ensures uniform contact along the edge of the plate, thus eliminating eccentric loading. When 1 kip (4.45 kN) or less of compressive load is applied, the slip gages should be engaged or attached. The purpose of engaging the deflection gage(s), after a slight load is applied, is to eliminate initial specimen settling deformation from the slip readings.

When the slip gages are in place, the compression load is applied at a rate not exceeding 25 kips (109 kN) per minute, or 0.003 in. (0.07 mm) of slip displacement per minute until the slip load is reached. The test should be terminated when a slip of 0.05 in. (1.3 mm) or greater is recorded. The load-slip relationship should preferably be monitored continuously on an X-Y plotter throughout the test, but in lieu of continuous data, sufficient load-slip data must be recorded to evaluate the slip load defined below.

### 3.4 Slip Load

Typical load-slip response is shown in Figure 4. Three types of curves are usually observed and the slip load associated with each type is defined as follows:

- (a) the maximum load provided this maximum occurs before a slip of 0.020 in. (0.5 mm) occurs (curve a)
- (b) the load at which the slip rate suddenly increases (curve b)
- (c) the load measured when the slip is 0.02 in. (20 mils, 0.5 mm). This definition controls when the load-slip curve shows a gradual change in response (curve c)

If a typical response curve is different from those shown in Figure 4, the Research Council on Structural Connections should be consulted.

### 3.5 Coefficient of Slip

The slip coefficient,  $k_s$ , for an individual specimen is calculated as follows:

$$k_s = \frac{\text{slip load}}{2 \times \text{clamping force}}$$

The average and the standard deviation of the ten specimens are to be calculated and reported. The slip coefficient corresponding to 75% confidence of a 1% probability of slip at service load (95% if 50 specimens are tested rather than 10 specimens) is to be calculated as follows (Ref. 43):

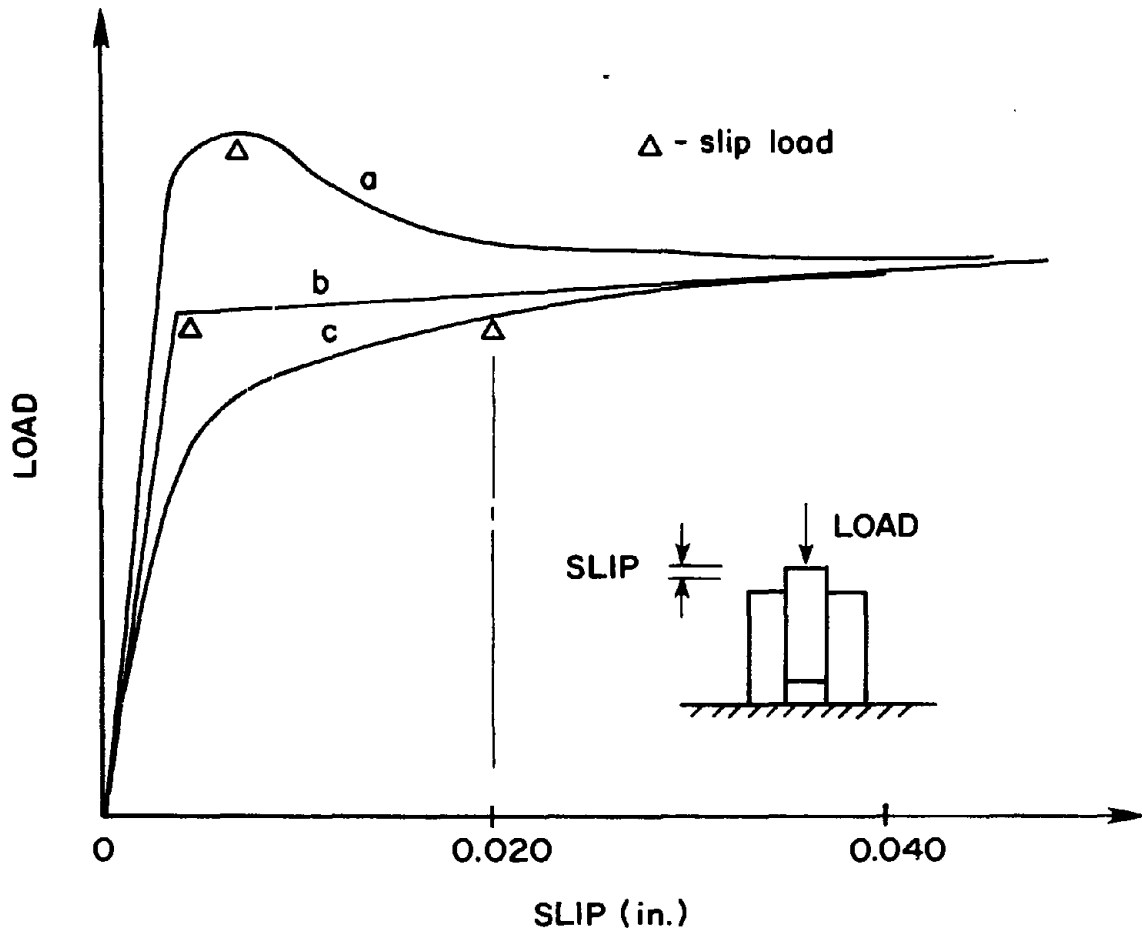


Figure 131. Definition of slip load

$$K_{1\%} = (\bar{K}_s - 3.0 \times s)$$

where  $\bar{K}_s$  = average slip coefficient of the ten specimens  
 $s$  = the standard deviation of the ten specimens

If the value of  $K_{1\%}$  multiplied by 1.45 is less than  $\bar{K}_s$ , the slip coefficient of the coating to be used for classification,  $K_{sc}$ , is equal to  $K_{1\%}$ . If  $K_{1\%}$  is greater than  $\bar{K}_s$ , then  $K_{sc}$ , the slip coefficient to be used for classification, is equal to  $\bar{K}_s$ . The slip coefficient for classification determined above is to be reported and the coating classified according to Table 1. The value of  $K_{sc}$  is rounded to two significant figures.

Table 1

Value of Slip Coefficient for Classification, $K_{sc}$	Classification of Coating
$0.19 \leq K_{sc} < 0.30$	A
$0.31 \leq K_{sc} < 0.37$	B
$0.38 \leq K_{sc} < 0.44$	C
$0.45 \leq K_{sc} < 0.53$	D
$0.54 \leq K_{sc}$	E

#### 4.0 Tension Creep Tests

The test method outlined is intended to ensure that the coating will not undergo significant creep deformation under service loading. The test also determines whether the loss in clamping force in the fastener due to the compression creep of the paint is large enough to reduce the slip load below the minimum value for the class of the coating determined in Section 3 above. Three replicate specimens are to be tested.

#### 4.1 Test Setup

Tension-type specimens, as shown in Figure 2, are to be used. The replicate specimens are to be linked together in a single chain-like arrangement, using loose pin bolts, so that the same load is applied to all specimens. The specimens shall be assembled so that the specimen plates are bearing against the bolt in a direction opposite to the applied tension loading. Care should be taken in the assembly of the specimens to ensure the centerline of the holes used to accept the pin bolts is in line with the bolts used to assemble the joint. The load level, specified in Section 4.2, shall be maintained constant within  $\pm 1\%$  by springs, load maintainers, servo controllers, dead weights, or other suitable equipment. The bolts used to clamp the specimens together shall be 7/8 in. (22 mm) A490 bolts. All bolts should come from the

same lot. The clamping force in the bolts should be a minimum of 49 kips (219 kN). The clamping force is to be determined by calibrating the bolt force with bolt elongation, if standard bolts are used. It is recommended that either load indicator washers be used to monitor the bolt force or special fasteners which control the clamping force by other means such as bolt torque be used. A minimum of three bolt calibrations must be performed using the technique selected for bolt force determination. The average of the three bolt calibration is to be calculated and reported. The method of measuring bolt force must ensure the clamping force is within  $\pm 2$  kips (12 kN) of the average value.

The relative slip between the outside plates and the center plates shall be measured to an accuracy of 0.001 in. (0.02 mm). This is to be measured on both sides of each specimen.

#### 4.2 Test Procedure

The load to be placed on the specimens is to be calculated as given below:

$$P_c = \text{average clamping force} \times \text{slip coefficient} \times 1.38$$

where the average clamping force, minimum of 49 kips (219 kN) is determined as outlined in Section 4.1. The slip coefficient is the minimum slip coefficient of the classification of the coating. The values are given in Table 1. The load is to be placed on the specimen and held for 1000 hours. The creep deformation of a specimen is calculated using the average readings of the two displacements on each side of the specimen. The difference between the average after 1000 hours and the initial average reading taken within one-half hour after loading the specimens is defined as the creep deformation of the specimen. This value is to be reported for each specimen. If the creep deformation of any specimen exceeds 0.005 in. (0.12 mm), the coating has failed the test for the classification. The coating may be retested using new specimens in accordance with this section at a load corresponding to a lower classification (lower value of slip coefficient).

If the value of creep deformation is less than 0.005 in. (0.12 mm) for all specimens, the specimens are to be loaded in tension to a load calculated as

$$P_u = P_c \times 1.45$$

The slip deformation which occurs at this load must be less than 0.015 in. (0.38 mm) for all specimens. If the deformation is greater than this value for any specimen, the coating is considered to have failed to meet the requirements for the classification. The value of this deformation for each specimen is to be reported.

#### Commentary

The slip coefficient under short-term static loading has been found to be independent of clamping force, paint thickness, and hole diameter. The slip coefficient can be easily determined using the hydraulic bolt test setup included in the following recommended specification. The slip load measured in this setup yields the slip coefficient directly since the clamping force is controlled. The slip coefficient,

$k_s$ , is given by

$$k_s = \frac{\text{slip load}}{2 \times \text{clamping force}}$$

The resulting slip coefficient has been found to correlate with both tension and compression tests of bolted specimens. However, tests of bolted specimens revealed that the clamping force may not be constant but decreases with time due to the compressive creep of the coating on the faying surfaces and under the nut and bolt head. The reduction of the clamping force can be considerable for joints with high clamping force and thick coatings, as much as a 20% loss. This reduction in clamping force causes a corresponding reduction in the slip load. The resulting reduction in slip load must be considered in the procedure used to determine the design allowable slip loads for the coating.

The loss in clamping force is a characteristic of the coating. Consequently, it cannot be accounted for by an increase in the factor of safety or a reduction in the clamping force used for design without unduly penalizing coatings which do not exhibit this behavior.

The creep deformation of the bolted joint under the applied shear loading is also an important characteristic and a function of the coating applied. Thicker coatings tend to creep more than thinner coatings. Rate of creep deformation increases as the applied load approaches the slip load. Extensive testing has shown that the rate of creep is not constant with time, rather it decreases with time. After 1000 hours of loading, the additional creep deformation is negligible.

The proposed test methods are designed to provide the necessary information to evaluate the suitability of a coating for slip critical bolted connections and to determine the slip coefficient to be used in the design of the connections. The initial testing of the compression specimens provide a measure of the scatter of the slip coefficient and means of classifying the coating into the design classification.

The creep tests are designed to measure the paint's creep behavior under the service loads determined by the paint's classification based on the compression test results. The post creep tests to the slip load associated with the design classification are to ensure that the loss of clamping force in the bolt does not reduce the slip load below that associated with the design classification. A490 bolts are specified, since the loss of clamping force is larger for these bolts than A325 bolts. The qualifying of the paint for use in a structure at an average thickness of 2 mils less than the test specimen is to ensure that a casual buildup of paint due to overspray, etc., does not jeopardize the coating's performance.

The use of 1 in. (25 mm) holes in the specimens is to ensure that adequate clearance is available for slip. Fabrication tolerances, coating buildup on the holes, and assembly tolerances reduce the apparent clearances.

There are many parts of the proposed specification where the statements reflect our best thoughts of methods to provide a reliable test and are not based on any data. For example, the limitations on

normal curing may be too broad or too restrictive. Opinions from paint experts are welcomed. Also, the statement in Section 1.2 dealing with changes in the composition of the paint, method of manufacture, etc., may be too restrictive, since no tolerances are provided.



TABLE 1.7.1A (continued)

ALLOWABLE DESIGN STRESSES—STRUCTURAL STEEL (All values in parenthesis are in MPa)					
Type	Structural Carbon Steel	High Strength Low-Alloy		High Yield Strength Quenched and Tempered Alloy Steel	
Shear in girder webs, gross section . . . . . $F_v=0.33F_y$	12,000 (82.737)	17,000 (117.211)	17,000 (117.211)	33,000 (227.527)	30,000 (206.842)
Bearing on milled stiffeners and other steel parts in contact (rivets and bolts excluded) . . . . . $0.80F_y$	29,000 (199.948)	40,000 (275.790)	40,000 (275.790)	80,000 (551.580)	72,000 (496.422)
Stress in extreme fiber or pins (4) . . . . . $0.80F_y$	29,000 (199.948)	40,000 (275.790)	40,000 (275.790)	80,000 (551.580)	72,000 (496.422)
Shear in pins $F_v=0.40F_y$	14,000 (96.526)	20,000 (137.895)	20,000 (137.895)	40,000 (275.790)	36,000 (248.211)
Bearing on pins not subject to rotation (9) . . . . . $0.80F_y$	29,000 (199.948)	40,000 (275.790)	40,000 (275.790)	80,000 (551.580)	72,000 (496.422)
Bearing on pins subject to rotation (such as used in rockers and hinges) . . . $0.40F_y$	14,000 (96.526)	20,000 (137.895)	20,000 (137.895)	40,000 (275.790)	36,000 (248.211)
Bearing on power-driven rivets and high strength bolts (or as limited by the allowable bearing on the fasteners) $1.35F_u$	78,500 (541.237)	<del>85,000 (606.738)</del>	<del>94,500 (657.848)</del>	<del>148,000 (1020.420)</del>	135,000 (930.790)

See page 141 for footnotes.

in standard or oversize holes.

$1.20F_u$	69,500 (479,000)	78,000 (537,000)	84,000 (579,000)	132,000 (909,000)	120,000 (827,000)
-----------	---------------------	---------------------	---------------------	----------------------	----------------------

in slotted holes when the force is applied perpendicular to the long direction of the slot.

$1.0F_u$	58,000 (400,000)	65,000 (448,000)	70,000 (482,000)	110,000 (758,000)	100,000 (689,000)
----------	---------------------	---------------------	---------------------	----------------------	----------------------

Table 1.7.41C2—Allowable Working Shear Stresses<sup>a</sup> for High Strength Bolts Used for Friction-Type Shear Connectors. Based Upon Surface Condition of Bolted Parts, in ksi (MPa).

Class of Surface <sup>b</sup>	Surface Condition of Bolted Parts	Standard Holes		Oversize Holes and Short Slotted Holes		Long Slotted Holes	
		M164 (A325)	M253 (A490)	M164 (A325)	M253 (A490)	M164 (A325)	M253 (A490)
A	Clean mill scale	18.0 (110.316)	30.0 (127.895)	13.5 (93.078)	17.0 (117.211)	11.5 (79.289)	14.5 (99.973)
B	Blast-cleaned carbon and low alloy steel	25.0 (172.369)	31.0 (213.737)	21.0 (144.790)	26.5 (182.710)	17.5 (120.658)	21.5 (148.237)
C	Blast-cleaned quenched and tempered steel	17.0 (117.211)	21.0 (144.790)	14.5 (99.973)	18.0 (124.105)	12.0 (82.737)	15.0 (103.421)
D	Hot-dip galvanized and roughened	18.5 (134.447)	24.5 (168.921)	16.5 (113.763)	20.5 (141.342)	13.5 (92.079)	17.0 (117.211)
E	Blast-cleaned, organic zinc rich paint	19.0 (131.000)	23.5 (162.026)	16.0 (110.316)	20.0 (137.895)	13.0 (89.632)	16.0 (110.316)
F	Blast-cleaned, inorganic zinc rich paint	26.5 (182.710)	33.5 (230.974)	22.5 (155.131)	28.5 (196.500)	18.5 (127.552)	23.5 (162.026)
G	Blast-cleaned, metallized with zinc	26.5 (182.710)	33.5 (230.974)	22.5 (155.131)	28.5 (196.500)	18.5 (127.552)	23.5 (162.026)
H	Blast-cleaned, metallized with aluminum	27.0 (186.158)	34.0 (234.421)	23.0 (158.579)	29.0 (199.948)	19.0 (131.000)	24.0 (166.474)
I	Vinyl Wash	15.0 (103.421)	18.5 (127.552)	12.5 (86.184)	16.0 (110.316)	10.5 (72.394)	13.0 (89.632)

<sup>a</sup> Values from this table are applicable only when they do not exceed the lowest appropriate allowable working stresses for bearing-type connections, taking into account the position of threads relative to shear planes and, if required, the 20% reduction due to joint length. (See Table 1.7.41C1 Footnote d)

<sup>b</sup> See Article 2.10.20(C) for further definition of Class of Surface.

Replace Table 1.7.41C2 as follows:

Class	Slip Coef.	Range <sup>(1)</sup> Slip Coef.	Surface Treatment	Standard Holes <sup>(2)</sup>	
				A325	A490
A	0.22	0.19-0.30	A588 millscale (epoxy topcoat)*	10	12
B	0.33	0.31-0.37	Other millscale (phenoxy-base organic zinc)(3)*	15	18
C	0.40	0.38-44	Hot dip galvanized and roughened (epoxy-base organic zinc)*	18	22
D	0.47	0.45-0.53	Blast cleaned (phenoxy-base organic zinc (4), inorganic 75% zinc)*	21	26
E	0.56	>0.54	Metallized with zinc or aluminum (inorganic 80% zinc)*	25	31

(1) A particular paint product is classified based on test evidence provided by the manufacturer using an approved test specification. A proposed test specification is given in Appendix A of this report.

(2) For oversize and short slotted holes, reduce the stresses to 0.85 of the value shown. For long slotted holes, reduce to 0.70 of the value shown.

(3) One brand of phenoxy-base organic zinc that satisfies the State of California Spec (90% zinc).

(4) One brand of phenoxy-base organic zinc that has 80% zinc.

\* Classification of particular paint products tested in this research program.

**Table 1.7.41C1—Allowable Working Stresses For High Strength Bolts<sup>a</sup> in ksi (MPa).**

Load Condition	Hole Type	AASHTO M164 <sup>f</sup> (ASTM A325) Bolts	AASHTO M253 (ASTM A490) Bolts
Applied Tension <sup>b</sup> (T)	Standard, oversize or slotted	39.5 (272.342)	48.5 (334.395)
Shear (F <sub>v</sub> ): Friction-Type Connection <sup>c</sup>	Standard	16.0 (110.316)	20.0 (137.895)
	Oversize	13.5 (93.079)	17.0 (117.211)
	Short slotted	13.5 (93.079)	17.0 (117.211)
	Long slotted	11.5 (79.289)	14.5 (99.973)
Shear (F <sub>v</sub> ): Bearing-Type Connection: <sup>d</sup>	Threads in any shear plane	19.0 (131.000)	25.0 (172.369)
	No threads in shear plane	Standard or slotted 27.0 (186.158)	Standard or slotted 36.0 (248.211)
Bearing <sup>e</sup> (f <sub>p</sub> )	Standard or slotted	$\frac{LF_u}{2.2d}$ or $(1.35)F_u$ (whichever is smaller)	
	Slotted	$\frac{LF_u}{2.2d}$ or $1.0 F_u$ whichever is smaller	

<sup>a</sup> The tabulated stresses, except for bearing stress, apply to the nominal area of bolts used in any grade of steel.

<sup>b</sup> For allowable working stresses when bolts are subjected to fatigue loading in tension, see Article 1.7.41(C)(4).

for all steels except for A588 steel (see Table 1.7.41(C)(2)).

<sup>c</sup> Applicable for contact surfaces with clean mill scale. When the designer has specified special treatment of the contact surfaces in a friction-type connection, values in Table 1.7.41(C)(2) may be substituted.

<sup>d</sup> In bearing-type connections whose length between extreme fasteners in each of the spliced parts measured parallel to the line of an axial force exceeds 50 inches (1.27m), tabulated values shall be reduced by 20 percent,

when no undeveloped fillers are used or 30 in. (0.76m) when undeveloped fillers are used.

<sup>e</sup> L is the distance in inches (m) measured in the line of force from the center line of a bolt to the nearest edge of an adjacent bolt or to the end of the connected part toward which the force is directed; d is the diameter of the bolts; and F<sub>u</sub> is the lowest specified minimum tensile strength of the connected parts.

<sup>f</sup> AASHTO M164 (ASTM A325) high strength bolts are available in three types, designated as types 1, 2 or 3. Type 3 shall be required on the plans when using unpainted AASHTO M222 (ASTM A588) steel.

TABLE 1.7.71A

Type of Fastener	Strength ( $\phi F$ )
Groove Weld <sup>1</sup>	1.00 $F_y$
Fillet Weld <sup>2</sup>	0.45 $F_u$
Low-Carbon Steel Bolts	
AASHTO M - - -	
(ASTM A 307)	
Tension	27 ksi (186.158 MPa)
Shear <sup>3</sup>	25 ksi (172.369 MPa)
Power-Driven Rivets	
AASHTO M228	
(ASTM A502)	
Shear - Grade 1	25 ksi (172.369 MPa)
Shear - Grade 2	30 ksi (206.842 MPa)
High-Strength Bolts	
AASHTO M 164	
(ASTM A325)	
Tension <sup>5</sup>	70 ksi (482.632 MPa)
Shear (Bearing-Type) <sup>3,4</sup>	60 ksi (413.685 MPa)
Bearing <sup>6</sup>	$\frac{LF_u}{1.18d}$ or 3.0 $F_u$ whichever is smaller
AASHTO M253	
(ASTM A490)	
Tension	87 ksi (599.843 MPa)
Shear (Bearing Type) <sup>3,4</sup>	80 ksi (551.580 MPa)
Bearing <sup>6</sup> , standard holes	$\frac{LF_u}{1.18d}$ or $\textcircled{3.0} F_u$ whichever is smaller 2.4
slotted holes	$\frac{LF_u}{1.18d}$ or 2.0 $F_u$ whichever is smaller

## FEDERALLY COORDINATED PROGRAM (FCP) OF HIGHWAY RESEARCH AND DEVELOPMENT

The Offices of Research and Development (R&D) of the Federal Highway Administration (FHWA) are responsible for a broad program of staff and contract research and development and a Federal-aid program, conducted by or through the State highway transportation agencies, that includes the Highway Planning and Research (HP&R) program and the National Cooperative Highway Research Program (NCHRP) managed by the Transportation Research Board. The FCP is a carefully selected group of projects that uses research and development resources to obtain timely solutions to urgent national highway engineering problems.\*

The diagonal double stripe on the cover of this report represents a highway and is color-coded to identify the FCP category that the report falls under. A red stripe is used for category 1, dark blue for category 2, light blue for category 3, brown for category 4, gray for category 5, green for categories 6 and 7, and an orange stripe identifies category 0.

### *FCP Category Descriptions*

#### **1. Improved Highway Design and Operation for Safety**

Safety R&D addresses problems associated with the responsibilities of the FHWA under the Highway Safety Act and includes investigation of appropriate design standards, roadside hardware, signing, and physical and scientific data for the formulation of improved safety regulations.

#### **2. Reduction of Traffic Congestion, and Improved Operational Efficiency**

Traffic R&D is concerned with increasing the operational efficiency of existing highways by advancing technology, by improving designs for existing as well as new facilities, and by balancing the demand-capacity relationship through traffic management techniques such as bus and carpool preferential treatment, motorist information, and rerouting of traffic.

#### **3. Environmental Considerations in Highway Design, Location, Construction, and Operation**

Environmental R&D is directed toward identifying and evaluating highway elements that affect

the quality of the human environment. The goals are reduction of adverse highway and traffic impacts, and protection and enhancement of the environment.

#### **4. Improved Materials Utilization and Durability**

Materials R&D is concerned with expanding the knowledge and technology of materials properties, using available natural materials, improving structural foundation materials, recycling highway materials, converting industrial wastes into useful highway products, developing extender or substitute materials for those in short supply, and developing more rapid and reliable testing procedures. The goals are lower highway construction costs and extended maintenance-free operation.

#### **5. Improved Design to Reduce Costs, Extend Life Expectancy, and Insure Structural Safety**

Structural R&D is concerned with furthering the latest technological advances in structural and hydraulic designs, fabrication processes, and construction techniques to provide safe, efficient highways at reasonable costs.

#### **6. Improved Technology for Highway Construction**

This category is concerned with the research, development, and implementation of highway construction technology to increase productivity, reduce energy consumption, conserve dwindling resources, and reduce costs while improving the quality and methods of construction.

#### **7. Improved Technology for Highway Maintenance**

This category addresses problems in preserving the Nation's highways and includes activities in physical maintenance, traffic services, management, and equipment. The goal is to maximize operational efficiency and safety to the traveling public while conserving resources.

#### **0. Other New Studies**

This category, not included in the seven-volume official statement of the FCP, is concerned with HP&R and NCHRP studies not specifically related to FCP projects. These studies involve R&D support of other FHWA program office research.

\* The complete seven-volume official statement of the FCP is available from the National Technical Information Service, Springfield, Va. 22161. Single copies of the introductory volume are available without charge from Program Analysis (HRD-3), Offices of Research and Development, Federal Highway Administration, Washington, D.C. 20590.

B85  
11

